Diese Dissertation haben begutachtet

Prof. Dr. Ulrich SCHUBERT

Prof. Dr. Nicola HÜSING

Dissertation

Synthesis and Characterization of Organically Modified Aluminum and Yttrium Alkoxides

ausgeführt zum Zwecke der Erlangung des akademischen Grades eines Doktors der technischen Wissenschaften

unter der Leitung von

o.Univ.Prof. Dipl.-Ing. Dr.rer.nat. Ulrich SCHUBERT

E165
Institut für Materialchemie

eingereicht an der Technischen Universität Wien
Fakultät für Technische Chemie

von

Dipl.-Ing. Robert LICHTENBERGER

Mat.Nr. 0126514

Schallergasse 9/18
1120 Wien

Wien, 05.02.2010

Dipl.-Ing. Robert Lichtenberger

"As an adolescent I aspired to lasting fame, I craved factual certainty, and I thirsted for a meaningful vision of human life – so I became a scientist. This is like becoming an archbishop so you can meet girls."

M. Cartmill

Für Alexandra, Jonas & Elias. Ihr seid meine Welt.

Acknowledgements

First of all I would like to express my gratitude to Prof. Ulrich Schubert for giving me the opportunity to work in his group and for the supervision of my thesis. His guidance and support throughout the last years provided me lots of freedom for scientific as well as personal development.

Special thanks to Stefan B. and Majka for their effort to measure all the crystals I showed them and solving the structures, no matter how futile it may have appeared in the beginning. Many thanks to Michael for doing numerous NMR experiments, always accompanied with inspiring discussions and useful advices.

Big thanks to my (*former*) colleagues Angelika, Bernhard (for providing "Eisernheit"), *Christian Mar.*, *Christoph R.*, *Claudia*, *Denisa*, *Denise*, *Doris*, *Elmar*, *Fatmir*, *Giedrius*, *Guido*, Harald, Hongzhi, Jakob, *Jingxia*, Maïa, Marco, Marina, Melitta, Michael, *Mirka*, Mohsin, *Nele*, *Ofer*, *Philipp*, *Ralf*, *René*, Rupali, Rupert (for repairing erverything), *Simas*, *Sorin*, *Stefan E.*, Stephan R., and Stephan K. for a pleasant working environment and lots of friendship, also outside university. Special thanks to Christian Mau., Christoph L., Robert P. (for being the other one), Stefan B. (for being the greatest fum hood buddy one can imagine), and Van An (for being the lady in the men's office) for making the "rear office" to the most exciting and enjoyable place to work.

I also want to thank Anna, Manuel (the "crystal-grower"), and Robert H. for their great practical work during their stays in our lab.

Thanks to Christian Heller, Doris Tisch, Manuel Schwabl, Niklas Pucher, and Ute Wolfesberger for being friends at as well as outside the university, sharing the desperate times PhD students have to pass, and for going All-In if necessary.

Greetings to my friends outside university, who always reminded me of the pleasures of "real life" and enriched my life. Special gratidue to the "Buam" from Linz, who joined my entire life.

I'm deeply indebt to my parents who supported me throughout my whole studies and always encouraged me to make my way, in the scientific and the real world. A big huge also to my brother Peter for being the big one and bringing me home if necessary.

Finally I want to dedicate this work to the most important persons in my lif: my wife Alexandra and my sons Jonas and Elias. Without you, all the work of the last years wouldn't have been possible (although I might have slept more). Thanks for your restless love and for making my life what it is: perfect.

Kurzfassung

Die Kontrolle der Reaktivität in Hydrolyse- und Kondensationsreaktionen durch die Modifizierung von Metallalkoxiden mit organischen Liganden ermöglicht ihre Verwendung als Vorstufen für Sol-Gel Materialien. Gleichzeitig wird dadurch auch die Struktur des resultierenden Materials beeinflusst und der Verbleib von organischen Liganden im Material eröffnet eine Strategie zur Synthese anorganisch-organischer Hybridmaterialien. Organische Liganden mit zusätzlichen funktionellen Gruppen können des Weiteren als Verknüpfungsstellen für kovalent Bindungen zwischen anorganischen und organischen Polymeren dienen. Ein Verstehen der Einflüsse der organischen Liganden auf die Struktur und Reaktivität der Vorstufen ist eine Voraussetzung für ein vorausschauendes Design neuer Sol-Gel (Hybrid-)Materialien.

Der erste Teil dieser Arbeit befasst sich mit der systematischen Untersuchung der Modifikation von Aluminiumalkoxiden mit *β*-diketonischen Verbindungen (*β*-Ketoester, Dialkylmalonate, *β*-Ketoamide). Die Produkte wurden in Lösung mittels NMR spektroskopischer Methoden und im Feststoff, falls möglich, durch Einkristall-Röntgendiffraktion untersucht.

Verbindungen des Typs Al(*β*-Ketoesterat)$_3$ wurde durch Reaktion von [Al(OR)$_3$]$_n$ (OR = O^{t}Bu, O^{i}Pr) mit drei Äquivalenten *β*-Ketoester erhalten. Alle Komplexe weisen eine einkernige oktaedrische Struktur auf. Verbindungen des Typs Al$_2$(*μ*-O^{i}Pr)$_2$(O^{i}Pr)(*β*-Ketoesterat)$_2$ – welche eine asymmetrisch substituierte zweikernige Struktur aufweisen – konnten nur durch Reaktion bei erhöhten Temperaturen oder durch Deoligomerisation von [Al(O^{i}Pr)$_3$]$_4$ vor der Substitutionsreaktion erhalten werden. Eine Ausnahme stellen *β*-Ketoester mit zusätzlichen Substituenten in der 4 Position dar, welche auf Grund der veränderten elektronischen Verhältnisse bereits bei Raumtemperatur Al$_2$(*μ*-O^{i}Pr)$_2$(O^{i}Pr)(*β*-Ketoesterate)$_2$ als Produkt lieferten. Für Ethyl-2-isopropylacetoacetat wurde Hydrodeacylierung als Nebenreaktion beobachtet. Analoge Verbindungen wurden auch für die Modifikation von Al(O^{i}Pr)$_3$ mit N,N-Diethylacetoacetamid erhalten. Es wurde kein Einfluss durch Veränderung der Ester-Funktionalität auf die Produkte beobachtet, ausgenommen für *tert.*-Butylacetoacetat, wo Umesterung auftrat.

Verbindungen des Typs Al(Dialkylmalonat)$_3$, Al$_2$(*μ*-O^{i}Pr)$_2$(O^{i}Pr)$_2$(Dialkylmalonat)$_2$, [Al(*μ*-O^{i}Pr)(Diisopropylmalonat)$_2$]$_2$ und Al$_3$(*μ*-OH)(*μ*-OEt)$_3$(Diethylmalonat)$_5$ wurde für die Modifikation von Aluminium Alkoxiden mit Dialkylmalonaten erhalten. [Al(*μ*-O^{i}Pr)(Diisopropylmalonat)$_2$]$_2$ wurde ausschließlich durch Kristallisation von Al$_2$(*μ*-O^{i}Pr)$_2$(O^{i}Pr)$_2$(Diisopropylmalonat)$_2$ erhalten. Eine Verbindung vom Typ Al$_3$(*μ*-OH)(*μ*-OEt)$_3$(Diethylmalonat)$_5$ wurde nur für die Modifikation mit Dialkylmalonaten erhalten. Umesterung wurde für Reaktionen von Al(O^{i}Pr)$_3$ mit Dimethyl- und Diethylmalonat beobachtet.

Der zweite Teil dieser Arbeit beschreibt die Synthese dreier neuer Yttriumcluster durch die Modifikation von Y$_5$O(O^{i}Pr)$_{13}$ mit Isopropylacetoacetat (^{i}prac). Y$_9$O(OH)$_9$(O^{i}Pr)$_8$(^{i}prac)$_8$

wurde durch Reaktion mit einem Äquivalent Ligand per Yttriumatom erhalten, während die Reaktion mit drei Äquivalenten $[Y_2(OH)(^{i}prac)_5]_2$ als Produkt ergab. Kristallisation von $[Y_2(OH)(^{i}prac)_5]_2$ aus Chloroform gab $Y_9O(OH)_9(^{i}prac)_{16}$, strukturell eng verwandt mit $Y_9O(OH)_9(O^{i}Pr)_8(^{i}prac)_8$. Diese Zusammenhänge zeigen die strukturelle Vielseitigkeit der Yttriumcluster.

Abstract

The control of reactivity towards hydrolysis and condensation of metal alkoxides by modification with organic ligands enables their use as precursors for sol-gel materials. Concomitantly the structure of the final material is influenced and retaining of the organic ligands in the final material opens a route to inorganic-organic hybrid materials. Organic ligands bearing additional functionalities furthermore may serve as anchoring points for covalent linkage between inorganic and organic polymers. Understanding the influence of the organic ligand on the structure and reactivity of the precursors is a prerequisite for a deliberate design of new sol-gel derived (hybrid) materials.

In the first part of this work a systematic study on modification of aluminum alkoxides with β-diketonic compounds (β-ketoesters, dialkylmalonates, β-ketoamides) was performed. The obtained products were characterized by NMR spectroscopic methods in solution as well as by single crystal XRD in the solid state, if possible.

Compounds Al(β-ketoesterate)$_3$ were obtained upon reaction of $[Al(OR)_3]_n$ (OR = O^{t}Bu, O^{i}Pr) with 3 equivalents of β-ketoester, all exhibiting a mononuclear octahedral structure. Complexes $Al_2(\mu\text{-}O^iPr)_2(O^iPr)(\beta\text{-ketoesterate})_2$ – which show a asymmetrically substituted dinuclear structure – could only be obtained upon reaction at elevated temperatures or by de-oligomerization of $[Al(O^iPr)_3]_4$ prior to the substitution reaction, except for β-ketoesters bearing additional substitutents in the 4 position, where the different electronic situation yields $Al_2(\mu\text{-}O^iPr)_2(O^iPr)(\beta\text{-ketoesterate})_2$ already at room temperature. For ethyl 2-isopropylacetoacetate hydrodeacylation was observed as competing reaction. Analogous compounds were also obtained for the modification of $Al(O^iPr)_3$ with N,N-diethyl acetoacetamide. No influence upon variation of the ester functionality on the products was observed, except for *tert.*-butyl acetoacetate, where transesterification was observed.

The compounds Al(dialkylmalonate)$_3$, $Al_2(\mu\text{-}O^iPr)_2(O^iPr)_2$(dialkylmalonate)$_2$, $[Al(\mu\text{-}O^iPr)(\text{diisopropylmalonate})_2]_2$, and $Al_3(\mu\text{-OH})(\mu\text{-OEt})_3$(diethylmalonate)$_5$ were obtained upon modification of aluminum alkoxides with dialyklmalonates. $[Al(\mu\text{-}O^iPr)(\text{diisopropylmalonate})_2]_2$ was exclusively obtained upon crystallization from $Al_2(\mu\text{-}O^iPr)_2(O^iPr)_2$(diisopropylmalonate)$_2$. A compound of the type $Al_3(\mu\text{-OH})(\mu\text{-OEt})_3$(diethylmalonate)$_5$ was only obtained for modification with dialkylmalonates. Transesterification was observed for reactions of $Al(O^iPr)_3$ with dimethyl and diethyl malonate.

In the second part of this work, modification of $Y_5O(O^iPr)_{13}$ with isopropylacetoacetate (^{i}prac), yielding three new clusters, is described. $Y_9O(OH)_9(O^iPr)_8(^i\text{prac})_8$ was obtained upon reaction with one equivalent of ligand per yttrium atom, whereas $[Y_2(OH)(^i\text{prac})_5]_2$ was obtained for the reaction with three equivalents. Crystallization of $[Y_2(OH)(^i\text{prac})_5]_2$ from chloroform yielded $Y_9O(OH)_9(^i\text{prac})_{16}$, structurally closely related to $Y_9O(OH)_9(O^iPr)_8(^i\text{prac})_8$, showing the structural versatility of yttrium clusters.

Parts of this work have been published

"Modification of aluminum alkoxides with dialkylmalonates" Lichtenberger, R.; Baumann, S. O.; Bendová, M.; Puchberger, M.; Schubert, U. *submitted for publication.*

"Modification of aluminum alkoxides with *β*-ketoesters: new insights into formation, structure and stability" Lichtenberger, R.; Baumann, S. O.; Puchberger, M.; Schubert U. *J. Sol-Gel Sci. Technol.* **2009**, *50*, 130–140.

Abreviations[i]

2θ	diffraction angle
^{t}Am	*tert.*-amyl
ax.	Axial
^{i}Bu	isobutyl
^{n}Bu	n-butyl
^{s}Bu	*sec.*-butyl
^{t}Bu	*tert.*-butyl
CL	chelating ligand
COSY	correlation spectroscopy
daa	diacetone alcoholate
edbp	2,2'-ethylenebis(4,6-di-*tert.*-butylphenolate)
en	ethylenediamine
Et	ethyl
Et_2acac	3,5-heptandionate
eq.	equatorial
equiv.	equivalent(s)
EXSY	exchange spectrsocopy
F	structure factor
fac	facial
GOF	goodness of fit
HMBC	heteronuclear multiple-bond correlation
HSQC	heteronuclear single quantum correlation
I	intensity
L	ligand
λ	wavelength
μ	absorption coefficient
Me	methyl
mer	meridional

[i] For abbreviations of reagents used in this work compare chapter 5.1 / Table 5-1.

MOCVD	metal-organic chemical vapor deposition
NMR	nuclear magnetic resonance
OAc	acetate
Ph	phenyl
^{i}Pr	isopropyl
^{n}Pr	n-propyl
q	scattering vector
S_N	nucleophilic substitution
thd	2,2,6,6-tetramethyl-3,5-heptandionate
tmp	2,2,6,6-tetramethylpiperidinate
XRD	X-ray diffraction
Z	number of formula units per unit cell

NMR Abbreviations

δ	chemical shift
s	singlet
d	doublet
t	triplet
quart	quartet
quint	quintet
sept	septet
m	multiplet
br	broad

Table of Contents

1 Introduction

New materials are an important topic in numerous fields of science and technology and play a key role in various applications from scientific to everyday use. The continuous demand for materials with improved or even new properties is a constant driving force for the development of new materials which have always been and are still one of the main driving forces of civilization. Since the beginning of mankind many significant steps in development were accompanied by the discovery of new materials and entire eras were named after them (*e.g.* Stone Age, Bronze Age,…). Today's rapid scientific and technological developments have exponentially raised the demand for novel materials but concomitantly also the rate of inventions in this field. Besides the quest for new and improved materials also the investigation of materials synthesis is of great interest in science and technology, since the increasing demand for high-tech materials requires easy, fast, and cheap production methods.

From a chemical point of view, materials are classically categorized into two groups, namely inorganic and organic materials, both classes reaching from natural to synthetic ones. In most cases, members of either group bear properties typical for the corresponding group – *e.g.* hardness, brittleness, and high density for inorganic materials or softness, flexibility, and low density for organic materials – although it is clear that there are numerous exceptions in both cases. Besides – or better in-between – these historically classified groups the field of inorganic-organic hybrid materials emerges. Although examples for such hybrids are known for thousands of years, *e.g.* the famous "Maya Blue"[1], this category of materials is a relatively young field in science. Starting in the late 1970's, this class of materials experienced a tremendous boost of interest by development of soft inorganic chemistry processes ("*chimie douce*"). Within these, the sol-gel process represents one of the most convenient and versatile approaches to inorganic materials, and hybrid materials derived thereof [2-4].

For an efficient and deliberate synthesis of new materials with defined and tunable properties, a comprehensive understanding of all steps and processes, from the starting materials to the final product, is essential. Therefore the investigation of precursors for material synthesis is of great interest to gain more information how structural and functional properties of the starting material do influence the corresponding properties of the final material, and whether and how these are influenced by each reaction step.

1.1 Sol-Gel Chemistry

Sol-gel processing is a relatively new method to synthesize oxidic materials by gelation instead of precipitation or crystallization. During this process, a molecular precursor reacts *via* progressive polycondensation steps to give a sol, which after gelation and removal of the solvent gives the final product [2, 4].

In this context, a sol describes a stable dispersion of colloidal crystalline or amorphous particles or polymers in a continuous liquid phase. The gel is a continuous, porous, and three-dimensional network of a solid phase supporting a continuous liquid phase. These networks can either be "colloidal" – if build from agglomerated dense particles – or "polymeric" – if the gel has a polymeric substructure. In both cases, the subunits can be connected either by covalent bonds, van der Waals interactions, or hydrogen bonds.

Gelation, *i.e.* the sol-gel transition, is characterized by a continuous increase of the viscosity until the gelation point, where a sudden and strong increase of the viscosity indicates the formation of a continuous 3D network. This means, that a continuous network through the whole sample is formed, but smaller clusters and aggregates still exist in the liquid phase. During gelation, the overall volume remains constant and the liquid is entrapped within the gel network. Bond formation does not stop at the gelation point since the liquid phase still can be seen as sol and smaller clusters are capable to aggregate with each other or to connect to the continuous network. This process is named aging and may have an important influence on the gels properties. Other processes involved in the aging are further condensation, dissolution or phase transitions.

Drying and evaporation of the solvent from the pores of a gel causes shrinkage and concomitant increase of the surface tension, resulting in a collapse of the pore walls and breakdown of the 3D network, giving powders as products, named xerogels. This breakdown of the network can be overcome by the method of supercritical drying (mostly with supercritical CO_2), where the liquid-gas interface is avoided and therefore surface tensions are avoided, resulting in monolithic porous products, also called aerogels. Alternatively, the sol can directly be processed to obtain products like films or fibers (Figure 1-1).

There are two classes of precursors for sol-gel materials, *viz.* inorganic and metal-organic. The former are sodium silicates ("Na_2SiO_3" or "water glass") for silica gels or metal salts for other metal oxide gels, whereas the latter in both cases are (transition) metal[ii] alkoxides. The differences for the precursors of non-silica based gels will be discussed below (compare chapter 1.2), but for silica based materials the main differences are as follows [5]:

- For silicon alkoxides, addition of water initiates gelation by generation of ≡Si-OH from ≡Si-OR groups, whereas for water glass based systems gelation is initiated by pH changes, generating ≡Si-OH from ≡Si-O^- groups.
- Silicon alkoxides are processed either neat or in an organic solvent (mostly an alcohol), whereas water-glass based systems are always reacted in water.
- Alkoxide-based systems are better controllable with respect to properties and morphology of the final materials due to a higher number of parameters which can be influenced, concomitantly making the system more complex.

[ii] In the following only "metal alkoxides" will be used for transition as well as for main group metal alkoxides, except silcon alkoxides.

Both types of precursors have in common that the processing conditions can be divided into two regimes: reactions under acidic or basic conditions, respectively. For each regime different reaction mechanisms dominate, leading to different materials morphologies and properties.

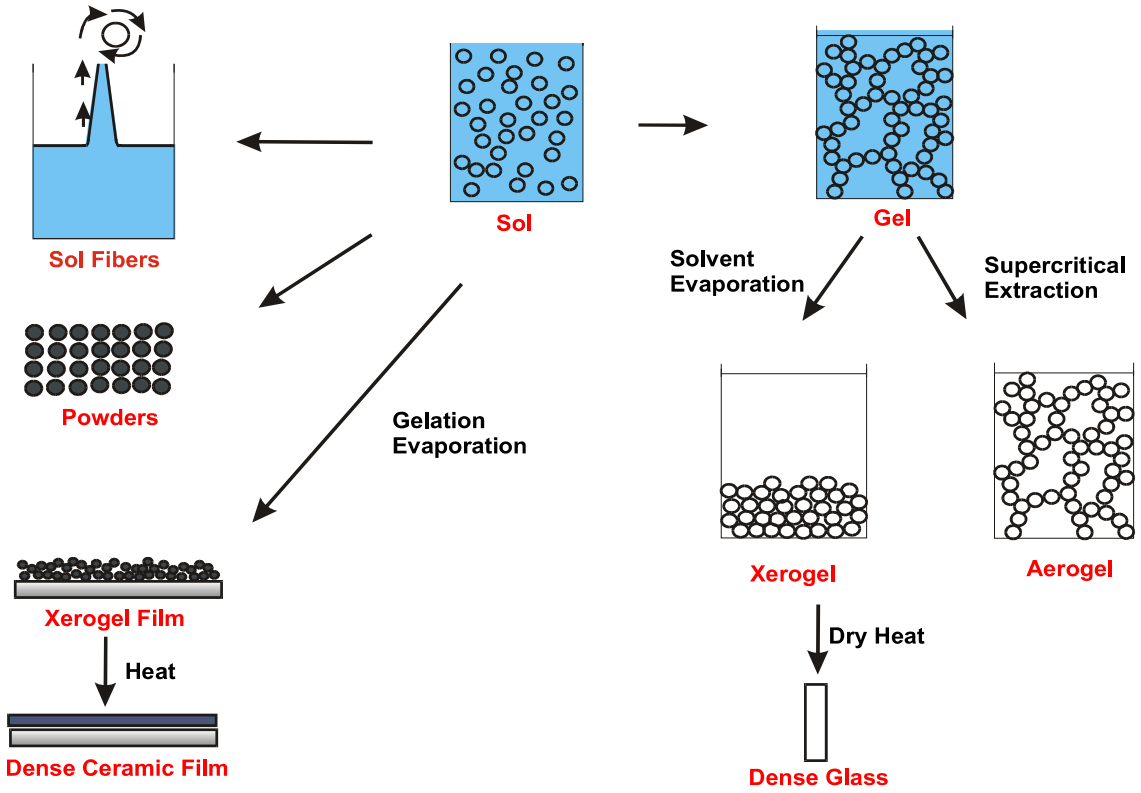

Figure 1-1 Sol-gel processing options.

1.2 Metal Alkoxides

As mentioned before, inorganic as well as metal organic precursors can be applied also for the preparation of non-silicate metal oxide gels by the sol-gel technique. As for silica gels, reactions with metal salts are mostly performed in water as solvent, leading to different aquo ($M–OH_2$), hydroxo (M–OH), and oxo (M=O or M–O–M) species, depending on the pH regime. Furthermore, for metal salts also the influence of the counterions X has to be taken into account. Depending on the stability of the M–X bond, the salt either can dissociate into discrete ions or the counterion can remain coordinated to the metal center. Especially when a strong metal-counterion interaction persists, this may have significant influences such as blocking of coordination sites or direction of reaction pathways (*trans* effect), and the counterions might remain in the final material. This all greatly influences also the final materials morphology and properties. As a matter of fact, these influences of the counterion are irrelevant for metal alkoxides.

Compared to silicon alkoxides, some important differences have to be taken into account for metal alkoxides [2, 6]:

- Due to their lower electronegativity and the resulting higher Lewis acidity, metal alkoxides are more reactive towards nucleophilic attack. This results in higher reaction rates in hydrolysis reactions.
- Most metals have more than one stable coordination number and tend to expand their coordination number when coordinatively unsaturated.

As a result, metal alkoxides tend to spontaneously form precipitates instead of homogeneous gels upon contact with water. Whereas hydrolysis and condensation of silicon alkoxides usually are catalyzed by an acid or a base, the reactivity of metal alkoxides often has to be lowered by chemical modifications. The reactivity towards hydrolysis therefore depends on the type of metal, *viz.* its electronegativity.

Additional to the electronic influences on the reactivity also the degree of oligomerization and solvation has an important influence on the reactivity. Metal alkoxides tend to saturate their coordination sphere by formation of alkoxo bridges or addition of donor molecules, *e.g.* solvent molecules (alcohols,…). (Figure 1-2)

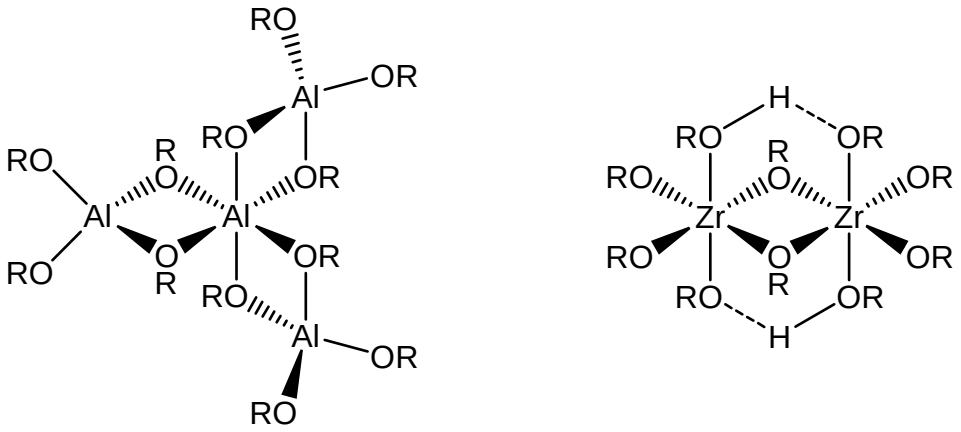

Figure 1-2 Examples for coordination expansion of metal alkoxides: oligomerization ($[Al(OR)_3]_4$, OR = O^iPr) [7, 8] (*left)*; oligomerization and addition of solvent molecules ($[Zr(OR)_4(ROH)]_2$, OR = O^iPr) [9] (*right*).

This is caused by the fact, that the usual coordination number of many metals is higher than their valency and therefore compensation of the charge is not sufficient to saturate the coordination sphere. The degree of oligomerization mainly depends on two factors:

- The tendency to oligomerize increases with the covalent radius of the metal.
- Larger alkoxo groups decrease the tendency to oligomerize due to increasing steric hindrance.

As mentioned, besides formation of alkoxo bridges, coordinative saturation can as well be reached by the coordination of donor molecules (Lewis bases), such as alcohols or amines. This coordination in general lowers the degree of oligomerization and therefore enhances reactivity towards hydrolysis or, more generally spoken, nucleophilic attack. As an example,

hydrolysis of $Zr(O^nPr)_4$ dissolved in ^nPrOH results in precipitates whereas homogeneous gels can be obtained from cyclohexane [10]. These observations show that alkoxo bridges are more stable towards hydrolysis than coordinated solvent molecules.

The formation of a sol and subsequently a gel from metal alkoxides mainly proceeds in a quite analogous way as for silicon alkoxides. In a first hydrolysis step, alkoxo groups at the metal center are replaced by hydroxo groups by nucleophilic substitution (S_N). This involves nucleophilic addition of a water molecule to the metal center followed by a proton transfer to an alkoxo ligand and subsequent elimination of an alcohol molecule (Scheme 1-1).

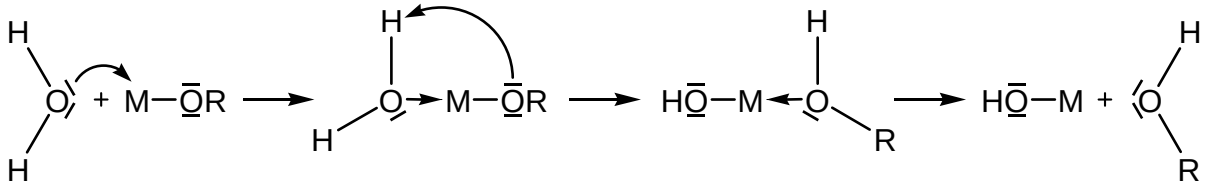

Scheme 1-1

Condensation reactions take place after hydrolysis, resulting in connection of the individual metal centers. Oxo bridges are formed by the attack of a hydroxo group at another metal center following a similar addition-elimination pathway as for the hydrolysis reaction. The released molecule can be either a water (oxolation) or an alcohol (alcoxolation) molecule (Scheme 1-2).

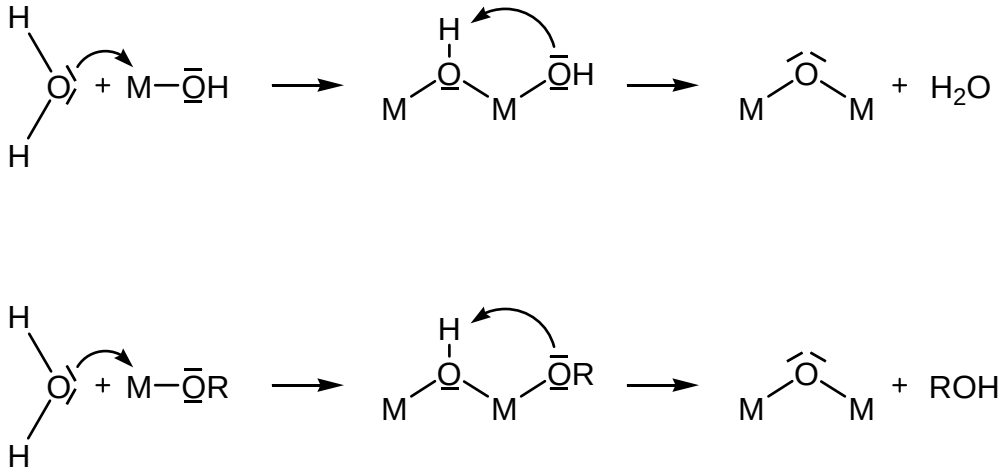

Scheme 1-2

For coordinatively unsaturated metal centers, *viz.* metal centers with coordinated solvent molecules – mostly water (X = H) or an alcohol (X = R) – condensation can occur under formation of hydroxo-bridges (olation) (Scheme 1-3)

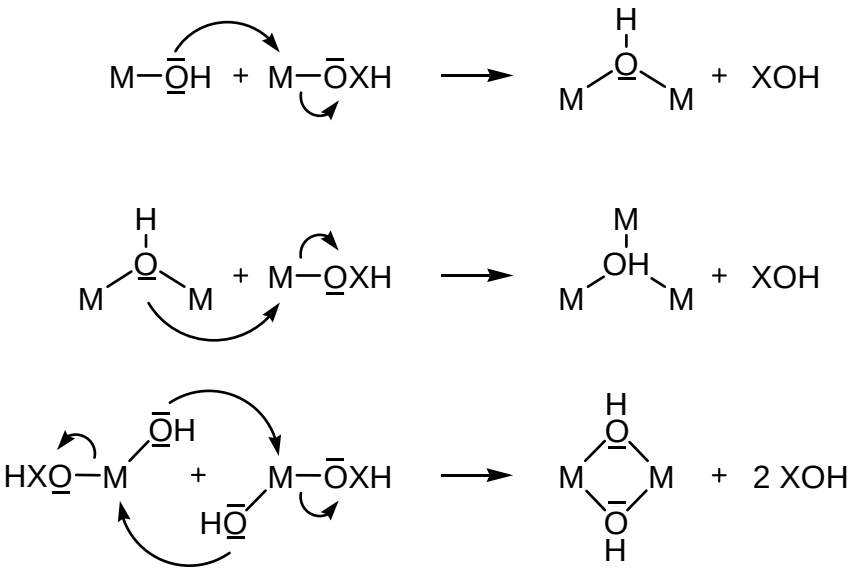

Scheme 1-3

As mentioned before, metal alkoxides tend to be too reactive upon hydrolysis and condensation and therefore yield precipitates instead of gels. To overcome this problem the reactivity towards nucelophilic attack has to be lowered. One of the most widely used methods is the replacement of alkoxo ligands by hydrolytically more stable ligands. Especially multidentate ligands are beneficial, because additionally to the strong coordination to the metal center caused by the chelate effect, the bi- or multidentate binding mode blocks free coordination sites at the metal center. Mostly anionic ligands, formed from compounds having an acidic proton which easily can be transferred to an alkoxo ligand, are used for this purpose. This leaves the overall charge of the complex unchanged but increases the coordination number at the metal center. These chelating ligands (CL) are introduced to the precursor in a simple substitution reaction (Scheme 1-4).

Scheme 1-4

The introduction of such ligands has additionally important chemical and structural effects on the precursors as well as on the final material [6]:

- The reduced number of hydrolyzable alkoxo groups lowers the reactivity and therefore favors the formation of gels instead of crystalline precipitates.
- Due to blocking of reactive sites, the degree of crosslinking in the inorganic network is decreased and therefore again the formation of gels compared to crystalline precipitates is favored.
- The reactivity of the remaining alkoxo groups may be influenced by electronic effects of the introduced ligand.

- Bidentate ligands my influence the stereochemistry of the nucleophilic attack either by electronic effects (alkoxo groups *trans* or *cis* to the chelating ligand) or by steric shielding.

All these effects have to be taken into account when metal alkoxides are modified but also can be used intentionally, for example to influence the final microstructure of the desired product. Additionally, modification with organic ligands allows the introduction of additional functionalities, *e.g.* complexing groups for the coordination of further metal ions or polymerizable groups for the connection to organic polymers (compare chapter 1.3).

1.2.1 Aluminum Alkoxides

Aluminum alkoxides were first prepared in the 19th century [11] and extensively studied since the 1950's [12, 13]. Due to the high Lewis acidity of the aluminum center and the fact, that the charge (valency) of the metal center (3+) is lower than the preferred and stable coordination numbers of aluminum (4–6), aluminum alkoxides tend to oligomerize. The degree of oligomerization of aluminum alkoxides is mainly determined by the type of alkoxo group, *e.g.* its electronic and steric properties. Increasing steric demand causes a decrease in oligomerization. For example, aluminum tri-*tert.*-butoxide is dimeric $[Al(O^tBu)_3]_2$, whereas aluminum tri-*sec.*-butoxide trimeric $[Al(O^sBu)_3]_3$, aluminum tri-isopropoxide tetrameric $[Al(O^iPr)_3]_4$, and aluminum tri-ethoxide oligomeric $[Al(OEt)_3]_n$, all at room temperature in toluene solution or in the solid state or, in the case of $[Al(O^sBu)_3]_3$, as neat liquid. The type of oligomeric structure for a given degree of oligomerization should lead to a preferred coordination environment for the metal center(s), according to Bradley's structural theory of metal alkoxides [14].

For dimeric $[Al(O^tBu)_3]_2$ a structure of two edge sharing tetrahedra (Figure 1-3) was predicted [12] and also verified by single crystal XRD [15] and NMR spectroscopy, showing the same structure in solid state and solution. The ^1H and ^{13}C NMR spectra show to sets of signals with relative intensities of 1:2 [8, 16], indicating the different chemical nature of the bridging and terminal alkoxo groups, whereupon only one broad signal for tetracoordinated aluminum can be observed in the ^{27}Al NMR spectrum [17]. This structure is also consistent with Bradley's structural theory on metal alkoxides [14, 18].

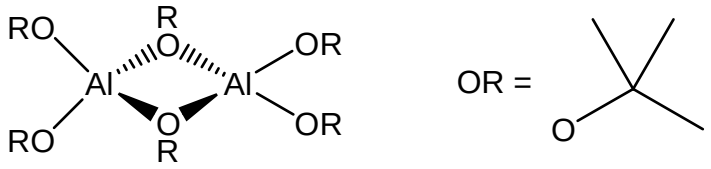

Figure 1-3 Schematic representation of $[Al(O^tBu)_3]_2$.

Replacement of the *tert.*-butoxo group by *sec.*-butoxide leads to trimeric $[Al(O^sBu)_3]_3$ [12, 17]. In this structure (Figure 1-4), a linear trimer with a central pentacoordinated and two terminal tetracoordinated aluminum centers is formed. This is of particular interest since

aluminum usually prefers tetra- or hexacoordination, which would be possible in a cyclic trimeric form (Figure 1-5), which also was suggested for trimeric $Al(O^iPr)_3$ (*vide infra*) [19]. For the linear trimer a higher average coordination number is obtained due to the pentacoordinated central atom.

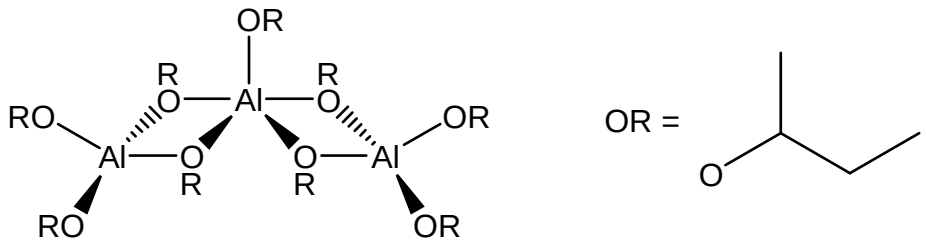

Figure 1-4 Schematic representation of $[Al(O^sBu)_3]_3$.

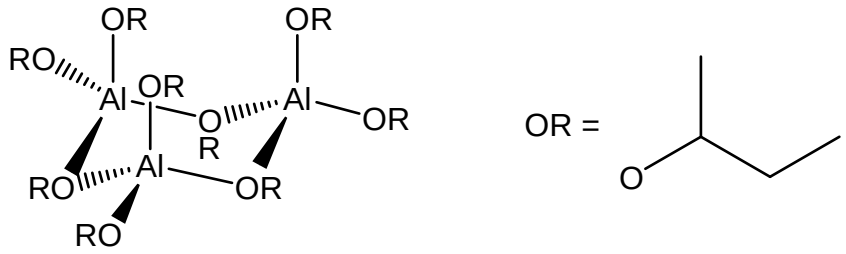

Figure 1-5 Schematic representation of a possible cyclic trimer of $[Al(O^sBu)_3]_3$.

For aluminum tri-isopropoxide the situation is more complex and the structure has been discussed for some time. Early publications predicted a tetrameric, cyclic structure (Figure 1-6) [20].

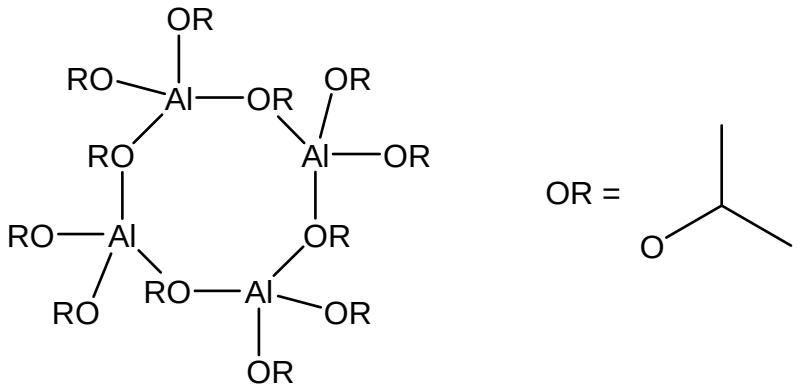

Figure 1-6 Schematic representation of a possible cyclic tetramer of $[Al(O^iPr)_3]_4$.

In contrast, Bradley [14, 21] suggested that an alkoxide undergoes the minimum degree of polymerization consistent with the maximum coordination number of the metal. For trivalent aluminum this would mean a dimer for tetracoordinated aluminum centers and an octamer for hexacoordinated aluminum centers. A tetrameric structure could be explained by a combination of tetra- and hexacoordination (Figure 1-7). As for the supposed cyclic structure, this structure is tetrameric as well, but the structure shown in Figure 1-7 has a

higher average coordination number per aluminum atom, due to the octahedrally coordinated central aluminum atom (3 x 4 + 6 = 18 → 4.5 per aluminum atom compared to 4 x 4 = 16 → 4.0 per aluminum atom). This structure was proven to be the correct one for $[Al(O^iPr)_3]_4$ in solid state and solution at room temperature [7, 8]. ^1H NMR spectroscopy shows two signals for the methine protons of the isopropoxo groups with relative intensities of 1:1 as expected, assigned to the bridging and terminal groups. The methyl protons of the isopropoxo groups split into three doublets with relative intensities of 1:1:2, resulting from a splitting of the signals for the bridging groups. This is explained by hindered rotation of the bridging isopropoxo groups and the resulting fixed orientation of the methyl groups [8]. ^{27}Al NMR confirms the structure, giving rise to signals for tetra- and hexacoordinated aluminum centers [17] in a 3:1 ratio [22].

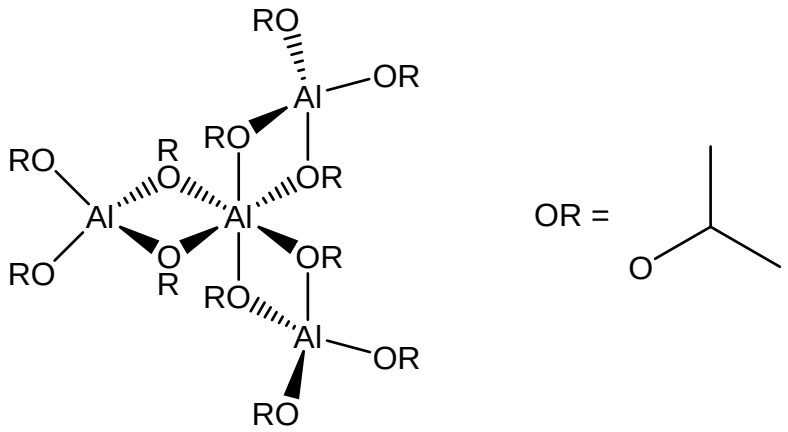

Figure 1-7 Schematic representation of $[Al(O^iPr)_3]_4$.

Solid aluminum isopropoxide is known to melt at about 140 °C and tends to give a super-cooled melt after cooling to room temperature, stable for several days, followed by slow recrystallization to give again $[Al(O^iPr)_3]_4$ [8, 23]. Molecular weight measurements showed that the melt has an average degree of association of about 2.8, suggesting mainly trimeric and partially dimeric species. For the trimeric structure a cyclic structure was also predicted (compare Figure 1-5) [8], but ^{27}Al NMR spectroscopy shows a signal for pentanuclear aluminum, indicating a structure analogous that of $[Al(O^sBu)_3]_3$ (compare Figure 1-4). Further investigations showed that the melt mainly consists of dimeric units at elevated temperatures, having a analogous structure to $[Al(O^tBu)_3]_2$ (compare Figure 1-3) [24]. It was confirmed that at room temperature the neat molten $Al(O^iPr)_3$ as well as solutions in toluene are mixtures of dimeric and trimeric species. In the vapor phase $Al(O^iPr)_3$ is dimeric as well [13] – monomeric $Al(O^iPr)_3$ is unknown.

The tetrameric structure analogous to the one shown in Figure 1-7 was also found for the aluminum alkoxides of benzyl alcohol and 4-chlorobenzyl alcohol in the solid state. Temperature dependent equilibria between tetra-, tri-, and dimeric species were observed also for these compounds, along with a concentration dependence of the degree of oligomerization in solution [25]. These results also indicate that branched primary alcohols tend to adopt this tetrameric structure.

Aluminum ethoxide forms oligomers $[Al(OEt)_3]_n$ with units lager than tetrameric (n > 4), proven by mass spectroscopy [26]. Linear structures according to Figure 1-8 were suggested [27].

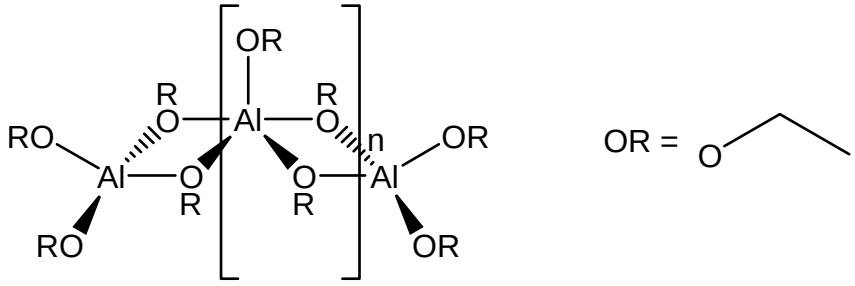

Figure 1-8 Schematic representation of $[Al(OEt)_3]_n$ (n > 4).

In contrast, aluminum 2,2,2-trichloroethoxide is dimeric in toluene solution with a structure analogous to $[Al(O^tBu)_3]_2$ (compare Figure 1-3). This is explained by the reduced nucleophilicity of the oxygen caused by the electron-withdrawing effect of the chlorine atoms [28].

The influence of the steric demand on the degree of oligomerization can be seen very well when comparing the alkoxides of different isomers of an alcohol. For the isomers of butanol, the *tert.*-butoxide gives dimeric $[Al(O^tBu)_3]_2$ (Figure 1-3), the *sec.*-butoxide trimeric $[Al(O^sBu)_3]_3$ (Figure 1-4) (*vide supra*), and the isobutoxide tetrameric $[Al(O^iBu)_3]_4$, structurally analogous to $[Al(O^iPr)_3]_4$ (compare Figure 1-7) [17]. This again confirms this structure to be the preferred one for aluminum alkoxides of branched primary alcohols. No reliable source was found for the structure of $Al(O^nBu)_3$. An analogous behavior can be observed for the alkoxides derived from different isomers of pentanol [13, 17].

It is also interesting to mention, that the complete exchange of O^iPr groups against O^tBu or O^tAm groups was first reported to be impossible and to yield only $[Al(\mu\text{-}O^iPr)(OR)_2]_2$ (OR = $^tBu/O^tAm$) [12, 13], indicating a stronger hindrance of the substitution of the bridging positions. Later it was shown that the complete exchange is not impossible but requires prolonged reaction times, also confirming a stronger hindrance for the bridging positions [16].

In general it can be said that in most cases the degree of oligomerization of aluminum alkoxides is not fixed, and equilibria between different species are often present. These equilibria show temperature dependence and in solution also concentration dependence, and depend on the type of solvent. Therefore, the given structures always have to be seen as "main" or "dominant" species but do not rule out the existence of minor proportions of other oligomers.

Aluminum alkoxides are a widely used starting material for metal alkoxide based sol-gel processes, especially $Al(O^sBu)_3$ and $Al(O^iPr)_3$. Beside their use in this solution-based materials preparation method they are also commonly used as precursors for MOCVD processes. Besides being used as starting materials for alumina-based materials, another

important field of application for aluminum alkoxides is their use as polymerization catalyst, especially for anionic ring-opening polymerizations of ε-caprolactones [29-31] or lactides [29, 32]. Mechanistic studies revealed a strong dependence of the reactivity on the degree of association [29, 30, 32] as well as on the presence of additional alcohol or diol molecules [31].

Another field of application of aluminum alkoxides is their catalytic activity in the Meerwein-Ponndorf-Verley reaction [33, 34]. In this reaction, aldehydes or ketones are reduced to alcohols by a hydride transfer from an alkoxo ligand, oxidizing it to a ketone itself. Again, a tremendous influence of the degree of oligomerization on the reactivity is observed [34].

Also relevant for the understanding of sol-gel processing is the field of higher condensed species like aluminum (hydr)oxoalkoxides, since they could be seen as partially hydrolyzed aluminum alkoxides and therefore can provide an insight into processes and intermediates occurring during hydrolysis/condensation processes in sol-gel reactions. Unfortunately, only few examples of aluminum (hydr)oxoalkoxides were isolated and structurally characterized [35-37]. The different compounds show versatile structural behavior, presenting metal-oxo-cores from Al_4 to Al_{11}. In the context of this work, the complex $Al_5(\mu_5\text{-}O)(\mu\text{-}O^iBu)_8(O^iBu)_8$ [36] is of particular interest, since it clearly has a structural relation to the structure of "yttrium isopropoxide" $Y_5(\mu_5\text{-}O)(\mu_3\text{-}O^iPr)_4(\mu\text{-}O^iPr)_4(O^iPr)_5$ [38] (compare chapter 1.2.2).

1.2.2 Yttrium Alkoxides

Much less is known about the structural and chemical behavior of yttrium alkoxides. For yttrium isopropoxide, the highly oxophilic character of yttrium and its tendency to attain the preferred coordination number of six or higher leads to deoxygenation of an isopropoxo ligand during preparation from neat yttrium and isopropanol [38]. Therefore, yttrium isopropoxide cannot be isolated as "$[Y(O^iPr)_3]_n$" but as $Y_5(\mu_5\text{-}O)(\mu_3\text{-}O^iPr)_4(\mu\text{-}O^iPr)_4(O^iPr)_5$ (Figure 1-9).

The only homoleptic yttrium alkoxides (without oxo or hydroxo groups) reported so far are $[Y(\mu,\kappa^2\text{-}OR)_2(OR)]_{10}$ (OR = OC_2H_4OMe) [39] (Figure 1-10) and $[Y_4(\mu_3,\kappa^2\text{-}OR)_3(\mu,\kappa^2\text{-}OR)_2(\mu,\kappa^1\text{-}OR)_3(OR)_4]_2$ (OR = $OC_2H_4O^iPr$) [40] (Figure 1-11). The former structure shows heptacoordinated yttrium centers whereas in the latter structure, the yttrium atoms are hexa-, hepta-, and octacoordinated, showing the capability of yttrium to attain higher coordination numbers than six, in contrast to aluminum. In both structures, the yttrium centers are stabilized by donation of the ether oxygens, leading to saturation of the coordination sphere.

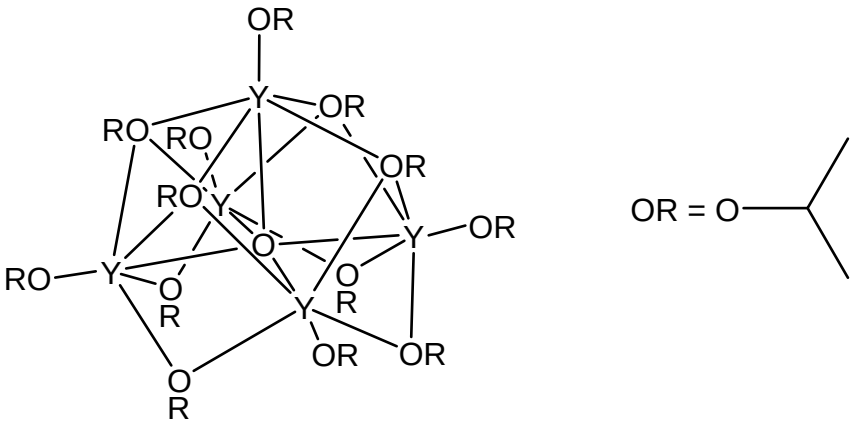

Figure 1-9 Schematic representation of $Y_5(\mu_5\text{-O})(\mu_3\text{-O}^i\text{Pr})_4(\mu\text{-O}^i\text{Pr})_4(\text{O}^i\text{Pr})_5$.

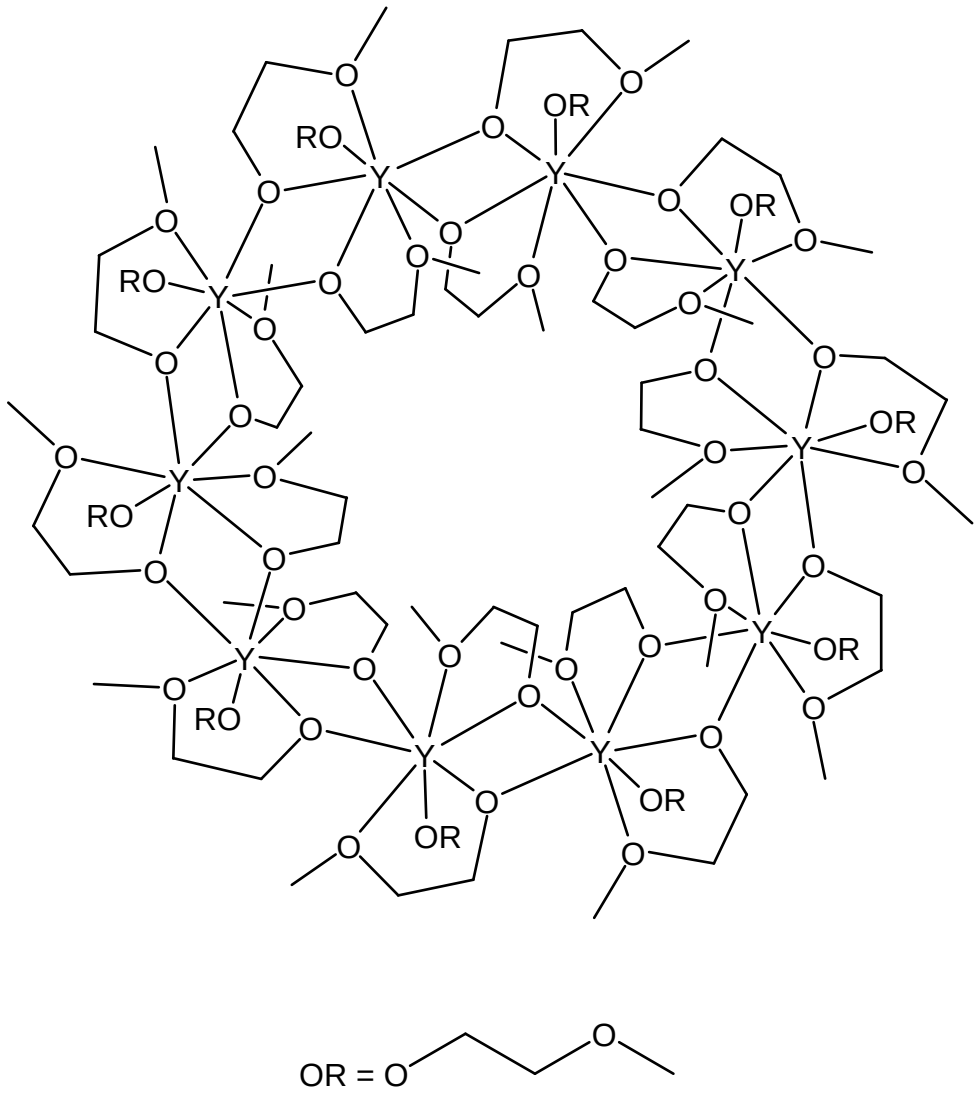

Figure 1-10 Schematic representation of $[Y(\mu,\kappa^2\text{-OR})_2(OR)]_{10}$ (OR = OC_2H_4OMe).

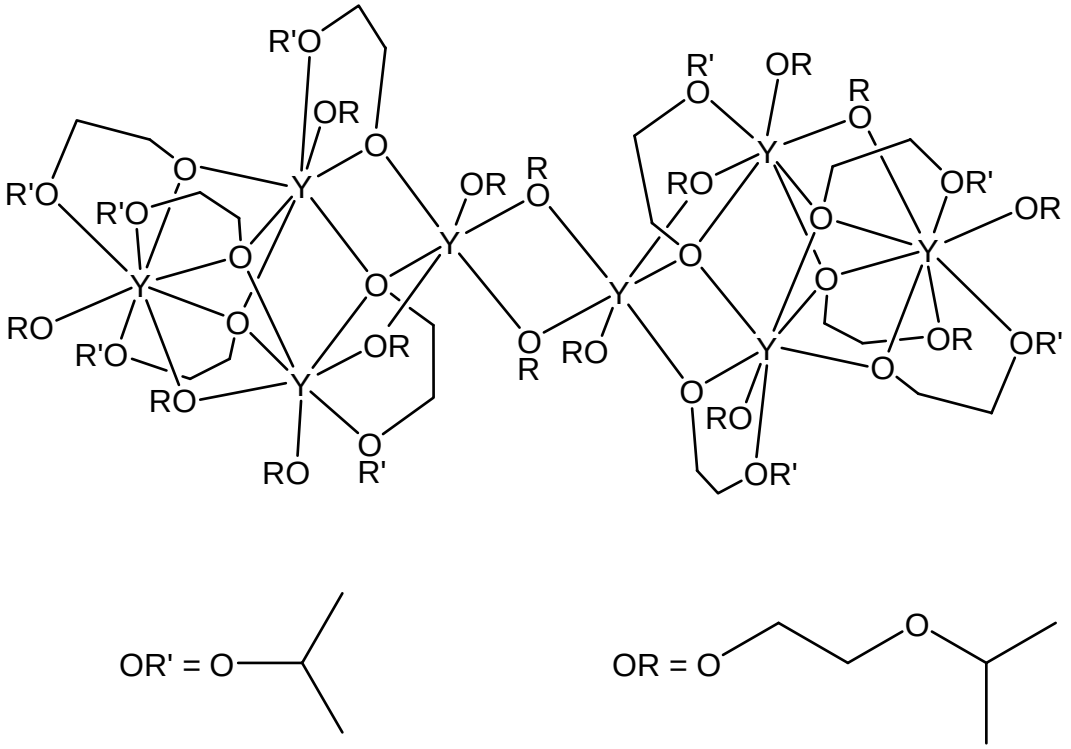

Figure 1-11 Schematic representation of $[Y_4(\mu_3,\kappa^2\text{-OR})_3(\mu,\kappa^2\text{-OR})_2(\mu,\kappa^1\text{-OR})_3(OR)_4]_2$ (OR = $OC_2H_4O^iPr$).

Another example for an yttrium alkoxide without oxo or hydroxo groups is $Y_3(\mu_3\text{-}O^tBu)_2(\mu\text{-}O^tBu)_3(O^tBu)_4(^tBuOH)_2$ [41], stabilized by the coordination of two alcohol molecules. $[Y_8(\mu_6\text{-O})(\mu_4\text{-O})_4(\mu_3\text{-O})(\mu_3\text{-}O^tBu)_2(\mu\text{-}O^tBu)_6(O^tBu)_4]_n$ [42], an yttrium oxo-alkoxide, was obtained upon removal of the stabilizing solvent molecules of the former compound.

The use of the sterically hindered alcohols with a second donor functionality like 3-ethoxymethyl-2,4-dimethyl-3-pentanol leads to a mononuclear complex with a suggested distorted octahedral coordination environment (Figure 1-12).

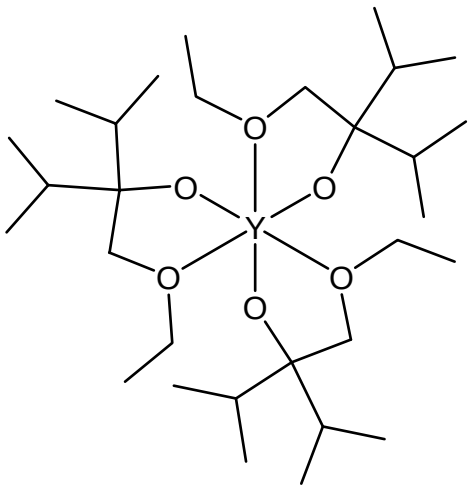

Figure 1-12 Schematic representation of $Y(OC(^iPr)_2CH_2OEt)_3$.

This again shows the influence of steric demand and saturation of coordination sites by additional donor functionalities on the degree of oligomerization [43].

Analogous to aluminum alkoxides, yttrium alkoxides are used as precursors for oxidic materials by sol-gel processing [44, 45] or MOCVD [45] as well as polymerization catalysts [46-48].

1.2.3 Modification of Metal Alkoxides

1.2.3.1 Modification of Aluminum Alkoxides

As mentioned before, aluminum 2,2,2-trichloroethoxide is dimeric in contrast to oligomeric $[Al(OEt)_3]_n$ as a result of the electron withdrawing effect of the chlorine atoms. As a consequence, the aluminum center is even more Lewis acidic, resulting in a higher tendency to coordinate donor molecules, *e.g.* pyridine, causing a further breakdown of the aggregates, giving monomeric species [28].

Results for the modification of $Al(O^iPr)_3$ with pyridine as donor ligand have also shown that the degree of oligomerization of the starting alkoxide has a strong influence on the reactivity. Whereas tetrameric $[Al(O^iPr)_3]_4$ is insoluble in pyridine, freshly distilled trimeric $[Al(O^iPr)_3]_3$ is well soluble, what is traced back to stabilization by complexation of pyridine [19, 49]. Figure 1-13 schematically represents the stabilization of an $Al(OR)_3$ unit (*e.g.* $Al(O^iPr)_3$) by an electron donating ligand D (*e.g.* pyridine).

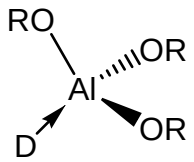

Figure 1-13 Schematic representation of the stabilization of an aluminum alkoxide $Al(OR)_3$ by a donor-ligand D.

These two examples already show that there is a bidirectional influence of the degree of oligomerization on the tendency towards coordination of donor molecules and *vice versa* a strong influence of the donor molecules on the degree of oligomerization. This tendency to affect the degree of oligomerization by coordination of donor molecules or (partial) replacement of alkoxo groups by other ligands is an important tool to control the reactivity of the alkoxides and has to be taken into account upon modification of alkoxides for this purpose. On the other hand, the influence of the alkoxo group on the degree of oligomerization and the structure remains upon modification and therefore the properties of modified metal alkoxides are influenced by both, the alkoxo group and the ligand used for substitution.

Examples for ligands commonly used for the modification of aluminum alkoxides are organic acids, β-diketones, amines, or aminoalcohols. Among these, the modification with acetylacetone (acac-H) and analogous β-diketones is studied best.

The modification of aluminum alkoxides and siloxides with acac-H, 3,5-heptandione (Et_2acac-H) and ethyl acetoacetate (etac-H) clearly shows that the dependence of the degree of oligomerization on the type and size of alkoxide after modification with a chelating ligand is retained. For the modification of $Al(O^iPr)_3$ with acac-H, dimeric $Al_2(\mu\text{-}O^iPr)_2(O^iPr)_2(acac)_2$ is initially formed, which upon storage gives trimeric $Al_3(\mu\text{-}O^iPr)_4(O^iPr)_2(acac)_3$ (Figure 1-14 *left*). In contrast, for the sterically more demanding $OSiMe_3$ siloxo group dimeric $Al_2(\mu\text{-}OSiMe_3)_2(OSiMe_3)_2(acac)_2$ is stable (Figure 1-14 *center*), and for the even bulkier $OSiPh_3$ group even monomeric $Al(OSiPh_3)_2(acac)$ could be isolated (Figure 1-14 *right*).

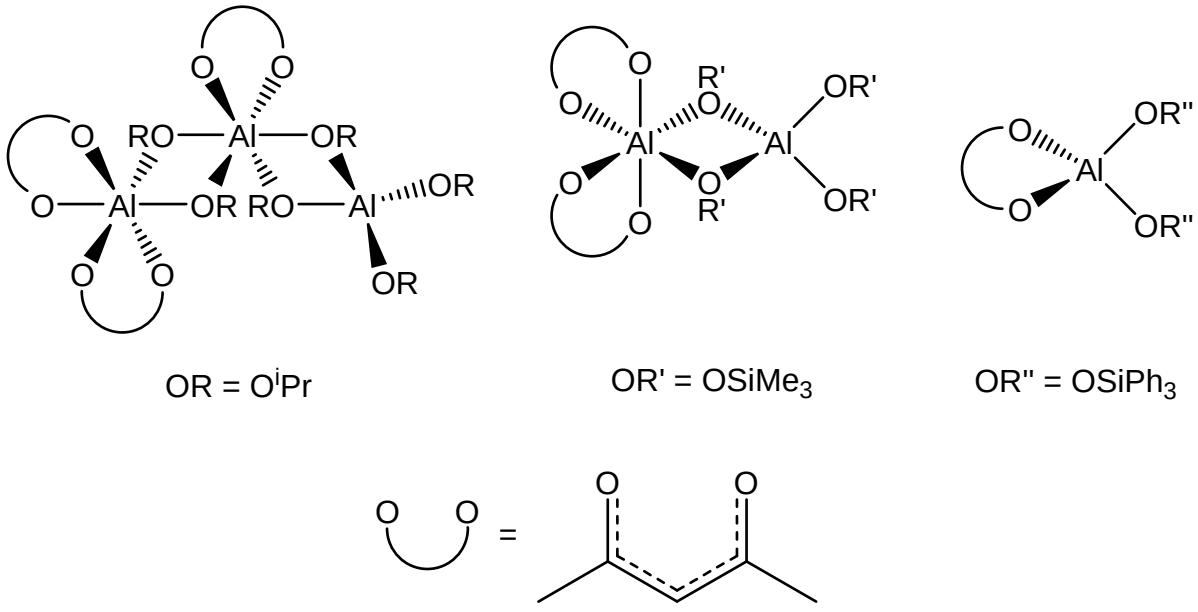

Figure 1-14 Schematic representation of $Al_3(\mu\text{-}O^iPr)_4(O^iPr)_2(acac)_3$ (*left*), $Al_2(\mu\text{-}OSiMe_3)_2(OSiMe_3)_2(acac)_2$ (*center*), and $Al(OSiPh_3)_2(acac)$ (*right*).

The use of OMe, *e.g.* a much smaller alkoxo group, leads to oligomeric, insoluble species. $Al_2(\mu\text{-}OSiMe_3)_2(OSiMe_3)_2(acac)_2$ shows a very interesting structure, characteristic for many modified aluminum alkoxides with one octahedral aluminum center coordinated by two acac ligands and two μ-$OSiMe_3$ groups and one tetrahedral aluminum center coordinated by two μ-$OSiMe_3$ and two terminal $OSiMe_3$ [50, 51]. The same structural motif is also found for $Al(O^iPr)_3$ modified with N-phenylsalicylidene imine [52, 53].

Modification of $Al(O^iPr)_3$ with two equiv. Et_2acac-H per aluminum atom gave dimeric $[Al(\mu\text{-}O^iPr)(Et_2acac)_2]_2$ (Figure 1-15) [50, 54]. This structure is of particular interest since other products of the general type $[Al(OR)(\beta\text{-diketonate})_2]_n$ were reported to be unstable and to give disproportionation products $Al_2(\mu\text{-}OR)_2(OR)_2(\beta\text{-diketonate})_2$ and $Al(\beta\text{-diketonate})_3$ [50]. Interestingly, in own experiments two compounds showing a dimeric structure with an Al/β-diketonate ratio of 1:2 wer obtained, *viz.* $[Al(\mu\text{-}O^iPr)(d^iprm)_2]_2$ and $[Al(\mu\text{-}O^sBu)(acac)_2]_2$

(compare chapter 3.2.3) [55]. These examples again show the influence of the alkoxo group as well as the ligand on the stability of the complexes formed.

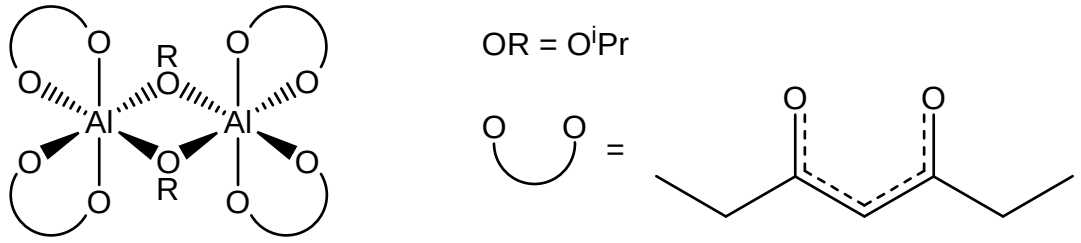

Figure 1-15 Schematic representation of [Al(μ-O^{i}Pr)(Et$_2$acac)]$_2$ (only one possible isomer shown).

The Al(β-diketonate)$_3$ compounds formed in the disproportionation reaction described above are octahedrally coordinated mononuclear complexes (Figure 1-16). This is the typical coordination geometry for aluminum centers coordinated with three chelating ligands, as reported for various ligands. These complexes and Al(acac)$_3$ in particular can be obtained by various preparation routes and were extensively studied. They are also the products for the substitution of all alkoxo groups from an aluminum alkoxide upon reaction with three equiv. of chelating ligand.

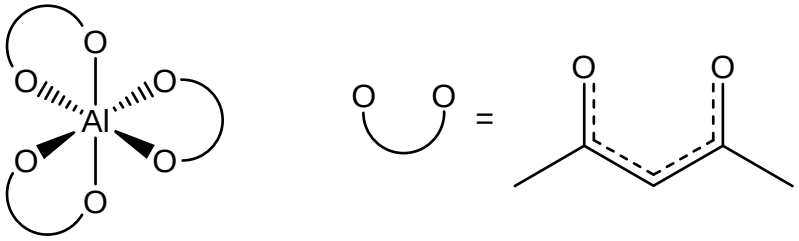

Figure 1-16 Schematic representation of Al(acac)$_3$.

Studies one the modification of Al(O^{s}Bu)$_3$ with β-diketones and β-ketoesteres show a dependence of the degree of substitution on the type of ligand. Furthermore, the β-diketonate and β-ketoesterate ligands show a different hydrolytic stability, with β-diketonates exhibiting a higher hydrolytic stability compared to β-ketoesters [56].

For the modification of Al(O^{i}Pr)$_3$ with semicarbazones [57, 58] or thiosemicarbazones [59] products with a substitution degree of 1:1, 1:2, and 1:3 were obtained. The 1:1 and 1:2 products were dimeric according to molecular weight determinations, whereas the 1:3 products were monomeric. In contrast to the analogous acac derivatives (*vide supra*), the 1:1 complex was suggested to be a dimer with two pentacoordinated aluminum centers, *viz.* [Al(μ-OiPr)(O^{i}Pr)(CL)]$_2$ (CL = semicarbazonate, thiosemicarbazonate) (Figure 1-17) [57-59]. The correctness of this proposed structure is in doubt since no analytical method capable of distinguishing between this structure and the well proven asymmetric dinuclear structure (compare Figure 1-14 *center*) was applied. The 1:2 products were reported to have an analogous structure as the β-diketonate derivatives (compare Figure 1-15), and the 1:3

complexes to be octahedral complexes. For the 1:1 and 1:2 products with semicarbazones, substitution reactions with *tert.*-butanol were performed, showing that the isopropoxo groups can be replaced by *tert.*-butoxo groups [57, 58]. This is of particular interest since no stable dimers were obtained for other ligands for the O^{t}Bu derivatives (compare chapters 3.1.1 and 3.2).

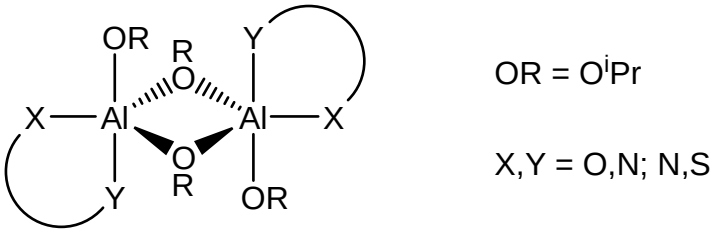

Figure 1-17 Schematic representation of postulated [Al(μ-OiPr)(O^{i}Pr)(CL)]$_2$ (CL = semicarbazonate, thiosemicarbazonate) (only one possible isomer shown).

Modification of aluminum tri-2-chlorophenoxide with acac-H and different β-ketoesters yielded also products of the general formulas Al(OR)$_2$(CL) and Al(CL)$_3$ (OR = 2-chlorophenoxide, CL = acac, β-ketoesterate), but molecular weight determination and IR spectroscopy revealed that in this case the monosubstituted products Al(OR)$_2$(CL) are monomeric (compare Figure 1-14 *right*), again showing the influence of the alkoxo group on the degree of oligomerization [60].

The complexes Al$_2$(μ-O^{i}Pr)$_2$(O^{i}Pr)$_2$(CL)$_2$ (CL = acac, etac) (*vide supra*) [50] were used as starting materials for the preparation of mixed ligand complexes. The starting complexes were reacted with different compounds L-H$_2$, *viz.* glycols [61] or thioalcohols [62], and L-H, *viz.* 8-hydroxyquinoline [63] or 2-pyridylmethanol [64]. The derivatives of the dianionic ligands (*viz.* glycolates and thioalcoholates) gave either dimers of the type (CL)$_2$Al(μ-O^{i}Pr)$_2$AlL or tetramers of the type (CL)$_2$Al(μ-O^{i}Pr)$_2$Al(μ-L)$_2$Al(μ-O^{i}Pr)$_2$Al(CL)$_2$ (Figure 1-18) [61, 62].

For 8-hydroxyquinoline and 2-pyridylmethanol, *viz.* monoanionic ligands, derivatives (CL)$_2$Al(μ-O^{i}Pr)$_2$Al(OiPr)L or (CL)$_2$Al(μ-O^{i}Pr)$_2$AlL$_2$ were alternatively obtained, depending on the molar ratio applied (Figure 1-19) [63, 64]. In all products, the initial dimeric structure was retained and no trimerization as observed for Al$_2$(μ-O^{i}Pr)$_2$(O^{i}Pr)$_2$(acac)$_2$ (giving Al$_3$(μ-O^{i}Pr)$_4$(O^{i}Pr)$_2$(acac)$_3$ upon aging in solution [50]) was reported.

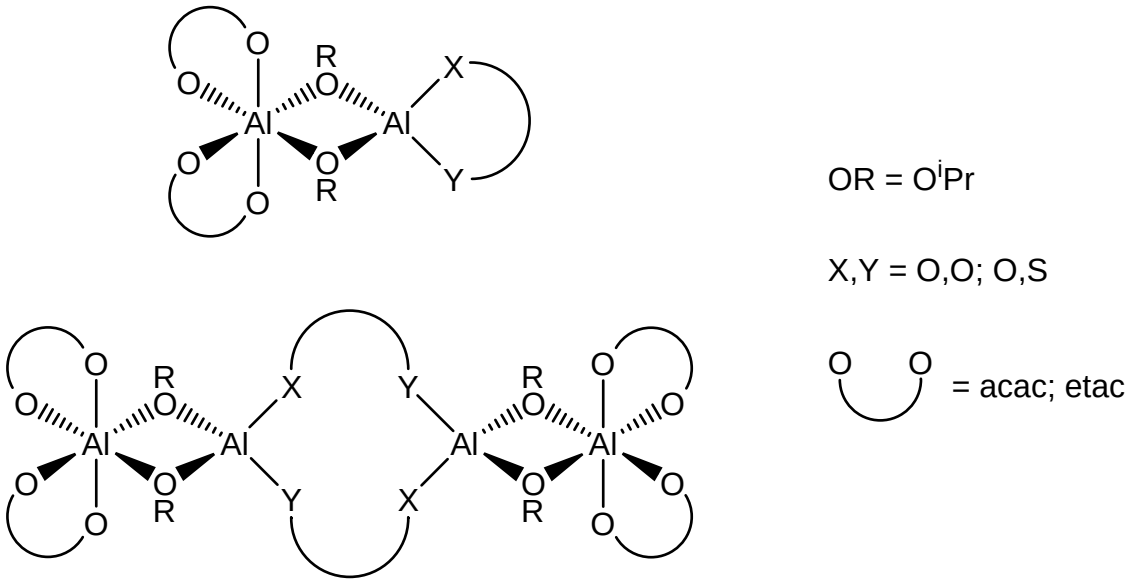

Figure 1-18 Schematic representation of $(CL)_2Al(\mu\text{-}O^iPr)_2AlL_2$ (*top*) and $(CL)_2Al(\mu\text{-}O^iPr)_2Al(\mu\text{-}L)_2Al(\mu\text{-}O^iPr)_2Al(CL)_2$ (*bottom*) (L = glycolate, thioalcoholate) (only one possible isomer shown for each case).

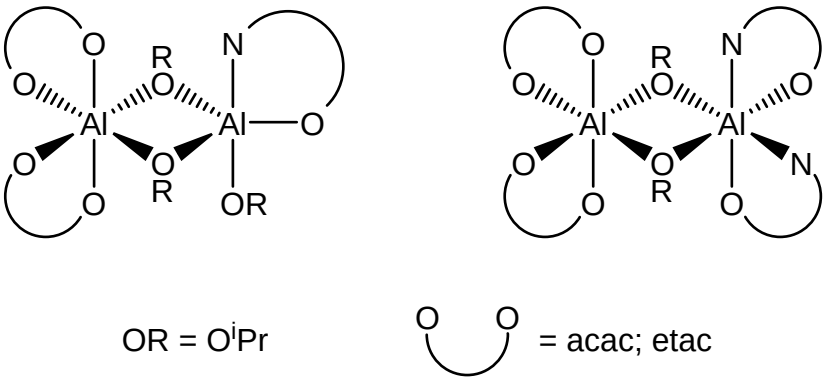

Figure 1-19 Schematic representation of $(CL)_2Al(\mu\text{-}O^iPr)_2Al(OiPr)L$ (*left*) or $(CL)_2Al(\mu\text{-}O^iPr)_2AlL_2$ (*right*) (L = 2-hydroxoquinolinate, 2-pyridylmethanolate) (only one possible isomer shown for each case).

Modification of $Al_2(\mu\text{-}O^iPr)_2(O^iPr)_2(CL)_2$ (CL = N-phenylsalicylideneiminate) [52], structurally analogous to $Al_2(\mu\text{-}O^iPr)_2(O^iPr)_2(acac)_2$, with various oximes yielded products analogous to those depicted in Figure 1-19, with one exception: for the reaction with one equiv. of 2-acetylthiophenyloxime a mononuclear, pentacoordinated complex with two chelating N-phenylsalicylideneiminate ligands and one monodentate oximate ligand was formed [53]. Again no influence of a dimer/trimer equilibrium analogous to $[Al(\mu\text{-}O^iPr)(O^iPr)(acac)]_n$ (n = 2, 3) was reported.

The tendency to stabilize lower coordination numbers by sterically more demanding groups can also be achieved by the use of sterically crowded alcohols or diols, *e.g.* 2,2'-ethylenebis(4,6-di-*tert.*-butylphenol) (edbp-H_2), stabilizing two aluminum centers in tetrahedral coordination geometry in $Al_2(\mu\text{-}O^iPr)_2(edbp)_4$ [65, 66].

Alternatively, large silanolates instead of alcoholates can be used for the same purpose. Their effect on the degree of oligomerization upon modification with acac-H was shown before [50], and also can be seen in the complex $Al_2(\mu\text{-}O^iPr)_2(O^iPr)_2(OSi(O^tBu)_3)_2$ [67].

For the modification with ethylenediamine (en), formation of a dimeric species with two tetrahedrally coordinated aluminum centers bridged by an en ligand was proposed [68-70]. At higher concentrations, the formation of polymeric species was observed [68]. Hydrazine is also capable to form adducts with aluminum alkoxides; the stability of the resluting complexes also depends on the type of alkoxide [71].

Modification of $Al(OR)_3$ (OR = OEt, O^nPr, O^iPr, O^sBu, O^tBu) with carboxylic acids (acetic, propionic, and 2-methylpropionic acid) in different stoichiometric ratios yielded compounds $Al(OR)_{3-n}(carboxylate)_n$ (n = 1, 2, 3), but no structural information was obtained. Esterification was observed for all reactions as side reaction. [72]

Modification of $Al(O^sBu)_3$ with acrylic acid resulted in a maximum degree of substitution of 1.6–1.7 acrylate ligands per aluminum center. This corresponds to a complete replacement of all terminal alkoxo groups of the trimeric structure, leading to $Al_3(\mu\text{-}O^sBu)_4(acrylate)_5$ (Figure 1-20 / compare also Figure 1-4). Reaction of acrylic acid with released *sec.*-butanol was proven as well, although the amount of formed butyl acrylate is negligible and no influence on the product by the water produced during the esterification was observed [73].

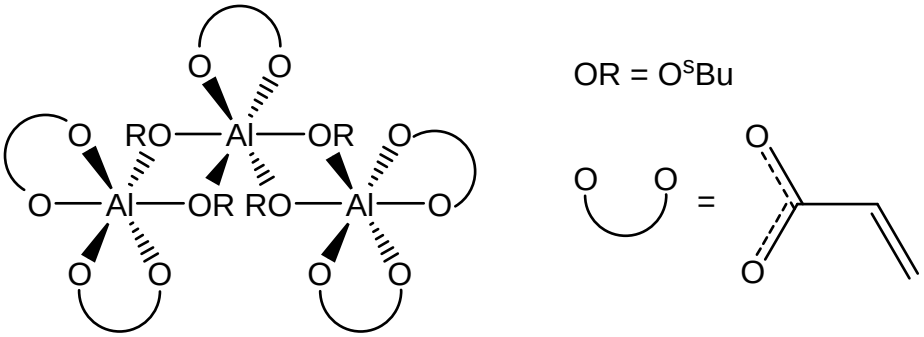

Figure 1-20 Schematic representation of $Al_3(\mu\text{-}O^sBu)_4(acrylate)_5$.

For the modification of $Al(O^sBu)_3$ with one molecule of diacetone alcohol (daa-H) per aluminum atom leads to a linear trimeric species with only pentacoordinated aluminum centers, explained by different binding modes of the daa ligand at the terminal aluminum centers (bidentate) and the central aluminum atom (monodentate) (Figure 1-21). Again only terminal O^sBu groups are replaced by daa. The trimer collapses to give tetrahedrally coordinated units at higher molar ratios of daa-H/Al [74].

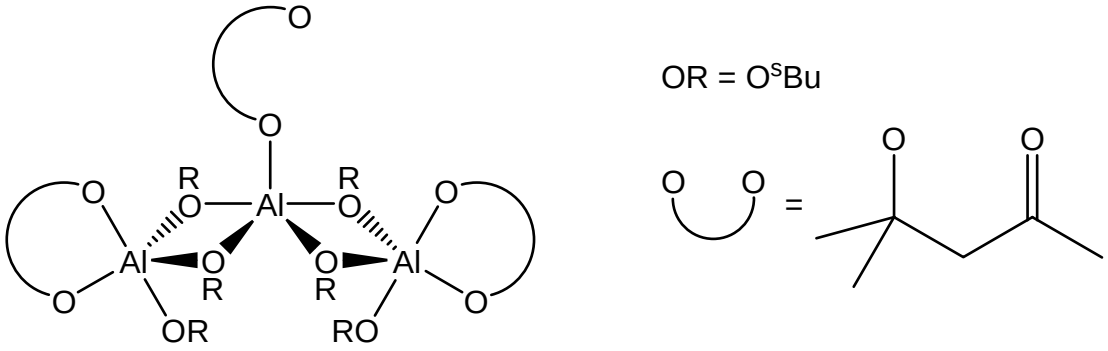

Figure 1-21 Schematic representation of $Al_3(\mu\text{-}O^sBu)_4(O^sBu)_2(daa)_3$ (only one possible isomer shown).

Modification of $Al(OCH_2CH_2OMe)_3$ or $Al(OCH_2CH_2OEt)_3$ with one equiv. of 8-hydroxyquinoline (quin-H) gave dimeric products $[Al(\mu\text{-}OR)(quin)_2]_2$ (R = CH_2CH_2OMe or CH_2CH_2OEt) with a stoichiometric ratio of Al/quin = 1:2, having two octahedrally coordinated aluminum centers, structurally analogous to $[Al(\mu\text{-}O^iPr)(Et_2acac)_2]_2$ (*vide supra* / compare Figure 1-15). Attempts to prepare analogous products with O^iPr or OEt bridges failed and only yielded $Al(quin)_3$ [75]. Although no coordination of the ether oxygen of the OCH_2CH_2OR ligands to the aluminum centers is observed, it apparently stabilizes the dimeric structures with a Al/quin ratio of 1:2.

Besides the described structures for aluminum alkoxides modified with different ligands, a wide variety of other modified aluminum alkoxides prepared by alternative preparation procedures – *viz.* not by substitution reactions from aluminum alkoxides – is reported in the literature [65, 76-78]. In most cases these complexes are formed from aluminum hydrides or alkyls of which, in a first reaction step, part of the hydride/alkyl groups is replaced by an organic ligand. In a second step the residual hydride/alkyl groups are (partially) replaced by alkoxo groups upon addition of alcohols and release of H_2 or alkanes, respectively. By these alternative procedures new structural motives can be observed, such as symmetric dimers [65, 76] or monomeric species [77] for Al/ligand ratios of 1:1. Since this work focuses on the *modification of* aluminum alkoxides, a closer discussion of these compounds would exceed the scope of this work and hence is omitted.

As the aluminum alkoxides themselves, also their modified derivatives find wide application as polymerization catalysts [79-82]. The ligands used for modification are often sterically demanding to gain control over the reactivity and the structure of the polymer, or even the chirality when chiral ligands are used.

1.2.3.2 Modification of Yttrium Alkoxides

Examples for the modification of yttrium alkoxides with organic ligands are extremely rare. The only yttrium compound prepared by substitution of alkoxo groups reported so far, which bear alkoxo groups as well as other ligands in the final structure, is $[Y_4(\mu_4\text{-O})(\mu\text{-OEt})_2(\mu\text{-aaa})_2(\text{aaa})_3]_2(\mu_3\text{-OH})_4(\mu_3\text{-OEt})_2$ (aaa = allyl acetoacetate) [44, 83]. This compound was obtained upon the reaction of $Y_5(\mu_5\text{-O})(\mu_3\text{-O}^i\text{Pr})_4(\mu\text{-O}^i\text{Pr})_4(\text{O}^i\text{Pr})_5$ with aaa-H and subsequent crystallization from an ethanol/toluene-mixture, causing exchange of the remaining O^iPr by OEt groups. It is assumed that initially $Y_4O(\mu\text{-O}^i\text{Pr})_5(\mu\text{-aaa})_2(\text{aaa})_3$ is formed which was spectroscopically identified.

Reaction of $Y_5(\mu_5\text{-O})(\mu_3\text{-O}^i\text{Pr})_4(\mu\text{-O}^i\text{Pr})_4(\text{O}^i\text{Pr})_5$ with three equiv. of 2,2,6,6-tetramethyl-3,5-heptandione (thd-H) per Y atom gave $Y(thd)_3$, showing that the Y_5 core can be degraded upon coordination to give a mononuclear, octahedrally coordinated yttrium complex [84].

The reaction between $Y_5(\mu_5\text{-O})(\mu_3\text{-O}^i\text{Pr})_4(\mu\text{-O}^i\text{Pr})_4(\text{O}^i\text{Pr})_5$ and acac-H shows that the substitution of O^iPr groups by β-diketones is not that straightforward in general. This reaction yielded dimeric $Y_2(\mu\text{-OAc})_2(\text{acac})_4(H_2O)_2$ (OAc = acetate), showing unexpected cleavage of the acetylacetone to give acetate [85].

1.3 Inorganic-Organic Hybrid Materials

As mentioned in the beginning, the developement of the sol-gel processing opened an easy way to and therefore boosted the development of inorganic-organic hybrid materials. The term hybrid materials is used for materials composed of molecular building blocks of different composition, in contrast to composite materials, whose macroscopic constituents show defined phase boundaries.

As for composite materials, the idea behind the development of such materials is the combination of the properties of both inorganic as well as organic compounds, *e.g.* combining the hardness of an inorganic crystalline material with the elasticity of an organic polymer resulting in a hard, but at the same still compliable material. Additionally, the processibility is greatly influenced. Hybrid materials mostly show a much more polymer-like behavior with respect to the processing parameters, overcoming the problem of the poor processibility of pure inorganic solid state materials, often requiring high temperatures.

Inorganic-organic hybrid materials are typically categorized into two classes [4]:

- *Class I* inorganic-organic hybrid materials show only weak interactions between the inorganic and organic phase, *e.g.* van der Waals or hydrogen bonding or weak electrostatic interactions (Figure 1-22).

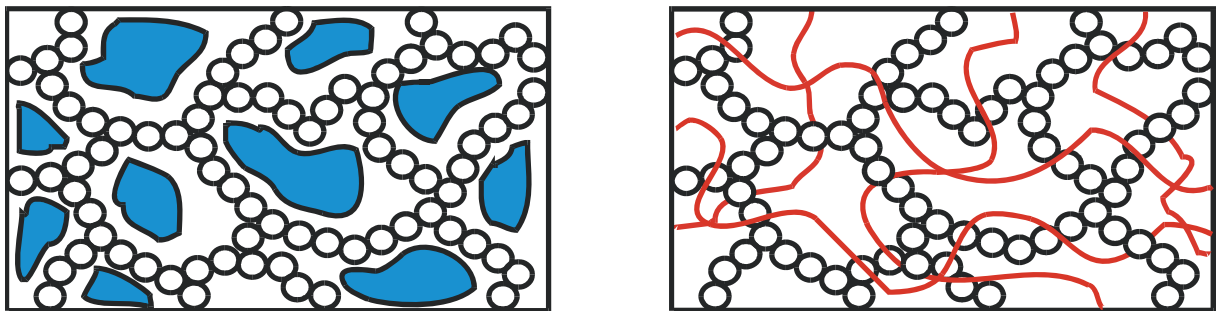

Figure 1-22 Inorganic-organic hybrid materials *without* covalent linkage between the inorganic and organic phase: molecules/particles embedded into an inorganic gel matrix (*left*); interpenetrating inorganic and organic polymer networks (*right*).

- *Class II* inorganic-organic hybrid materials show strong interactions between the inorganic and organic phase, *e.g.* covalent or coordinative bonding (Figure 1-23).

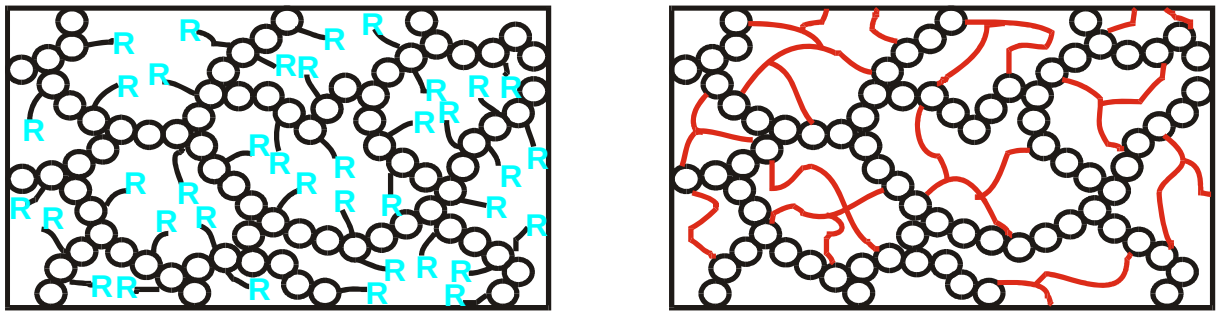

Figure 1-23 Inorganic-organic hybrid materials *with* covalent linkage between the inorganic and organic phase: organic groups attached to an inorganic polymer network (*left*); dual inorganic-organic hybrid polymer network (*right*).

It is clear that there is a steady transition from *Class I* to *Class II* hybrid materials since also the strength of chemical interactions changes gradually.

Class I hybrid materials with organic molecules embedded in an inorganic network (Figure 1-22 *left*) can be prepared by dissolution or dispersion of the molecules in the precursor solution and subsequent gelation of the inorganic part. Gelation of inorganic precursors in a solution of an organic polymer leads to interpenetrating inorganic and organic polymer networks (Figure 1-22 *right*). *Class II* hybrid materials with organic groups covalently linked to the inorganic network (Figure 1-23 *left*) can be obtained by sol-gel processing of precursors bearing organic groups stable against hydrolysis. If these organic groups bear additional functionalities, these can be copolymerized with organic monomers, leading to a dual inorganic-inorganic hybrid polymer network (Figure 1-23 *right*). The preparation of inorganic-organic hybrid polymers can be achieved either by an in-situ formation of both networks, the formation of an inorganic network around a pre-formed organic structure (organic polymers bearing metal alkoxo (end)groups), or the formation of an organic polymer around a preformed inorganic structure (inorganic polymers/gels bearing polymerizable groups).

In principle the preparation of hybrid materials can be categorized into two different approaches [86]:

- *In situ formation*: The inorganic as well as the organic phase are formed *in situ* from molecular precursors to give the final hybrid material.
- *Building blocks*: Previously prepared and well defined building blocks are combined to give the final hybrid material, with at least partial retainment of the original integrity.

Both approaches have different advantages and disadvantages. For example, due to the (partial) retention of the building blocks – and therewith their properties – in the latter approach, structure-property predictions are eased. On the other hand, the great influence of a variety of parameters – *e.g.* reaction conditions or precursor proportions – allows the variation of the properties within a wide range for *in situ* formed materials. The possible use of single source precursors also allows an exact adjustment of the stoichiometry and the phase ratios, respectively. An example for the former approach is the sol-gel processing of organically modified silicon alkoxides, whereas intercalation products of organic polymers in layered inorganic materials is a well known and widely applied group of hybrid materials prepared following the building block approach.

There is a wide variety of possibilities to influence the properties of the final hybrid materials by variation of the

- chemical composition
- ratio
- structure
- distribution

of the inorganic and organic precursor (parts), respectively.

As discussed before (compare chapter 1.2), the inorganic structure of a hybrid material obtained from organically modified alkoxide precursors is strongly influenced by the substitution of alkoxo groups. The reduction of the number of hydrolyzable alkoxo groups leads to a lower degree of cross-linking in the final material and also the stereochemistry and directionality of the gel and product formation can be influenced. But concomitantly also the structure of the organic phase is influenced by the addition of precursors with anchoring points for covalent linkage. For example, precursors bearing more than one polymerizable C=C double bond can act as cross-linkers and therefore increase the branching of the organic polymer, analogous to the use of organic cross-linkers to obtain cross-linked organic polymers. Finally it also has to be taken into account that an inter-phase is formed between the inorganic and organic phases, often showing different properties than the bulk phases. Especially for hybrid materials composed of very small regimes, the proportion of inter-phase can overcome those of the bulk phases and therefore the properties of this inter-phase might dominate the overall properties. This also reflects one of the big advantages and chances of hybrid materials: creation of new properties, neither originating directly from the inorganic nor the organic phase, but resulting from the interplay of both phases.

2 Research Goals and Scope of Work

This work focuses on the synthesis and characterization of precursors for sol-gel derived (hybrid) materials. The sol-gel process was developed and is well studied and understood for silicon-based materials, but to a much lesser extend for other metal based systems. For example, the high reactivity of metal alkoxides – a widely used class of precursors for metal oxide materials prepared by the sol-gel route – upon hydrolysis and the hydrolytic instability of metal-carbon bonds are some of the most crucial differences for the sol-gel processing of silicon- compared to metal-based materials [5, 6].

To overcome these problems, modification of metal alkoxides with chelating ligands is a well known and widely applied way for the control of reactivity of metal alkoxide sol-gel precursors. For the use as precursors for sol-gel derived inorganic-organic hybrid materials the introduction of additional functionalities as anchoring point for a covalent linkage to the organic matrix is feasible [87].

Various publications deal with the synthesis of metal oxide materials by the sol-gel process from alkoxides modified with a variety of organic ligands. Unfortunately, in many cases characterization of the final materials properties was the main focus and a detailed study of the precursors was neglected. Since for an efficient and deliberate synthesis of new materials knowledge about the structures and reactivities of the precursors is an essential prerequisite, systematic studies on the modification of metal alkoxides with organic ligands are of great interest.

The aim of this work was a systematic investigation of the modification of aluminum alkoxides with *β*-diketonic ligands, *viz.* *β*-diketones, *β*-ketoesters, dialkylmalonates, and acetoacetamides. The influence of variations of the ester functionalities as well as of the type of parent alkoxide on the structure, stability, and reactivity of the modified precursors was of main interest. Additionally, the influence of variations of the reaction conditions during preparation on the precursors was of interest. Since some of the ligands as well as the metal alkoxide bear alkoxo (amido) functionalities, it was of additional interest whether interactions between these groups have to be taken into account, *e.g.* transesterification. The possibility of introducing additional functionalities by the ester group also was of interest, opening a way to precursors for inorganic-organic hybrid polymers with an anchoring point for covalent linkage between the two phases.

Furthermore, the known dependence of the degree of oligomerization of metal alkoxides on their reactivity, in particular also after modification with organic ligands, was only incompletely investigated so far, in particular for aluminum alkoxides, which are known to show a complex oligomerization behavior. Therefore a more detailed study of the dependence of the parent alkoxides degree of oligomerization on the modification reactions is desirable for a better understanding of the processes involved in modification of metal alkoxides.

In a further step, expansion of the obtained findings on the modification of yttrium alkoxides was desired. Yttrium was chosen as another trivalent metal center since it is known to show a complex coordination behavior with coordination numbers up to nine. Additionally, yttrium is known to form oxo/hydroxo species upon the preparation of its alkoxides. Therefore a wider variety of structures can be expected compared to aluminum, including alkoxo/hydroxo/oxo-complexes. The findings for the modification of yttrium alkoxides may be supportive for the understanding of the structural and chemical behavior of alkoxide based yttrium precursors and yttrium oxide based materials.

Results obtained for the modification of yttrium alkoxides may also be applied to alkoxides of other trivalent metal alkoxides, in particular lanthanide alkoxides, since it is established that lanthanides often behave analogous to yttrium – sometimes actually denoted as “pseudo-lanthanide”. These opens the route to functional inorganic/organic hybrid materials, which, additionally to the modification of the mechanical properties by the incooperation of inorganic material into an organic matrix (or *vice versa*), exhibit special electronic, magnetic, or – as in the case of lanthanide based materials – optical properties.

3 Results and Discussion

3.1 Modification of Aluminum Alkoxides with *β*-Ketoesters

As elucidated before, modification of aluminum alkoxides with *β*-diketonates and *β*-ketoesters is a well known and often applied procedure. In earlier work, substitution of alkoxo groups by chelating ligands was driven to completion and monitored by the azeotropic removal of the liberated ^{i}PrOH with benzene from the reaction solution at elevated temperatures [12]. In later publications it was shown that this is not necessary, for example for the modification of aluminum alkoxides with acac-H [50] or of titanium alkoxides with *β*-ketoesters [88, 89], and that the substitution proceeds at room temperature in toluene [50]. The latter reaction was chosen as starting point for the preparation of various aluminum alkoxide derivatives by the modification with a series of *β*-ketoesters (Scheme 3-1).

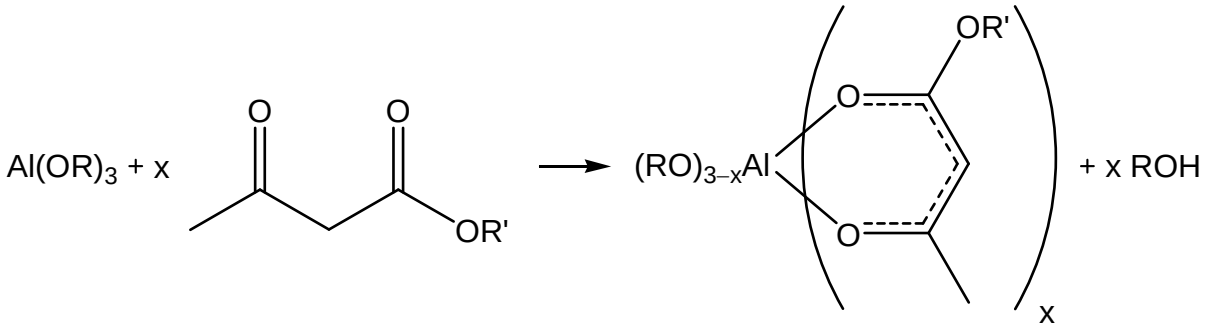

Scheme 3-1

3.1.1 Modification with *β*-Ketoalkylesters

As first part of the investigations the influence of varying the steric demand of the ester functionality was investigated. Therefore Al($O^{i}Pr$)$_3$ was reacted with methyl (meac-H), ethyl (etac-H), isopropyl (^{i}prac-H), and *tert.*-butyl (^{t}buac-H) acetoacetate (Figure 3-1).

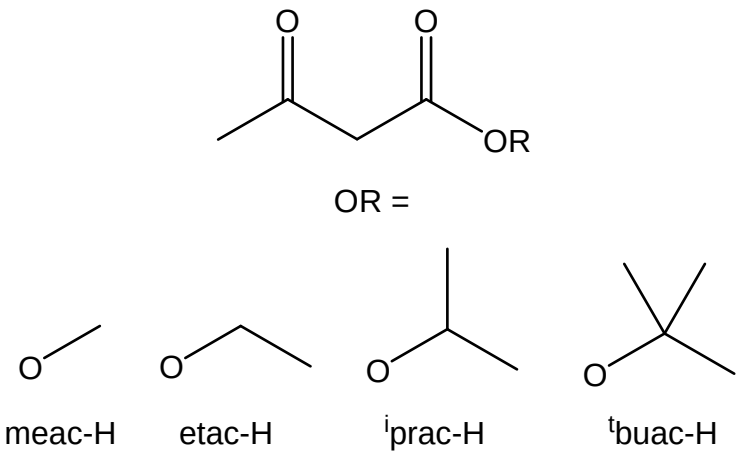

Figure 3-1 *β*-Ketoalkylesters used for the modification of aluminum alkoxides.

3.1.1.1 Al(*β*-ketoesterate)$_3$ Complexes

Although Al(*β*-ketoesterate)$_3$ complexes are no classical sol-gel precursors because they are lacking readily hydrolyzable Al–OR groups, they are of interest for a better understanding of the coordination behavior of the *β*-ketoesterate ligands and also for the complete characterization of compounds with a lower degree of substitution. The complexes were prepared by addition of three equiv. of *β*-ketoester to the alkoxide (Scheme 3-2).

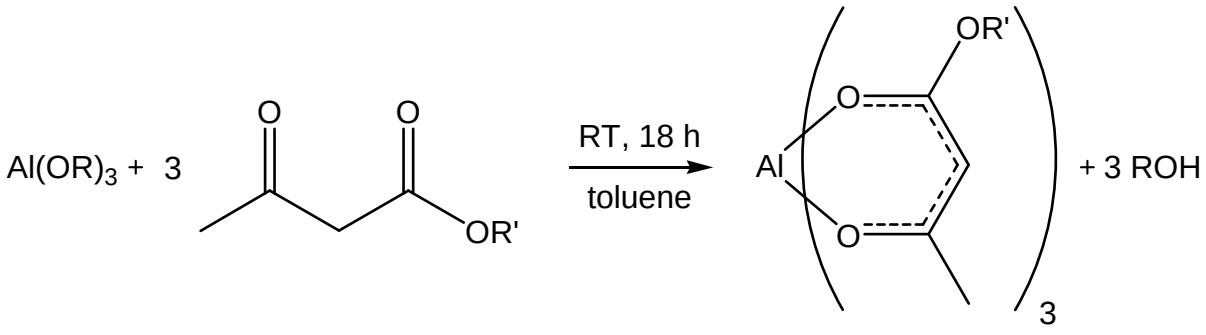

OR = O^{i}Pr, O^{t}Bu

OR' = OMe, OEt, O^{i}Pr, O^{t}Bu

Scheme 3-2

This general reaction works for Al(O^{i}Pr)$_3$ and Al(O^{t}Bu)$_3$ with all esters at room temperature to give Al(meac)$_3$ (**1a**), Al(etac)$_3$ (**1b**), Al(^{i}prac)$_3$ (**1c**), and Al(^{t}buac)$_3$ (**1d**) as pure products in quantitative yields. Elevated reaction temperatures did not change the products. After the reaction the volatiles were removed *in vacuo* and the products isolated as microcrystalline precipitates or powders.

Coordination of the *β*-ketoesterate ligands during this reaction was monitored by ^{1}H NMR spectroscopy, showing the disappearance of the signals of the C***H***$_2$ group between the two carbonyl groups of the non-coordinated esters (2.96–2.93 ppm) and the appearance of the signals for the corresponding C***H*** proton of the deprotonated and coordinated ligand (4.99–4.81 ppm) (Figure 3-2). In all cases complete coordination was observed at least after 18 h of stirring in toluene at room temperature, and prolonged reaction times did not result in any changes according to ^{1}H NMR spectroscopy.

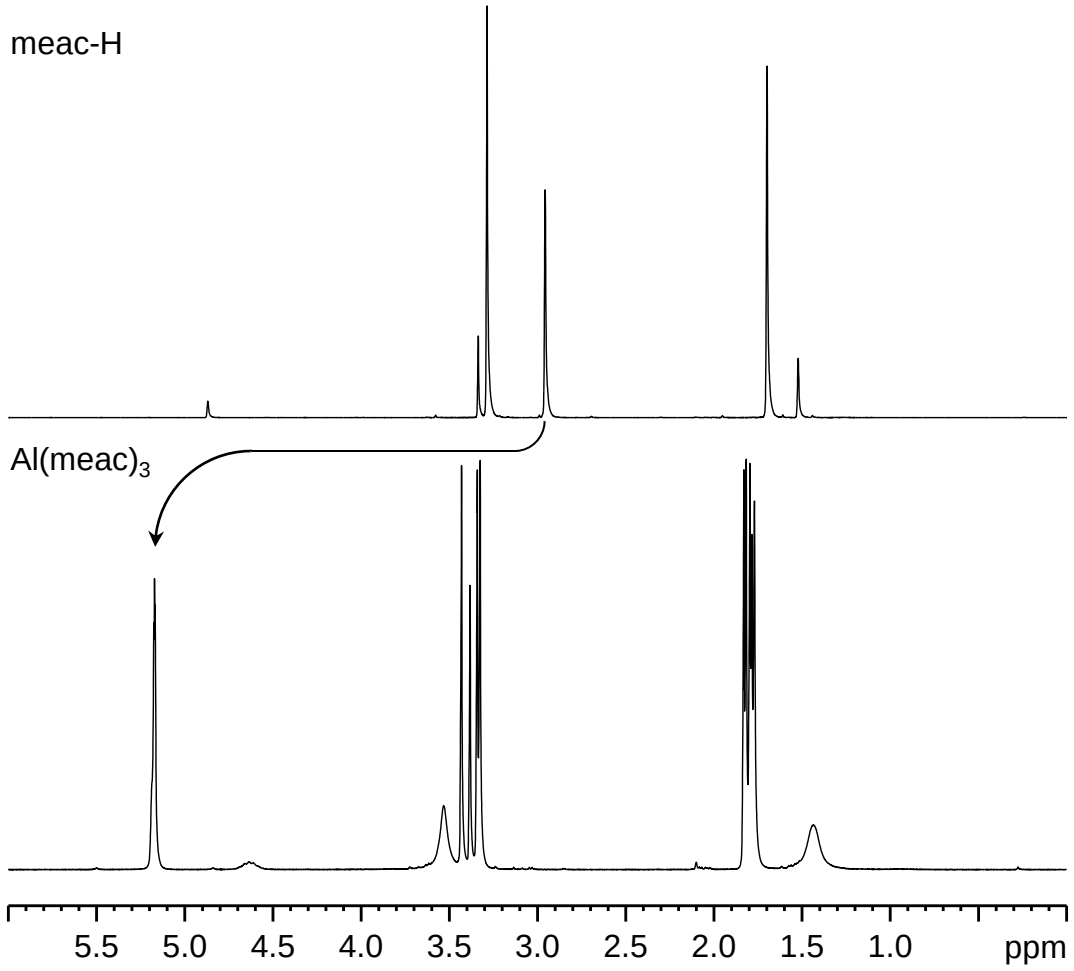

Figure 3-2 Comparison of the spectra of meac-H (*top*) and Al(meac)$_3$ (**1a**) (*bottom*), indicating the shift of the signal for the C***H*** group in Al(meac)$_3$ compared to the C***H***$_2$ group in meac-H (in C_6D_6).

In addition to the described preparation of **1a**–**1d** (according to Scheme 3-2), a first attempt to prepare compounds [Al(O^{i}Pr)$_2$(*β*-ketoesterate)]$_n$ (compare chapter 3.1.1.2) by reaction of [Al(O^{i}Pr)$_3$]$_4$ with one molar equivalent of *β*-ketoester per aluminum atom at room temperature (Scheme 3-1) did not yield the desired products. Even after prolonged reaction times at room temperature, only mixtures of Al(*β*-ketoesterate)$_3$ (**1a**–**1d**) and unsubstituted [Al(O^{i}Pr)$_3$]$_4$ were obtained for all esters used (Scheme 3-3).

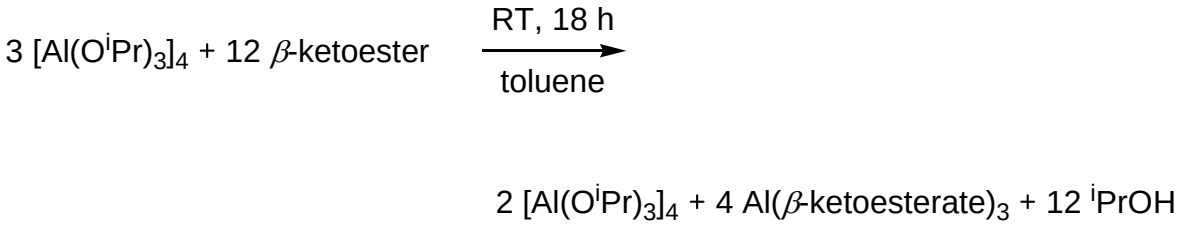

Scheme 3-3

Since upon substitution of O^iPr groups by *β*-ketoesters and subsequent formation of Al(*β*-ketoesterate)$_3$ the tetrameric structure has to be broken up it is assumed that intermediate $[Al(O^iPr)_x(\beta\text{-ketoesterate})_{3-x}]_n$ species react more readily with *β*-ketoesters than $[Al(O^iPr)_3]_4$, leading to exclusive formation of Al(*β*-ketoesterate)$_3$ (**1a**–**1d**) and conservation of tetrameric $[Al(O^iPr)_3]_4$. To the best of my knowledge, this behavior was not described in literature so far.

The crystal structure of $Al(^tbuac)_3$ (**1d)** was previously reported [90]. The ^{27}Al NMR chemical shift of 4.8 ppm in the NMR spectrum of Al(etac)$_3$ (**1b**) is in line with the octahedral coordination of the aluminum atom (Figure 3-3) [17].

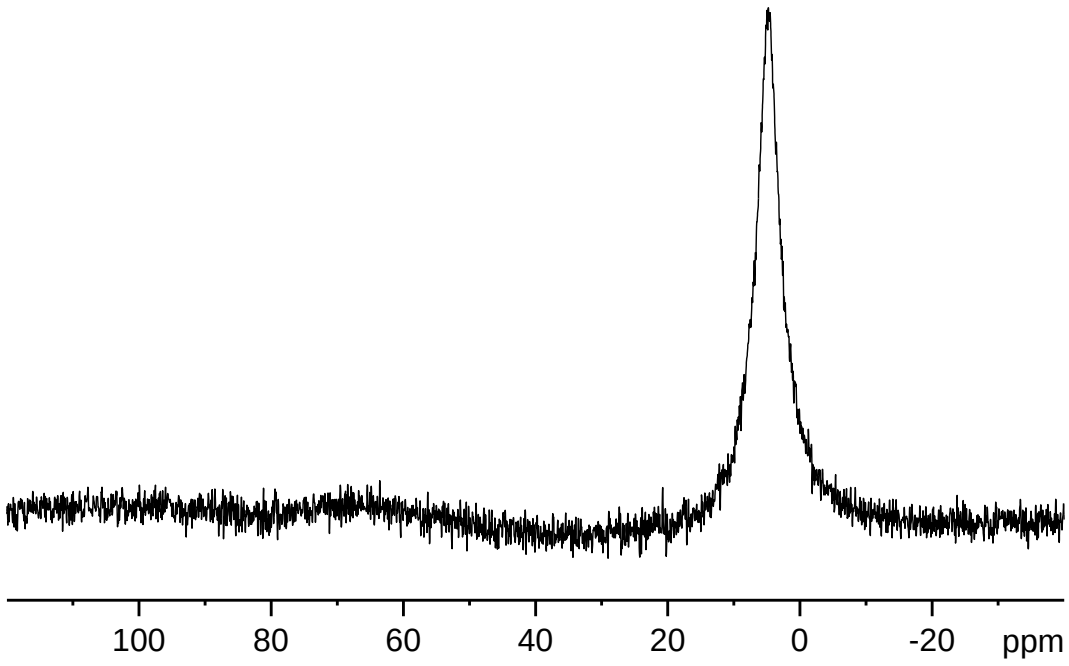

Figure 3-3 ^{27}Al NMR spectrum of **1b** (in $[D_8]$toluene).

^1H and ^{13}C NMR spectra of the Al(*β*-ketoesterate)$_3$ compounds showed up to 4 signal sets for the ester groups. This is a result of the coexistence of different isomers in solution, *viz.* a C_3 symmetric isomer with the keto and ester oxygen atoms, respectively, in *fac* arrangement and a C_1 symmetric isomer with *mer* arrangement. In the C_3 symmetric complex, all ligands are symmetry equivalent giving rise to one set of signals in the NMR spectra, whereas for the

C_1 symmetric complex all ligands are non-equivalent, causing one set of signals for each ligand (Figure 3-3).

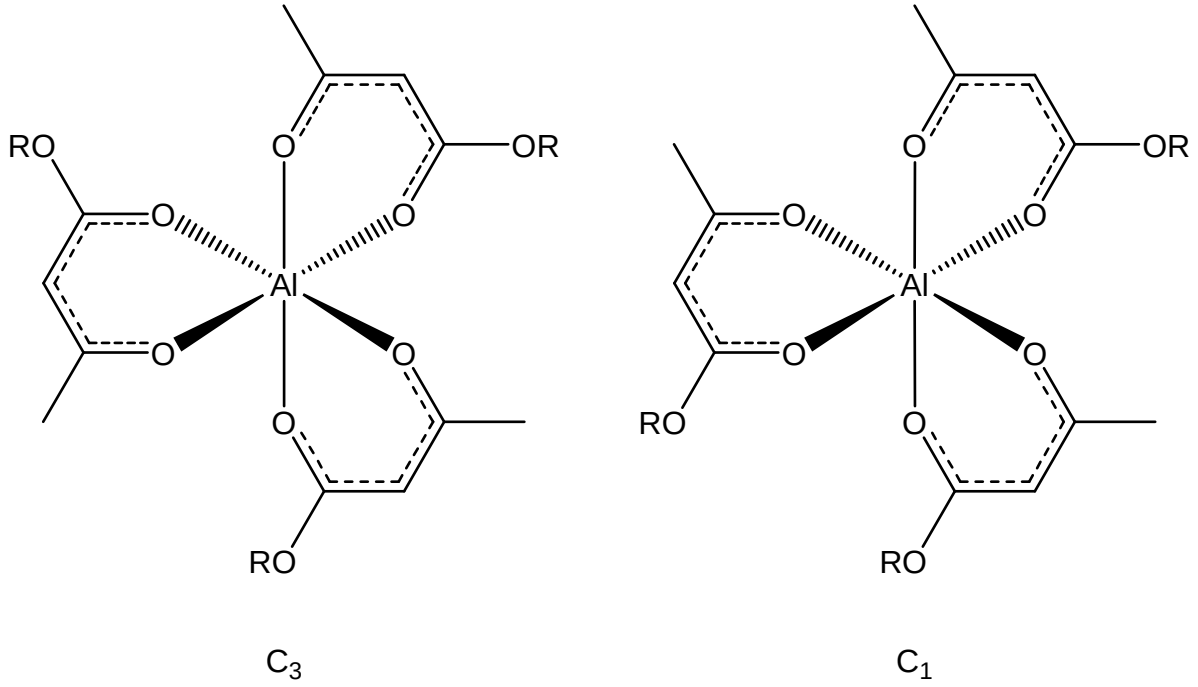

Figure 3-4 Schematic representation of the possible isomers of Al(β-ketoesterate)$_3$ complexes (only one enantiomer shown for each case).

As a matter of fact, each isomer forms a pair of enantiomers, which in the context of the NMR studies has no further consequences. Although it could not be determined which signals originate from which isomer, the observation of four signal sets of equal intensity in the ^{1}H NMR spectra corresponds to a 1:3 ratio of C_3 and C_1 symmetric species. Since there are three times more possible C_1 than C_3 isomers this means that no isomer is energetically favored in solution. Variable temperature NMR showed that the isomers can transform into each other. Coalescence was observed above 80 °C, causing an averaged signal set (Figure 3-5).

EXSY experiments confirmed exchange of the β-ketoesterate signals between the different isomers. The methyl region of the EXSY spectrum of **1b** is given in Figure 3-6, showing exchange for the C***H***$_3$CO (1.90–1.80 ppm) and OC***H***$_3$ (1.12–0.92 ppm) signals.

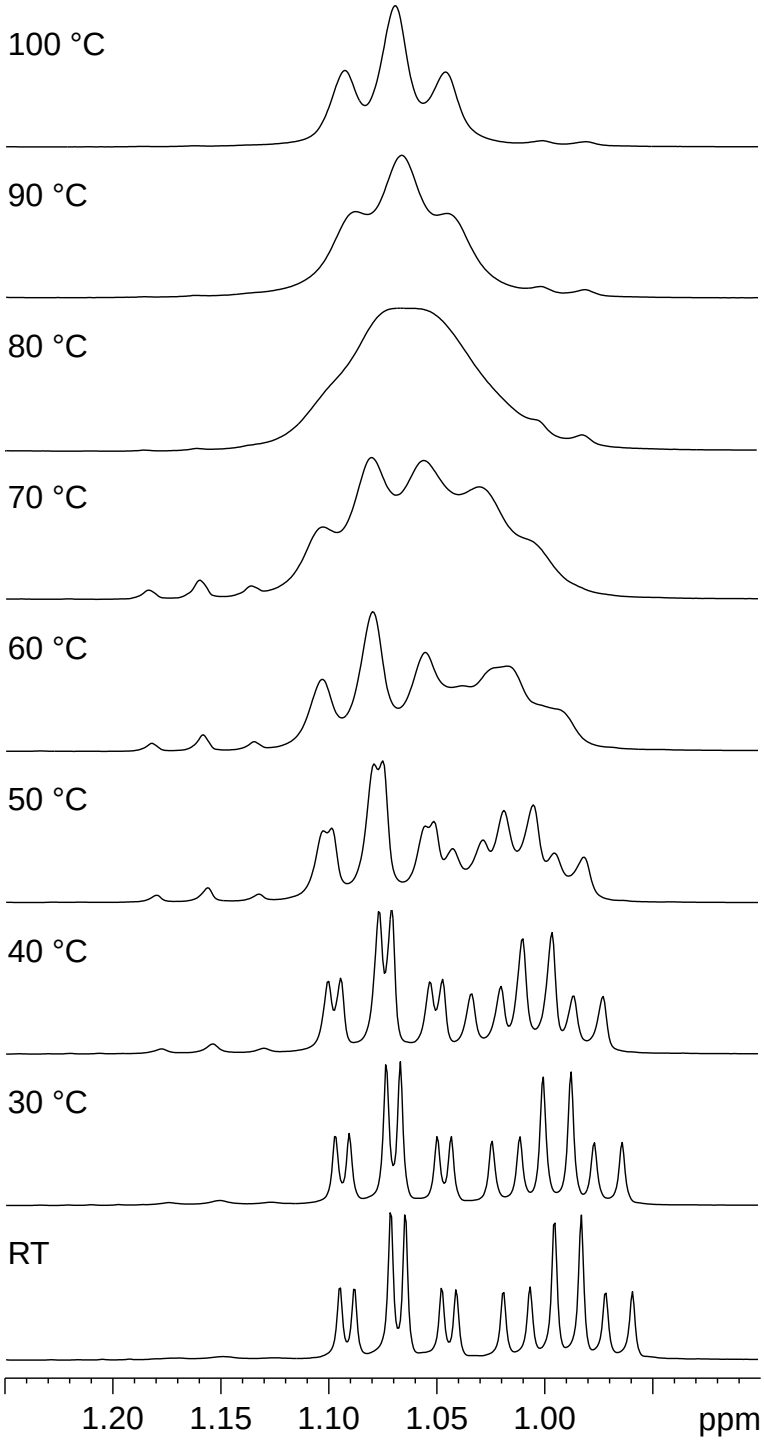

Figure 3-5 Variable temperature ^{1}H NMR spectra of **1b** showing coalescence above 80 °C (in [D_8]toluene).

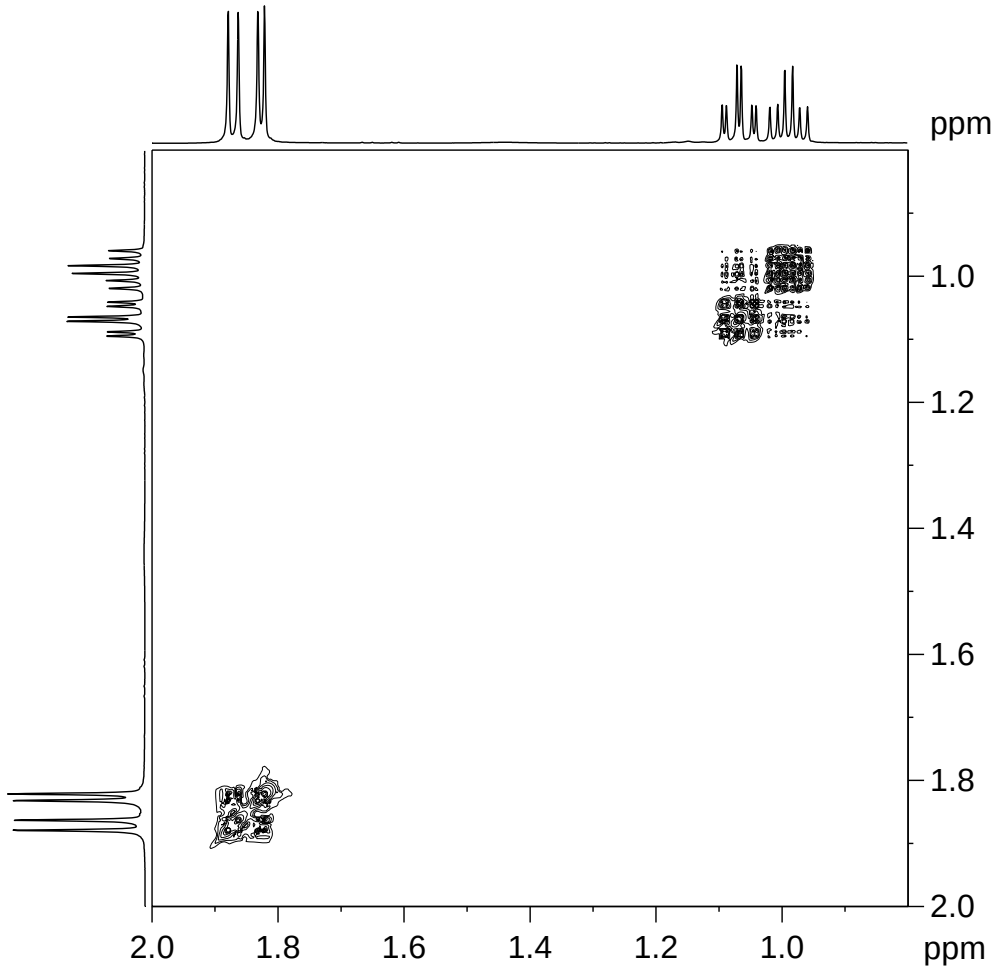

Figure 3-6 EXSY spectrum of **1b** (in [D_8]toluene).

No significant influence on the ^{1}H and ^{13}C NMR shifts of CO***CH***CO upon variation of the ester functionality of the ligands was observed for the Al(*β*-ketoesterate)$_3$ complexes **1a**–**1d** (Table 3-1), only for the ^{13}C resonances a minimal trend to higher values with increasing steric demand can be interpreted. Also the other ^{1}H and ^{13}C NMR shifts of the ligands were not significantly influenced by variation of the ester group.

Table 3-1 ^{1}H and ^{13}C NMR shifts of CO***CH***CO of **1a**–**1d**.

	^{1}H (COC***H***CO)[a]	^{13}C (CO***C***HCO)[b]
1a	5.17	85.0/84.7/84.5
1b	5.18/5.17	85.2/85.0/84.8
1c	5.16	85.6/85.4/85.1
1d	5.13/5.10/5.08	86.4/86.2/86.1/85.8

[a] in C_6D_6

[b] in [D_8]toluene

3.1.1.2 $Al_2(\mu\text{-}O^iPr)_2(O^iPr)_2(\beta\text{-ketoesterate})_2$ Complexes

Heating the solutions from the reaction of $Al(O^iPr)_3$ with one equiv. of β-ketoester in toluene at room temperature, containing $Al(\beta\text{-ketoesterate})_3$ and $[Al(O^iPr)_3]_4$ along with liberated ^{i}PrOH (compare chapter 3.1.1.1 / Scheme 3-3), to 120 °C overnight resulted in the formation of the anticipated $[Al(O^iPr)_2(\beta\text{-ketoesterate})]_n$ derivatives (Scheme 3-4).

$$[Al(O^iPr)_3]_4 + 2\ Al(\beta\text{-ketoesterate})_3 \xrightarrow[\text{toluene}]{\text{120 °C, 18 h}} 6/n\ [Al(O^iPr)_2(\beta\text{-ketoesterate})]_n$$

Scheme 3-4

The general validity of this reaction pathway was proven by the reaction of isolated $Al(\beta\text{-ketoesterate})_3$ and $[Al(O^iPr)_3]_4$ in appropriate stoichiometric ratios in toluene (without free alcohol), giving the same results. After cooling to room temperature no redistribution to $Al(\beta\text{-ketoesterate})_3$ and $[Al(O^iPr)_3]_4$ occurred. This proves, that:

- the monosubstituted product is the most stable species for an Al/β-ketoester ratio of 1:1.
- the formation of $Al(\beta\text{-ketoesterate})_3$ at room temperature as described above is due to a kinetic effect.

The same result was also obtained for an alternative preparation route, where a toluene solution of $[Al(O^iPr)_3]_4$ was thermally pre-treated. This is known to cause de-oligomerization of the tetrameric units [24, 33]. According to literature, the solution consists mainly of dimeric and trimeric species after fast cooling to room temperature, but some tetrameric $[Al(O^iPr)_3]_4$ is still present or reformed. This was confirmed by ^{27}Al NMR spectroscopy, showing a broad signal for pentacoordinated aluminum of trimeric species in the range from about 45 to 15 ppm, as well as a sharp signal at about 0 ppm for hexacoordinated aluminum of the tetramer, besides signals from about 80 to 50 ppm for tetracoordinated aluminum of di-, tri-, and tetrameric species (Figure 3-7) [17].

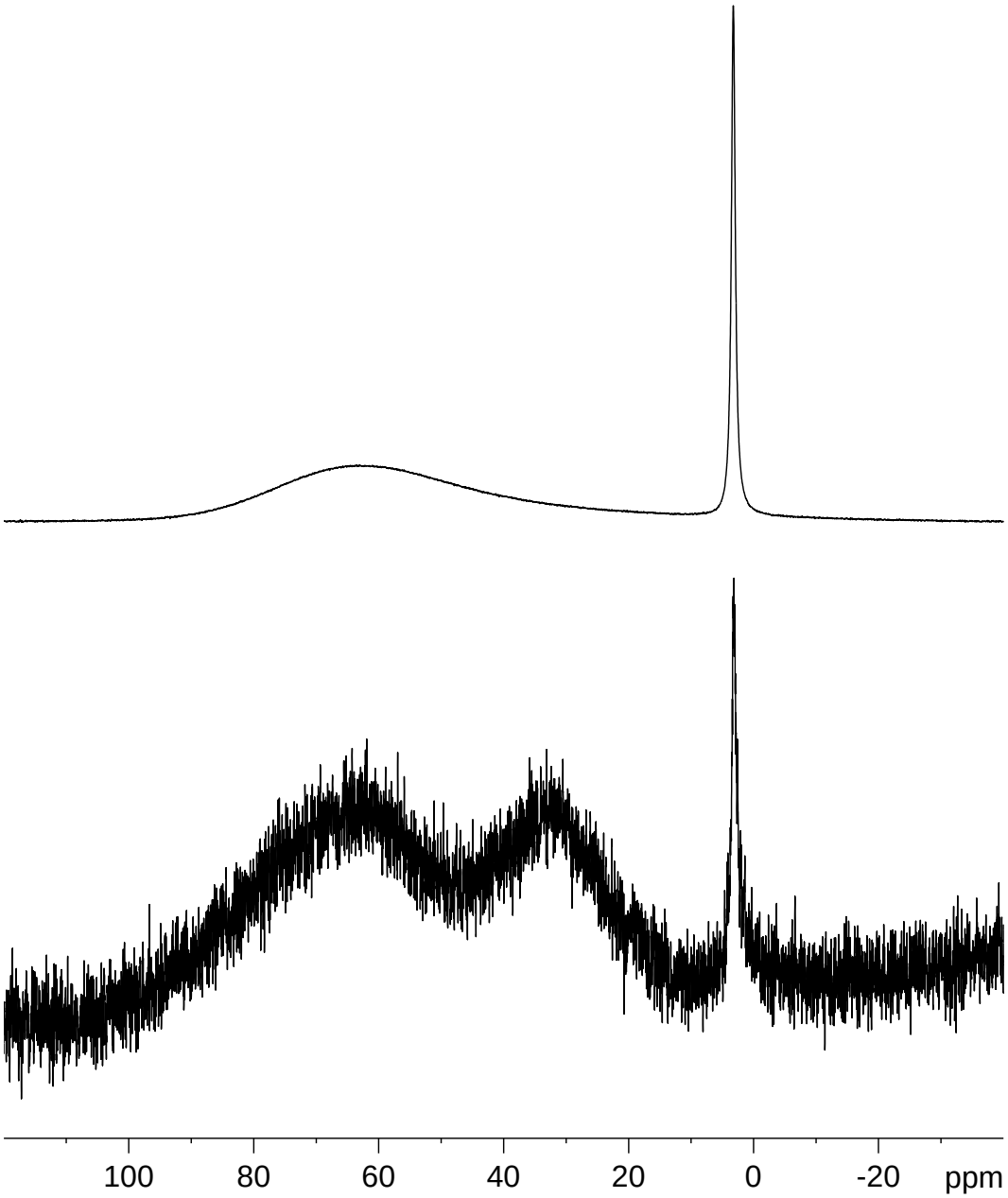

Figure 3-7 ^{27}Al NMR spectra of $[Al(O^iPr)_3]_4$ before (*top*) and $[Al(O^iPr)_3]_{<4}$ after (*bottom*) thermal treatment (in $[D_8]$toluene).

^{1}H NMR and HSQC spectroscopy additionally clearly confirmed the breakup of the tetrameric units (Figure 3-8).

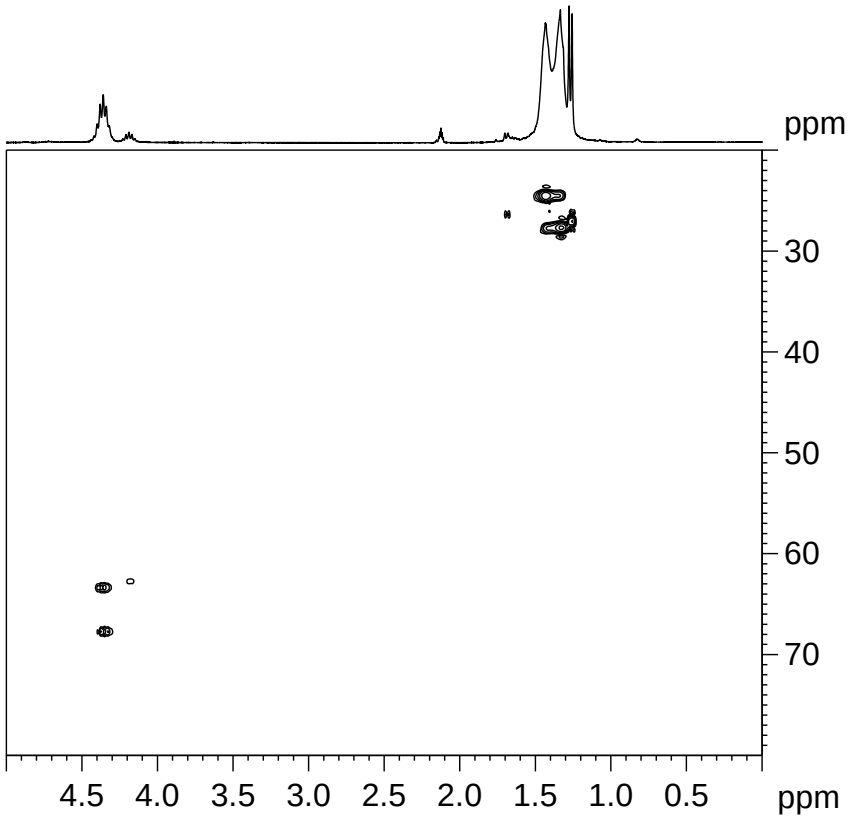

Figure 3-8 HSQC spectrum of $[Al(O^iPr)_3]_{<4}$ (in $[D_8]$toluene).

After de-oligomerization of tetrameric $[Al(O^iPr)_3]_4$, the solution was cooled to room temperature, the *β*-ketoester was added and allowed to react for several hours. The resulting product was identified to be the same as for the two reaction pathways described before, which means that pre-heating of the parent alkoxide and subsequent reaction with the ligand at room temperature results in the same products as the in-situ heating of a mixture of the metal alkoxide and the ligand. These results lead to the following conclusions:

- Re-formation of $[Al(O^iPr)_3]_4$ from the dimer and trimer is slow at room temperature.
- The dimer and trimer react faster with the *β*-ketoesters than the tetramer.
- The dimer and trimer react also faster than intermediate $[Al(O^iPr)_x(\beta\text{-ketoesterate})_{3-x}]_n$ species, giving directly the monosubstituted compounds.

All $[Al(O^iPr)_2(\beta\text{-ketoesterate})]_n$ derivatives show two ^1H NMR signals for the methine protons of the O^iPr groups, indicating the existence of two chemically different alkoxo groups. According to literature results [50] for the modification of aluminum alkoxides and siloxides with acac-H and the single crystal XRD analysis of **2d** reported below, the derivatives are asymmetrically substituted, alkoxo-bridged dimers (Figure 3-9).

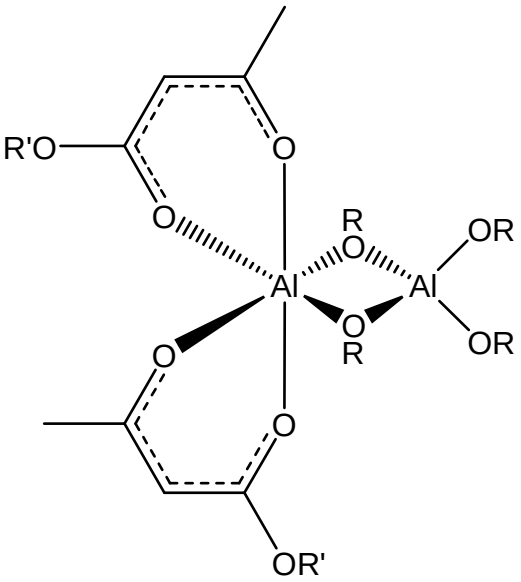

C_1

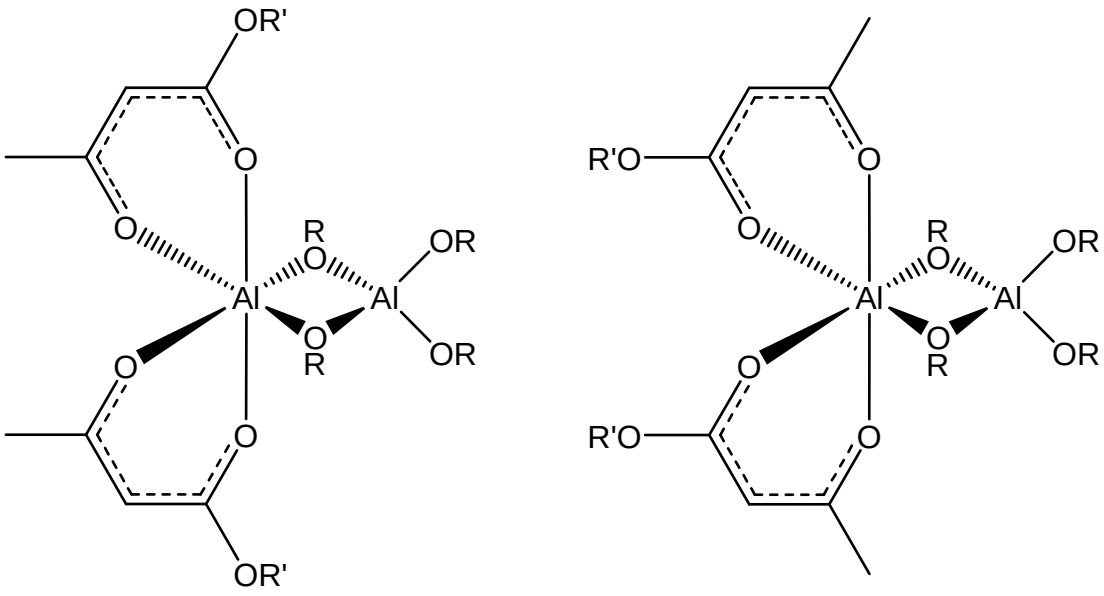

C_2

Figure 3-9 Schematic representation of the possible isomers of $Al_2(\mu\text{-}OR)_2(OR)_2(\beta\text{-ketoesterate})_2$ (OR = O^iPr) (only one enantiomer shown for each case).

These compounds are isostructural to $Al_2(\mu\text{-}OSiMe_3)_2(OSiMe_3)_2(acac)_2$ [50, 51]. In this structure, one aluminum center is tetrahedrally coordinated by two bridging and two terminal alkoxo groups, whereas the other aluminum center is octahedrally coordinated by two chelating β-diketonate ligands and the two bridging alkoxo groups. Given the asymmetric nature of the β-ketoesterate ligands, this results in three possible isomers for complexes

2a–**2d,** one C_1 and two C_2 symmetric (Figure 3-9), each forming a pair of enantiomers, giving six stereoisomers in total. In the NMR spectra, the C_2 symmetric complexes should show one set of signals for the ester ligands and two sets for the O^iPr groups (one for the bridging and one for the terminal) and splitting of these signals in two sets each for the C_1 symmetric complex. Since, in some cases, more than two signal sets were observed for the *β*-ketoesterate ligands and only two signals for the methine protons of the O^iPr groups, different isomers coexist in solution for which the O^iPr signals are not distinguishable. All signals were assigned by COSY, HSQC, and HMBC spectroscopy, showing the coexistence of more than one species in solution. The methine signals of the O^iPr groups are clearly assigned to bridging and terminal groups, but in the C***H***$_3$ region multiple signal overlap was observed and thus a definite assignment is difficult. The $Al_2(\mu\text{-}O^iPr)_2(O^iPr)_2(\beta\text{-ketoesterate})_4$ complexes also show small signals beside a sharp main signal for the COC***H***CO proton, indicating the presence of one dominating species besides small proportions of the other isomers. Only $Al_2(\mu\text{-}O^iPr)_2(O^iPr)_2(^t\text{buac})_4$ (**2d**) gave three signals of almost equal intensity, showing the stability of the different isomers to be almost equal in solution.

Intermolecular ligand exchange between the different species was observed in EXSY experiments for all complexes. For the complexes **2a**, **2c**, and **2d** splitting of the methyl protons of the OMe, O^iPr and O^tBu ester groups, respectively, was also observed in the ^{1}H NMR spectra. Whereas this results in two signals of equal intensity for the ^{i}prac (**2c**) and ^{t}buac (**2d**) derivative, one main signal at 3.66 ppm was found for the meac (**2a**) derivative, along with three smaller signals at 3.77, 3.58, and 3.30 ppm. The splitting of these signals is explained by the different chemical environments for ester groups of ligands with the ester carboxy group in axial position[iii], *i.e.* directed to the second aluminum center, and equatorial position, *i.e.* directed away from the second aluminum center. The additional signals in the ^{1}H NMR spectrum of **2a** are explained by different chemical shifts of the OMe groups for the different isomers, resulting from a different *trans* influence of ester and keto carbonyl groups, which is more pronounced for **2a** than for **2c** or **2d** because the methyl group in **2a** is located one bond closer to the carbonyl group.

The corresponding region of the EXSY spectrum of $Al_2(\mu\text{-}O^iPr)_2(O^iPr)_2(\text{meac})_4$ (**2a**) is reproduced in Figure 3-10, showing exchange between all of these four signals.

[iii] "Axial" and "equatorial" position refers to the $Al_2(\mu\text{-OR})_2$ plane.

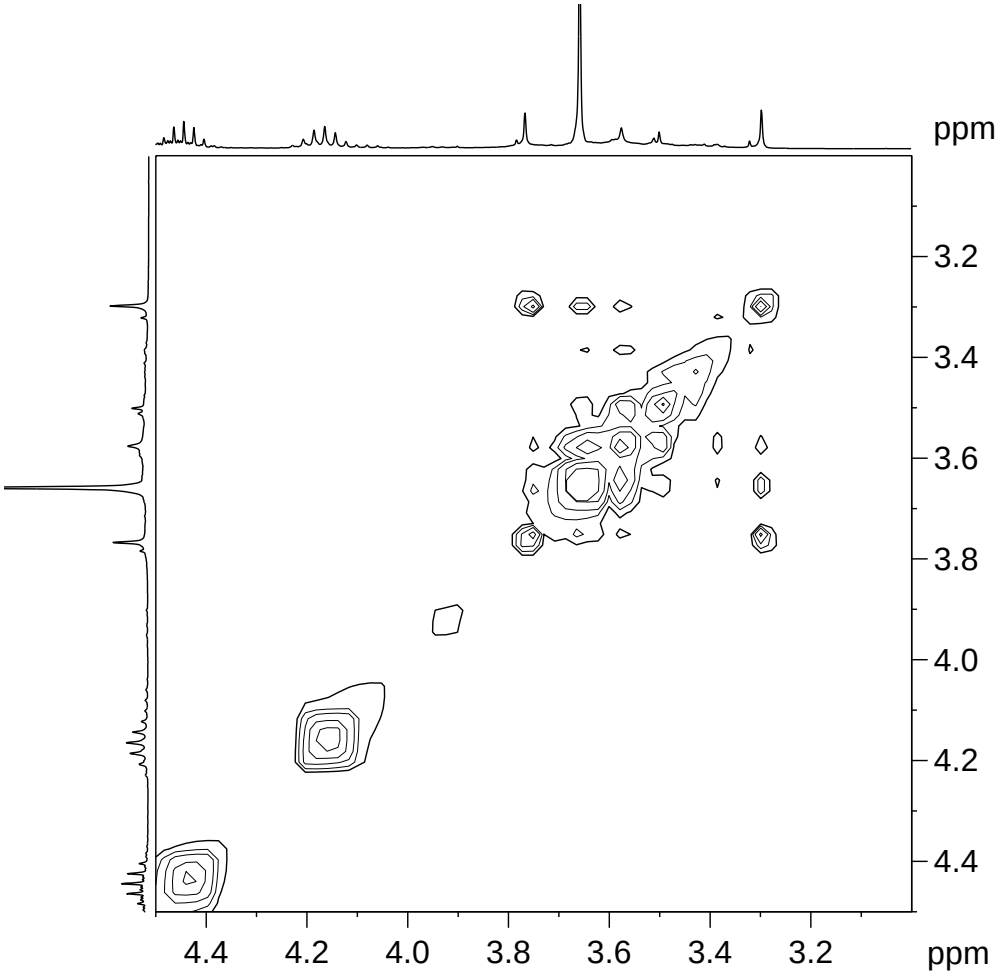

Figure 3-10 EXSY spectrum of **2a** (in $[D_8]$toluene).

In accordance with the NMR spectrum of $[Al(O^iPr)_3]_4$, the signals for the bridging O^iPr groups are shifted to lower field compared to the terminal groups. The shifts of the O^iPr methine protons for the $[Al(OR)_2(\beta\text{-ketoesterate})]_n$ derivatives are compared with that of $[Al(O^iPr)_3]_4$ in Table 3-2. The methine proton signals for all complexes are upfield shifted, corresponding to the reduced Lewis acidity of the substituted aluminum center. For the known analogous acac derivative $Al_2(\mu\text{-}O^iPr)_2(O^iPr)_2(acac)_4$ [50] an analogous upfield shift of the μ-OC***H***Me_2 proton signal was observed, but with significantly higher intensity (4.28 ppm).

Table 3-2 ^{1}H NMR shifts of the Al–O^{i}Pr groups of [Al(O^{i}Pr)$_3$]$_4$ and **2a**–**2d** (in C_6D_6).

	μ-OC***H***Me$_2$	OC***H***Me$_2$	μ-OCH(C***H***$_3$)$_2$	OCH(C***H***$_3$)$_2$
[Al(O^{i}Pr)$_3$]$_4$	4.69	4.41	1.68/1.39[a]	1.32
2a	4.45	4.16	1.49–1.30[b]	1.49–1.30[b]
2b	4.48	4.18	1.48	1.39
2c	4.50	4.21	1.48	1.39
2d	4.55	4.28	1.62–1.25[c]	1.62–1.25[c]

[a] splitting of μ-O^{i}Pr groups [7]

[b] overlap of bridging and terminal OCH(C***H***$_3$)$_2$

[c] overlap with COOC(C***H***$_3$)$_3$

A slight trend to higher ppm values with increasing size of the ester OR groups for the ^{1}H NMR signals of the methine protons was observed. Corresponding ^{13}C NMR signals are not influenced by the ester OR group. The ^{1}H and ^{13}C NMR signals of CO***CH***CO showed no significant change upon variation of the ester functionality, although a slight trend to higher values was observed for the ^{13}C resonances.

Compared to the Al(β-ketoesterate)$_3$ complexes **1a-1d** the ^{1}H NMR resonances for COC***H***CO are upfield shifted. In Table 3-3 the ^{1}H and ^{13}C NMR shifts of CO***CH***CO are compared for the Al(β-ketoesterate)$_3$ (**1a-1d**) and Al$_2$(μ-O^{i}Pr)$_2$(O^{i}Pr)$_2$(β-ketoesterate)$_4$ (**2a-2d**) complexes (compare also Table 3-1). For the ^{13}C resonances no significant difference between the mono- and trisubstituted products was observed. For the other ^{1}H and ^{13}C NMR signals of the β-ketoesterate ligands no significant differences were observed, neither for a variation of the ester functionality nor for the different degrees of substitution.

Table 3-3 Comparison of ^{1}H and ^{13}C NMR shifts of CO***CH***CO of **1a**–**1d** and **2a**–**2d**.

	Al(β-ketoesterate)$_3$			Al$_2$(μ-O^{i}Pr)$_2$(O^{i}Pr)$_2$(β-ketoesterate)$_4$	
	^{1}H (COC***H***CO)[a]	^{13}C (CO***C***HCO)[b]		^{1}H (COC***H***CO)[a]	^{13}C (CO***C***HCO)[b]
1a	5.17	85.0/84.7/84.5	**2a**	5.07 (5.06)[c]	85.5
1b	5.18/5.17	85.2/85.0/84.8	**2b**	5.10 (5.08)[c]	86.0
1c	5.16	85.6/85.4/85.1	**2c**	5.06 (5.04)[c]	86.5
1d	5.13/5.10/5.08	86.4/86.2/86.1/85.8	**2d**	5.06/5.04/4.98	87.4/86.2

[a] in C_6D_6

[b] in [D$_8$]toluene

[c] values in brackets: signals of minor components with different coordination geometry

The ^{27}Al NMR spectrum of **2d** also confirmed the dinuclear structure, giving rise to a broad, relatively weak signal for tetrahedrally coordinated aluminum from 100–40 ppm, with a maximum at 71 ppm, and a sharp one at 2.4 ppm for octahedrally coordinated aluminum (Figure 3-11) [17].

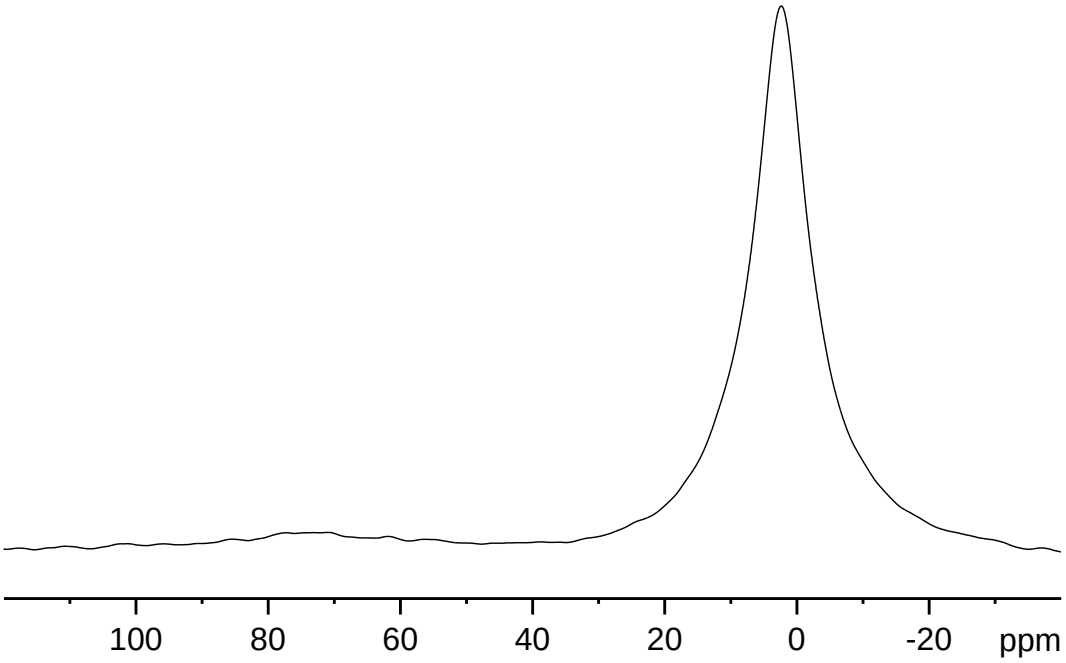

Figure 3-11 ^{27}Al NMR spectrum of **2d** (in C_6D_6).

As mentioned before, crystals suitable for single crystal XRD were obtained for $Al_2(\mu\text{-}O^iPr)_2(O^iPr)_2(^t\text{buac})_4$ (**2d**). Although the quality of the data set was affected by formation of thin platelets and partial decomposition of the crystal during the measurement, the dimeric nature of the compound with one octahedrally and one tetrahedrally coordinated aluminum atom was confirmed (Figure 3-12). The C_1 isomer (compare Figure 3-9) with the two ester groups occupying an equatorial and an axial position was found. Selected bond distances and angles are given in Table 3-4.

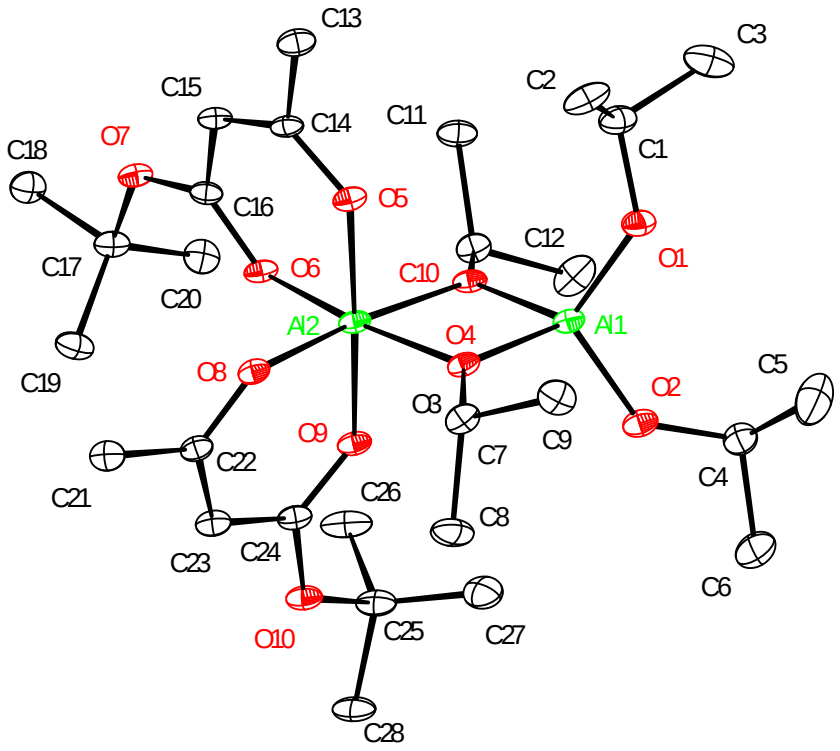

Figure 3-12 Molecular Structure of $Al_2(\mu\text{-}O^iPr)_2(O^iPr)_2(^tbuac)_2$ (**2d**), showing 30 % thermal ellipsoids (hydrogen atoms omitted for clarity).

Table 3-4 Selected bond distances [pm] and angles [°] of **2d**.

Al(1)−O(1)	171.4(5)	Al(2)−O(6)	190.4(4)
Al(1)−O(2)	171.5(4)	Al(2)−O(8)	185.0(4)
Al(1)−O(3)	180.4(4)	Al(2)−O(9)	192.6(4)
Al(1)−O(4)	180.0(4)	O(5)−C(14)	128.1(6)
Al(2)−O(3)	190.1(4)	O(6)−C(16)	126.9(6)
Al(2)−O(4)	191.7(4)	O(8)−C(22)	129.7(7)
Al(2)−O(5)	187.2(4)	O(9)−C(24)	125.7(7)
O(1)−Al(1)−O(2)	113.5(2)	O(4)−Al(2)−O(9)	87.4(2)
O(3)−Al(1)−O(4)	113.2(2)	O(5)−Al(2)−O(6)	91.0(2)
Al(1)−O(3)−Al(2)	100.4(2)	O(5)−Al(2)−O(8)	89.4(2)
Al(1)−O(4)−Al(2)	99.9(2)	O(6)−Al(2)−O(8)	92.9(2)
O(3)−Al(2)−O(4)	77.1(2)	O(6)−Al(2)−O(9)	86.0(2)
O(3)−Al(2)−O(5)	89.9(2)	O(8)−Al(2)−O(9)	90.8(2)
O(3)−Al(2)−O(8)	96.2(2)	O(3)−Al(2)−O(6)	170.9(2)
O(3)−Al(2)−O(9)	93.1(2)	O(4)−Al(2)−O(8)	172.9(2)
O(4)−Al(2)−O(5)	92.8(2)	O(5)−Al(2)−O(9)	177.0(2)
O(4)−Al(2)−O(6)	93.9(2)		

The Al–O distances of the chelating ^{t}buac are longer for the "ester" oxygen compared to that of the "keto" oxygen. An additional *trans* influence from the bridging alkoxo groups causes shorter bond lengths for the equatorial bonds. The Al–O bond distances of the ^{t}buac ligands decrease in the order Al–$O^{ester,ax}$ (192.6(4) pm) > Al–$O^{ester,eq}$ (190.4(4) pm) > Al–$O^{keto,ax}$ (187.2(4) pm) > Al–$O^{keto,eq}$ (185.0(4) pm). *Vice versa*, the different substituents trans to the bridging alkoxo groups result in an asymmetric bridging situation (Al(2)–O(3) 190.1(4) pm and Al(2)–O(4) 191.7(4) pm). The ketoesterate ligand with the ester oxygen (O(6)) trans to the bridging O^{i}Pr group shows an envelope-like conformation with the aluminum atom deviating from the O–C–CH–C–O plane whereas the other is nearly planar and only slightly twisted (Figure 3-11). Analogous conformations were observed for other *β*-diketonate [50, 54, 91], *β*-ketoesterate [90] and dialkylmalonate (compare chapter 3.2) derivatives of aluminum. Interestingly, in the structurally analogous compound $Al_2(\mu\text{-}OSiMe_3)_2(OSiMe_3)_2(acac)_2$ both acac ligands show an envelope conformation [50, 54].

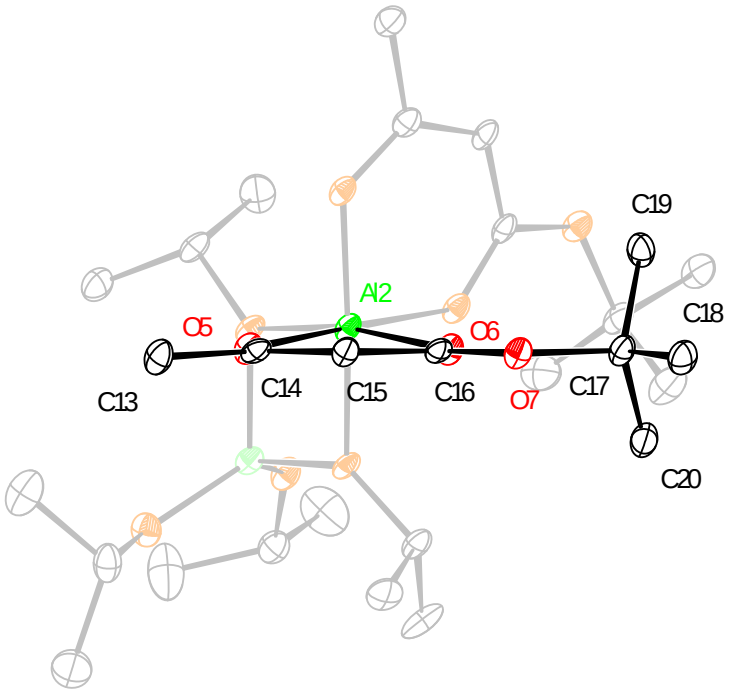

Figure 3-13 View of the envelop-like conformation of one of the ^{t}buac ligands in **2d**.

The Al–(*μ*-O) distances Al(2)–O(3) and Al(2)–O(4) are significantly longer than Al(1)–O(3) (180.4(4) pm) and Al(1)–O(4) (180.0(4) pm), showing the bond distances from the bridging oxygen atoms to the octahedral aluminum center to be significantly longer than to the tetrahedral center. As expected, the distances Al(1)–O(1) (171.4(5) pm) and Al(1)–O(2) (171.5(4) pm) of the terminal alkoxo groups are distinctly shorter than that of the bridging.

Comparison of the molecular structure in the solid state obtained by single crystal XRD and the results of the NMR spectroscopic investigations in solution clearly show that the asymmetric dimeric structure is retained in solution, although dynamic isomerization processes and coexistence of the different isomers can be observed in solution.

Attempts to prepare analogous compounds bearing Al–O^{t}Bu groups instead of the Al–O^{i}Pr groups by using $[Al(O^tBu)_3]_2$ instead of $[Al(O^iPr)_3]_4$ as starting material failed and only yielded the corresponding Al(*β*-ketoesterate)$_3$ complexes and – for substitution degrees lower than three – unreacted $[Al(O^tBu)_3]_2$. This is traced back to the higher steric demand of the O^{t}Bu groups which makes them too big to occupy the bridging position besides an octahedrally coordinated aluminum center.

3.1.1.3 [Al(OR)(*β*-ketoesterate)$_2$]$_n$ Complexes

Attempts to obtain *β*-ketoesterate derivatives of the general formula [Al(OR)(*β*-ketoesterate)$_2$]$_n$, *i.e.* with an Al/*β*-ketoesterate ratio of 1:2, starting from $[Al(O^iPr)_3]_4$ or $[Al(O^tBu)_3]_2$ failed. Direct reaction of $[Al(O^iPr)_3]_4$ with two equiv. of *β*-ketoester per aluminum – analogous to reaction with one or three equiv. – yielded only mixtures of Al(*β*-ketoesterate)$_3$ (**1a**–**1d**) and $Al_2(\mu\text{-}O^iPr)_2(O^iPr)_2$(*β*-ketoesterate)$_2$ (**2a**–**2d**) (Figure 3-14).

Some compounds with a general formula $[Al(\mu\text{-}OR)(CL)_2]_2$ (CL = acac [50], Et$_2$acac [50, 54], etac [50], quin [75]) are reported in literature (compare chapter 1.2.3.1). The *β*-diketonate and *β*-ketoesterate derivatives of aluminum isopropoxide are reported to be quite unstable and to disproportionate to give $Al(CL)_3$ and $Al_2(\mu\text{-}O^iPr)_2(O^iPr)_2(CL)_2$ [50] (Scheme 3-5). Therefore, it is assumed, that an analogous reaction takes place for the other *β*-ketoesterate derivatives reported in this work, although no evidence was found that the $[Al(\mu\text{-}OR)$(*β*-ketoesterate)$_2]_2$ species are formed as intermediates.

$$2\ Al_2(\mu\text{-}OiPr)_2(\beta\text{-ketoesterate})_4 \longrightarrow 2\ Al(\beta\text{-ketoesterate})_3 + Al_2(\mu\text{-}OiPr)_2(OiPr)_2(\beta\text{-ketoesterate})_2$$

Scheme 3-5

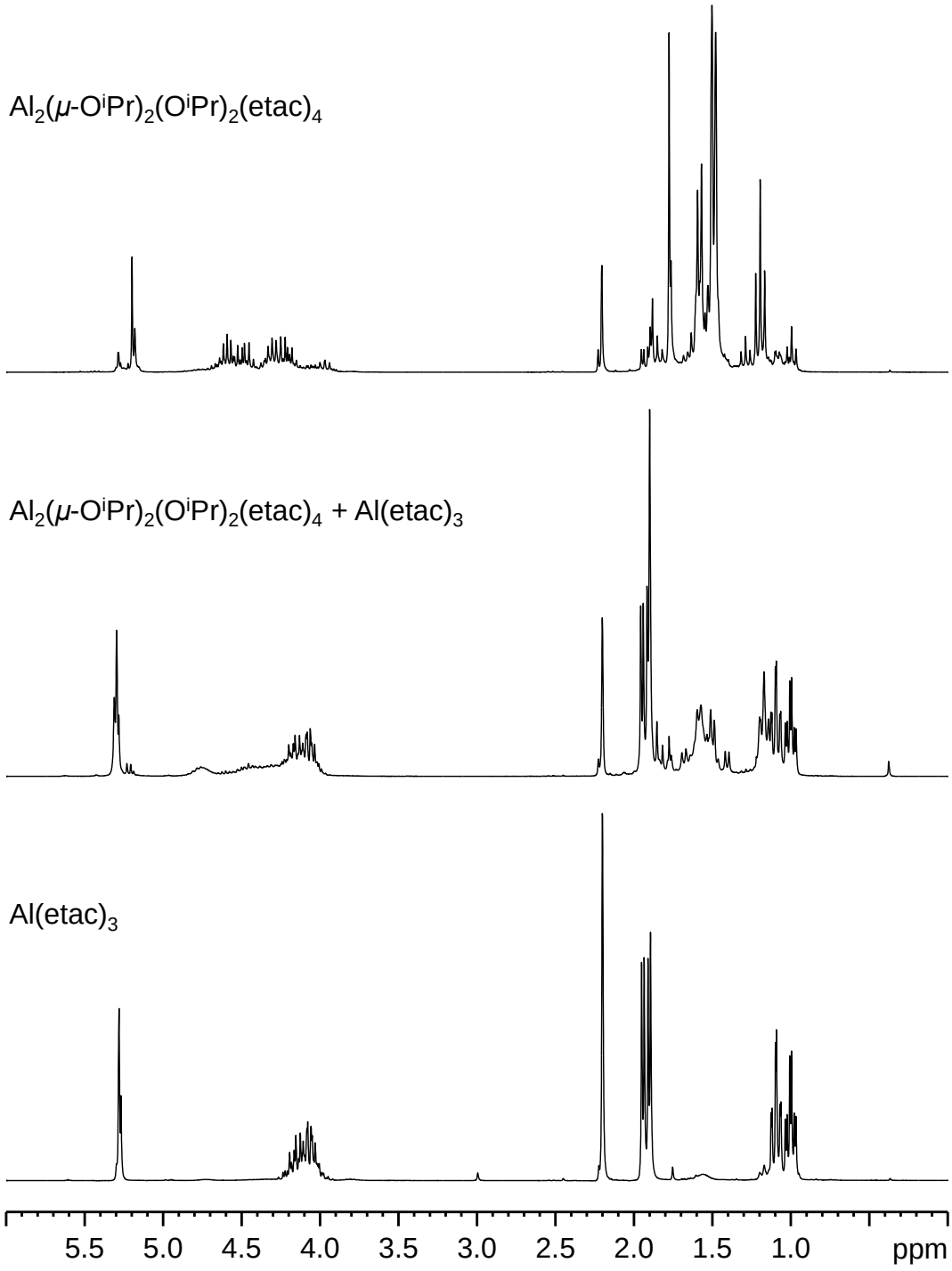

Figure 3-14 ^{1}H NMR spectra of products of the reaction of $[Al(O^{i}Pr)_3]_4$ with one (*top*), two (*center*), and three (*bottom*) equivalents of etac-H (in C_6D_6).

3.1.1.4 Transesterification

It is known that transesterification (Scheme 3-6) can occur as a possible side reaction during the reaction of metal alkoxides with esters [92] or can be used selectively as a preparative synthetic method [93]. *β*-Ketoesters are also capable to undergo transesterification

in the presence of alcohols without additional catalyst [94]. It was reported that coordination of the *β*-ketoesters to metal centers, *e.g.* aluminum, inhibits the transesterification reaction [95].

Scheme 3-6

Transesterification would change the structural and chemical properties of the modified metal alkoxides; for *β*-ketoesters with a functional OR group (compare chapter 3.1.2) this would also result in the loss of the organic functionality. Transesterification as possible side reaction was studied for the reaction of the *β*-ketoesters with $[Al(O^iPr)_3]_4$ by NMR spectroscopy. If transesterification would occur, isopropyl acetoacetate derivatives would be formed. ^{1}H NMR spectroscopy allows easy monitoring of transesterification, because the signal of the methine proton of the formed isopropyl acetoacetate at 5.15–4.85 ppm (in $Al(\mu\text{-}O^iPr)_2(O^iPr)_2(^i\text{prac})_2$), 5.35 ppm (in $Al(^i\text{prac})_3$), or 4.91 (^{i}prac-H) is considerably shifted to higher ppm values compared to the signals of all the other esters. Additional evidence can be obtained from HMBC experiments which show long-range coupling between the methine proton and a carbonyl carbon of the ester group if the isopropyl ester was formed.

In no case transesterification was observed, neither at room temperature nor at 120 °C, except for the reaction of $[Al(O^iPr)_3]_4$ with *three* equivalents of ^{t}buac-H at 120 °C. $Al(^t\text{buac})_3$ (**1d**), formed at room temperature, reacts at 120 °C overnight with the liberated ^{i}PrOH still present in the reaction solution to give $Al(^t\text{buac})_{3-x}(^i\text{prac})_x$ along with free ^{t}BuOH (Scheme 3-7 / Figure 3-15). Longer reaction times eventually led to complete substitution of all O^{t}Bu groups by ^{i}PrOH, giving $Al(^i\text{prac})_3$ (**1c**). Interestingly, no transesterification was observed for the reaction of $[Al(O^iPr)_3]_4$ with *one* equivalent of ^{t}buac-H, after heating for 18 h to 120 °C, and crystalline $Al_2(\mu\text{-}O^iPr)_2(O^iPr)_2(^t\text{buac})_4$ (**2d**) was the only product. Based on these results it is assumed that the steric demand of the O^{t}Bu group in $Al(^t\text{buac})_3$ favors transesterification and formation of sterically less demanding $Al(^t\text{buac})_{3-x}(^i\text{prac})_x$ species. Since one ^{t}buac ligand in **2d** is replaced by two O^{i}Pr groups, the steric constraint might be low enough not to cause transesterification in this case.

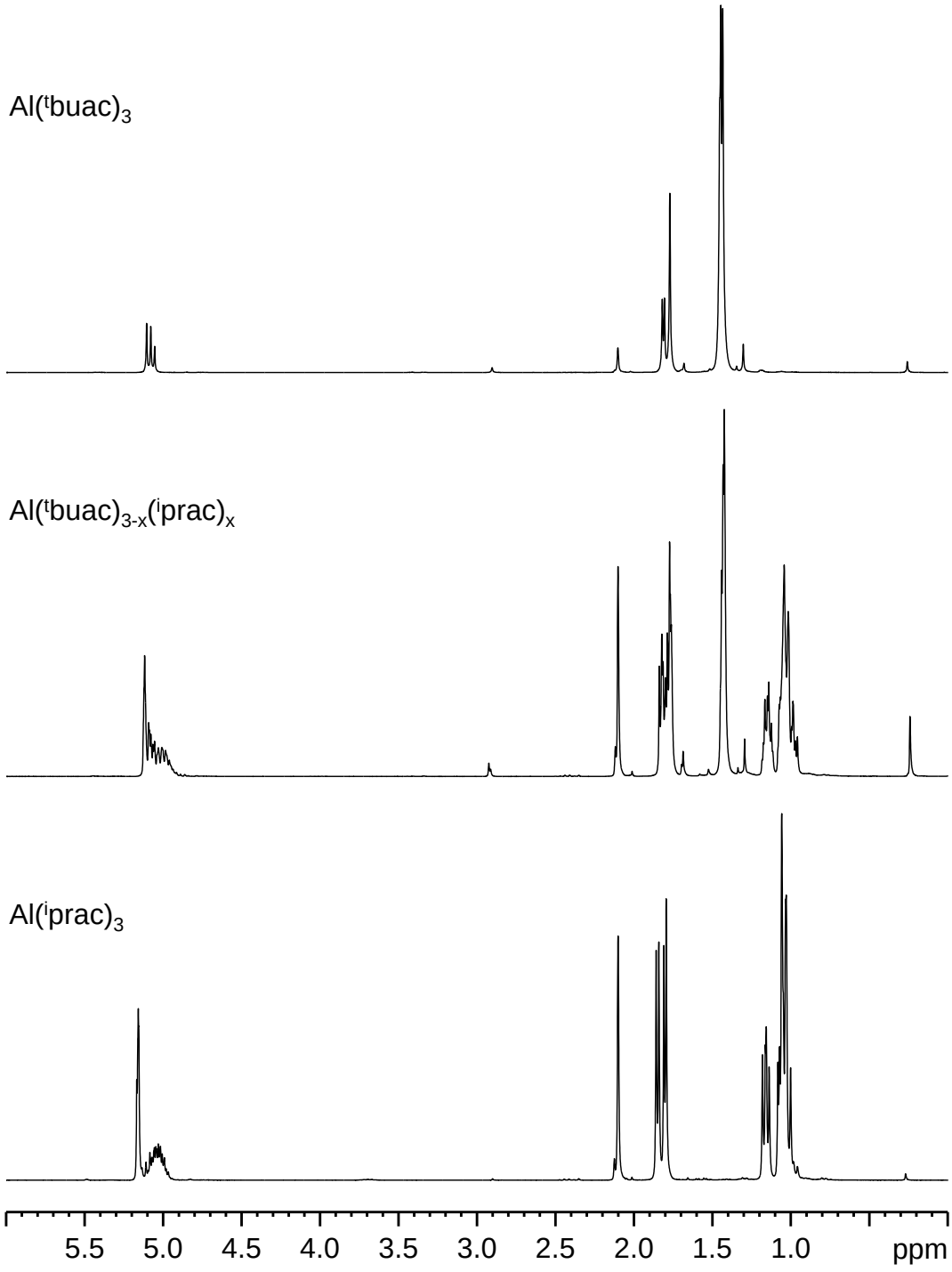

Figure 3-15 ^{1}H NMR spectra of Al(^{t}buac)$_3$ (**1d**) (*center*), Al(^{t}buac)$_{3-x}$(^{i}prac)$_x$, and Al(^{i}prac)$_3$ (**1c**) (*bottom*), showing the proceeding transesterification.

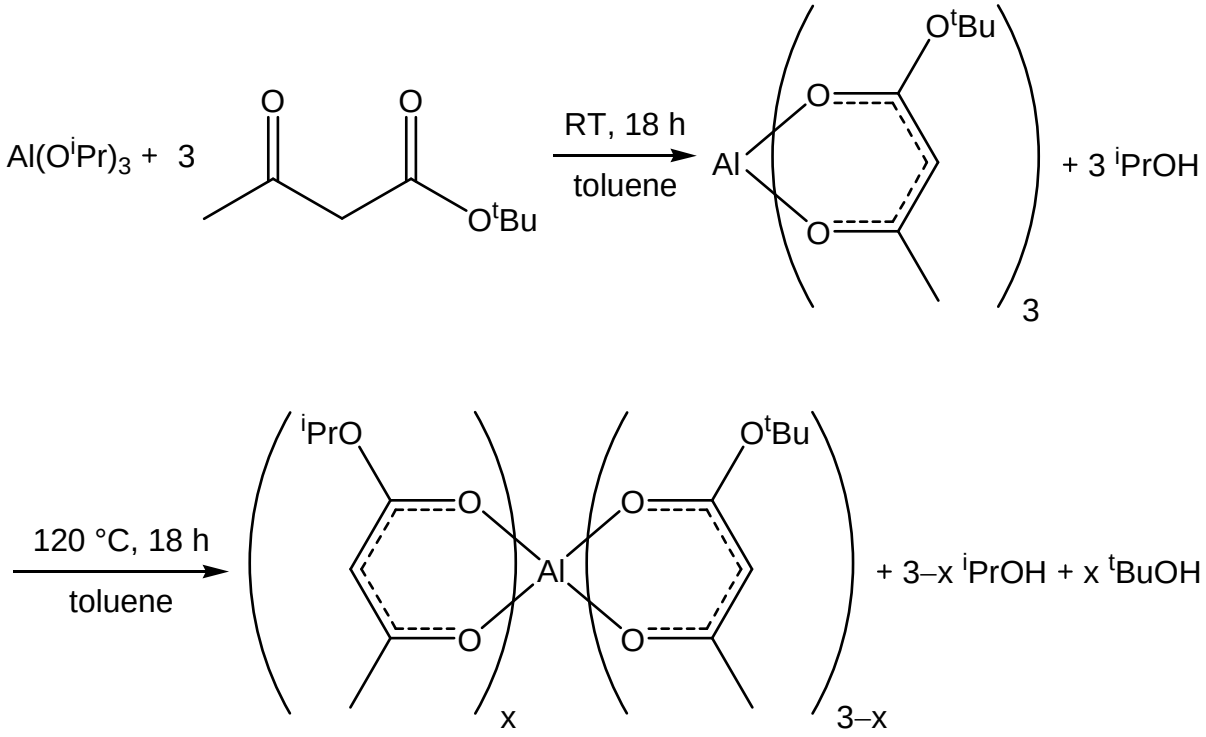

Scheme 3-7

This reaction was studied in more detail by NMR spectroscopy, recording spectra *in situ* at 80°C in intervals of 2 and 4 h, respectively. Figure 3-16 shows the time dependence of the ratio between free ^{i}PrOH and ^{t}BuOH, representing the degree of transesterification.

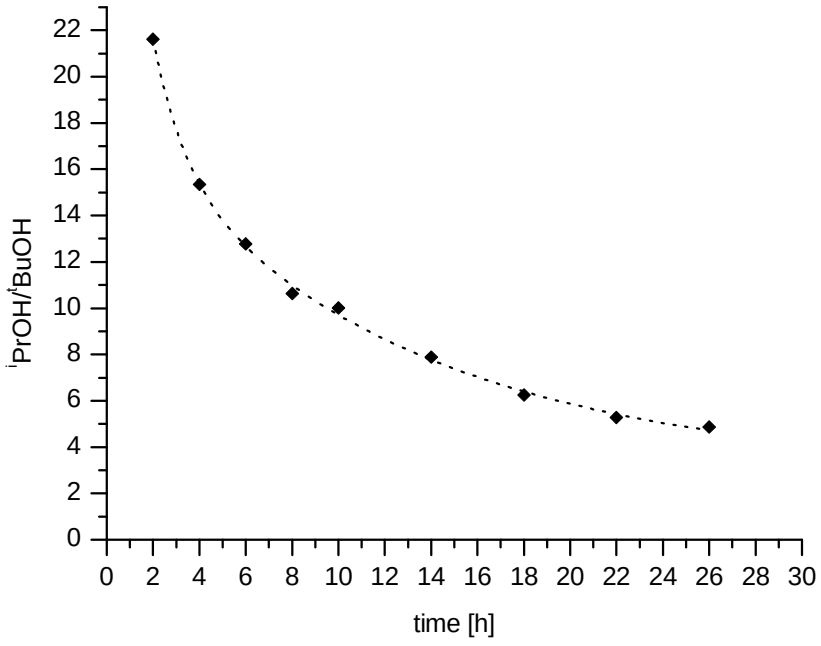

Figure 3-16 Monitoring of transesterification through time dependence of ^{i}PrOH/^{t}BuOH ratio at 80 °C(in [D_8]toluene).

3.1.2 Modification with Functional *β*-Ketoesters

As outlined before, the use of chelating ligands for the modification of metal alkoxides also opens the possibility to introduce organic functionalities, beside the control of the reactivity during hydrolysis. Since the chelating ligands are bound much stronger to the metal center, they remain at least partially in the final material, and the functionalities introduced are available in the material. This opens for example the possibility to obtain precursors for inorganic/organic hybrid materials, where non-functional ligands, such as the *β*-ketoesters described in chapter 3.1.1, may regulate the polarity of the inorganic phase and provide miscibility with the organic phase. The use of ligands bearing additional functionalities provides an anchoring point for a covalent linkage between an inorganic and an organic network, leading to covalently linked inorganic-organic hybrid polymers (compare chapter 1.3)

The use of *β*-ketoesters allows the introduction of an additional functionality by the ester group. In this work, the two *β*-ketoesters allyl acetoacetate (aaa-H) and 2-(methacryloyloxy)ethyl acetoacetate (meaa-H) (Figure 3-10) where used for the modification of $Al(O^iPr)_3$, both bearing a polymerizable C=C double bond as additional functional group.

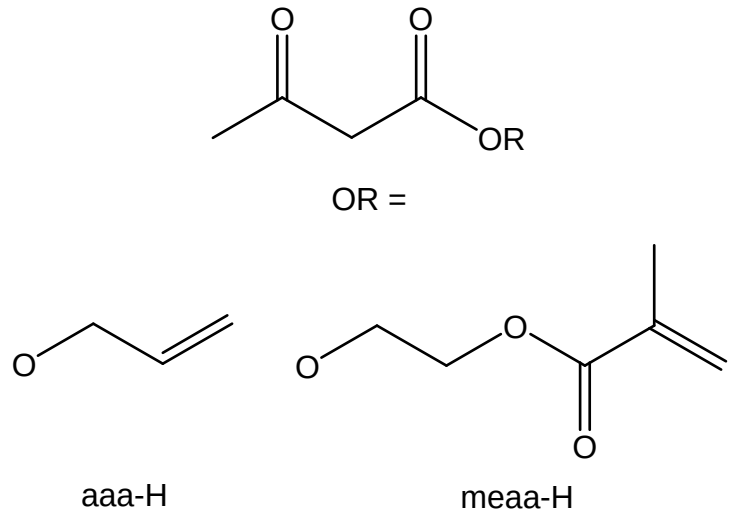

Figure 3-17 Functional *β*-ketoesters used for the modification of aluminum alkoxides.

Reaction of $Al(O^iPr)_3$ with one or three equiv. of aaa-H, following the reaction described for the modification with *β*-ketoalkylesters (compare chapter 3.1.1 / Scheme 3-2), yielded the desired compounds $Al(aaa)_3$ (**1e**) and $Al_2(\mu\text{-}O^iPr)_2(O^iPr)_2(aaa)_2$ (**2e**), respectively. The formation and the structure of both complexes was confirmed by NMR spectroscopy, as well as the retention of the allyl functionality, indicated by the signals at 5.95–5.55 ($OCH_2C\boldsymbol{H}=CH_2$) and 5.10–4.85 ppm ($OCH_2CH=C\boldsymbol{H}_2$) for **1e**, and 6.05–5.85 ($OCH_2C\boldsymbol{H}=CH_2$) and 5.30–5.00 ppm ($OCH_2CH=C\boldsymbol{H}_2$) for **2e** (Figure 3-13).

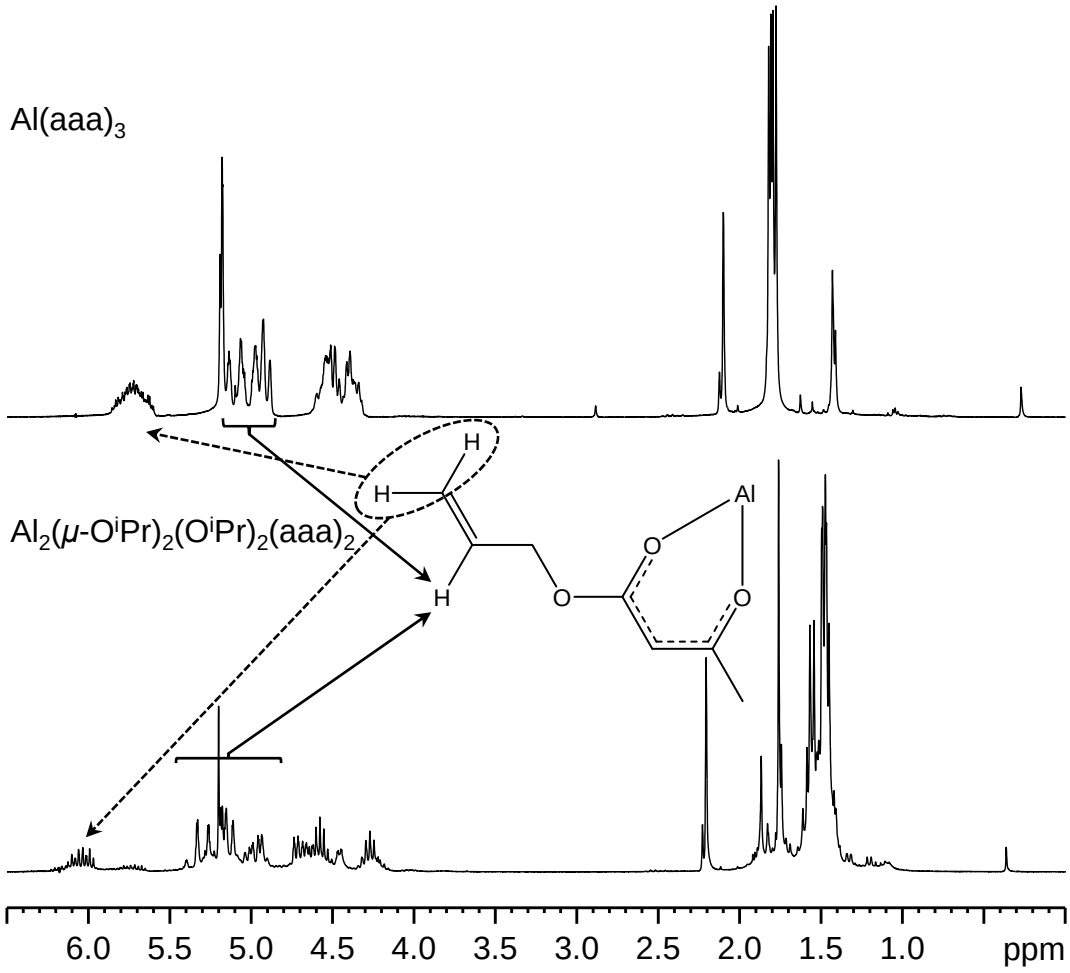

Figure 3-18 ^{1}H NMR spectra of **1e** (*top*) and **2e** (*bottom*) showing the preservation of the polymerizable C=C double bond (in C_6D_6).

The preparation of $Al_2(\mu\text{-}O^iPr)_2(O^iPr)_2(meaa)_2$ (**2f**) according to the described reaction failed due to "gelation" during the reaction at elevated temperatures, indicating thermal instability of the ligand under these reaction conditions. Therefore, the alternative synthetic pathway described above (compare chapter 3.1.1.2), *i.e.* thermal pre-treatment of the alkoxides and subsequent addition of the ligand at room temperature, was applied, giving the desired products. Characterization by NMR spectroscopy showed the expected coordination of the *β*-ketoester giving rise to a signal at 5.05 ppm for the COC***H***CO proton. Signals for the =C***H***$_2$ protons of the methacrylate group at 6.12 and 5.18 ppm showed retention of the polymerizable double bond (Figure 3-19). The small signal at 6.06 ppm results from minor impurities of $Al(meaa)_3$ (**1f**), which is formed because some tetrameric $[Al(O^iPr)_3]_4$ is still present in the pre-treated $Al(O^iPr)_3$ solution, as mentioned before (compare chapter 3.1.1.2). The additional signals at about 2.10 ppm result from residual toluene.

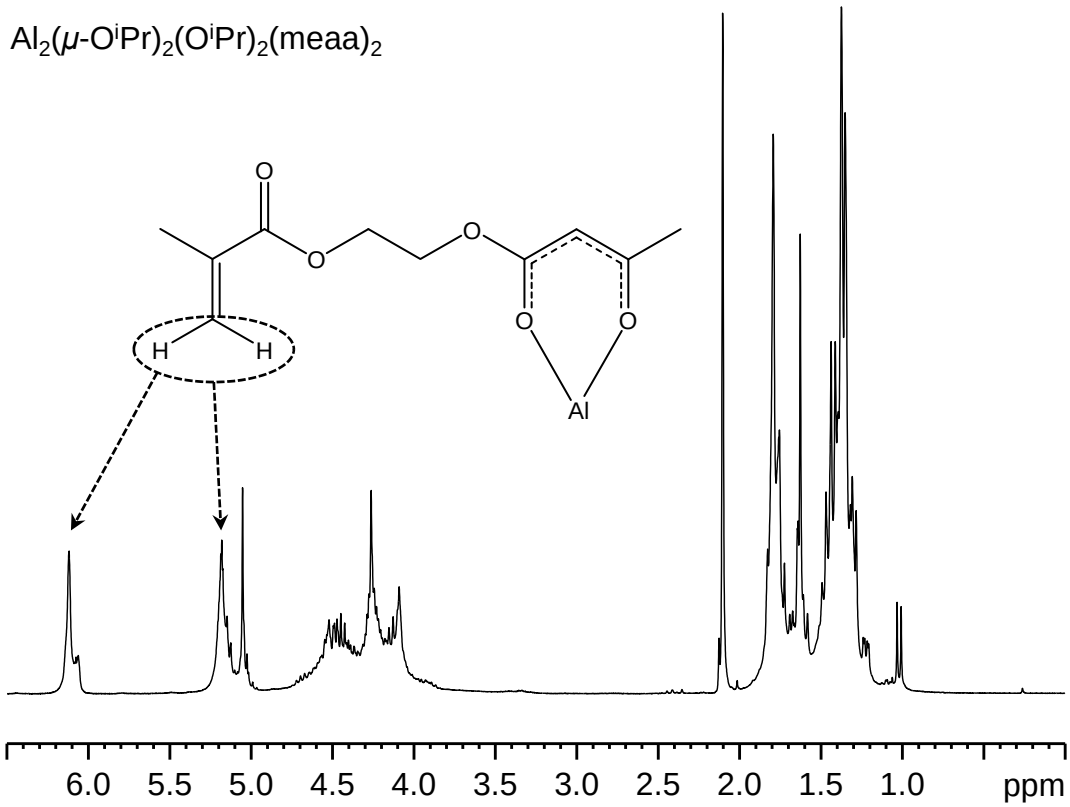

Figure 3-19 ^{1}H NMR spectra of **2e** indicating the preservation of the polymerizable C=C double bond (in C_6D_6).

These results show, that the alternative preparation route, *i.e.* thermal de-oligomerization of $[Al(O^iPr)_3]_4$ prior to ligand substitution under mild reaction conditions (room temperature), opens the possibility of using temperature-sensitive ligands for the modification of $Al(O^iPr)_3$.

It is obvious that for the preparation of $Al(meaa)_3$ (**1f**) the "conventional" route can be applied as well, since no elevated temperatures are needed in this case. $Al(meaa)_3$ is readily formed at room temperature upon addition of three equiv. of meaa-H (per aluminum) to $[Al(O^iPr)_3]_4$ in toluene. Coordination of the ligand and preservation of the methacrylic double bond was again confirmed by ^{1}H NMR spectroscopy (Figure 3-20), giving signals for the COC***H***CO protons at 5.14 ppm and for the =C$\boldsymbol{H}_2$ protons at 6.12/6.08 and 5.25 – 5.15 ppm, respectively. The splitting of the signals at 6.12/6.08 is explained by the coexistence of different isomers, *i.e.* C_1 or C_3 symmetric complexes (compare chapter 3.1.1.1 / Figure 3-4).

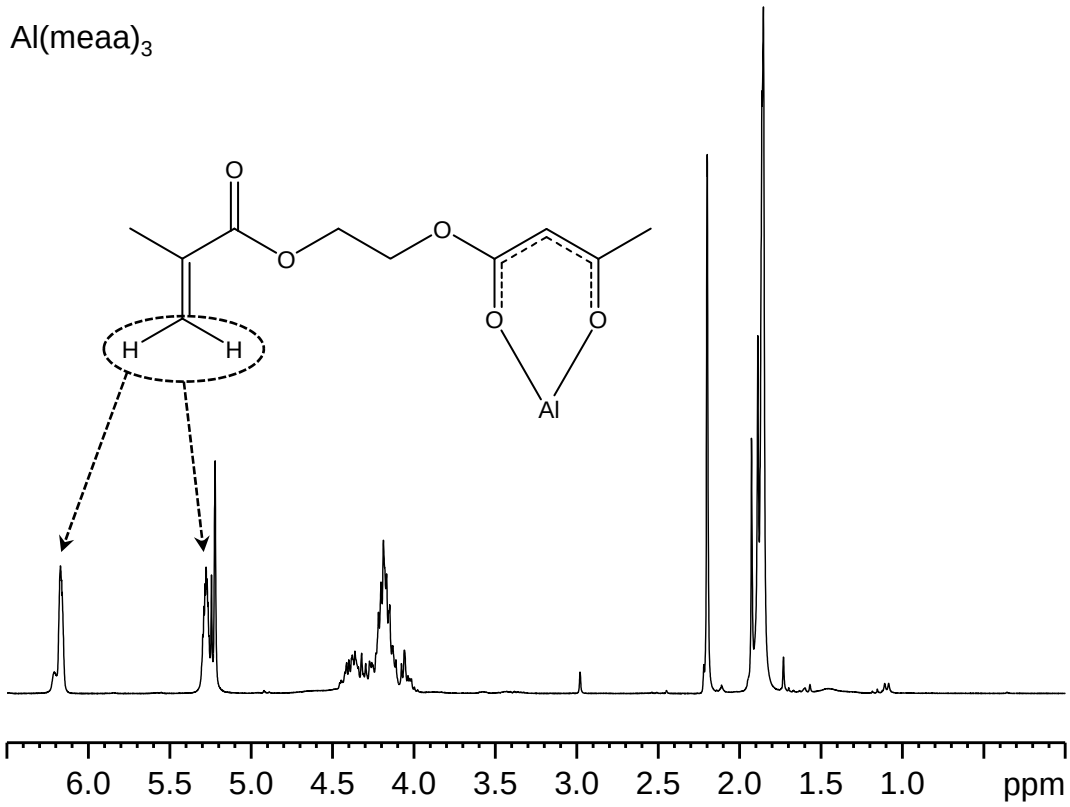

Figure 3-20 ^{1}H NMR spectra of Al(meaa)$_3$ (**1f**) indicating the preservation of the polymerizable C=C double bond (in C_6D_6).

No transesterification was observed in any case, which corresponds to the results for the *β*-ketoalkylesters. For meaa-H transesterification can occur at two positions, *viz.* the acetoacetic ester or the methacrylic ester functionality could be cleaved, leading to either isopropyl acetoacetate or isopropyl methacrylate as by-product. None of these reactions was observed, confirming the stability of the ligand under the reaction conditions applied. In the case of the *β*-ketoesters bearing additional functionalities this is of particular interest, since here transesterification would mean that the functionality is transferred to an Al–OR group, which in course of the sol-gel processing would be cleaved by hydrolysis and would therefore not be available in the final material.

3.1.3 Modification with Modified *β*-Ketoesters[iv]

Based on the results for the modification with different *β*-ketoesters with an unsubstituted acetoacetate moiety, the influence of substituents in the 4 position (methyl 4-methoxyacetoacetate, ethyl 4,4,4-trifluoroacetoacetate) or 2 position (ethyl 2-isopropylacetoacetate) of the ester was studied (Figure 3-21).

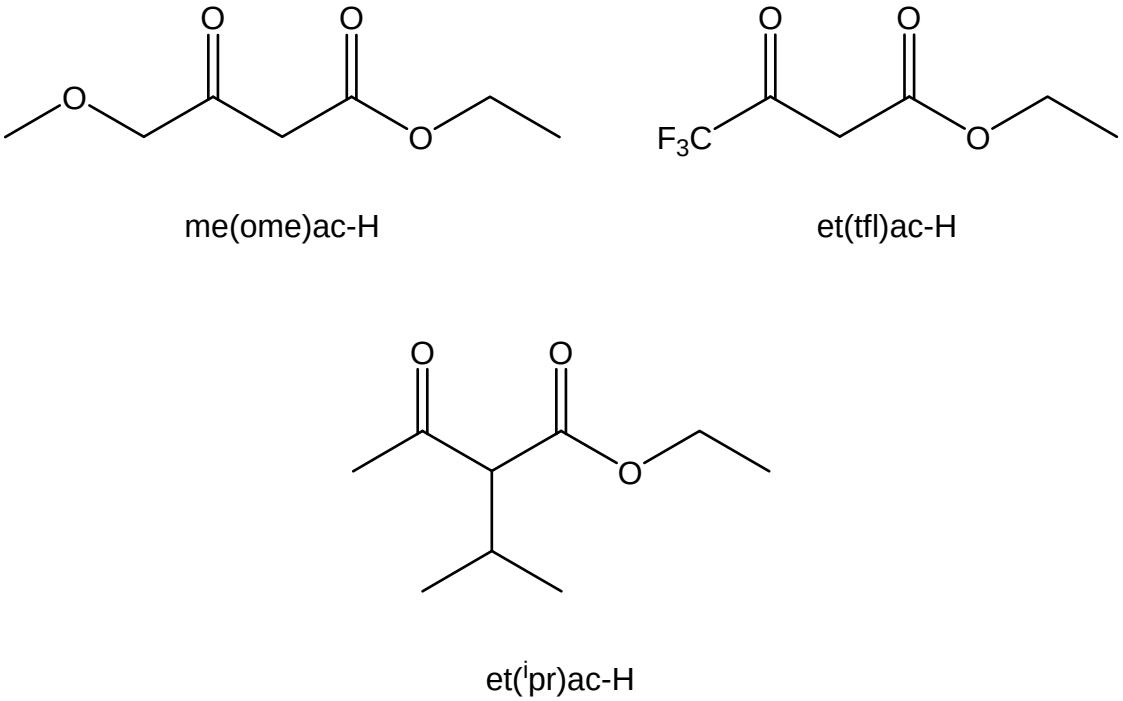

Figure 3-21 Modified *β*-ketoesters used for the modification of aluminum alkoxides.

Modifications were carried out analogous to those for unmodified *β*-ketoesters[iv], *viz.* addition of the ligand to a solution of $Al(O^iPr)_3$ or $Al(O^tBu)_3$ in toluene and subsequent stirring at room temperature and elevated temperatures (compare chapter 3.1.1 / Scheme 3-2).

3.1.3.1 Modification with me(ome)ac-H and et(tfl)ac-H

To study the influence of substituents in the 4 position of the *β*-ketoesters, reactions with me(ome)ac-H and et(tfl)ac-H were carried out. Both ligands reacted readily at room temperature. For a stoichiometric ratio of 1:3 the expected complexes $Al(me(ome)ac)_3$ (**1g**) and $Al(et(tfl)ac)_3$ (**1h**) were obtained starting either from $Al(O^iPr)_3$ or $Al(O^tBu)_3$, which were characterized by NMR spectroscopy.

The ^1H NMR spectra of the complexes showed significantly higher shifts compared to the analogous complexes of the unmodified *β*-ketoesters for the COC***H***CO protons,

[iv] In this context, "*modified β*-ketoesters" refers to *β*-ketoesters bearing additional substituents at the *β*-keto moiety besides the ester functionality, and "*unmodified β*-ketoesters" refers to *β*-ketoesters bearing *no* additional substituents at the *β*-keto moiety besides the ester functionality (compare chapters 3.1.1 and 3.1.2).

viz. 5.89/5.87/5.86 ppm for **1g** compared to 5.17 ppm for Al(meac)$_3$ (**1a**) and 5.60/5.55 for **1h** compared to 5.18/5.17 ppm for Al(etac)$_3$ (**1b**). This reflects the influence of the substituents at the 4 position on the electronic properties of the ligand, showing the deshielding effect at the 2 position caused by the electron withdrawing effect of the OMe group (**1g**) and fluorine atoms (**1h**), respectively. In the ^{13}C NMR spectrum of **1h** also a significant shift to higher field was observed for the keto carbonyl carbon (170.0–169.2 ppm), being less shifted than the ester carbonyl carbon (176.1–176.0 ppm). This weaker deshielding of the keto carbonyl carbon compared to the ester carbonyl carbon was only observed for the et(tfl)ac ligand.

For the reaction of Al(O^{i}Pr)$_3$ with one equiv. of ligand, interestingly no formation of Al(*β*-ketoesterate)$_3$ and unreacted [Al(O^{i}Pr)$_3$]$_4$ was observed as for the unmodified *β*-ketoesters (compare chapter 3.1.1.1 / Scheme 3-3). NMR spectroscopy revealed that for these modified *β*-ketoesters the 1:1 products Al$_2$(*μ*-O^{i}Pr)$_2$(O^{i}Pr)$_2$(me(ome)ac)$_2$ (**2g**) and Al$_2$(*μ*-O^{i}Pr)$_2$(O^{i}Pr)$_2$(et(tfl)ac)$_2$ (**2h**) were obtained already at room temperature. Heating of the reaction solutions did not cause any changes of the products.

^{1}H NMR spectroscopy also showed a deshielding of the COC***H***CO protons compared to the unmodified analogs, giving resonances at 5.78 ppm for **2g** and 5.57 ppm for **2h**, respectively, compared to 5.07 for Al$_2$(*μ*-O^{i}Pr)$_2$(O^{i}Pr)$_2$(meac)$_2$ (**2a**) and 5.10 ppm Al$_2$(*μ*-O^{i}Pr)$_2$(O^{i}Pr)$_2$(etac)$_2$ (**2b**), respectively. Compared to the trisubstituted analogs (**1g** and **1h**), the signals are slightly less shifted, corresponding to the observations for the unmodified derivatives. The signals for the Al–O^{i}Pr groups all appear in the same range as for the unmodified complexes and no influence of the additional substituents at the *β*-ketoester ligands was observed. The ^{13}C NMR resonances of the carbonyl carbons of **2h** showed a similar reversion as for **1h**.

Although no influence can be observed on the ^{1}H NMR signals, it is assumed that the additional substituents influence the electronic structure of the residual Al–O^{i}Pr groups upon coordination in a different way than the unmodified ligands do, *i.e.* the ligands have a different *trans* influence, and therefore formation of the monosubstituted dimeric products is favored over the formation of the trisubstituted monomeric complexes, as it is observed for the unmodified *β*-ketoesters.

As for the unmodified analogs derived from meac-H (**1a** and **2a**) and etac-H (**1b** and **2b**), no transesterification reactions were observed.

3.1.3.2 Modification with et(^{i}prac)-H

For the reaction of Al(O^{i}Pr)$_3$ with three equiv. of et(^{i}pr)ac-H, at room temperature no coordination was observed at all, indicating a lower reactivity of *β*-ketoesters with a substituent in 2 position (due to a lowering of the acidity of the proton in the 2 position caused by the electron donating effect of the alkyl group). Heating to 100 °C finally resulted in coordination and isolation of a product after removal of the volatiles *in vacuo*. NMR spectroscopy revealed a structure analogous to unmodified *β*-ketoester derivatives, *viz.* Al(et(^{i}pr)ac)$_3$ (**1i**). Compound **1i** was alternatively obtained starting from Al(O^{t}Bu)$_3$.

For the reaction of $Al(O^iPr)_3$ with one equiv. of et(^{i}pr)ac-H following an analogous reaction procedure as described above for **1i** yielded $Al(\mu\text{-}O^iPr)_2(O^iPr)_2(et(^i pr)ac)_2$ (**2i**) with an analogous structure as the unmodified homologue **2b**, as determined by NMR spectroscopic methods.

Since it is known that analogous reactions of $Al(O^sBu)_3$ with acetylacetonate derivatives substituted in the 3 position lead to hydrodeacylation as competing reaction [96], the reaction of $Al(O^iPr)_3$ with one equiv. et(^{i}pr)ac)-H was also studied in terms of side reactions. Therefore the reaction was performed directly in [D_8]toluene, and the products formed were characterized without removal of the volatiles. ^{1}H and ^{13}C NMR as well as COSY, HSQC, and HMBC spectroscopy revealed the formation of various byproducts besides formation of **2i**. Due to the asymmetric nature of et(^{i}pr)ac-H compared to 3-substituted acac-H derivatives, four different products can be formed by hydrodeacylation (Figure 3-22), and especially the carbonate species is known to be unstable and can decompose to give further products.

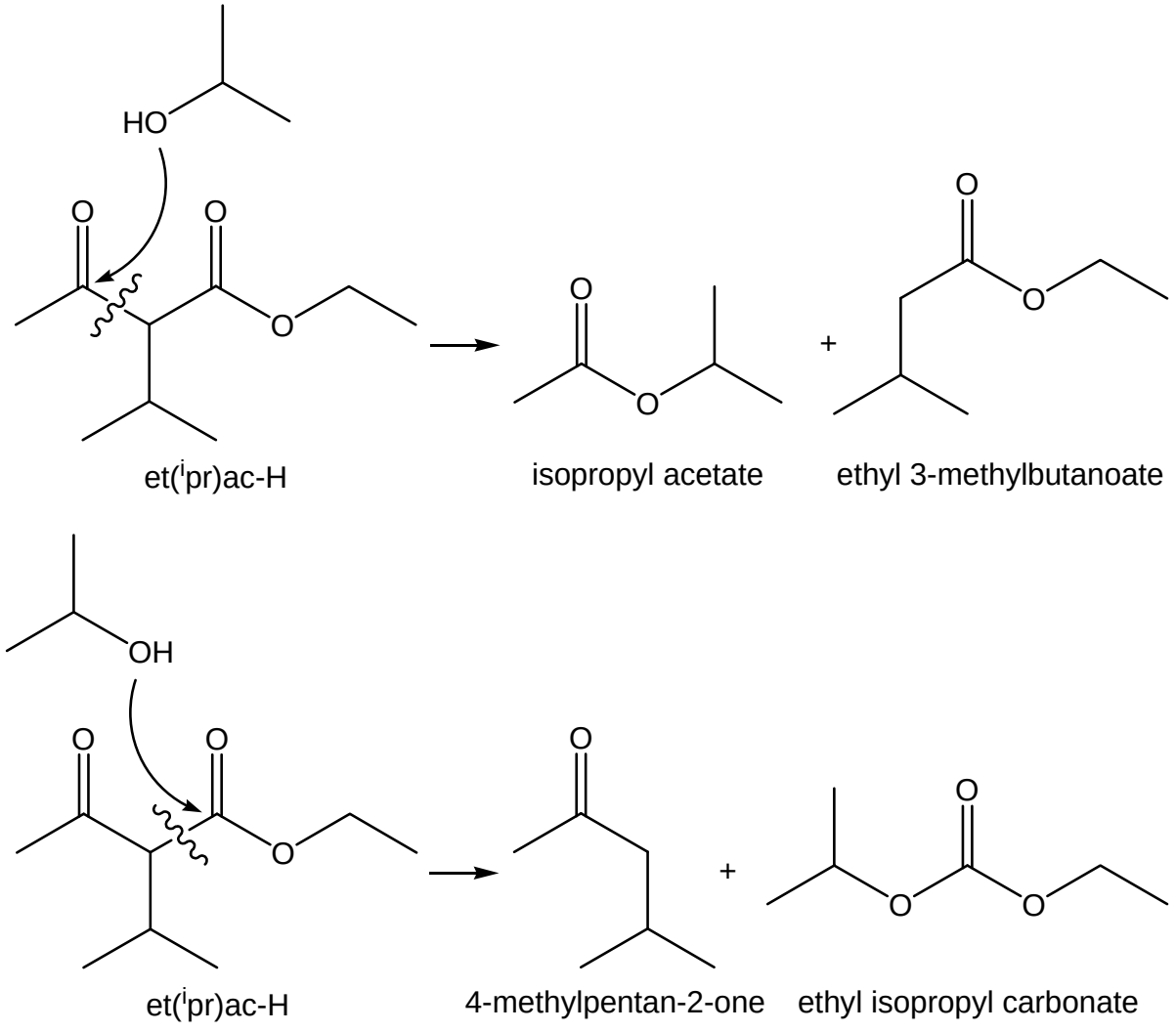

Figure 3-22 Schematic representation of possible hydrodeacylation reactions and products thereof.

The multitude of signals could not be assigned to the respective products and therefore no evidence can be given, which products are (preferentially) formed. Only the formation of 4-methylpentan-2-one can be definitely assured by the presence of a ***C***O resonance at 203.5 ppm in the ^{13}C NMR spectrum, since all other ***C***O resonances are in the range of 170–190 ppm. In this range multiple signals are detected, indicating the formation of different compounds.

This is another example for a competing reaction to the ligand substitution and coordination besides the reported hydrodeacylation of 3-substituted acac-H derivatives [96]. Another example is the lactame formation as competing reaction to the coordination of lysine [97]. In both cases a clear dependence on the type of metal center was observed, showing a dependence of the degree of the side-reaction in the series Al >> Zr > Ti, indicating a main influence of the Lewis acidity of the metal center.

3.1.4 Conclusions

Reaction of $Al(OR)_3$ (OR = O^{t}Bu, O^{i}Pr) with three equivalents of *β*-ketoesters (meac-H, etac-H, ^{i}prac-H, ^{t}buac-H, aaa-H, meaa-H, me(ome)ac-H, et(tfl)ac-H) at room temperature in toluene yielded products of the general formula Al(*β*-ketoesterate)$_3$ (**1a**–**1h**), except et(^{i}pr)ac-H, where elevated temperatures had to be applied to obtain Al(et(^{i}pr)ac)$_3$ (**1i**). The reaction was straightforward, and no influence of the *β*-ketoester or the alkoxide on the formation or structure of the product was observed, with one exception: The complex Al(^{t}buac)$_3$ (**1d**) underwent transesterification in the presence of ^{i}PrOH at elevated temperatures, giving Al(^{i}prac)$_x$(^{t}buac)$_{3-x}$. This behavior is attributed to the steric bulk of the O^{t}Bu groups, since it is not observed for a lower substitution degree. This side-reaction has to be taken into account especially for the reaction of Al(O^{i}Pr)$_3$ with ^{t}buac-H, since during this reaction *in situ* generated ^{i}PrOH is capable to undergo transesterification with the substitution product. All Al(*β*-ketoesterate)$_3$ (**1a**–**1i**) complexes are mononuclear octahedral complexes, giving rise to C_1 and C_3 symmetric isomers due to the asymmetric chelating ligand, coexisting in solution without preference.

Reaction of [Al(O^{i}Pr)$_3$]$_4$ with one equivalent of *β*-ketoester at room temperature did not give the anticipated monosubstituted products, except for me(ome)ac-H and et(tfl)ac-H. For all other ligands, initially formed Al(*β*-ketoesterate)$_3$ had to be reacted with residual [Al(O^{i}Pr)$_3$]$_4$ at elevated temperatures to give Al$_2$(*μ*-O^{i}Pr)$_2$(O^{i}Pr)$_2$(*β*-ketoesterate)$_2$ (**2a**–**2e**, **2g**-**2i**). This procedure worked for all ligands excepted for meaa-H, where it failed due to thermal instability of the ligand. The resulting derivatives **2a**–**2i** were stable at room temperature in solution as well in isolated form. This indicates that Al$_2$(*μ*-O^{i}Pr)$_2$(O^{i}Pr)$_2$(*β*-ketoesterate)$_2$ is the thermodynamically stable compound and Al(*β*-ketoesterate)$_3$ is formed for kinetic reasons. For the ligands me(ome)ac-H and et(tfl)ac-H – modified in the 4 position compared to the unmodified ligands meac-H and etac-H – the complexes Al$_2$(*μ*-O^{i}Pr)$_2$(O^{i}Pr)$_2$(me(ome)ac)$_2$ (**2g**) and Al$_2$(*μ*-O^{i}Pr)$_2$(O^{i}Pr)$_2$(et(tfl)ac)$_2$ (**2h**) were directly formed upon reaction at room temperature, indicating an influence of the electronic properties of the ligand on the reaction kinetics.

The monosubstituted products were asymmetric dimers with one aluminum atom coordinated by two *β*-ketoesterate ligands, connected to the second, tetrahedrally coordinated aluminum center bearing two additional O^iPr groups, by two bridging O^iPr groups. Due to the asymmetric nature of the *β*-ketoesterate ligands one C_1 and two C_2 symmetric isomers could be formed. It was shown, that in most cases more than one isomer coexist in solution. The C_1 symmetric isomer crystallized for $Al_2(\mu\text{-}O^iPr)_2(O^iPr)_2(^tbuac)_2$ **2d** and was characterized by single crystal XRD.

For the preparation of $Al_2(\mu\text{-}O^iPr)_2(O^iPr)_2(meaa)_2$ (**2f**), an alternative synthetic procedure was applied, *viz.* thermal de-oligomerization of $[Al(O^iPr)_3]_4$ and subsequent addition of the ligand after cooling to room temperature. This procedure allows using temperature sensitive ligands and proves the dependence of the reaction kinetics on the degree of oligomerization of the aluminum alkoxide. Preservation of the polymerizable C=C double bond was proven, and thus a possible precursor for covalently linked dual inorganic-organic hybrid polymers was synthesized.

The formation of $Al_2(\mu\text{-}O^iPr)_2(O^iPr)(et(^ipr)ac)_2$ (**2i**) was accompanied by the formation of different byproducts resulting from hydrodeacylation reactions as side reaction competing to coordination.

The kinetic control on the product formation, *viz.* the formation of Al(*β*-ketoesterate)$_3$ instead of $Al_2(\mu\text{-}O^iPr)_2(O^iPr)_2$(*β*-ketoesterate)$_2$ at room temperature, was not described for reactions of aluminum alkoxides with *β*-diketones or *β*-ketoesters until present and is in contrast to reports for reactions with acac-H [50].

The alkoxo group of the esters had no influence on the structure of the products and only minor influence on the electronic properties, reflected in slightly different ^1H NMR shifts of the bridging and terminal O^iPr groups of the monosubstituted dimers. Additional functionalities at the *β*-keto moiety in the modified *β*-ketoesters did not cause structural changes, although the product formation was influenced (*vide supra*). Furthermore the additional substituents only affected the electronic structure of the *β*-ketoesterate ligands itself, but no influence on the Al–O^iPr groups was observed (by means of NMR spectroscopic methods).

Compared to $Al_2(\mu\text{-}O^iPr)_2(O^iPr)_2(acac)_2$, aging to trinuclear $Al_3(\mu\text{-}O^iPr)_4(O^iPr)_2(acac)_3$ was not observed for the corresponding *β*-ketoesterate derivatives [50]. Thus, significant differences in reactivity of *β*-ketoesters and *β*-diketones with $[Al(O^iPr)_3]_4$ are noticed, since the structures of the formed derivatives may be different, depending on the side conditions (temperature, time). This may have important consequences if those ligands are used to modify aluminum alkoxides for sol-gel processing.

Only Al(*β*-ketoesterate)$_3$ was obtained for the reaction of $Al(O^tBu)_3$ with *β*-ketoesters, independent of the stoichiometric ratio or the reaction conditions. This is traced back to the higher steric demand of the O^tBu group compared to the O^iPr group, making it unsuitable for the bridging position.

Compounds of the general formula $[Al(OR)(\beta\text{-ketoesterate})_2]_n$ were not obtained in any case. Corresponding reactions yielded only mixtures of $Al(\beta\text{-ketoesterate})_3$ and $Al_2(\mu\text{-}OR)_2(OR)_2(\beta\text{-ketoesterate})_2$ (OR = O^iPr) or $[Al(OR)_3]_2$ (OR = $O^tBu)_3$. This is in agreement with literature reports, indicating a low stability of compounds $[Al(\mu\text{-}O^iPr)(CL)_2]_n$ (CL = acac, etac) [50]

3.2 Modification of Aluminum Alkoxides with Dialkylmalonates

Based on the results for the modification of aluminum alkoxides with *β*-diketones [50, 51, 54] and *β*-ketoesters (compare chapter 3.1), the modification with dialkylmalonates was studied (Figure 3-23). To the best of my knowledge, the direct modification of aluminum alkoxides with dialkylmalonates was not reported yet.

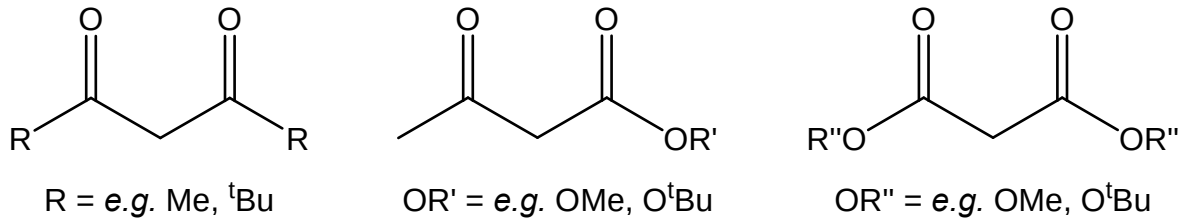

Figure 3-23 Comparison of the schematic structures of *β*-diketones, *β*-ketoesters, and dialkylmalonates.

Analogous studies as for the modification of *β*-keto alkylesters were carried out with the corresponding dialkylmalonates, *viz.* dimethyl- (dmem-H), diethyl- (detm-H), diisopropyl- (d^{i}prm-H), and di-*tert.*-butylmalonate (d^{t}bum-H) (Figure 3-24).

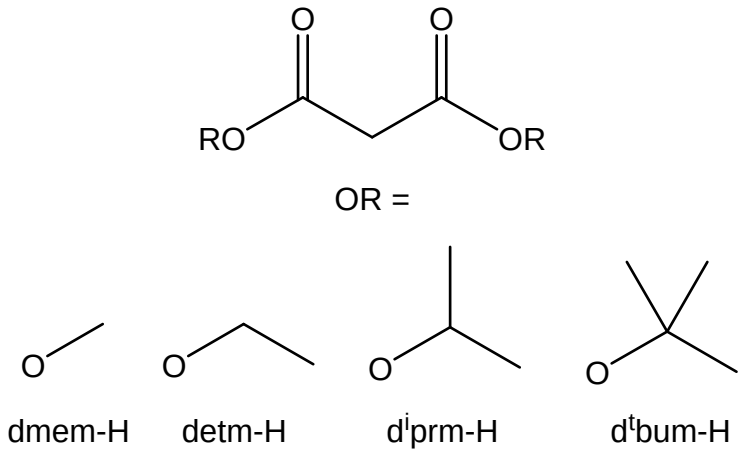

Figure 3-24 Dialkylmalonates used for the modification of aluminum alkoxides.

As expected, dialkylmalonates showed a lower reactivity towards substitution reactions with aluminum alkoxides compared to *β*-ketoesters, due to the presence of a second OR substituent and therefore a lowered tendency to form the reactive enolic form. For the reaction with Al(O^{i}Pr)$_3$, no coordination of the dialkylmalonate was observed at room temperature, and modification of Al(O^{t}Bu)$_3$ was very slow at room temperature (approx. 20 % conversion after 3 d). Elevated temperatures accelerated the reactions of Al(O^{t}Bu)$_3$ significantly and also allowed the modification of Al(O^{i}Pr)$_3$. However, significantly longer reaction times were necessary compared to the reactions of *β*-ketoesters with aluminum alkoxides.

3.2.1 Al(dialkylmalonate)$_3$ Complexes

Monomeric complexes Al(dmem)$_3$ (**3a**), Al(detm)$_3$ (**3b**), Al(d^{i}prm)$_3$ (**3c**), and Al(d^{t}bum)$_3$ (**3d**) were obtained by reaction of Al(O^{t}Bu)$_3$ with the corresponding malonate[v] in a 1:3 stoichiometric ratio in toluene at room temperature to 80 °C (Scheme 3-8). Reaction was slow (4–11 days) but nevertheless proceeded already at room temperature. Due to the lack of residual Al–OR groups, complexes **3a**–**3d** are not conventional precursors for sol-gel processing[vi], but as for the Al(*β*-ketoesterate)$_3$ analogs (compare chapter 3.1.1.1) their characterization is of interest for a better understanding of the coordination behavior of malonate ligands towards aluminum and is also essential for a complete understanding and interpretation of other products with a lower degree of substitution (*vide infra*). As a matter of fact, these complexes also prove the possibility to directly replace O^{i}Pr groups at the aluminum center by malonates without requiring additional reagents for deprotonation of the malonate.

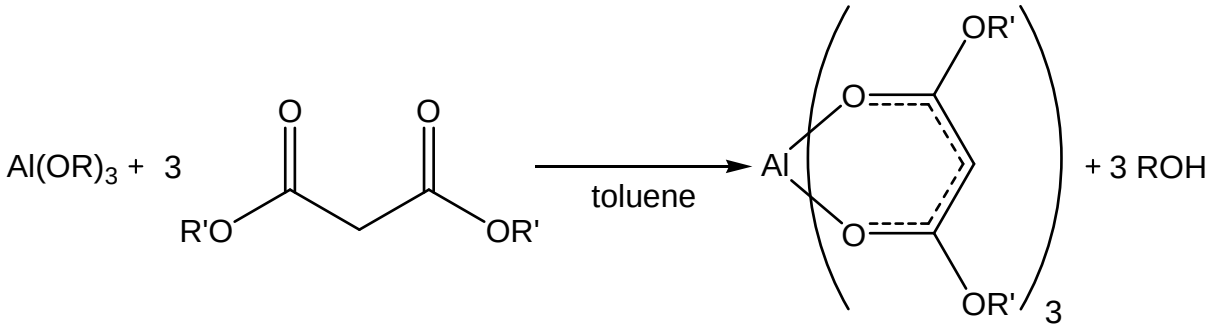

OR = O^{i}Pr; OR' = O^{i}Pr, O^{t}Bu

OR = O^{t}Bu; OR' = OMe, OEt, O^{i}Pr, O^{t}Bu

Scheme 3-8

Complexes Al(d^{i}prm)$_3$ (**3c**) and Al(d^{t}bum)$_3$ (**3d**) were also obtained by reacting Al(O^{i}Pr)$_3$ with d^{i}prm-H or d^{t}bum-H in toluene at 60° or 80°C. Although the reactions were slow, as they were with Al(O^{t}Bu)$_3$, Al(O^{i}Pr)$_3$ did not react with malonates at room temperature at all. The reaction between Al(O^{i}Pr)$_3$ and diprm-H was also done following an alternative reaction sequence described before for *β*-ketoesters (compare chapter 3.1.1.2), where [Al(O^{i}Pr)$_3$]$_4$ is thermally treated before addition of the ligand, causing de-oligomerization of the tetrameric units to give a solution of di, tri- and tetrameric species. The smaller units showed higher reactivity towards substitution by *β*-ketoesters, and the same was observed for malonates.

These results lead to some conclusions:

[v] In terms of a better readability, "malonate(s)" is used synonymously to "dialkylmalonates"

[vi] Of course, also the dialkylmalonato ligands can be hydrolyzed under harsh conditions and therefore also the Al(dialkylmalonate)$_3$ complexes **3a**–**3d** can act as precursors for alumina materials.

- The reaction rate of the substitution is inversely correlated to the degree of oligomerization of the aluminum alkoxide.
- The lower degree of oligomerization of $[Al(O^tBu)_3]_2$ compared to $[Al(O^iPr)_3]_4$ leads to higher reaction rates for the former, despite the higher steric demand of the O^tBu groups compared to the O^iPr groups, which lowers the reactivity towards substitution reactions.

Complexes **3a** and **3b** could not be prepared from $Al(O^iPr)_3$ since transesterification occurred as side reaction (compare chapter 3.2.5).

Compound **3c** also was prepared by an alternative, solvent-free reaction procedure, in which $Al(O^iPr)_3$ was reacted with 10 equiv. of d^iprm-H. Since neither $[Al(O^iPr)_3]_4$ nor $Al(d^iprm)_3$ (**3c**) are well soluble in d^iprm-H and the reaction mixture stayed heterogeneous even at 120 °C, it is supposed that thermally de-oligomerized $Al(O^iPr)_3$ species were dissolved in d^iprm-H, where they reacted to give $Al(d^iprm)_3$ (**3c**), which then precipitated. Of course, mono- and disubstituted intermediates also have to be soluble in d^iprm-H.

NMR spectroscopic characterization of **3a**–**3d** in solution (C_6D_6, [D_8]toluene) confirmed the expected symmetric octahedral structure showing only one signal for CO***C*H**CO in the ^{1}H (4.81–4.99 ppm) and ^{13}C (66.2–69.0 ppm) NMR spectra as well as for ***C***O (175.5–175.9 ppm). Interestingly, the signals for $OCH(C\boldsymbol{H}_3)_2$ in **3c** split into two doublets, whereas only one signal for $COOC(C\boldsymbol{H}_3)_3$ in **3d** was observed. No significant influence on the ^{1}H and ^{13}C NMR shifts upon variation of the ester alkoxo group was found. ^{27}Al NMR spectroscopy of **3c** additionally confirmed the structure, showing only one sharp signal for octahedrally coordinated aluminum at 5.3 ppm (Figure 3-25) [17].

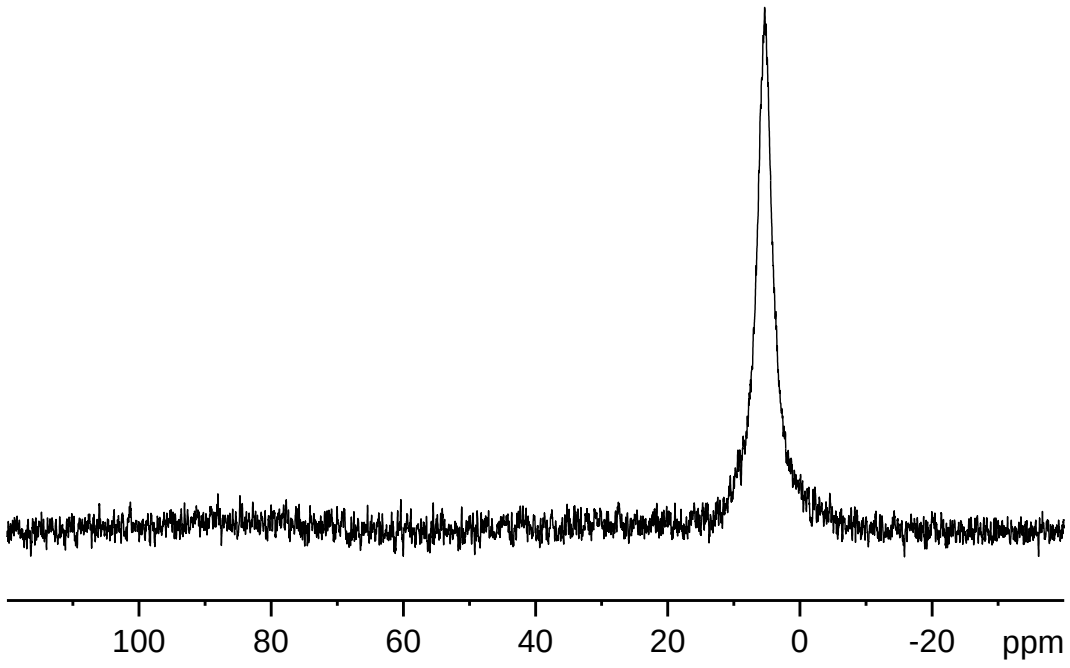

Figure 3-25 ^{27}Al NMR spectrum of **3c** (in [D_8]toluene).

Single crystal XRD of **3a** (Figure 3-26), **3c** (Figure 3-27), and **3d** (Figure 3-28) revealed nearly ideal octahedral coordination around the central aluminum atom, with negligible differences in Al–O bond distances (186.8(1)–189.3(1) pm) and bite angles of the malonates very close to 90° (90.35(7)°–91.83(6)°). Interestingly, the bond distances are distinctly shorter than those observed for Al–O^{ester} bonds in Al(^{t}buac)$_3$ [90] (193.0(2)–195.1(2) pm) and are more in the range of the Al–O^{keto} distances (185.7(2)–186.8(2) pm) in the same complex [90] or in Al(acac)$_3$ (188.0(2) pm) [91]. Selected bond distances and angles are given in Table 3-5 (**3a**), Table 3-6 (**3c**), and Table 3-7 (**3d**).

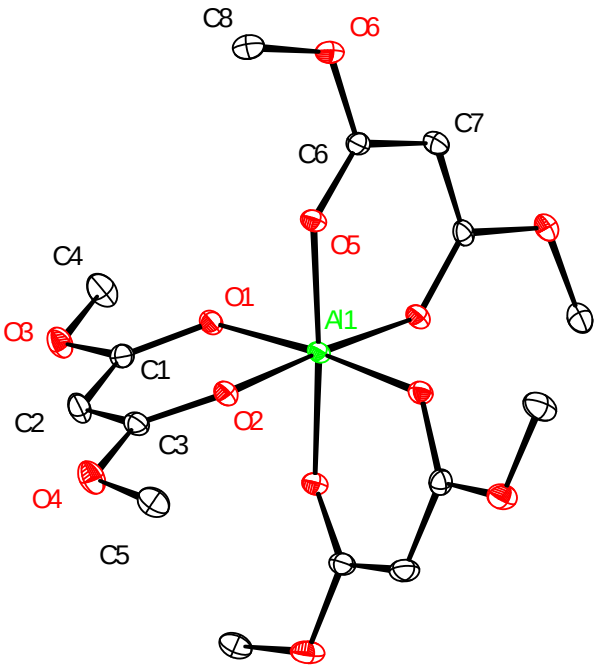

Figure 3-26 Molecular structure of Al(dmem)$_3$ (**3a**), showing 30 % thermal ellipsoids (hydrogen atoms omitted for clarity).

Table 3-5 Selected bond distances [pm] and angles [°] of **3a**.

Al(1)−O(1)	189.14(12)	Al(1)−O(5)	186.88(12)
Al(1)−O(2)	189.33(12)		
O(1)–Al(1)–O(1)[a]	175.00(8)	O(2)–Al(1)–O(2)[a]	89.40(8)
O(1)–Al(1)–O(2)	90.53(5)	O(2)–Al(1)–O(5)	89.56(5)
O(1)–Al(1)–O(2)[a]	85.92(5)	O(2)–Al(1)–O(5)[a]	175.78(5)
O(1)–Al(1)–O(5)	90.00(5)	O(5)–Al(1)–O(5)[a]	91.76(8)
O(1)–Al(1)–O(5)[a]	93.48(5)		

Symmetry transformations used to generate equivalent atoms:
[a] -x,y,-z+1/2

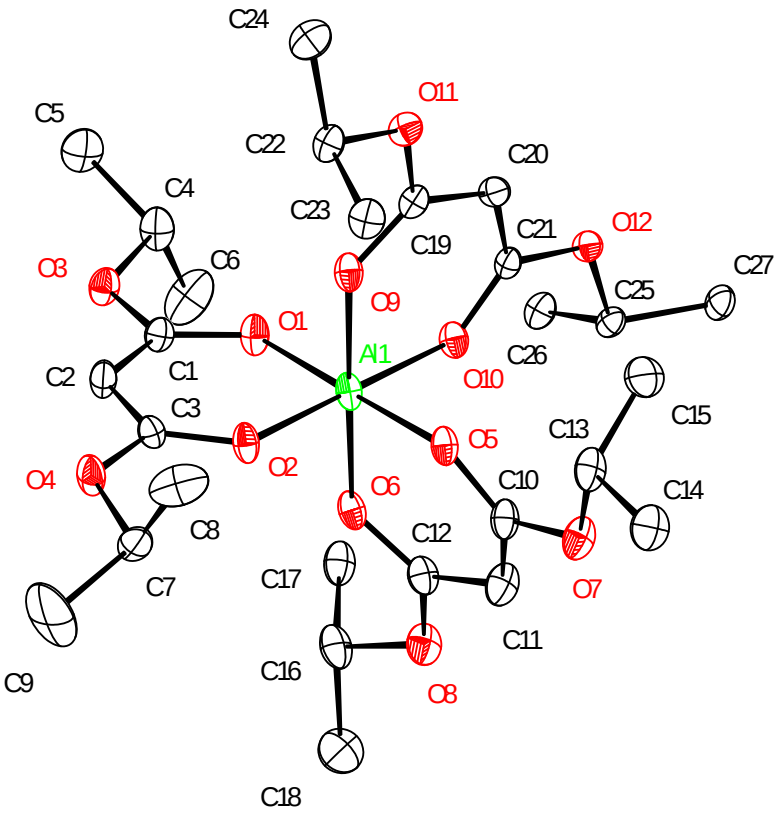

Figure 3-27 Molecular structure of Al(d^{i}prm)$_3$ (**3c**), showing 30 % thermal ellipsoids (hydrogen atoms omitted for clarity).

Table 3-6 Selected bond distances [pm] and angles [°] of **3b**.

Al(1)−O(1)	188.82(15)	Al(1)−O(6)	187.22(16)
Al(1)−O(2)	186.77(14)	Al(1)−O(9)	187.78(15)
Al(1)−O(5)	188.62(14)	Al(1)−O(10)	188.75(14)
O(1)−Al(1)−O(2)	91.83(6)	O(2)−Al(1)−O(10)	179.44(7)
O(1)−Al(1)−O(5)	179.06(7)	O(5)−Al(1)−O(6)	90.35(7)
O(1)−Al(1)−O(6)	90.19(7)	O(5)−Al(1)−O(9)	88.73(7)
O(1)−Al(1)−O(9)	90.72(7)	O(5)−Al(1)−O(10)	90.53(6)
O(1)−Al(1)−O(10)	88.71(6)	O(6)−Al(1)−O(9)	178.86(7)
O(2)−Al(1)−O(5)	88.93(6)	O(6)−Al(1)−O(10)	88.73(6)
O(2)−Al(1)−O(6)	91.13(7)	O(9)−Al(1)−O(10)	90.60(6)
O(2)−Al(1)−O(9)	89.53(7)		

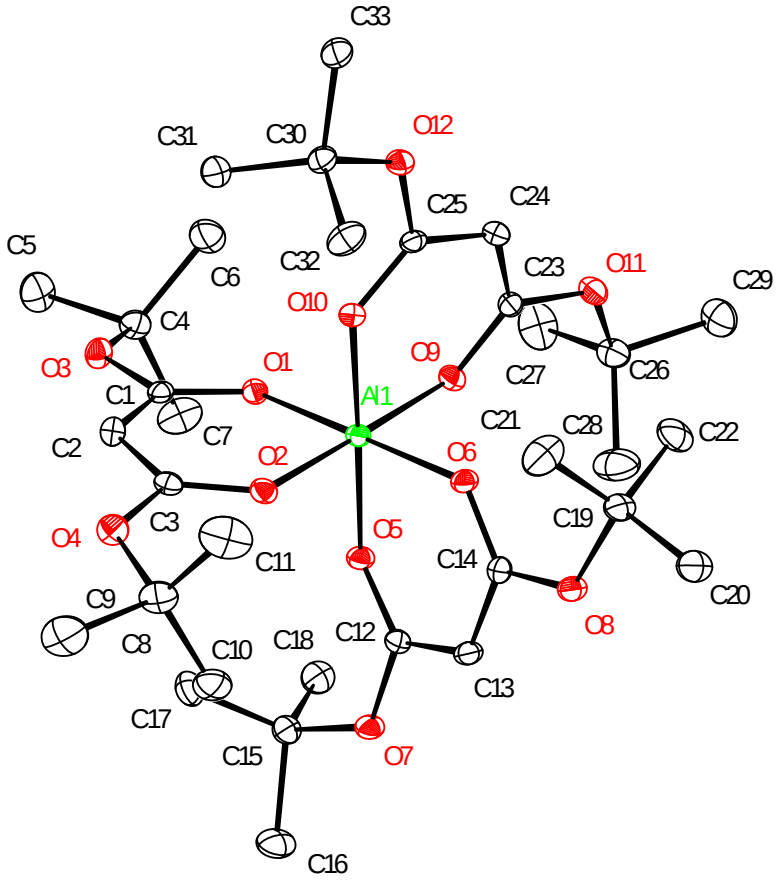

Figure 3-28 Molecular structure of Al(d^{t}bum)$_3$ (**3d**), showing 30 % thermal ellipsoids (hydrogen atoms omitted for clarity).

Table 3-7 Selected bond distances [pm] and angles [°] of **3d**.

Al(1)−O(1)	187.42(10)	Al(1)−O(6)	188.29(10)
Al(1)−O(2)	187.80(10)	Al(1)−O(9)	186.90(10)
Al(1)−O(5)	188.02(10)	Al(1)−O(10)	188.50(10)
O(1)−Al(1)−O(2)	91.36(4)	O(2)−Al(1)−O(10)	87.94(4)
O(1)−Al(1)−O(5)	88.26(4)	O(5)−Al(1)−O(6)	90.39(4)
O(1)−Al(1)−O(6)	177.99(5)	O(5)−Al(1)−O(9)	91.28(4)
O(1)−Al(1)−O(9)	88.69(4)	O(5)−Al(1)−O(10)	177.73(5)
O(1)−Al(1)−O(10)	91.90(4)	O(6)−Al(1)−O(9)	89.85(5)
O(2)−Al(1)−O(5)	89.80(5)	O(6)−Al(1)−O(10)	89.50(4)
O(2)−Al(1)−O(6)	90.13(5)	O(9)−Al(1)−O(10)	90.98(4)
O(2)−Al(1)−O(9)	178.92(5)		

In all three complexes, two of the metallacycles formed by the coordination of the malonate ligand exhibit an envelope-like conformation with aluminum atom deviating from the O–C–CH–C–O plane, whereas the third metallacycle exhibits a nearly planar or slightly

twisted conformation (compare chapter 3.1.1.2 / Figure 3-13). The same combination of ligand conformations was observed for the mentioned *β*-diketonate and *β*-ketoesterate derivatives [90, 91].

3.2.2 $Al_2(\mu\text{-}O^iPr)_2(O^iPr)_2(dialkylmalonate)_2$ Complexes

For the reaction of $Al(O^iPr)_3$ with one equivalent of d^iprm-H or d^tbum-H per aluminum, dinuclear complexes $Al_2(\mu\text{-}O^iPr)_2(O^iPr)_2(d^iprm)_2$ (**4c**) and $Al_2(\mu\text{-}O^iPr)_2(O^iPr)_2(d^tbum)_2$ (**4d**) were obtained. Similar to the reactions with three equivalents of malonates, higher reaction temperatures and longer reaction times had to be applied compared to the preparation of analogous *β*-ketoesterate substituted complexes (compare chapter 3.1.1.2). Preparation of the analogous compounds of dmem-H/detm-H failed due to the same reasons as for the trisubstituted complexes, *i.e.* transesterification (compare chapters 3.2.1 / 3.2.5).

The structure of **4c** and **4d** consist of one tetrahedrally coordinated aluminum center surrounded by two terminal and two bridging O^iPr groups, whereas the second aluminum center is octahedrally coordinated by two bridging O^iPr groups and two chelating malonate ligands (Figure 3-29), *i.e.* the complexes show an analogous structure as the homologous *β*-ketoesterate derivatives (compare chapter 3.1.1.2 / Figure 3-9), proven in solution by NMR spectroscopy and for **4d** also in the solid state by single crystal XRD.

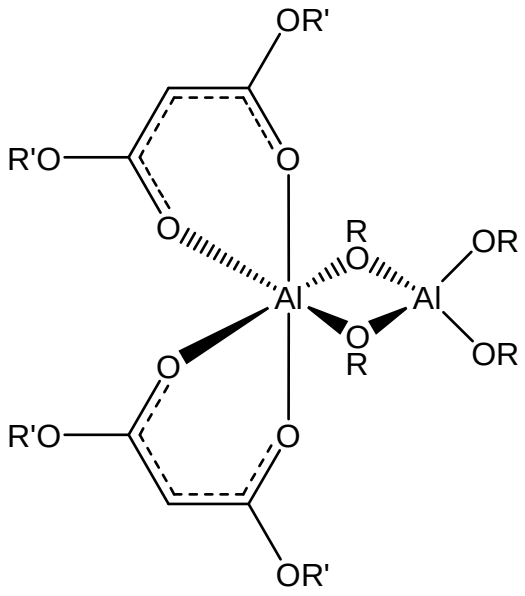

OR = O^iPr; OR' = O^iPr, O^tBu

Figure 3-29 Schematic representation of $Al_2(\mu\text{-}O^iPr)_2(O^iPr)_2(malonate)_2$ (**4c** and **4d**).

Contrary to *β*-ketoesterate substituted complexes, only one isomer is expected because of the symmetric malonate ligands. This was confirmed by NMR spectroscopy, showing only one signal for the COC***H***CO proton at 4.83 (**4c**) and 4.68 (**4d**) ppm, respectively. The methine

protons for the terminal (t) and bridging (b) Al–O^{i}Pr groups are clearly distinguished at 4.26 (t)/4.52 (b) ppm (**4c**) and 4.34 (t)/4.52 (b) ppm (**4d**), respectively. The ^{13}C NMR resonances (63.5 (t) and 66.3 (b) for **4c**/63.5 (t) and 65.8 (b) for **4d**) also confirm the dinuclear structure. The methyl protons of the bridging O^{i}Pr groups give rise to two signals. This splitting might result from different environments caused by hindered rotation, *viz.* being directed to the octahedrally or tetrahedrally coordinated aluminum center.

The signals for the malonate–O^{i}Pr (**4c**) and O^{t}Bu (**4d**) methyl protons also split in four and two signals, respectively. This indicates different environments of the malonate ester groups *trans* to another carboxylic group or *trans* to a bridging O^{i}Pr group, *e.g.* directed to or away from the second aluminum center. A splitting of the malonate methine protons was observed (4.96/5.41 ppm) for **4c** also. Additionally, the OCHC(C***H***$_3$)$_2$ methyl protons in **4c** for each of these two types of ester O^{i}Pr groups further split into two doublets. This indicates a preferential orientation of the O^{i}Pr groups which results in two non-equivalent environments for each methyl group.

EXSY spectra show exchange of the signals for the bridging/terminal Al–O^{i}Pr groups and additionally for the two O^{i}Pr (in **4c**)/O^{t}Bu (in **4d**) groups of the malonate ligands (Figure 3-30). Exchange between Al–O^{i}Pr and malonate–OR groups was not observed.

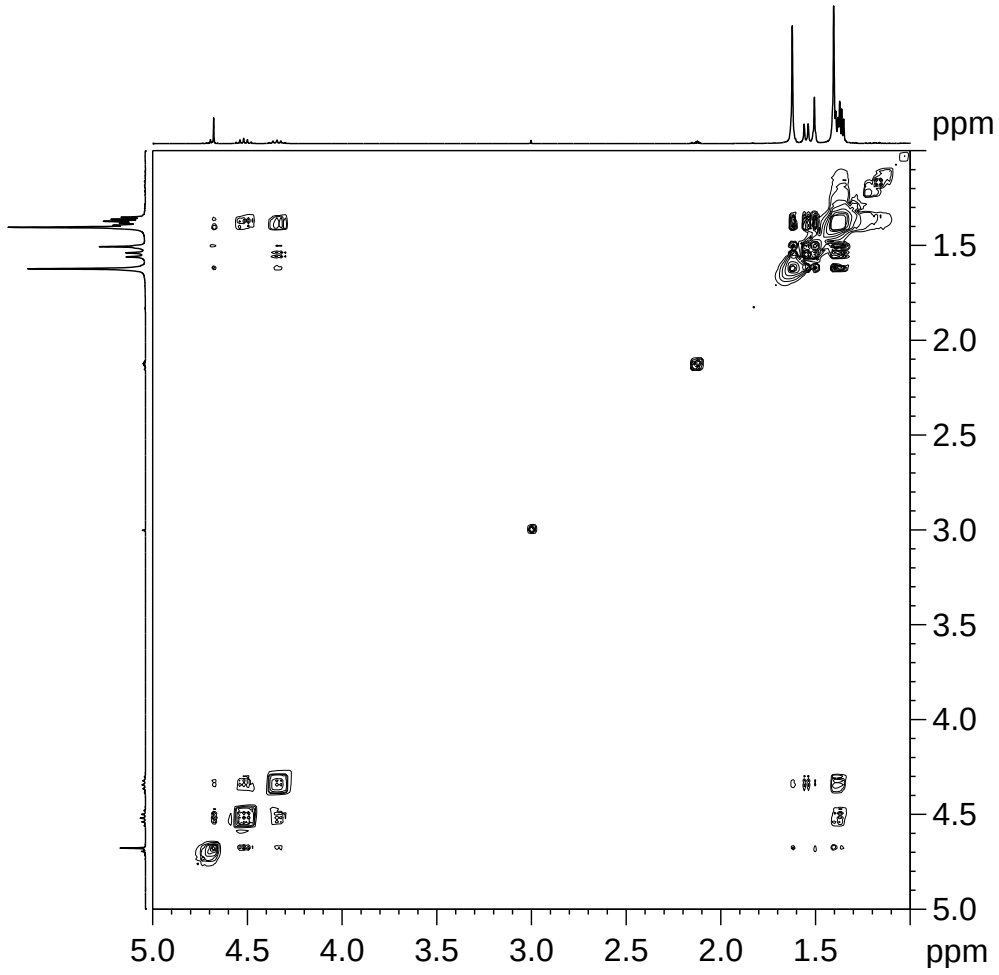

Figure 3-30 EXSY spectrum of **4d** (in [D$_8$]toluene).

^{27}Al NMR spectra of **4c** and **4d** (Figure 3-30) additionally supported the structure. Both spectra showed a broad signal assigned to tetrahedrally coordinated aluminum between 130–20 ppm with maxima at about 65 (**4c**) and 80 (**4d**) ppm, respectively, and one sharp signal at 5.1 (**4c**) or 4.8 (**4d**) ppm, assigned to octahedrally coordinated aluminum [17]. Integration of the signals revealed almost the expected 1:1 ratio, although integration is somewhat difficult because of the broad signal for tetrahedrally coordinated aluminum.

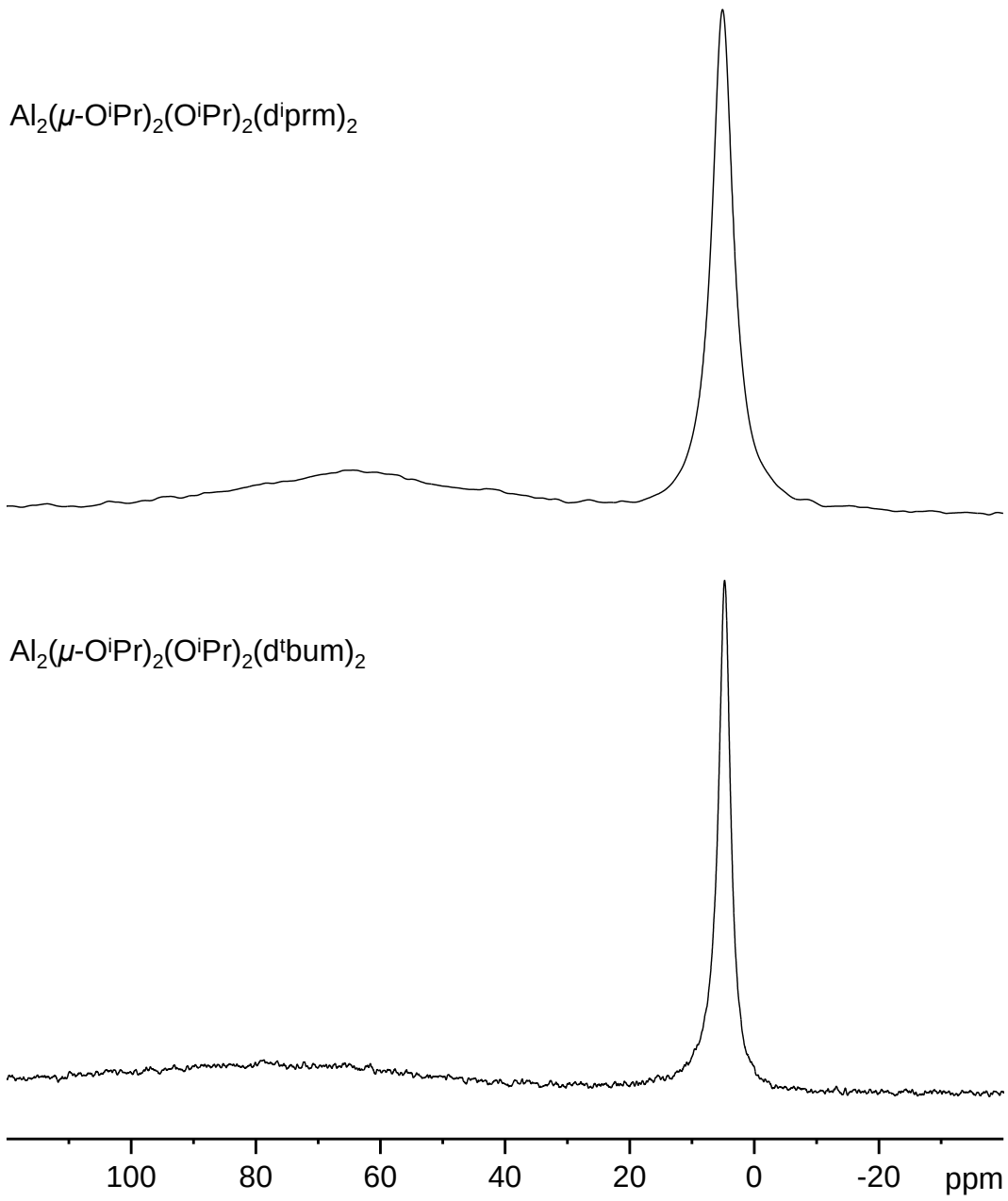

Figure 3-31 ^{27}Al NMR spectra of **4c** and **4d** (in [D_8]toluene)

The single crystal structure analysis of **4d** was in agreement with that derived from NMR spectra in solution (Figure 3-32). The bite angles for the two malonate ligands at the octahedral aluminum center are 90.29(7)° and 90.39(7)°. One of the malonate ligands again

shows a slightly envelop-like conformation, whereas the other one is nearly planar. Interestingly, no *trans* effect on the Al–O bond distances (188.26(15)–188.98(17) pm) was observed for the malonate ligands. The angle between the two bridging O^{i}Pr groups O(3)–Al(2)–O(4) at the octahedral aluminum center is only 76.61(7)° and leads to a distortion of the coordination octahedron. As expected, the bond distances Al(2)–O(3) and Al(2)–O(4) between the octahedral aluminum center and the bridging O^{i}Pr are significantly longer than those from the tetrahedral aluminum center to the bridging units, *viz.* 190.34(17) and 190.21(16) pm *vs.* 179.78(16) (Al(1)–O(3)) and 179.13(17) (Al(1)–O(4)) pm. In addition, the O(3)–Al(1)–O(4) angle at the tetrahedral aluminum center (82.17(7)°) is larger than that at the octahedral center, as expected, because of the different coordination geometry. Both bond distances to the terminal O^{i}Pr groups Al(1)–O(1) and Al(1)–O(2) of 169.82(19) and 169.78(18) pm are significantly shorter than those to the bridging O^{i}Pr groups. Comparison with $Al_2(O^iPr)_4(^tbuac)_2$ (**2d**) shows similar bond distances and angles, with the Al–O^{malonate} bond distances lying between those for Al–O^{ester} (190.4(4)–192.6(4) pm) and Al–O^{keto} (185.0(4)–187.2(4) pm) (compare chapter 3.1.1.2). Selected bond distances and angles are given in Table 3-8.

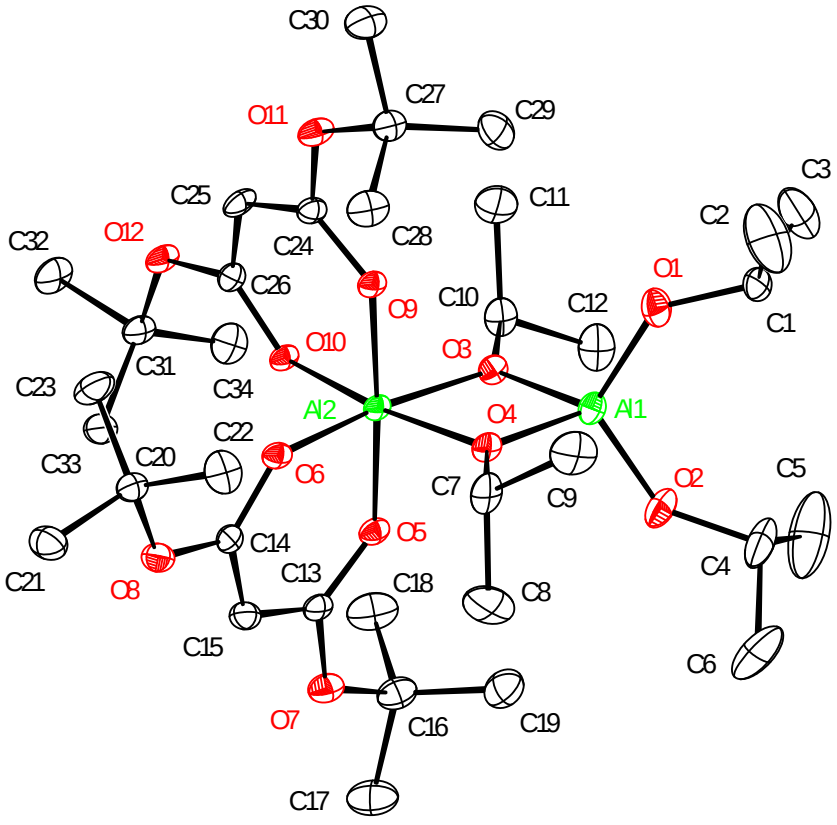

Figure 3-32 Molecular structure of $Al_2(\mu\text{-}O^iPr)_2(O^iPr)_2(d^tbum)_2$ (**4d**), showing 30 % thermal ellipsoids (hydrogen atoms omitted for clarity).

Table 3-8 Selected bond distances [pm] and angles [°] of **4d**.

Al(1)−O(1)	169.82(19)	Al(2)−O(4)	190.21(16)
Al(1)−O(2)	169.78(18)	Al(2)−O(5)	188.98(17)
Al(1)−O(3)	179.78(16)	Al(2)−O(6)	188.62(17)
Al(1)−O(4)	179.13(17)	Al(2)−O(9)	188.40(16)
Al(2)−O(3)	190.34(17)	Al(2)−O(10)	188.26(15)
O(1)−Al(1)−O(2)	117.60(10)	O(4)−Al(2)−O(6)	94.34(7)
O(1)−Al(1)−O(3)	111.63(9)	O(4)−Al(2)−O(9)	88.59(7)
O(1)−Al(1)−O(4)	114.30(9)	O(4)−Al(2)−O(10)	170.97(8)
O(2)−Al(1)−O(3)	114.03(9)	O(5)−Al(2)−O(6)	90.29(7)
O(2)−Al(1)−O(4)	112.00(9)	O(5)−Al(2)−O(9)	176.75(8)
O(3)−Al(1)−O(4)	82.17(7)	O(5)−Al(2)−O(10)	87.55(7)
O(3)−Al(2)−O(4)	76.61(7)	O(6)−Al(2)−O(9)	87.37(7)
O(3)−Al(2)−O(5)	88.92(7)	O(6)−Al(2)−O(10)	94.58(7)
O(3)−Al(2)−O(6)	170.83(7)	O(9)−Al(2)−O(10)	90.39(7)
O(3)−Al(2)−O(9)	93.75(7)	Al(1)−O(3)−Al(2)	100.46(7)
O(3)−Al(2)−O(10)	94.51(7)	Al(1)−O(4)−Al(2)	100.75(7)
O(4)−Al(2)−O(5)	93.84(7)		

The structure of **4d** shows two different environments for the methyl groups of the bridging O^{i}Pr groups, which correlates with the observation of two signals in the solution ^{1}H NMR spectrum (*vide supra*) and therefore indicates that these O^{i}Pr groups do not rotate freely in solution.

3.2.3 [Al(μ-O^{i}Pr)(d^{i}prm)$_2$]$_2$

Storage of Al$_2$(μ-O^{i}Pr)$_2$(O^{i}Pr)$_2$(d^{i}prm)$_2$ (**4c**), a colorless oil, at room temperature under argon atmosphere resulted in the formation of colorless crystals. Single crystal XRD surprisingly revealed that [Al(μ-O^{i}Pr)(d^{i}prm)$_2$]$_2$ (**5c**) had crystallized rather than **4c** (Figure 3-33). This is of special interest, since attempts to prepare **5c** directly from Al(O^{i}Pr)$_3$ with two equivalents of d^{i}prm-H at 100 °C had failed, and only mixtures of Al$_2$(μ-O^{i}Pr)$_2$(O^{i}Pr)$_2$(d^{i}prm)$_2$ (**4c**) and Al(d^{i}prm)$_3$ (**3c**) had been obtained. Interestingly, prolonged storage (one month) of a solution containing a mixture of **4c** and **3c**, resulting from an attempt to directly react Al(O^{i}Pr)$_3$ with two equiv. d^{i}prm-H, resulted in a clean comproportionation to give [Al(μ-O^{i}Pr)(d^{i}prm)$_2$]$_2$ (**5c**) as sole product. [Al(μ-OR)(β-diketonate)$_2$]$_2$ derivatives were reported to disproportionate to Al$_2$(μ-OR)$_2$(OR)$_2$(β-diketonate)$_2$ and Al(β-diketonate)$_3$ [50], but the observed rearrangement was not described in the literature and also not observed for β-ketoesterate derivatives (compare chapter 3.1.1.3).

Other products which of course have to be formed during the rearrangement from **4c** to **5c** could not be identified so far by means of the used spectroscopic or crystallographic methods, although the formation of $[Al(O^iPr)_{3-x}(d^iprm)_x]_n$ (x < 1) species is assumed and appears to be evident.

It is also remarkable that the rearrangement of **4c** to give **5c** only takes place upon storage of the isolated product – storage of a solution of **4c** in [D_8]toluene at room temperature did not show any changes within one month. This indicates, that the crystallization process during the formation of **5c** from oily **4c** is an important driving force for the formation of **5c**. Although **5c** is stable in solution at room temperature, temperature dependent NMR spectroscopy revealed that compound **5c** was not stable in solution ([D_8]toluene) at elevated temperatures (80 °C), but decomposed to give $Al(d^iprm)_3$ (**3c**) and additional, not identified species.

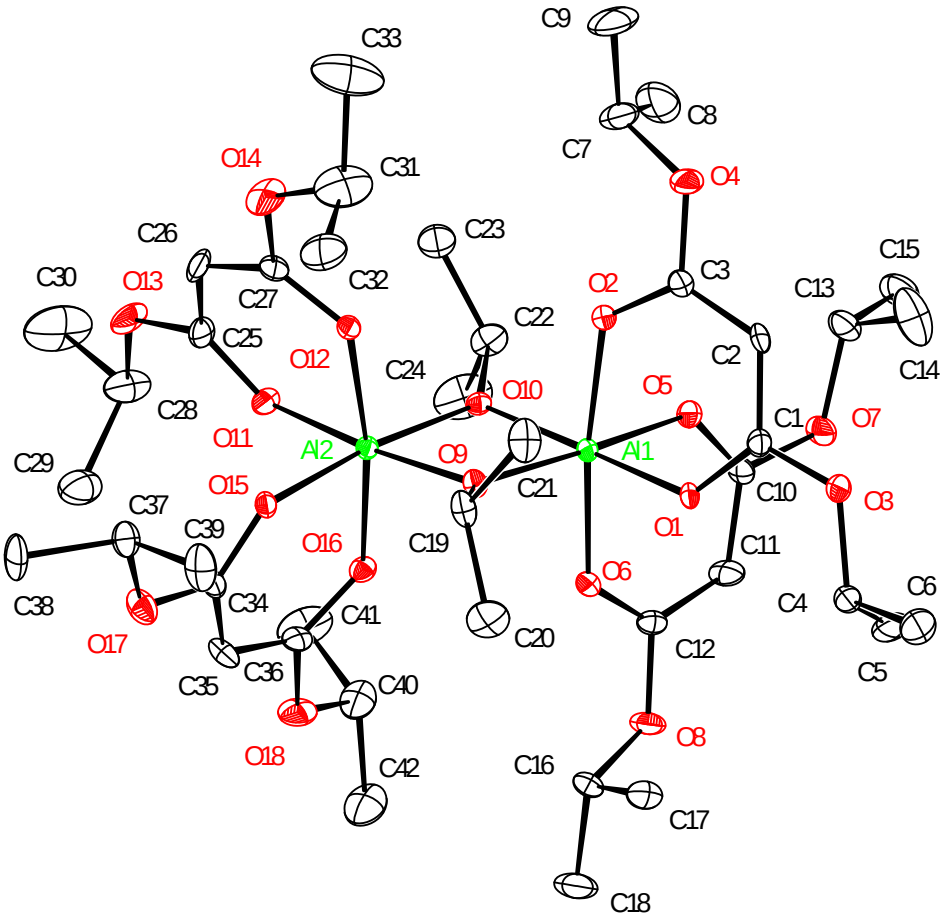

Figure 3-33 Molecular structure of $[Al(\mu\text{-}O^iPr)(d^iprm)_2]_2$ (**5d**), showing 30 % thermal ellipsoids (hydrogen atoms omitted for clarity).

The structure of **5c** can formally be derived from that of **4d** by substitution of the two terminal O^iPr ligands and thus converting the tetrahedral aluminum center in an octahedral, leading to a dimer with two equal aluminum centers. Only one structure analysis of a structurally analogous *β*-diketonate modified aluminum alkoxide has been reported in literature, *viz.* that of $[Al(\mu\text{-}O^iPr)(Et_2acac)_2]_2$ [54], although it was also observed for some other ligand classes (compare chapter 1.2.3.1). Al–O bond distances to the malonate ligands

are 190.1(4)–192.5(4) pm and the bite angles 88.8(2)°–89.3(2)°, which means longer bond distances and smaller bite angles compared to the monosubstituted dimeric compound $Al_2(\mu\text{-}O^iPr)_2(O^iPr)_2(d^tbum)_2$ **4d**[vii] (compare chapter 3.2.2 / Figure 3-32). This results from the more crowed situation due to the two octahedral centers compared to one octahedral center neighbored by a tetrahedral in **4c**. At each aluminum center, one coordinated malonate ligand has an envelope-like conformation whereas the other is nearly planar (as in **3c**). The angles between the aluminum centers and the bridging O^iPr groups are 77.6(2)° (O(9)–Al(1)–O(10)) and 77.9(2)° (O(9)–Al(2)–O(10)), and the corresponding Al–O bond distances 186.7(4)–188.7(4) pm. In contrast to the malonate ligands, these distances are shorter than those between the octahedrally coordinated aluminum center and the bridging O^iPr group in **4c**. This is a result of the significantly shorter bond distances to the tetrahedrally coordinated aluminum center in **4c**, leading to an elongation of the "opposite" bonds. Both C–O bonds of the bridging O^iPr groups are bent towards the same side of the $Al_2(\mu\text{-}O^iPr)_2$-plane, resulting in one methyl group being closer and the other more distant to the plane, supporting the observation of two methyl signals in the ^1H and ^{13}C NMR spectra. Additionally, the O–Al–O axes perpendicular to the $Al_2(\mu\text{-}O^iPr)_2$ plane are not parallel but slightly twisted. Selected bond distances and angles are given in Table 3-9.

It is also interesting to mention that from the two possible geometric isomers, *viz.* meso and *d,l* (Figure 3-34), for **5c** the *d,l* form crystallizes at room temperature, in contrast to the known structure of $[Al(\mu\text{-}O^iPr)(Et_2acac)_2]_2$, which crystallized in the meso form [50, 54].

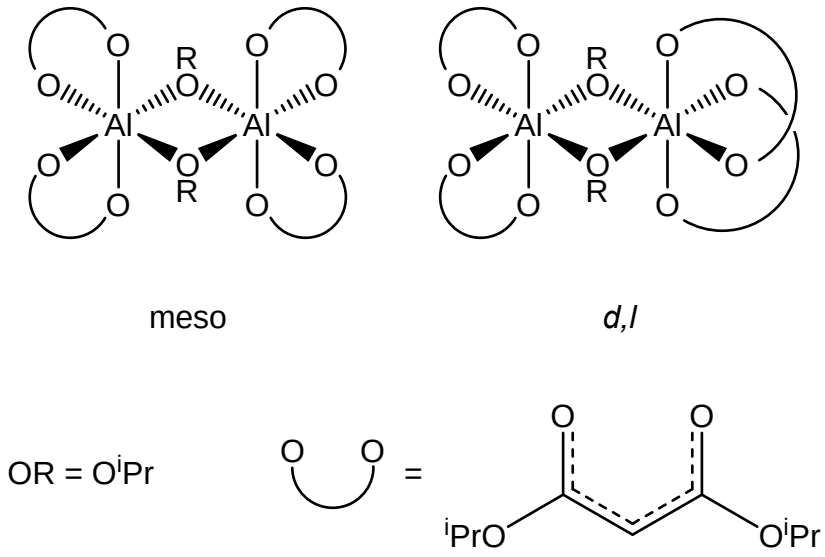

Figure 3-34 Schematic representation of possible meso and *d,l* geometries for $[Al(\mu\text{-}O^iPr)(d^iprm)_2]_2$ (**5c**).

[vii] Although compounds **4d** and **5c** bear different dialkylmalonate ligands (**4d**: d^tbum/**5c**: d^iprm), this should not have significant influences on the Al–O distances and O–Al–O angles. No significant influences were also observed for the trisubstituted mononuclear complexes Al(dialkylmalonate)$_3$ (**3c**: malonate = d^iprm, **3d**: malonate = d^tbum).

The bond lengths and bite angles are nearly the same as in $[Al(\mu\text{-}O^iPr)(Et_2acac)_2]_2$ [54], but this structure shows a higher symmetry, without the bending of the μ-O^iPr groups and the twisting of the O–Al–O axes.

Table 3-9 Selected bond distances [pm] and angles [°] of **5c**.

Al(1)−O(1)	190.8(4)	Al(2)−O(9)	187.7(4)
Al(1)−O(2)	190.1(4)	Al(2)−O(10)	186.7(4)
Al(1)−O(5)	190.5(4)	Al(2)−O(11)	191.0(4)
Al(1)−O(6)	190.7(4)	Al(2)−O(12)	191.6(4)
Al(1)−O(9)	186.8(4)	Al(2)−O(15)	1.92.5(4)
Al(1)−O(10)	188.7(4)	Al(2)−O(16)	192.3(4)
O(1)−Al(1)−O(2)	88.90(18)	O(9)−Al(2)−O(11)	174.3(2)
O(1)−Al(1)−O(5)	89.50(18)	O(9)−Al(2)−O(12)	89.03(18)
O(1)−Al(1)−O(6)	86.00(18)	O(9)−Al(2)−O(15)	94.06(17)
O(1)−Al(1)−O(9)	97.92(18)	O(9)−Al(2)−O(16)	97.84(18)
O(1)−Al(1)−O(10)	175.04(19)	O(10)−Al(2)−O(11)	96.93(18)
O(2)−Al(1)−O(5)	85.84(18)	O(10)−Al(2)−O(12)	97.06(18)
O(2)−Al(1)−O(6)	172.95(19)	O(10)−Al(2)−O(15)	171.58(18)
O(2)−Al(1)−O(9)	96.14(18)	O(10)−Al(2)−O(16)	89.98(18)
O(2)−Al(1)−O(10)	89.48(18)	O(11)−Al(2)−O(12)	89.28(17)
O(5)−Al(1)−O(6)	89.24(18)	O(11)−Al(2)−O(15)	91.24(18)
O(5)−Al(1)−O(9)	172.3(2)	O(11)−Al(2)−O(16)	84.40(18)
O(5)−Al(1)−O(10)	95.05(18)	O(12)−Al(2)−O(15)	85.03(17)
O(6)−Al(1)−O(9)	89.39(18)	O(12)−Al(2)−O(16)	171.07(19)
O(6)−Al(1)−O(10)	96.00(18)	O(15)−Al(2)−O(16)	88.78(17)
O(9)−Al(1)−O(10)	77.61(17)	Al(1)−O(9)−Al(2)	102.23(19)
O(9)−Al(2)−O(10)	77.86(17)	Al(1)−O(10)−Al(2)	101.89(19)

NMR spectroscopy confirmed the conversion of **4c** to **5c**. The spectra of **5c** were completely different to that of **4c**. The ^{1}H NMR signals for COC***H***CO and Al–OC***H***Me_2 were both shifted to higher ppm values, *viz.* 4.91 and 4.76 ppm, and only one quintet for Al–OC***H***Me_2 was observed. The formation of $Al(d^iprm)_3$ could also be excluded (Figure 3-35). The signals for COOC***H***Me_2 split into two slightly overlapping quintets at 5.17 and 5.28 ppm, caused by the different environments of the malonate–O^iPr groups directed to and away from the second aluminum center. Analogous to **4c**, the signals for the malonate methyl groups split into four doublets (two of them overlapping), again indicating preferential orientation of the malonate O^iPr groups with non-equivalent environments for the methyl groups. The methyl proton resonances for the bridging Al–O^iPr groups also split into two doublets, indicating hindered rotation of these groups and two different environments for the

methyl groups. This confirms that the dimeric structure with two aluminum centers, each coordinated by two malonate ligands and bridged by two O^{i}Pr groups, is retained in solution.

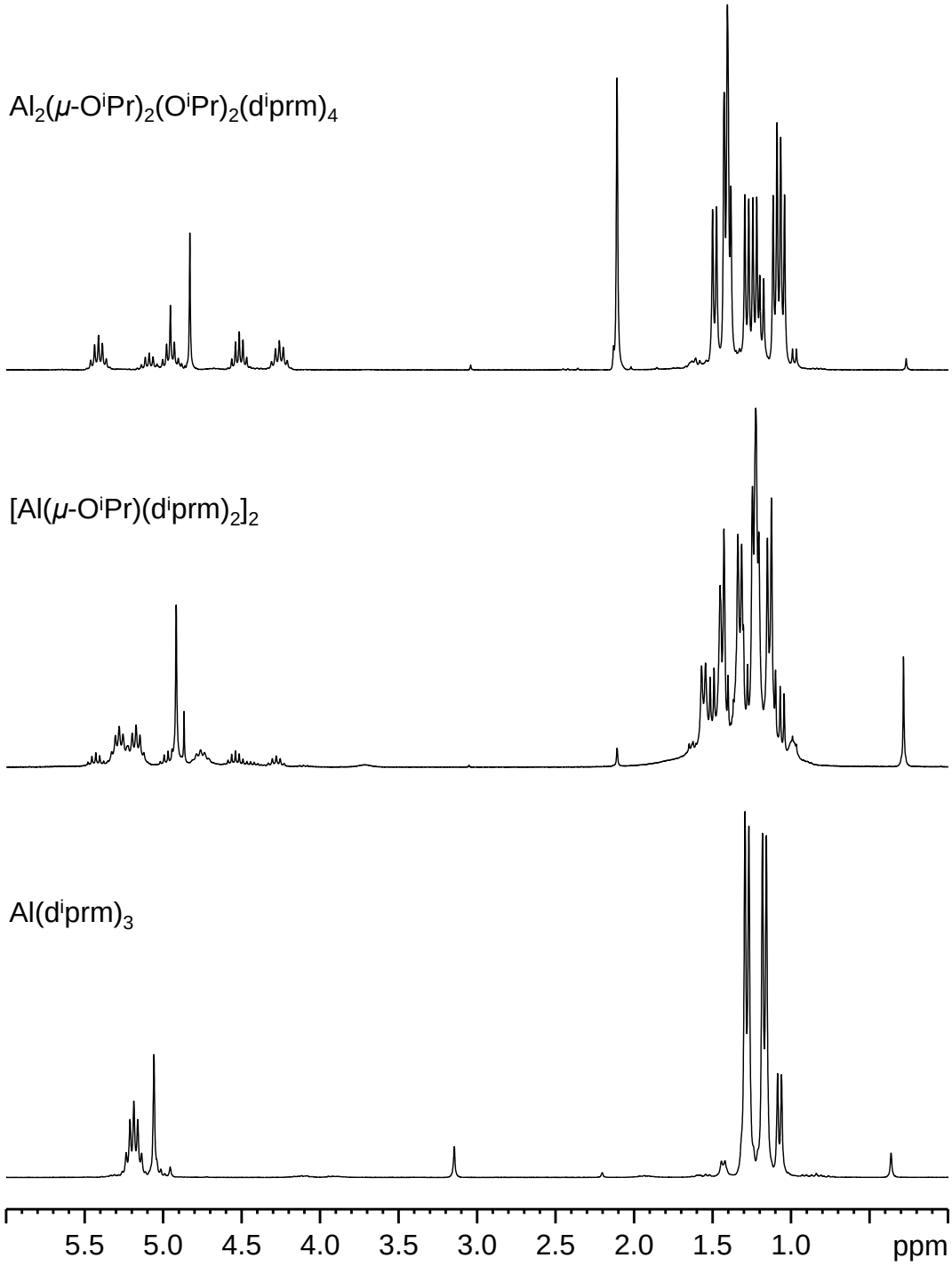

Figure 3-35 ^{1}H NMR spectra of $Al_2(\mu\text{-}O^iPr)_2(O^iPr)_2(d^iprm)_2$ (**4c**) (*top*), [Al(μ-O^iPr)(d^iprm)$_2$]$_2$ (**5c**) (*center*), and Al(d^iprm)$_3$ (**3c**) (*bottom*) (in C_6D_6).

EXSY spectroscopy revealed signals corresponding to exchange between the two AlOC*H*Me$_2$ protons, indicating a fluctuating behavior of these groups (Figure 3-36). ^{27}Al NMR spectroscopy further revealed the anticipated structure giving a single signal for hexacoordinated aluminum at 3.5 ppm (Figure 3-37).

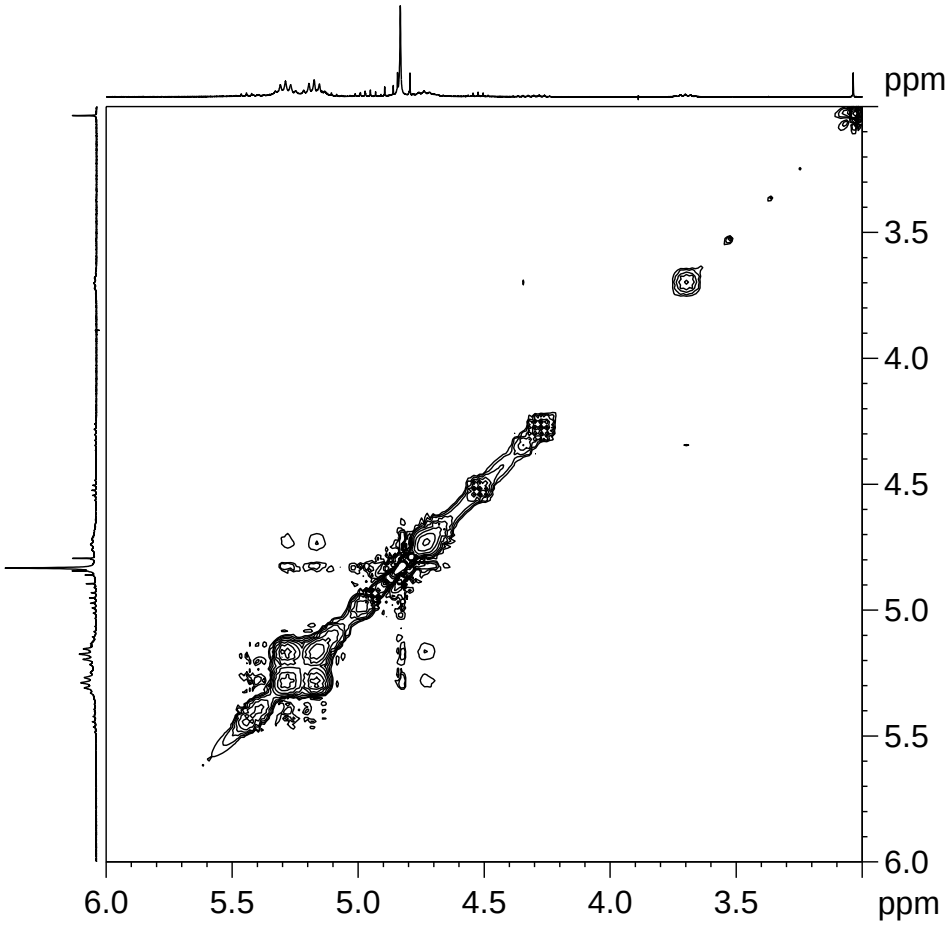

Figure 3-36 EXSY spectrum of **5c** (in [D_8]toluene).

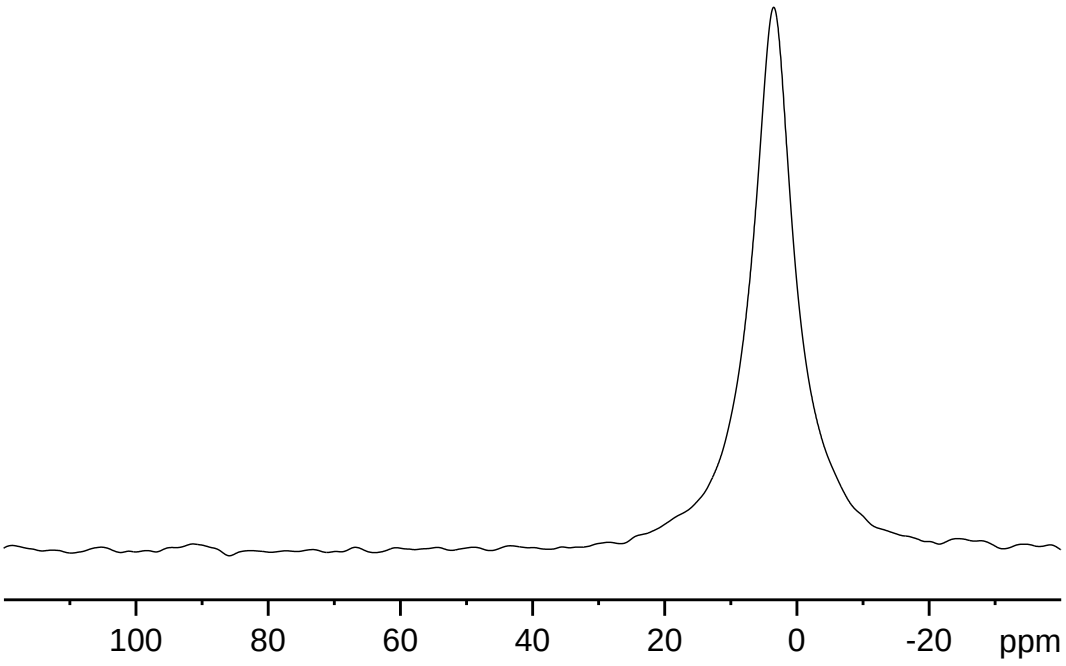

Figure 3-37 ^{27}Al NMR spectrum of **5c** (in [D_8]toluene).

3.2.3.1 EXCURSUS: [Al(μ-O^{s}Bu)(acac)$_2$]$_2$

For the reaction of Al(O^{s}Bu)$_3$ with one equiv. of acac-H in toluene at room temperature two types of crystals suitable for single crystal XRD were obtained upon recrystallization from the reaction solution. Acicular crystals were identified as Al(acac)$_3$, whereas the rhombohedrally shaped crystals were shown to be [Al(μ-O^{s}Bu)(acac)$_2$]$_2$ (Figure 3-38) [55]. Other species with a lower degree of substitution were not identified, but have to be formed considering the overall stoichiometry of the reaction.

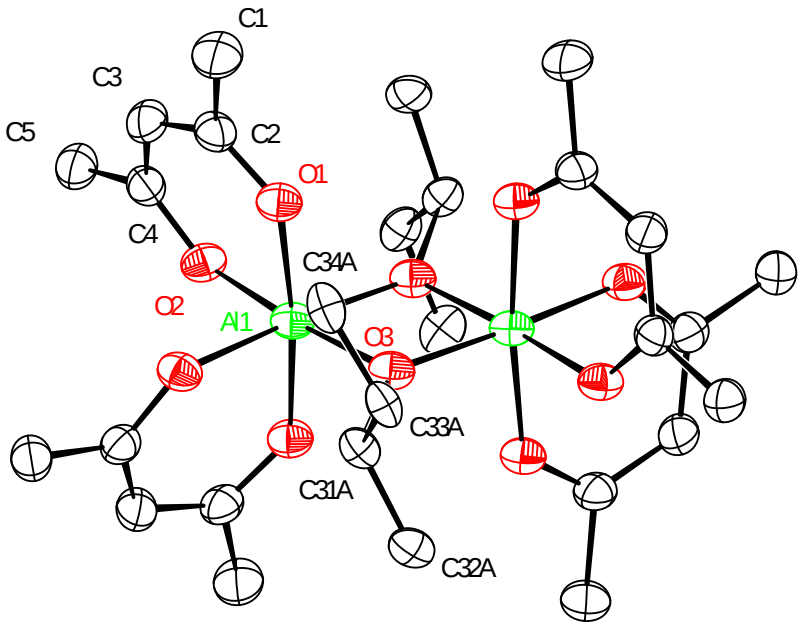

Figure 3-38 Molecular structure of [Al(μ-O^{s}Bu)(acac)$_2$]$_2$ showing 30 % thermal ellipsoids (hydrogen atoms omitted for clarity).

The structure is analogous to those of [Al(μ-O^{i}Pr)(d^{i}prm)$_2$]$_2$ (**5c**) (compare chapter 3.2.3 / Figure 3-33) and [Al(μ-O^{i}Pr)(Et$_2$acac)$_2$]$_2$ (compare chapter 1.2.3.1 / Figure 1-15) [50, 54] and crystallizes as *d,l* isomer, like the former and different to the latter. The Al–O^{keto} bond distances Al(1)–O(1) (189.8(1) pm) and Al(2)–O(2) (189.6(2) pm) show virtually no *trans* influence and are only slightly shorter than those of [Al(μ-O^{i}Pr)(Et$_2$acac)$_2$]$_2$ (189.2(5)–192.7(5) ppm) or **5c** (190.1(4)–192.5(4) pm). The Al–O^{i}Pr bond distances (187.3(2) pm) are also comparable to the analogous structures (186.6(5)–186.9(5) pm for [Al(μ-O^{i}Pr)(Et$_2$acac)$_2$]$_2$ or 186.7(4)–188.7(4) pm for **5c**). Selected bond distances and angles are given in Table 3-10.

Table 3-10 Selected bond distances [pm] and angles [°] of $[Al(\mu\text{-}O^sBu)(acac)_2]_2$.

Al(1)–O(1)	189.78(16)	Al(1)–O(3)	187.29(15)
Al(1)–O(2)	189.63(18)		
O(1)–Al(1)–O(1)[b]	173.51(12)	O(2)–Al(1)–O(2)[b]	89.73(11)
O(1)–Al(1)–O(2)	89.14(7)	O(2)–Al(1)–O(3)	174.04(8)
O(1)–Al(1)–O(2)[b]	86.26(7)	O(2)–Al(1)–O(3)[a]	96.15(7)
O(1)–Al(1)–O(3)	90.30(5)	O(3)–Al(1)–O(3)[a]	77.98(10)
O(1)–Al(1)–O(3)[a]	94.75(6)	Al(1)–O(3)–Al(1)[a]	102.02(10)

Symmetry transformations used to generate equivalent atoms:
[a] -x+0,-y+1/2,z+0; [b] y-1/4,x+1/4,-z+5/4

This structure is another example for the dependence of the stability of $[Al(\mu\text{-}OR)_2(\beta\text{-diketonate})_2]_2$ compounds on the type and combination of ligands. Whereas the analogous acac derivative of $Al(O^iPr)_3$ was reported to be unstable and disproportionate to give the mono- and trisubstituted products [50], the disubstituted product of $Al(O^sBu)_3$ reported here appears to be a stable complex, since it is obtained from a stoichiometric reaction (Al/acac ratio). As for **5c**, crystallization might be a crucial driving force for the formation and stabilization of $[Al(\mu\text{-}O^sBu)(acac)_2]_2$. On the other hand, $[Al(\mu\text{-}O^iPr)_2(Et_2acac)_2]_2$ is stable whereas the analogous acac derivative is unstable, as mentioned before. Therefore, besides the type of chelating ligand, also the combination of chelating ligand and alkoxide appear to be important for the stability of the different disubstituted complexes.

3.2.4 $Al_3(\mu\text{-}OH)(\mu\text{-}OEt)_3(detm)_5$

Since the preparation of $Al(detm)_3$ (**3b**) from $Al(O^iPr)_3$ and detm-H failed because of transesterification (compare chapters 3.2.1 / 3.2.5), an alternative preparative route was explored to avoid transesterification, starting from $Al(OEt)_3$ instead of $Al(O^iPr)_3$. Because $Al(OEt)_3$ is oligomeric in the solid state (compare chapter 1.2.1), it is only sparingly soluble in most organic solvents, including toluene. However, at least partial thermal de-oligomerization and subsequent partial solubility was expected, as for $Al(O^iPr)_3$. Therefore, $Al(OEt)_3$, dispersed in toluene, was reacted with three equiv. of detm-H at 90 °C. The solution immediately cleared upon heating. Monitoring of the reaction by ^1H NMR spectroscopy clearly revealed coordination of the malonate, but significant differences to the spectrum of **3b** were observed and greater proportions of unreacted detm-H were detected (Figure 3-39).

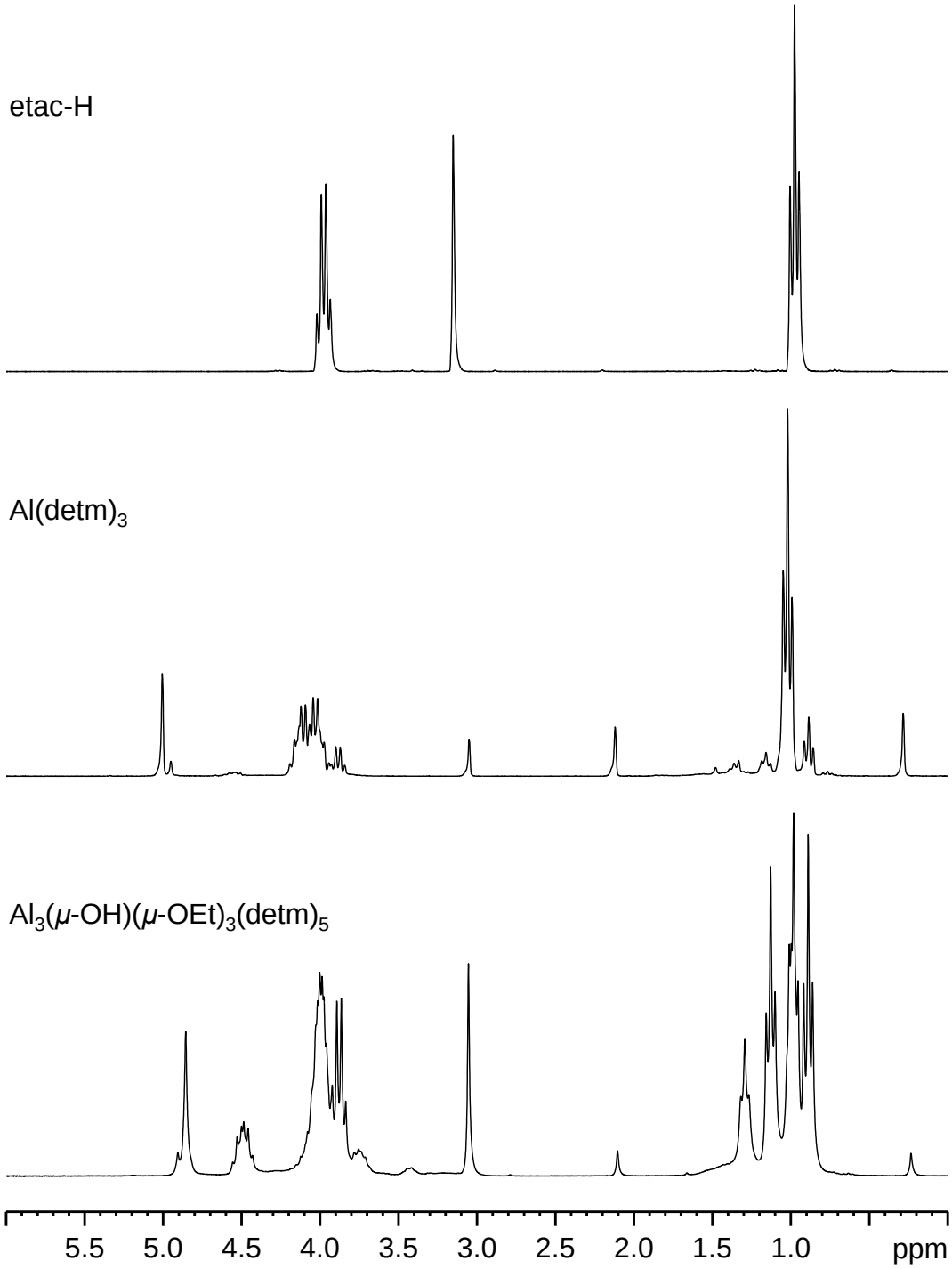

Figure 3-39 ^{1}H NMR spectra of etac-H (*top*), Al(detm)$_3$ (**3b**) (*center*), and $Al_3(\mu\text{-OH})(\mu\text{-OEt})_3(detm)_5$ (**6b**) (*bottom*) (in C_6D_6),

Removal of all volatiles and storage of the obtained oil for a few days at room temperature yielded crystals, which upon single crystal XRD analysis turned out to be $Al_3(\mu\text{-OH})(\mu\text{-OEt})_3(detm)_5$ (**6b**) (Figure 3-40).

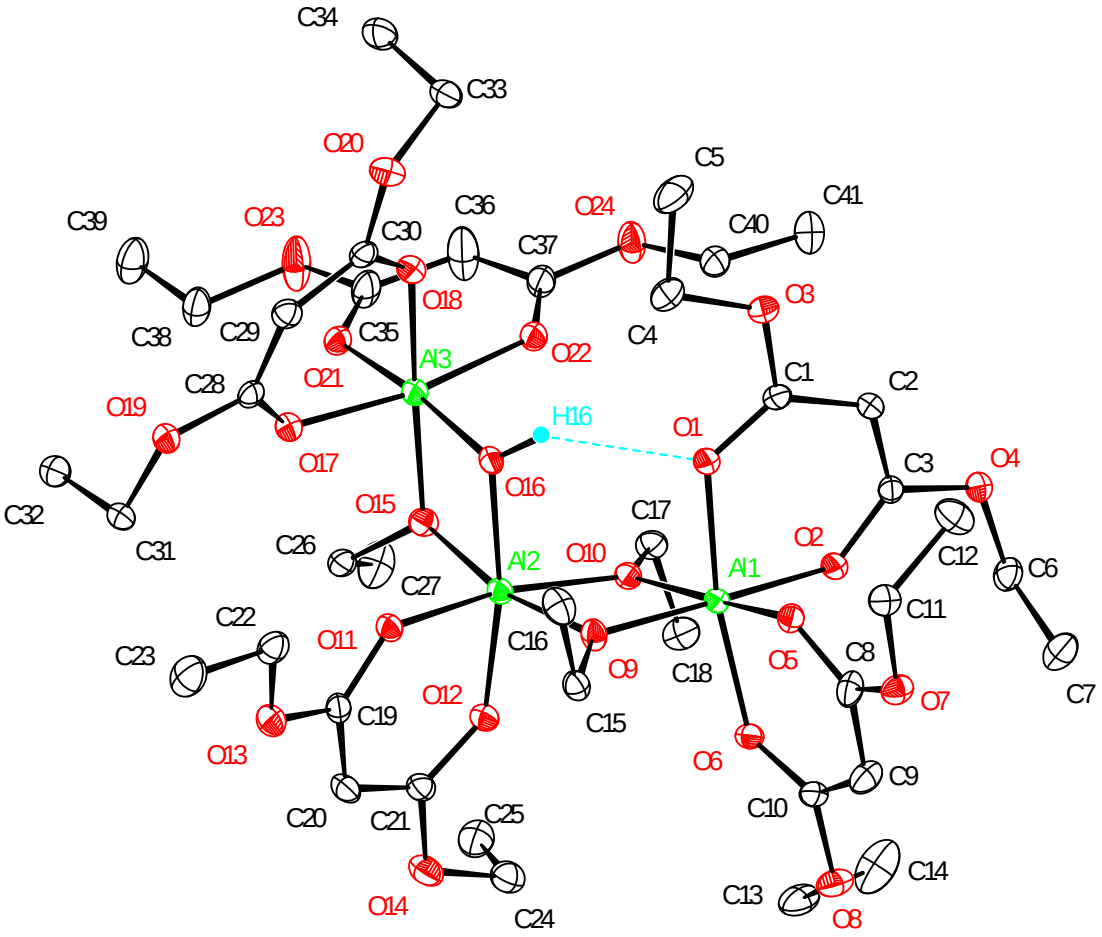

Figure 3-40 Molecular structure of $Al_3(\mu\text{-}OH)(\mu\text{-}OEt)_3(detm)_5$ (**6b**), showing 30 % thermal ellipsoids (carbon-bond hydrogen atoms omitted for clarity).

The crystal structure of **6b** shows three octahedrally coordinated aluminum centers. The two terminal aluminum centers are coordinated by two malonate ligands each, whereas the central one is coordinated only by one malonate, leading to an overall Al/malonate ratio of 3:5. One terminal aluminum center (Al(1)) is connected to the central Al(2) by two bridging OEt groups, while the second terminal aluminum center (Al(3)) is connected by only one bridging OEt group and a bridging hydroxo group. Again, one of the malonates at each terminal aluminum center has enveloped conformation and the other is nearly planar, as is the malonate ligand at the central aluminum atom. No *trans* effect was observed, resulting in Al–$O^{malonate}$ bond distances of 188.57(11)–191.45(11) pm, except for Al(1)–O(1), which is 194.76(11) pm. This slight elongation is traced back to a hydrogen bond between the hydroxo hydrogen H(16) and O(1) of 220.8(16) pm. The bite angles of the malonates are between 88.29(5)° and 89.56(5)°. The bond distances between the aluminum centers and the bridging oxygen atoms are in the range 184.42(11)–189.57(11) pm, not showing significant differences for the hydroxo group compared to the OEt groups. Selected bond distances and angles are given in Table 3-11.

Table 3-11 Selected bond distances [pm] and angles [°] of **6b**.

Al(1)−O(1)	194.76(11)	Al(2)−O(15)	189.04(11)
Al(1)−O(2)	188.57(11)	Al(2)−O(16)	187.62(12)
Al(1)−O(5)	189.81(12)	Al(3)−O(15)	188.91(12)
Al(1)−O(6)	191.45(11)	Al(3)−O(16)	184.88(12)
Al(1)−O(9)	184.42(11)	Al(3)−O(17)	189.24(11)
Al(1)−O(10)	184.93(11)	Al(3)−O(18)	190.77(12)
Al(2)−O(9)	189.26(11)	Al(3)−O(21)	188.92(12)
Al(2)−O(10)	189.57(11)	Al(3)−O(22)	191.03(11)
Al(2)−O(11)	191.43(11)	O(16)−H(16)	78.8(14)
Al(2)−O(12)	190.83(12)	O(1)···H(16)	220.8(16)
O(1)−Al(1)−O(2)	89.26(5)	O(11)−Al(2)−O(15)	97.17(5)
O(1)−Al(1)−O(5)	83.62(5)	O(11)−Al(2)−O(16)	87.86(5)
O(1)−Al(1)−O(6)	170.68(5)	O(12)−Al(2)−O(15)	92.50(5)
O(1)−Al(1)−O(9)	92.67(5)	O(12)−Al(2)−O(16)	168.76(5)
O(1)−Al(1)−O(10)	91.16(5)	O(15)−Al(2)−O(16)	77.52(5)
O(2)−Al(1)−O(5)	92.26(5)	O(15)−Al(3)−O(16)	78.23(5)
O(2)−Al(1)−O(6)	84.66(5)	O(15)−Al(3)−O(17)	89.76(5)
O(2)−Al(1)−O(9)	172.86(5)	O(15)−Al(3)−O(18)	172.00(5)
O(2)−Al(1)−O(10)	95.53(5)	O(15)−Al(3)−O(21)	93.07(5)
O(5)−Al(1)−O(6)	89.56(5)	O(15)−Al(3)−O(22)	97.64(5)
O(5)−Al(1)−O(9)	94.79(5)	O(16)−Al(3)−O(17)	94.94(5)
O(5)−Al(1)−O(10)	170.57(5)	O(16)−Al(3)−O(18)	94.15(5)
O(6)−Al(1)−O(9)	94.23(5)	O(16)−Al(3)−O(21)	171.26(5)
O(6)−Al(1)−O(10)	96.43(5)	O(16)−Al(3)−O(22)	91.17(5)
O(9)−Al(1)−O(10)	77.56(5)	O(17)−Al(3)−O(18)	88.48(5)
O(9)−Al(2)−O(10)	75.28(5)	O(17)−Al(3)−O(21)	85.63(5)
O(9)−Al(2)−O(11)	90.90(5)	O(17)−Al(3)−O(22)	171.24(5)
O(9)−Al(2)−O(12)	96.98(5)	O(18)−Al(3)−O(21)	94.58(5)
O(9)−Al(2)−O(15)	167.73(5)	O(18)−Al(3)−O(22)	84.82(5)
O(9)−Al(2)−O(16)	93.63(5)	O(21)−Al(3)−O(22)	89.29(5)
O(10)−Al(2)−O(11)	165.55(5)	Al(1)−O(10)−Al(2)	102.82(5)
O(10)−Al(2)−O(12)	89.22(5)	Al(1)−O(9)−Al(2)	103.13(5)
O(10)−Al(2)−O(15)	97.16(5)	Al(2)−O(15)−Al(3)	101.09(5)
O(10)−Al(2)−O(16)	97.07(5)	Al(2)−O(16)−Al(3)	103.15(6)
O(11)−Al(2)−O(12)	88.29(5)	O(16)−H(16)···O(1)	144.6(17)

The structure of **6b** is to some extend related to that of $Al_3(\mu\text{-}O^iPr)_4(O^iPr)_2(acac)_3$ [50, 51] (compare chapter 1.2.3.1 / Figure 1-14), with an Al/acac ratio of 1:1. The structure of **6b** can formally be derived by substitution of the two terminal O^iPr groups by chelating ligands and replacement of one of the bridging OR groups by a hydroxo group. However, a structural analog to **6a** was not observed for acac or O^iPr derivatives. There are also no structural analogs to $Al_3(\mu\text{-}O^iPr)_4(O^iPr)_2(acac)_3$ for malonate or β-ketoesterate derivatives.

All resonances of the ^1H and ^{13}C NMR spectra were assigned based on the structure, but no resonance for Al–O***H*** was observed. Only one resonance for the methyl and two for the methylene protons for all three Al–OEt groups were observed at 1.33 and 3.72–3.84/4.43–4.60 ppm in the ^1H NMR spectrum. The ^{13}C NMR spectrum showed only two signals at 18.4 and 56.6 ppm for the methyl and methylene carbons of the Al–OEt groups. The methyl groups of the five detm ligands resulted in two triplets of equal intensity at 0.99 and 1.14 ppm in the ^1H NMR spectrum. In the ^{13}C NMR spectrum, the malonate OEt groups exhibited two resonances each for the methyl and methylene carbon at 14.4/14.6, and at 60.0/60.1 ppm. Single resonances were observed for CO***C******H***CO in the ^1H (4.91 ppm) and ^{13}C (66.4 ppm) NMR spectra as well as for ***C***O (175.4 ppm). EXSY spectra indicated exchange between the signals at 3.72-3.84 and 3.92-4.12 ppm and between the signals at 3.92–4.12 and 4.43–4.60 ppm. The signal at 3.72-3.84 ppm originates only from Al–OC$\boldsymbol{H}_2$Me and the signal at 4.43–4.60 ppm only from COOC$\boldsymbol{H}_2$Me, whereas the signals at 3.92–4.12 ppm results from overlapping signals of both types of OEt groups. Since no exchange between the signals at 3.72–3.84 and 4.43–4.60 ppm was observed, it is assumed that exchange happens only between Al–OEt groups or between malonate–OR groups, but not between Al– and malonate–OR groups. ^{27}Al NMR spectroscopy showed only one signal at 5.9 ppm, in line with the existence of only octahedrally coordinated aluminum (Figure 3-41) [17]. A slight broadening of the signal compared to those for octahedral aluminum in **3c**, **4c**, **4d**, and **5c** was observed and is probably caused by the presence of three different aluminum centers.

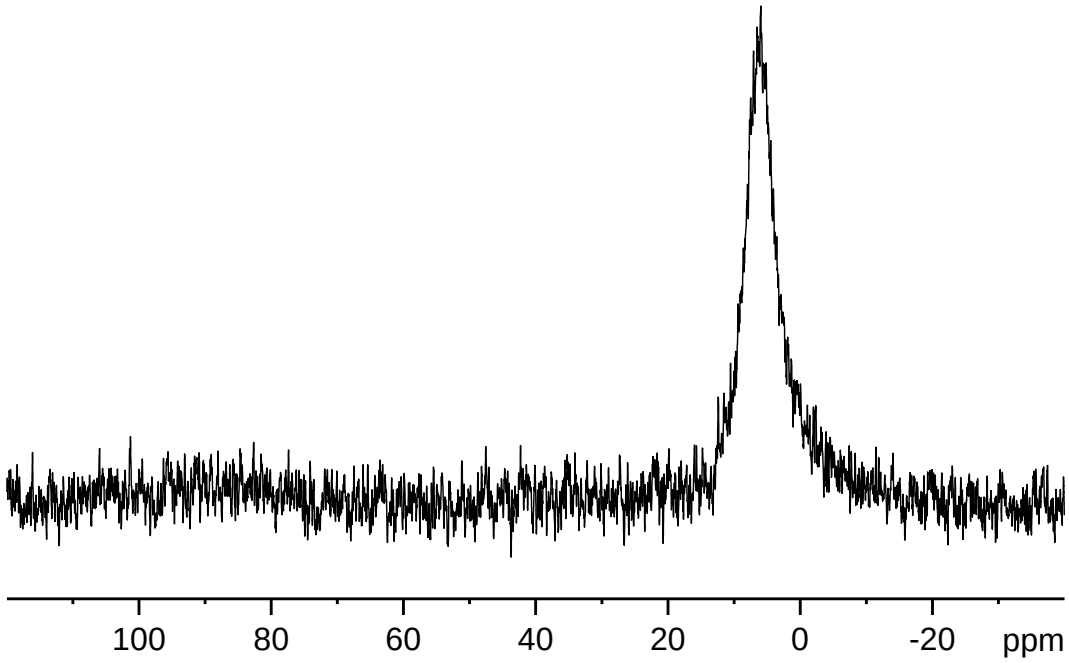

Figure 3-41 ^{27}Al NMR spectrum of **6b** (in [D_8]toluene).

At present, the origin of the hydroxo group is not clear, but it is strongly assumed that it results from cleavage of an OEt group with transfer of a proton to the oxygen and release of ethylene. The other possibility, partial hydrolysis during the reaction or of the used $Al(OEt)_3$, can be excluded since all operations were carefully carried out under exclusion of moisture and the reaction was reproducible. Furthermore, no partial hydrolyzed species were observed in other experiments starting from $Al(OEt)_3$ or another aluminum alkoxide. Formation of **6b** was also observed in a different experiment without the use of $Al(OEt)_3$. During attempts to crystallize Al(detm)$_3$ (**3b**) directly from the reaction solution of $Al(O^tBu)_3$ and detm-H in toluene, which contained **3b**, liberated ^{t}BuOH and some unreacted detm-H, formation of **6b** was also observed after some weeks by ^{1}H NMR spectroscopy. This observation proofs that

- the use of $Al(OEt)_3$ is not essential for the formation of **6b** and
- **6b** is a stable compound.

This also supports the postulated cleavage of an OEt group. Furthermore, the cleavage of Al–OR groups to give Al–OH and olefins was confirmed for the thermal decomposition of aluminum alkoxides, including $Al(OEt)_3$. Although this reaction was observed at higher temperatures only, it proves that the postulated reaction is in principle possible [98].

3.2.5 Transesterification

As for *β*-ketoesters [94], also malonates are reported to undergo transesterification reactions in presence of alcohols also in the absence of catalysts [99]. As denoted before, reactions of $Al(O^iPr)_3$ with dmem-H or detm-H were less straightforward than the

modification with d^{i}prm-H or d^{t}bum-H (compare chapters 3.2.1 and 3.2.2). No reaction was observed at all at room temperature (as for d^{i}prm-H or d^{t}bum-H), but after heating to elevated temperatures products were obtained exhibiting complex ^{1}H NMR spectra with multiple, broad, and overlapping resonances. Although coordination of malonate molecules was confirmed (appearance of signals at about 5 ppm for COC***H***CO), a closer look revealed that transesterification, *i.e.* exchange of the malonate–OR groups against O^{i}Pr groups, had taken place concomitantly, which was *inter alia* indicated by the formation of free d^{i}prm-H and coordinated d^{i}prm. The formation of **3a** or **3b** for the reaction with three equiv. of malonate per aluminum atom, *e.g.* partial formation of the intended products, could not be confirmed. Transesterification was not quantitative since twice as much OR groups than O^{i}Pr groups were present, and malonate species with both O^{i}Pr and OMe/OEt groups as well as Al(OEt)$_x$/Al(OMe)$_x$ species were spectroscopically identified. Furthermore, the formation of completely substituted complexes Al(malonate)$_3$ could not be confirmed.

Since the reactivity of Al(O^{i}Pr)$_3$ towards substitution with malonates was shown to be temperature dependent (compare chapter 3.2.1) and that transesterification occurs only at elevated temperatures for reactions with *β*-ketoesters (compare chapter 3.1.1.4), it was tried to coordinate dmem-H or detm-H to thermally pre-treated and deoligomerized Al(O^{i}Pr)$_3$ at room temperature in toluene. A solution of [Al(O^{i}Pr)$_3$]$_4$ in toluene was thus heated to reflux for 3 d and, after cooling to room temperature, dmem-H or detm-H was added. After stirring overnight at room temperature, coordination of the malonate was confirmed by NMR spectroscopy, but again transesterification was observed to a large extent. These results demonstrate that

- thermal de-oligomerization accelerates coordination of the malonate ligands and enables the reaction at room temperature, but also that
- thermal de-oligomerization and reaction at room temperature does not prevent transesterification.

In contrast to the results obtained for the modification with *β*-ketoesters (compare chapter 3.1.1.4), variation of the stoichiometric ratios did not cause any changes. Reaction of Al(O^{i}Pr)$_3$ with dmem-H and detm-H in an Al/malonate ratio of 1:1 gave also product mixtures through transesterification at the ester group as well as the aluminum center.

Compared to Al(O^{i}Pr)$_3$, transesterification was not observed for Al(O^{t}Bu)$_3$ in any case, showing that the tendency to undergo transesterification depends on the steric demand of the Al–OR group as well as on the malonate–OR group. In contrast to the reactions with *β*-ketoesters (compare chapter 3.1.1.4), where transesterification was observed only in cases where the attacking alkoxo group was “smaller” than the ester alkoxo group, *viz.* for *β*-ketoesters the attack of the “smaller” O^{i}Pr at “bigger” ^{t}buac, transesterification occurred for malonates upon attack of the “bigger” O^{i}Pr at “smaller” dmem-H or detm-H. On the other hand, O^{t}Bu groups appear to be sterically too demanding to attack the ester functionalities, since no transesterification was observed in reactions starting from Al(O^{t}Bu)$_3$.

3.2.6 Conclusions

It was shown that malonates are versatile ligands for the modification of aluminum alkoxides and are a good alternative to *β*-diketone or *β*-ketoester derivatives, although ligand substitution requires higher reaction temperatures and longer reaction times due to the fact that deprotonation of the malonic esters is less favorable.

Products with an Al/malonate ratio of 1:3 (**3c**), 1:2 (**5c**) and 1:1 (**4c**) were obtained for the reaction of $Al(O^iPr)_3$ with d^iprm-H. However, **5c** was not obtained by the direct reaction of aluminum alkoxide with two equivalents of malonate but formed spontaneously from **4c** upon storage. This is of particular interest, since analogous *β*-diketonate or *β*-ketoesterate derivatives were reported to be unstable and to decompose to give Al(*β*-diketonate)$_3$ and $Al_2(\mu\text{-}O^iPr)_2(O^iPr)_2$(*β*-diketonate)$_2$ upon storage in solution at room temperature. Complexes $Al_2(\mu\text{-}O^iPr)_2(O^iPr)_2(d^iprm)_2$ (**4c**) and $Al_2(\mu\text{-}O^iPr)_2(O^iPr)_2(d^tbum)_2$ (**4d**) with an Al/malonate ratio of 1:1 have analogous structures as the corresponding *β*-ketoester derivatives (compare chapter 3.1.1.2), *i.e.* they are dinuclear complexes with one octahedrally coordinated aluminum center bearing two malonate ligands connected, by two bridging O^iPr groups, to the second, tetrahedrally coordinated aluminum center, bearing two additional terminal O^iPr groups. $[Al(\mu\text{-}O^iPr)(d^iprm)_2]_2$ (**5c**) is a C_2-symmetric dimer, again analogous to a known *β*-diketonate derivative [50, 54], with two octahedrally coordinated aluminum centers connected by two μ-O^iPr groups.

Modification with dmem-H or detm-H resulted in partial transesterification in the case of $Al(O^iPr)_3$, but not with $Al(O^tBu)_3$. This leads to the conclusion that the tendency to undergo transesterification depends on the malonate as well as on the aluminum alkoxo groups. The use of $Al(O^tBu)_3$ also allowed obtaining complexes Al(malonate)$_3$ for all ligands used (**3a**–**3d**), but no products with an Al/malonate ratio of 1:1 or 1:2 were obtained. This indicates that the O^tBu group is sterically too demanding to enable formation of Al–O^tBu–Al bridges, which are necessary to stabilize substitution products by means of coordination expansion.

Finally, the unexpected product $Al_3(\mu\text{-}OH)(\mu\text{-}OEt)_3(detm)_5$ (**6b**) was obtained, bearing an Al–OH group, most likely formed by scission of an OEt group. This is supported by the fact that **6b** was obtained by two independent experiments.

3.3 Modification of Aluminum Alkoxides with *β*-Ketoamides

Based on the successful modification of aluminum alkoxides with *β*-ketoesters and dialkylmalonates it was tried to modify aluminum alkoxides in an analogous manner with N,N-diethyl acetoacetamide (Figure 3-42).

The modification of metal alkoxides with *β*-ketoamides is described very rarely in literature. Only the modification of $Zr(O^iPr)_4$ with N,N-diethyl acetoacetamide [100] and of $Ti(O^iPr)_4$ with *o*-hydroxy benzamide [101], was reported. Other *β*-ketoamido complexes of titanium and zirconium were obtained by a "transesterification/transamidation" reaction between a titanium or zirconium amide with *β*-ketoesters [102].

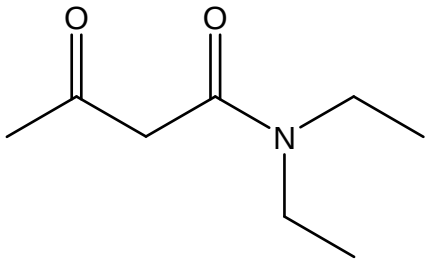

detaca-H

Figure 3-42 N,N-Diethyl acetoacetamide used for the modification of aluminum alkoxides.

The reaction of $Al(O^iPr)_3$ with three equiv. detaca-H in toluene at room temperature yielded – after removal of the volatiles *in vacuo* – a slightly greenish oil, which upon storage crystallized. Single crystal XRD revealed $Al(detaca)_3$ (**7b**) as product (Figure 3-43). Heating of the reaction solution to elevated temperatures did not cause any change of the product (according to NMR spectroscopy).

From the possible C_1 and C_3 symmetric isomers (compare chapter 3.1.1.1 for analogous Al(*β*-ketoesterate)$_3$ complexes), the C_1 symmetric crystallized exclusively. The Al–O bond distances are in the range of 187.1(1)–189.6(1) pm. The average $Al–O^{keto}$ distances (187.1(1)–187.4(1) pm) are shorter than the $Al–O^{amido}$ distances (187.4(1)–189.6(1) pm), as expected. Interestingly, one of the $Al–O^{amido}$ bonds (Al(1)–O(6)) is significantly shorter than the other two. This cannot be explained by a *trans* influence, since it is a bond *trans* to another $Al–O^{amido}$ bond (Al(1)–O(2)). Also for the $Al–O^{keto}$ bonds no significant *trans* influence was observed. The bite angles of the acetoacetamide ligands are all slightly above 90° (90.63(5)°–91.53(5)°). Selected bond distances and angles are given in Table 3-12.

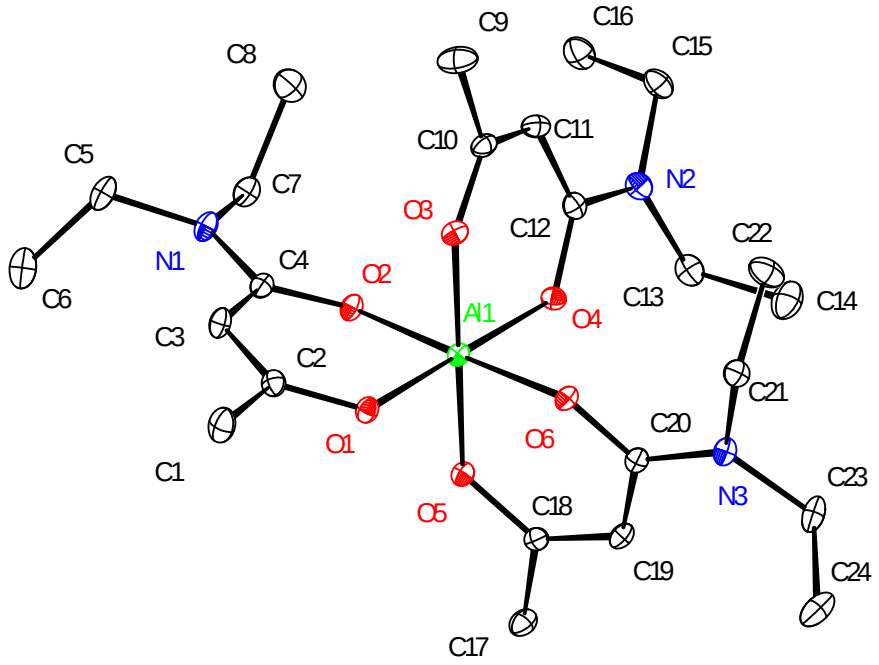

Figure 3-43 Molecular structure of Al(detaca)$_3$ (**7b**), showing 30 % thermal ellipsoids (hydrogen atoms omitted for clarity).

Table 3-12 Selected bond distances [pm] and angles [°] of **7b**.

Al(1)–O(1)	1871.2(11)	Al(1)–O(4)	189.64(11)
Al(1)–O(2)	1892.6(11)	Al(1)–O(5)	187.31(11)
Al(1)–O(3)	1874.0(11)	Al(1)–O(6)	187.42(11)
O(1)–Al(1)–O(2)	91.54(5)	O(2)–Al(1)–O(6)	178.40(5)
O(1)–Al(1)–O(3)	88.88(5)	O(3)–Al(1)–O(4)	90.62(5)
O(1)–Al(1)–O(4)	178.55(5)	O(3)–Al(1)–O(5)	178.43(5)
O(1)–Al(1)–O(5)	92.47(5)	O(3)–Al(1)–O(6)	89.54(5)
O(1)–Al(1)–O(6)	89.93(5)	O(4)–Al(1)–O(5)	88.06(5)
O(2)–Al(1)–O(3)	89.83(5)	O(4)–Al(1)–O(6)	88.71(5)
O(2)–Al(1)–O(4)	89.82(5)	O(5)–Al(1)–O(6)	91.28(5)
O(2)–Al(1)–O(5)	89.32(5)		

Compared to Al(^{t}buac)$_3$ [90], the Al–O^{keto} bond distances are quite similar, but the Al–O^{amido} bond distances in **7b** are significantly shorter (187.4(1)–189.6(19) pm) than the Al–O^{ester} bond distances in Al(^{t}buac)$_3$ (192.99(19)–195.1(2) pm). This also shows, that there is a much smaller difference between the Al–O^{keto} and Al–O^{amido} bond distances in (**7b**) than between the Al–O^{keto} and Al–O^{ester} bond distances in Al(^{t}buac)$_3$. The Al–O^{keto} bond distances are quite comparable to those of Al(acac)$_3$ [91] (187.98(22) pm) and the Al–O^{amido} bond

distances to the Al–O^{ester} bond distances of the malonate derivatives **3a**, **3c**, and **3d** (186.8(1)–189.3(1) pm).

The ^{1}H and ^{13}C NMR spectra confirmed the structure, giving sets of signals for the carbonyl groups and CO***CH***CO as observed for the Al(*β*-ketoesterate)$_3$ complexes (**1a**–**1d**) (compare chapter 3.1.1.1). Coexistence of the C_1 symmetric and the C_3 symmetric isomers could be confirmed, since four signals can be observed in the ^{13}C NMR spectrum for the keto ***C***O as well as for the CO***C***HCO. The resonances for the ethyl groups give broad signals in the ^{1}H as well as in the ^{13}C spectra, indicating dynamics, *viz.* rotation, of the amido group at room temperature in C_6D_6.

Reaction of Al($O^{i}Pr$)$_3$ with one equivalent of detaca-H in toluene at room temperature did not yield **7b** and unreacted [Al($O^{i}Pr$)$_3$]$_4$ as observed for reactions with *β*-ketoesters (compare chapter 3.1.1.1 and 3.1.1.2), but yielded Al$_2$(*μ*-$O^{i}Pr$)$_2$($O^{i}Pr$)$_2$(detaca)$_2$ (**8b**), similar to the modification with *β*-ketoesters bearing additional subtituents in the 4 position (compare chapter 3.1.3.1). The dimeric structure was revealed by ^{1}H and ^{13}C NMR spectroscopy, showing dynamics of the amido functionaltiy as observed for the trisubstituted product (**7b**). These results show that the different electronic influence of the amido functionality compared to an ester functionailty leads to a preferrential formation of the monosubstituted dimeric compound.

These results prove, that the substitution reaction between aluminum alkoxides and acetoacetamides is an easily applicable alternative for the modification of aluminum alkoxides with other *β*-diketonate compounds. This is the first report on the modification of aluminum alkoxides and also the first single crystal structure of an acetoacetamido ligand coordinated to an aluminum center. Since the C(O)–N amido bond is known to be more stable than a C(O)–O ester bond – what is also reflected by the fact, that metal amides can react with *β*-ketoesters to give metal alkoxides and *β*-ketoamides [102] – this opens a route to a new class of ligands, for which transesterification should be less a problem than for *β*-ketoesters or dilakylmalonates.

3.4 Modification of Yttrium Alkoxides

Based on the results for the modification of aluminum alkoxides with *β*-ketoesters and dialkylmalonates, analogous methods were applied to yttrium alkoxides. In contrast to aluminum, yttrium is able to form structures with coordination numbers higher than six. Furthermore, already the "pure" yttrium isopropoxide is a polynuclear alkoxo/oxo-cluster (compare chapter 1.2.2) [38].

3.4.1 $Y_9O(OH)_9(O^iPr)_8(^i prac)_8$[viii]

First experiments were carried out using isopropyl acetoacetate (^{i}prac-H) as ligand to avoid complications by transesterification as possible side reaction. Reaction of one equiv. of ^{i}prac-H (calculated for "$Y(O^iPr)_3$")[ix] with yttrium isopropoxide in toluene at room temperature showed complete coordination of the ligand (confirmed by ^{1}H NMR spectroscopy / compare chapter 3.1.1.1). In contrast to the analogous reaction with aluminium alkoxide, no changes of the spectrum were observed upon heating of the reaction solution, indicating the formation of the final product already at room temperature. Recrystallization of the white powder – obtained by evaporation of the volatiles *in vacuo* – from toluene at room temperature yielded colorless crystals. Single crystal structure analysis revealed $Y_9(\mu_5\text{-}O)(\mu_4\text{-}OH)(\mu_3\text{-}OH)_8(\mu\text{-}O^iPr)_8(^i prac)_8$ (**9c**) as product (Figure 3-44).

This structure is one of the rare examples of homometallic yttrium clusters with alkoxo-groups and additional organic ligands. Analogous examples from the literature are octanuclear $[Y_4O(OEt)_2(aaa)_5]_2(OH)_4(OEt)_2$[x] [44, 83], prepared by a related reaction procedure also starting from $Y_5O(O^iPr)_{13}$[xi]. Other copmpounds are $[Y(tmp)_2(OEt)]_2$[xii] and $[Y(tmp)_2]_2(OEt)(O^nBu)$[xiii] (tmp = 2,2,6,6-tetramethylpiperidinate), respectively [103], prepared from YCl_3 as yttrium source, or $Y_3(OR)_5(acac)_4$[xiv] (OR = OCH_2CH_2OMe), which was obtained upon raction of $[Y(OR)_3]_{10}$[xv] (OR = OC_2H_4OMe) with $Cu(acac)_2$ as byproduct in an attempt to prepare yttrium/copper bimetallic MOCVD precursors [104].

[viii] For the sake of clarity, the formulas of the yttrium complexes are denoted in a concentrated form without indication and differentiation of the coordination modes, *e.g.* $Y_9O(OH)_9(O^iPr)_8(^i prac)_8$ represents $Y_9(\mu_5\text{-}O)(\mu_4\text{-}OH)(\mu_3\text{-}OH)_8(\mu\text{-}O^iPr)_8(^i prac)_8$. Formulas indicating the binding modes of all ligands will be given in footnotes.

[ix] Corresponding to 0.22 equiv. of ^{i}prac-H per $Y_5(\mu_5\text{-}O)(\mu_3\text{-}O^iPr)_4(\mu\text{-}O^iPr)_4(O^iPr)_5$, *viz.* 1.08 equiv. of ^{i}prac-H per ytrrium atom.

[x] $[Y_4(\mu_4\text{-}O)(\mu\text{-}OEt)_2(\mu\text{-}aaa)_2(aaa)_3]_2(\mu_3\text{-}OH)_4(\mu_3\text{-}OEt)_2$

[xi] $Y_5(\mu_5\text{-}O)(\mu_3\text{-}O^iPr)_4(\mu\text{-}O^iPr)_4(O^iPr)_5$

[xii] $[Y(tmp)_2(\mu\text{-}OEt)]_2$

[xiii] $[Y(tmp)_2]_2(\mu\text{-}OEt)(\mu\text{-}O^nBu)$

[xiv] $Y_3(\mu_3,\kappa^2\text{-}OR)_2(\mu,\kappa^2\text{-}OR)_2(\mu,\kappa^1\text{-}OR)(acac)_4$

[xv] $[Y(\mu,\kappa^2\text{-}OR)_2(OR)]_{10}$

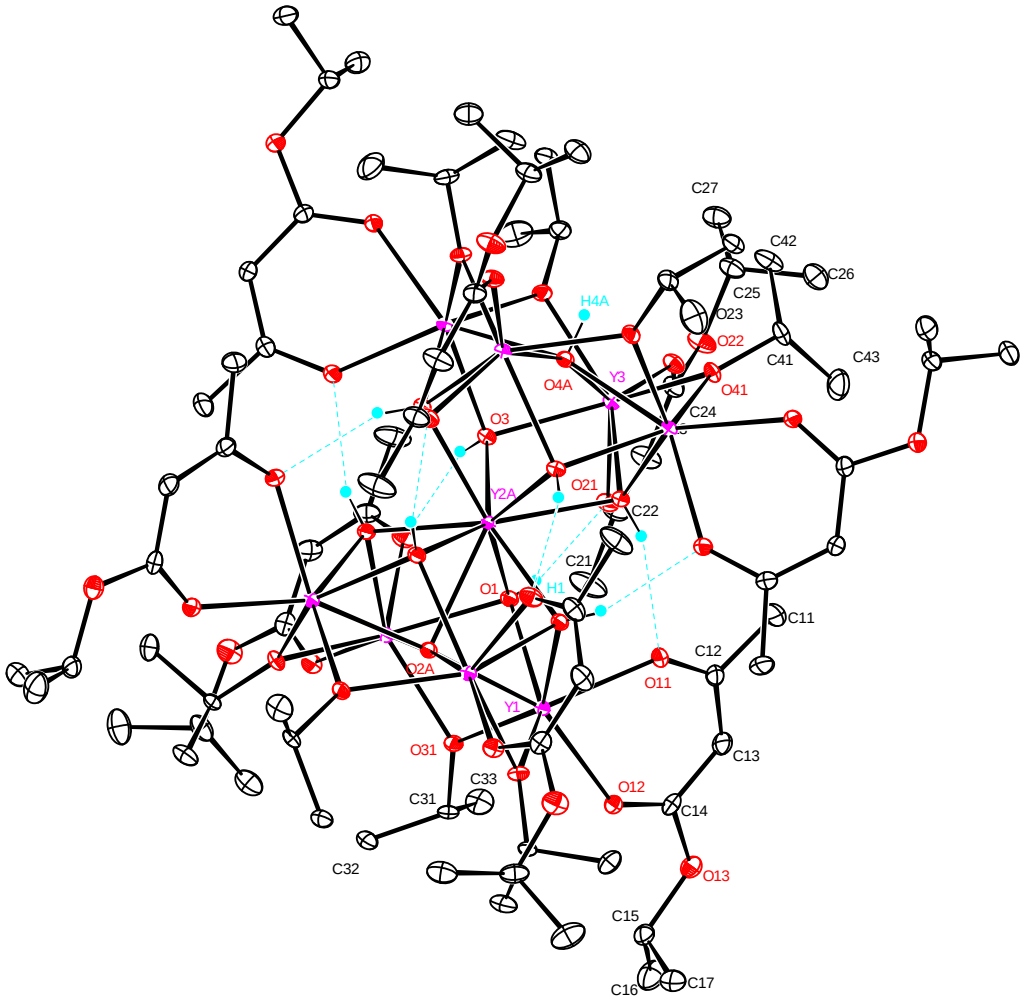

Figure 3-44 Molecular structure of $Y_9O(OH)_9(O^iPr)_8(^iprac)_8$ (**9c**), showing 30 % thermal ellipsoids (carbon-bond hydrogen atoms omitted for clarity).

The structure exhibits an Y_9 core (Figure 3-45), which was already reported in the literature as a structural motive for another yttrium complex, *viz.* $[Na(EtOH)_6][Y_9O_2(OH)_8(etac)_{16}]$[xvi] [105]. Another compound showing the same Y_9 core is presented in this work, *viz.* $Y_9O(OH)_9(^iprac)_{16}$[xvii] (**11c**) (compare chapter 3.4.3). In both cases only *β*-ketoesterate and oxo/hydroxo ligands are coordinated to the yttrium centers and no yttrium bonded alkoxo groups are present. The complex reported in the literature is charged, in contrast to the two Y_9 clusters reported in this work, which are neutral.

[xvi] $[Na(EtOH)_6][Y_9(\mu_4\text{-}O)_2(\mu_3\text{-}OH)_8(\mu\text{-}etac)_8(etac)_8]$
[xvii] $Y_9(\mu_5\text{-}O)(\mu_4\text{-}OH)(\mu_3\text{-}OH)_8(\mu\text{-}^iprac)_8(^iprac)_8$

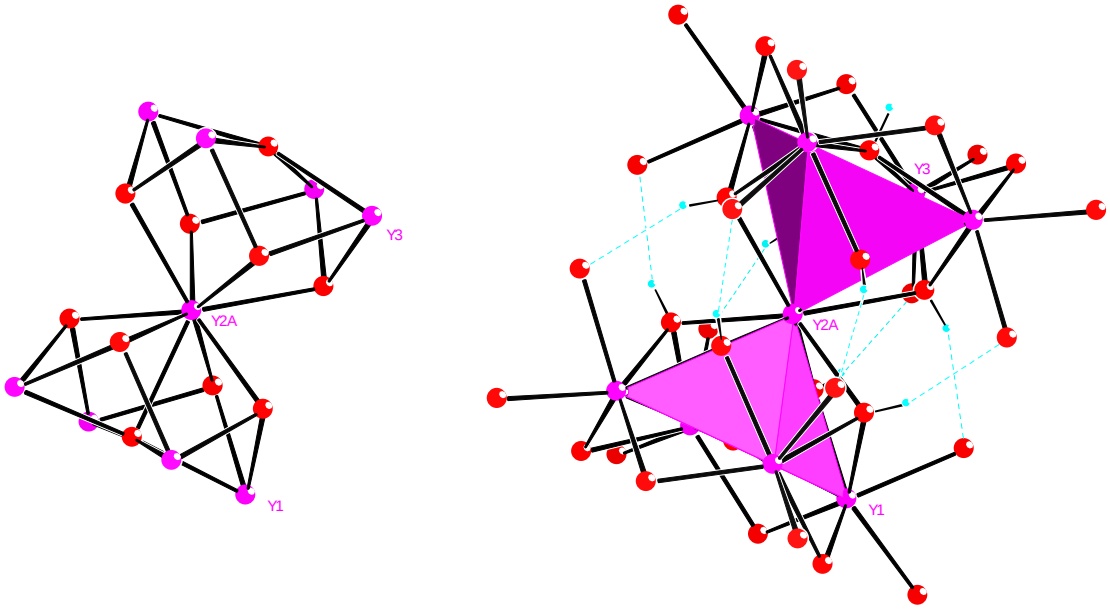

Figure 3-45 Y_9 core of **9c** showing the yttrium and μ_5-O, μ_4-OH, and μ_3-OH atoms (*left*) and the first coordination sphere of the yttrium atoms and the Y_5 pyramids (*right*).

The structure can be described by two square pyramids formed by five yttrium atoms connected through their vertices. The eight yttrium atoms of the basal planes are each seven-coordinated by one bidentate ^{i}prac, two μ-O^{i}Pr, two μ_3-OH and one μ_5-O or μ_4-OH, respectively. The "central" yttrium atom is coordinated by eight μ_3-OH and one μ_5-O, resulting in a coordination number of nine. The coordination geometry of the eight seven-coordinated yttrium atoms can be described as capped trigonal prismatic, whereas the central yttrium atom is surrounded by a capped square antiprism, where the μ_5-O atom caps one of the base planes of the prism (Figure 3-46).

The structural motif of the square-pyramidal Y_5 arrangement with an oxygen atom in the center of the square base is also found in the structure of yttrium isopropoxide [38], which is the starting material for the preparation of the compound. This reflects the stability of this structural motive. The basal planes of the two pyramids are rotated 90° with respect to each other, leading to a four-fold a rotational axis (Figure 3-47).

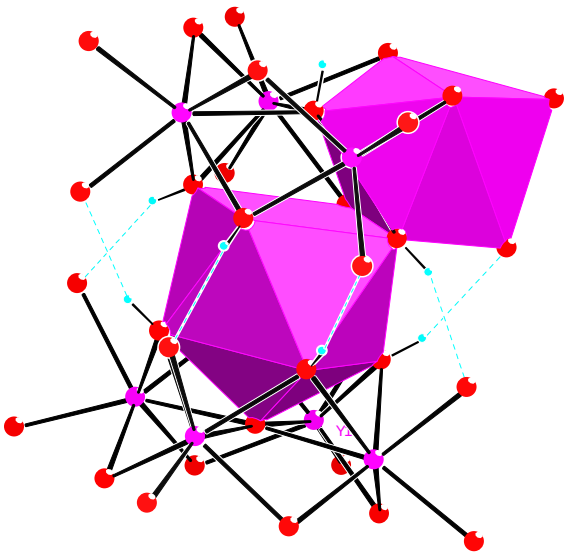

Figure 3-46 Coordination polyhedra of the yttrium atoms in **9c**.

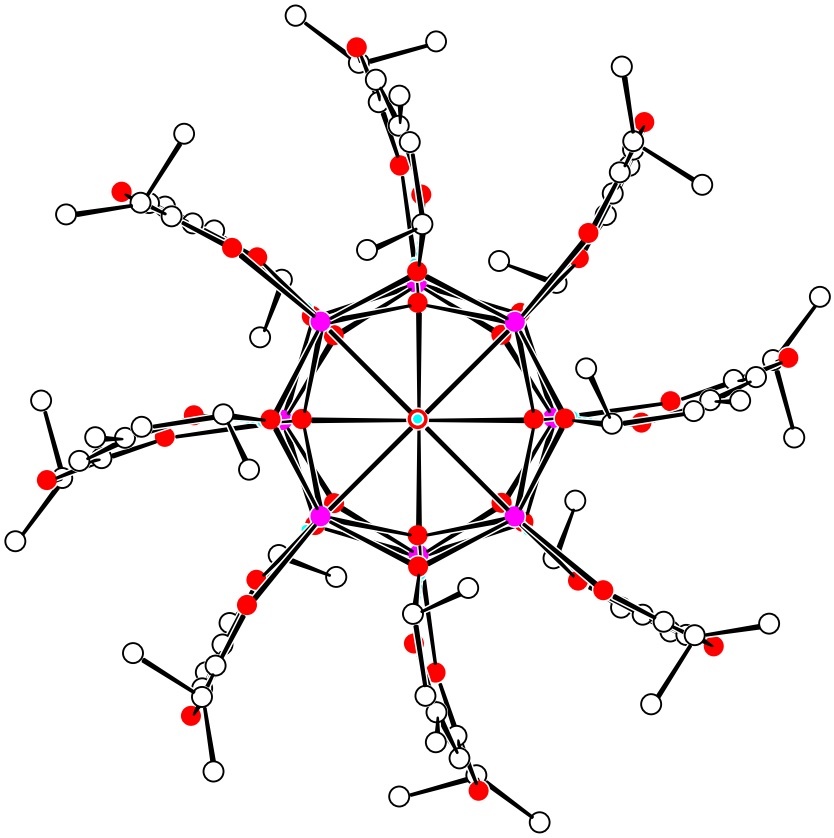

Figure 3-47 View along the C_4 axis of **9c**.

The two different "sides" of the structure, *i.e.* the side with the μ_5-O (O(2)) and the side with the μ_4-OH (O(4)) in the center of the basal planes of the square pyramides, can clearly be distinguished by means of bond distances and angles. The Y(2)–O(2) distance (2.484(9) pm) is significantly shorter than for Y(2)--O(4) (3.198(9) pm), leading to a bond in the former case and a non-bonding situation in the latter. This is also reflected by the fact, the the position of O(2) sligthly deviates from the Y(1) plane, lying "inside" the Y_5 pyramide, whereas O(4) clearly is positioned "outside" the pyramide. Compared to the known, structurally analogous $[Na(EtOH)_6][Y_9O_2(OH)_8(etac)_{16}]$, these distances are longer (2.89(2) pm) and shorter (2.94(2) pm), respectively, corresponding to a μ_5-binding mode of O(2). The same influence is seen for the Y(2)--Y(1) (3.499(6) pm) and Y(2)--Y(3) (3.749(6) pm) distances, showing that the formation of the Y(2)–O(2) bond leads to a contraction of the whole Y_5 pyramid, again with shorter distances for the μ_5-O side and longer distances for the μ_4-OH side compared to $[Na(EtOH)_6][Y_9O_2(OH)_8(etac)_{16}]$. This contraction is also reflected in shorter Y(1)--Y(1) distances (3.3774(8) pm compared to 3.4245(8) pm for Y(3)--Y(3)) but both shorter than in $[Na(EtOH)_6][Y_9O_2(OH)_8(etac)_{16}]$ (3.560(3)–3.593(3) pm). Analogous influences are also observed for the Y–(μ_3-OH) and Y–(μ-O^{i}Pr) distances. As expected, the Y–O^{ester} bond distances (2.326(3) and 2.301(3) pm) are slightly longer than the Y–O^{keto} distances (2.299(3) and 2.281(3) pm), but for this bonds with slightly longer distances for the Y(1) side. The bite angles of the ^{i}prac ligands are 73.70(10)° (Y(1)) and 74.03(10)° (Y(3)), respectively. Selected bond distances are given in Table 3-13.

Table 3-13 Selected bond distances [pm] and angles [°] of **9c**.

Y(1)–O(1)	228.8(2)	Y(3)–O(22)	230.1(2)
Y(1)–O(1)^a	230.7(2)	Y(3)–O(3)	229.1(2)
Y(1)–O(11)	230.0(2)	Y(3)–O(3)^a	228.9(2)
Y(1)–O(12)	232.6(2)	Y(3)–O(41)	227.6(2)
Y(1)–O(2A)	238.91(6)	Y(3)–O(41)^b	229.0(2)
Y(1)–O(31)	229.0(2)	Y(3)–O(4A)	244.45(12)
Y(1)–O(31)^a	226.5(2)	O(1)–H(1)	80.6(18)
Y(2A)–O(1)	233.8(3)	O(3)–H(3)	80.1(18)
Y(2A)–O(2A)	248.3(11)	O(4A)–H(4A)	84(2)
Y(2A)–O(3)	246.4(3)	O(21)···H(1)	220(2)
Y(3)–O(21)	228.3(2)	O(11)^b···H(3)	217(2)
O(1)–Y(1)–O(1)^a	79.97(10)	O(22)–Y(3)–O(3)^a	136.96(8)
O(1)–Y(1)–O(11)	79.18(8)	O(22)–Y(3)–O(4A)	143.78(19)
O(1)–Y(1)–O(12)	124.16(7)	O(3)–Y(2A)–O(3)^a	71.78(10)
O(1)–Y(1)–O(2A)	65.50(14)	O(3)–Y(2A)–O(3)^c	112.0(2)
O(1)–Y(1)–O(31)	74.83(8)	O(3)–Y(3)–O(3)^a	78.23(10)
O(1)–Y(1)–O(31)^a	141.25(7)	O(3)–Y(3)–O(4A)	70.50(15)
O(1)^a–Y(1)–O(11)	76.39(8)	O(3)^a–Y(3)–O(41)^b	138.01(7)
O(1)^a–Y(1)–O(12)	135.84(7)	O(3)^a–Y(3)–O(4A)	70.53(15)

Table 3-13 (cont.)

O(1)[a]–Y(1)–O(2A)	65.22(14)	O(31)–Y(1)–O(31)[a]	107.60(11)
O(1)[a]–Y(1)–O(31)	140.55(7)	O(41)–Y(3)–O(21)	124.22(8)
O(1)[a]–Y(1)–O(31)[a]	74.92(8)	O(41)–Y(3)–O(22)	92.19(7)
O(1)–Y(2A)–O(1)[a]	78.33(10)	O(41)–Y(3)–O(3)	138.29(7)
O(1)–Y(2A)–O(1)[c]	126.5(2)	O(41)–Y(3)–O(3)[a]	74.60(8)
O(1)–Y(2A)–O(2A)	63.27(12)	O(41)–Y(3)–O(41)[b]	106.81(11)
O(1)–Y(2A)–O(3)	74.13(7)	O(41)–Y(3)–O(4A)	70.89(11)
O(1)–Y(2A)–O(3)[a]	74.29(7)	O(41)[b]–Y(3)–O(22)	84.91(7)
O(1)–Y(2A)–O(3)[b]	140.70(8)	O(41)[b]–Y(3)–O(3)	74.29(8)
O(1)–Y(2A)–O(3)[c]	140.93(8)	O(41)[b]–Y(3)–O(4A)	70.67(11)
O(11)–Y(1)–O(12)	73.67(8)	Y(1)–O(1)–Y(1)[b]	94.59(8)
O(11)–Y(1)–O(2A)	130.95(19)	Y(1)–O(1)–Y(2A)	98.30(11)
O(11)–Y(1)–O(31)	126.44(8)	Y(1)[b]–O(1)–Y(2A)	97.75(11)
O(11)–Y(1)–O(31)[a]	121.61(8)	Y(1)–O(2A)–Y(2A)	91.79(18)
O(12)–Y(1)–O(2A)	154.88(18)	Y(1)–O(2A)–Y(1)[a]	89.944(12)
O(12)–Y(1)–O(31)	83.61(7)	Y(1)–O(2A)–Y(1)[c]	176.4(4)
O(12)–Y(1)–O(31)[a]	94.18(7)	Y(1)–O(31)–Y(1)[b]	95.69(8)
O(2A)–Y(1)–O(31)	76.79(11)	Y(2A)–O(3)–Y(3)[b]	104.07(10)
O(2A)–Y(1)–O(31)[a]	77.25(12)	Y(2A)–O(3)–Y(3)	104.01(10)
O(2A)–Y(2A)–O(3)	124.00(11)	Y(3)–O(3)–Y(3)[b]	96.79(8)
O(21)–Y(3)–O(22)	73.92(8)	Y(3)–O(4A)–Y(3)[a]	88.92(5)
O(21)–Y(3)–O(3)	80.51(8)	Y(3)–O(4A)–Y(3)[c]	164.2(4)
O(21)–Y(3)–O(3)[a]	80.26(8)	Y(3)–O(41)–Y(3)[a]	97.18(8)
O(21)–Y(3)–O(41)[b]	124.59(8)	O(1)–H(1)···O(21)	165(3)
O(21)–Y(3)–O(4A)	142.11(19)	O(3)–H(3)···O(11)[b]	163(3)
O(22)–Y(3)–O(3)	128.84(7)	O(22)–Y(3)–O(3)[a]	136.96(8)

Symmetry transformations used to generate equivalent atoms:
[a] y,-x+1/2,z; [b] -y+1/2,x,z; [c] -x+1/2,-y+1/2,z

As can be expected for steric reasons, the ester functionalities of the ^{i}prac ligands are directed away from the center of the structure. The cluster is further stabilized by the formation of eight H-bonds between the μ_3-OH groups and the keto carbonyl oxygens of the ^{i}prac ligands (2.165(40) pm for O(11)···H(3) and 2.185(50) pm for O(21)···H(1)). These hydrogen bonds also determine the orientation of the β-ketoesterate ligands, since hydrogen bonds are preferentially formed to the keto carbonyl oxygen.

Compound **9c** crystallized in the tetragonal space group *P*4/n. The packing arrangement of the Y_9 clusters leads to large voids, forming channels along the *c* axis (Figure 3-48). These channels are filled with four toluene molecules per Y_9 cluster.

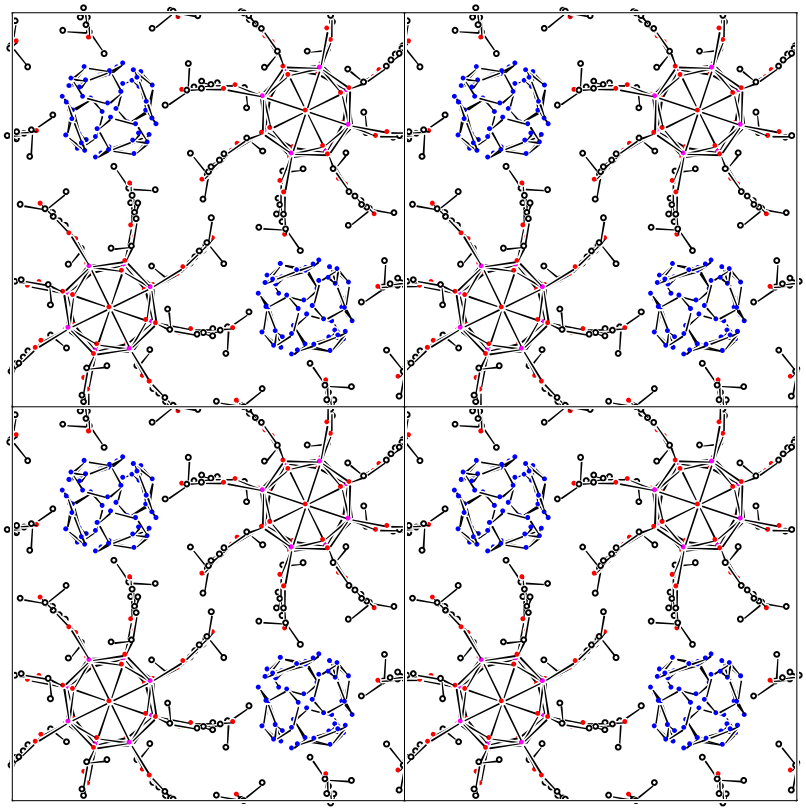

Figure 3-48 Representation of a 2x2x2 super cell of **9c**, along the *c* axis (hydrogen atoms omitted for clarity, carbon atoms of solvent molecules colored blue).

3.4.2 $[Y_2(OH)(^i prac)_5]_2$[xviii]

In an analogous reaction of yttrium isopropoxide with three equiv. of ^{i}prac-H (calculated for "$Y(O^iPr)_3$")[xix], a white precipitate formed after several days of stirring in toluene at room temperature, which was recrystallized directly from the reaction solution, yielding colorless crystals. A single crystal structure analysis revealed $[Y_2(\mu_3\text{-}OH)(\mu\text{-}^i prac)_3(^i prac)_2]_2$ (**10c**) as product (Figure 3-49). Refluxing of the reaction solution for several hours, causing dissolution of the precipitate, did not change the product.

[xviii] $[Y_2(\mu_3\text{-}OH)(\mu\text{-}^i prac)_3(^i prac)_2]_2$

[xix] Corresponding to 0.65 equiv. of ^{i}prac-H per $Y_5(\mu_5\text{-}O)(\mu_3\text{-}O^iPr)_4(\mu\text{-}O^iPr)_4(O^iPr)_5$, *viz.* 3.25 equiv. of ^{i}prac-H per ytrrium atom.

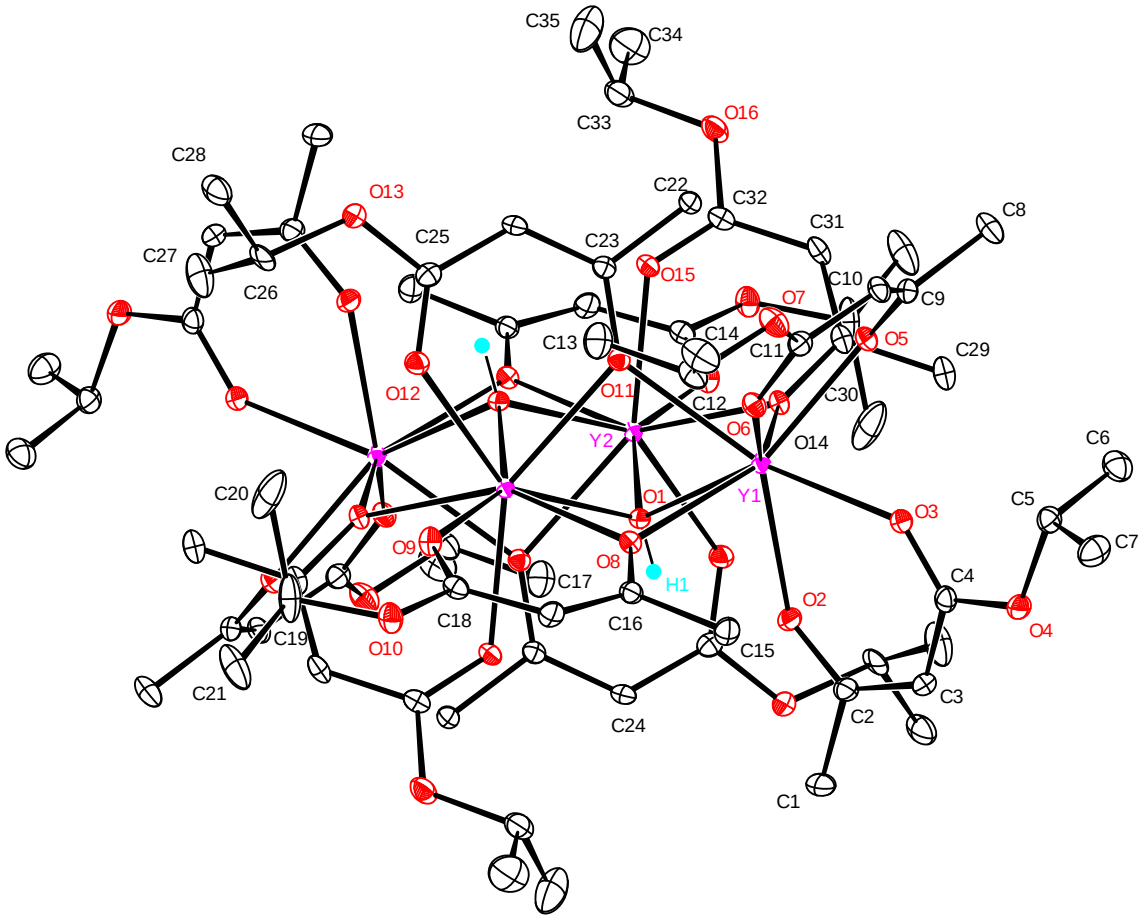

Figure 3-49 Molecular structure of $[Y_2(OH)(^{i}prac)_5]_2$ (**10c**), showing 30 % thermal ellipsoids (carbon-bond hydrogen atoms omitted for clarity).

This product shows complete replacement of the O^{i}Pr groups, and only β-ketoesterate and hydroxo groups as ligands. The μ_5-O atom from the parent $Y_5O(O^{i}Pr)_{13}$ is also replaced. The structure exhibits an Y_4 core (Figure 3-50) with two distinguishable eight-coordinated yttrium atoms. Of the overall ten ^{i}prac ligands, four are chelating but six ^{i}prac ligands exhibit a bridging-chelating binding mode. Bridging occurs exclusively by the keto carbonyl group whereas the ester carbonyl group coordinates to one of the bridged yttrium centers.

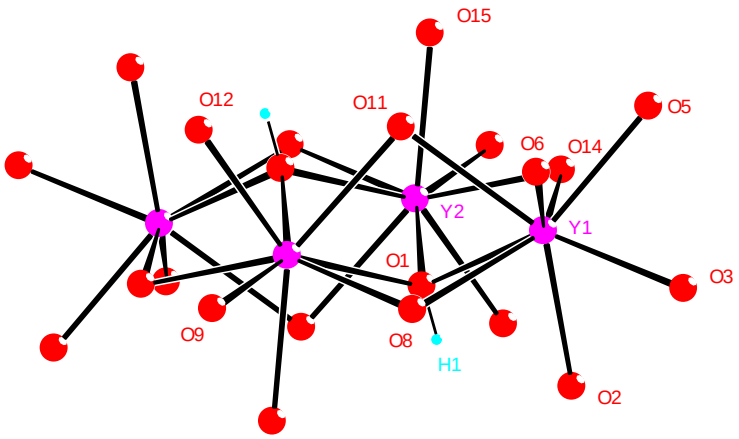

Figure 3-50 Y_4 core of **10c** showing the first coordination sphere of the yttrium atoms.

One type of yttrium atoms (Y(1)) is coordinated by two "terminal" bidentate ^{i}prac ligands, one hydroxo group and the keto groups of three bridging ^{i}prac ligands. The other type of yttrium centers (Y(2)) is coordinated by two hydroxo groups and chelated by three bridging ^{i}prac ligands, *i.e.* is coordinated by the keto and ester carbonyl group of the bridging ^{i}prac ligands. The Y(1) centers show a distorted dodecahedral coordination geometry whereas the coordination around Y(2) is better described as a distorted square antiprism (Figure 3-51).

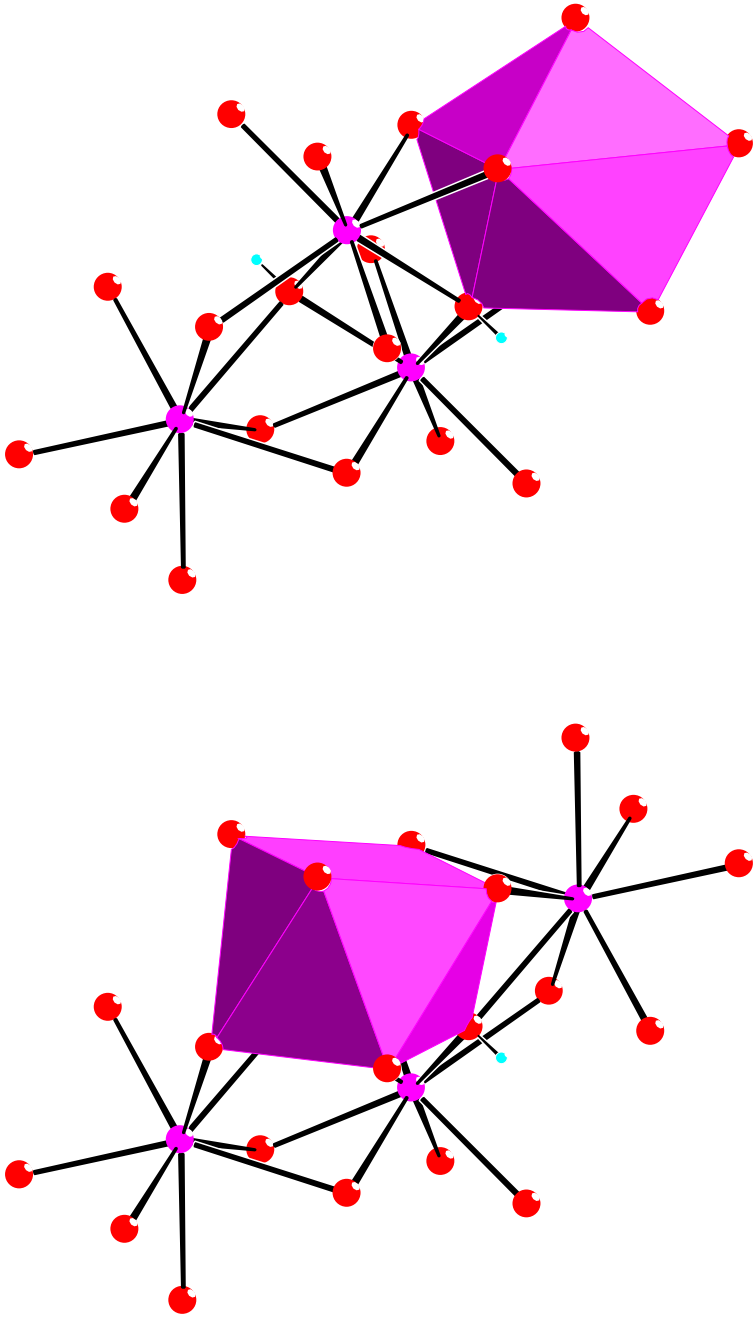

Figure 3-51 Coordination polyhedral of the Y(1) (*top*) and Y(2) (*bottom*) atoms in **10c**.

Comparison of this structure with the known analogous compound $[Y_2(OH)(acac)_5]_2$[xx] [106] shows, that both structures exhibit an analogous Y_4 core. Whereas **10c** has four "terminal" and six bridging ^{i}prac ligands, $[Y_2(OH)(acac)_5]_2$ has six "terminal" and only four bridging ^{i}prac ligands. This causes a higher average coordination number of the yttrium atoms in **10c** (Figure 3-52).

[xx] $[Y_2(\mu_3\text{-}OH)(\mu\text{-}acac)_2(acac)_3]_2$

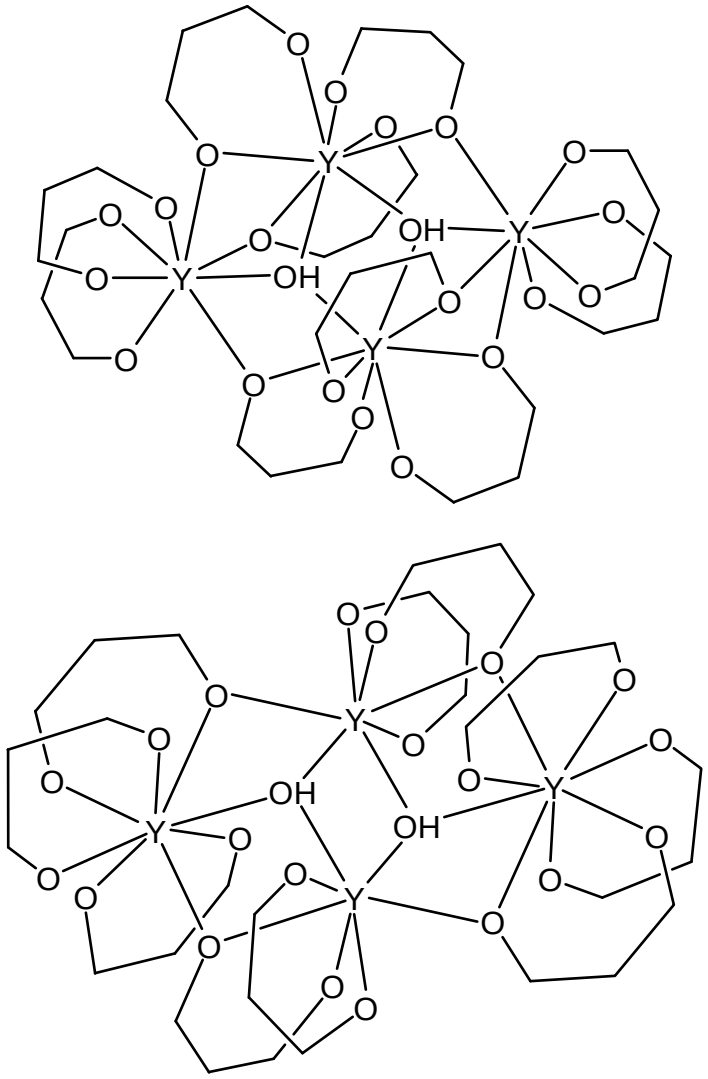

Figure 3-52 Schematic representations of **10c** (*top*) and $[Y_2(OH)(acac)_5]_2$ (*bottom*) (methyl and ester groups omitted for clarity).

The Y_4 structural motive can also be found in $[Y_4O(OEt)_2(aaa)_5]_2(OH)_4(OEt)_2$[xxi] [44, 83] (compare chapter 1.2.3.2), when it is not seen as being built from two connected $Y_4O(OEt)_2(aaa)_5$ units (derived from $Y_5O(O^iPr)_{13}$) but formally as "$[Y_4O(OH)_2(OEt)(OEt)_2(aaa)_5]_2$".

The four yttrium centers in **10c** are co-planar. Two centers each are bridged by one or two ^{i}prac ligands. Each μ_3-OH is capping an Y_3 triangle, one above and one below the Y_4 plane. The Y--Y distances are 6.479(2) (Y(1)--Y(1)), 3.722(1) (Y(2)--Y(2)), and 3.589(1) and 3.878(1) (Y(1)--Y(2)), respectively, quite similar to those of known $[Y_2(OH)(acac)_5]_2$.

The Y–O bond distances are 2.275(2)–2.365(3) for the μ_3-OH, and range from 2.275(2)–2.325(2) for $Y–O^{keto,t}$, over 2.298(2)–2.347(2) for $Y–O^{ester}$ to 2.372(3)–2.452(2) for $Y–(\mu\text{-}O^{keto})$, showing the expected elongation for the bridging compared to the terminal keto

[xxi] $[Y_4(\mu_4\text{-}O)(\mu\text{-}OEt)_2(\mu\text{-}aaa)_2(aaa)_3]_2(\mu_3\text{-}OH)_4(\mu_3\text{-}OEt)_2$

groups as well as slightly longer distances for the ester groups compared to the (terminal) keto groups, with all distances in the range of those in $[Y_2(OH)(acac)_5]_2$. The average Y–(μ-O^{keto}) distances are longer for Y(1) (2.439(2) pm), than for Y(2) (2.390(3) pm). The two non-bridging ^{i}prac ligands show nearly planar conformation. Of the three bridging ^{i}prac ligands, two also exhibit more or less planar conformation with the Y(1)--Y(2) axis lying approximately in the plane of the coordinating O–C–C(H)–C–O plane. The third ^{i}prac ligand (coordinating via O(14) and O(15)) shows a clear envelope-like conformation (compare chapter 3.1.1.2 / Figure 3-13) and is strongly twisted with respect to the Y(1)--Y(2) axis. As a result, this ligand shows a very strong envelope-like conformation, but with a very planar O–C–C(H)–C–O plane. Selected bond distances and angles are given in Table 3-14.

Table 3-14 Selected bond distances [pm] and angles [°] of **10c**.

Y(1)–O(1)	236.5(2)	Y(2)–O(1)	230.0(2)
Y(1)–O(2)	232.5(2)	Y(2)–O(1)^{a}	227.5(2)
Y(1)–O(3)	233.2(2)	Y(2)–O(8)^{a}	238.4(2)
Y(1)–O(5)	227.5(2)	Y(2)–O(9)^{a}	232.7(2)
Y(1)–O(6)	234.7(2)	Y(2)–O(11)^{a}	241.3(2)
Y(1)–O(8)	243.6(2)	Y(2)–O(12)^{a}	229.8(2)
Y(1)–O(11)	245.2(2)	Y(2)–O(14)	237.2(2)
Y(1)–O(14)	242.8(2)	Y(2)–O(15)	234.3(2)
O(1)–Y(1)–O(2)	67.81(7)	O(5)–Y(1)–O(11)	93.87(7)
O(1)–Y(1)–O(3)	138.49(7)	O(5)–Y(1)–O(14)	73.12(7)
O(1)–Y(1)–O(5)	137.50(7)	O(5)–Y(1)–O(6)	73.63(7)
O(1)–Y(1)–O(6)	131.55(7)	O(5)–Y(1)–O(8)	143.32(7)
O(1)–Y(1)–O(8)	67.87(7)	O(6)–Y(1)–O(11)	74.46(7)
O(1)–Y(1)–O(11)	68.57(7)	O(6)–Y(1)–O(14)	139.07(7)
O(1)–Y(1)–O(14)	67.11(7)	O(6)–Y(1)–O(8)	70.52(7)
O(1)^{a}–Y(2)–O(8)^{a}	70.20(7)	O(8)^{a}–Y(2)–O(11)^{a}	70.90(7)
O(1)^{a}–Y(2)–O(9)^{a}	139.13(7)	O(8)^{a}–Y(2)–O(12)^{a}	113.93(7)
O(1)^{a}–Y(2)–O(11)^{a}	70.69(7)	O(8)^{a}–Y(2)–O(14)	150.13(7)
O(1)^{a}–Y(2)–O(12)^{a}	141.39(7)	O(8)^{a}–Y(2)–O(15)	80.48(7)
O(1)^{a}–Y(2)–O(14)	114.39(7)	O(8)^{a}–Y(2)–O(9)^{a}	73.88(7)
O(1)^{a}–Y(2)–O(15)	79.41(7)	O(8)–Y(1)–O(11)	69.39(7)
O(1)–Y(2)–O(1)^{a}	71.12(8)	O(8)–Y(1)–O(14)	133.70(7)
O(1)–Y(2)–O(11)^{a}	75.41(7)	O(9)^{a}–Y(2)–O(11)^{a}	114.76(7)
O(1)–Y(2)–O(12)^{a}	84.00(8)	O(9)^{a}–Y(2)–O(12)^{a}	72.04(8)
O(1)–Y(2)–O(14)	69.08(7)	O(9)^{a}–Y(2)–O(14)	88.24(7)
O(1)–Y(2)–O(15)	113.72(7)	O(9)^{a}–Y(2)–O(15)	76.01(7)

Table 3-14 (cont.)

O(1)–Y(2)–O(8)[a]	135.05(7)	O(11)[a]–Y(2)–O(12)[a]	74.81(7)
O(1)–Y(2)–O(9)[a]	149.30(7)	O(11)[a]–Y(2)–O(14)	138.97(7)
O(2)–Y(1)–O(11)	134.27(7)	O(11)[a]–Y(2)–O(15)	143.95(7)
O(2)–Y(1)–O(14)	90.75(7)	O(11)–Y(1)–O(14)	84.66(7)
O(2)–Y(1)–O(3)	70.71(7)	O(12)[a]–Y(2)–O(14)	81.57(7)
O(2)–Y(1)–O(5)	128.13(7)	O(12)[a]–Y(2)–O(15)	138.75(7)
O(2)–Y(1)–O(6)	128.89(7)	O(14)–Y(2)–O(15)	71.95(7)
O(2)–Y(1)–O(8)	82.07(7)	Y(1)–O(1)–Y(2)	112.45(8)
O(3)–Y(1)–O(11)	149.95(7)	Y(1)–O(1)–Y(2)[a]	101.32(8)
O(3)–Y(1)–O(14)	115.43(7)	Y(1)–O(11)–Y(2)[a]	95.07(7)
O(3)–Y(1)–O(5)	72.86(8)	Y(1)–O(14)–Y(2)	107.77(8)
O(3)–Y(1)–O(6)	75.93(8)	Y(1)–O(8)–Y(2)[a]	96.22(7)
O(3)–Y(1)–O(8)	105.13(7)	Y(2)–O(1)–Y(2)[a]	108.88(8)

Symmetry transformations used to generate equivalent atoms:
[a] -x,-y,-z+2

3.4.3 $Y_9O(OH)_9(^{i}prac)_{16}$[xxii]

Another Y cluster was obtained by slow evaporation of $CDCl_3$ from an NMR tube sealed with a cap and Parafilm® containing $[Y_2(OH)(^{i}prac)_5]_2$ (**10c**) (compare chapter 3.4.2), resulting in big cubic crystals. Single crystal XRD revealed $Y_9(\mu_5\text{-}O)(\mu_4\text{-}OH)(\mu_3\text{-}OH)_8(\mu\text{-}^{i}prac)_8(^{i}prac)_8$ (Figure 3-53) as product.

This structure exhibits the same Y_9 core as $Y_9O(OH)_9(O^{i}Pr)_8(^{i}prac)_8$ (**9c**) (compare chapter 3.4.1 / Figure 3-45), but the $O^{i}Pr$ groups are replaced by additional ^{i}prac ligands. These ^{i}prac ligands are bridging-chelating, bridging two yttrium centers by the keto carbonyl oxygen. The ester carbonyl oxygens of the eight μ-^{i}prac ligands coordinate to one of the eight yttrium atoms in the "corners" each. Therefore the yttrium atoms increase their coordination number from seven to eight compared to **9c**. This leads to a distorted dodecahedral coordination geometry for these eight yttrium atoms (Figure 3-54), whereas the "central" yttrium atom is nine-coordinated in a capped tetragonal antiprismatic coordination geometry, analogous to **9c**.

[xxii] $Y_9(\mu_5\text{-}O)(\mu_4\text{-}OH)(\mu_3\text{-}OH)_8(\mu\text{-}^{i}prac)_8(^{i}prac)_8$

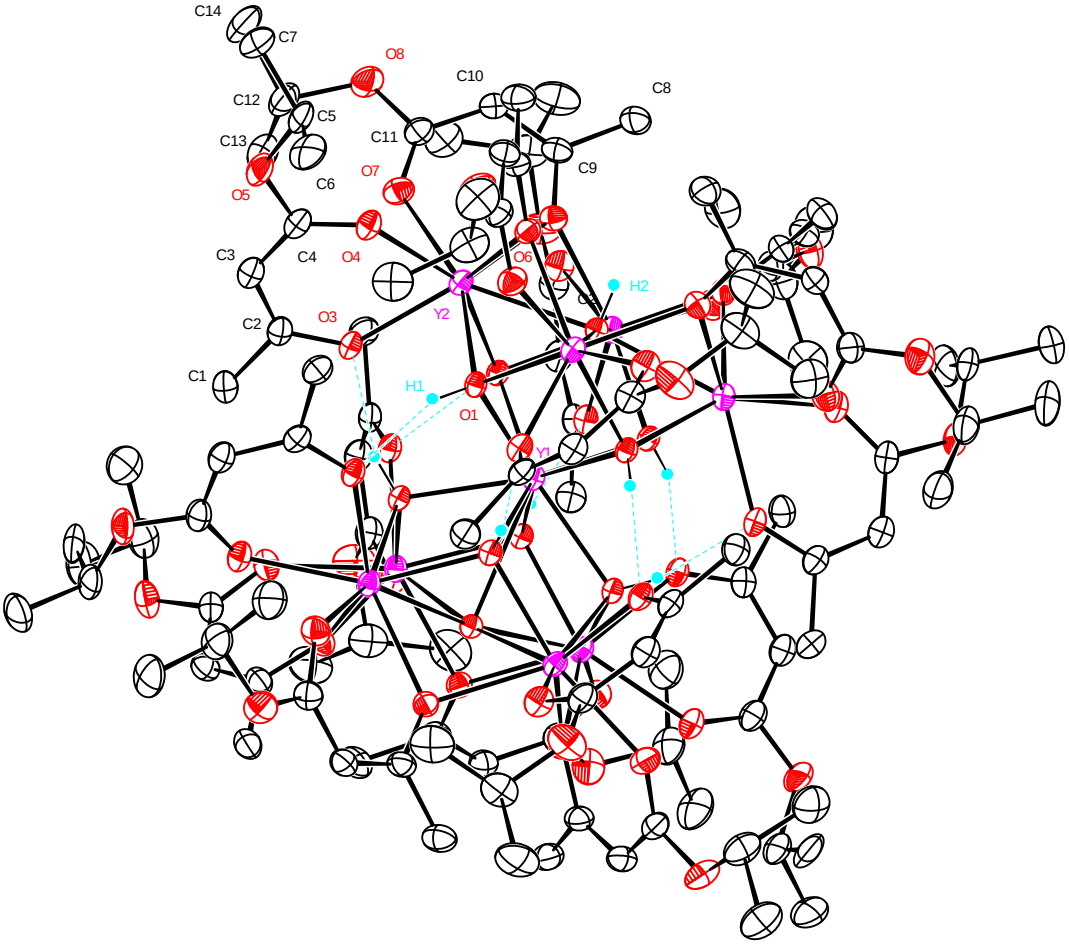

Figure 3-53 Molecular structure of $Y_9O(OH)_9(^{i}prac)_{16}$ (**11c**), showing 30 % thermal ellipsoids (carbon bond hydrogen atoms omitted for clarity).

This structure is analogous to that of known $[Na(EtOH)_6][Y_9O_2(OH)_8(etac)_{16}]$ [105], except the fact, that **11c** is a neutral compound, due to the presence of one μ_4-OH group instead one of the μ_4-O atoms. In the anionic compound both O^{2-} groups are considered as μ_4-O, whereas for **11c** the O^{2-} is μ_5-O with an additional bond to the central yttrium atom.

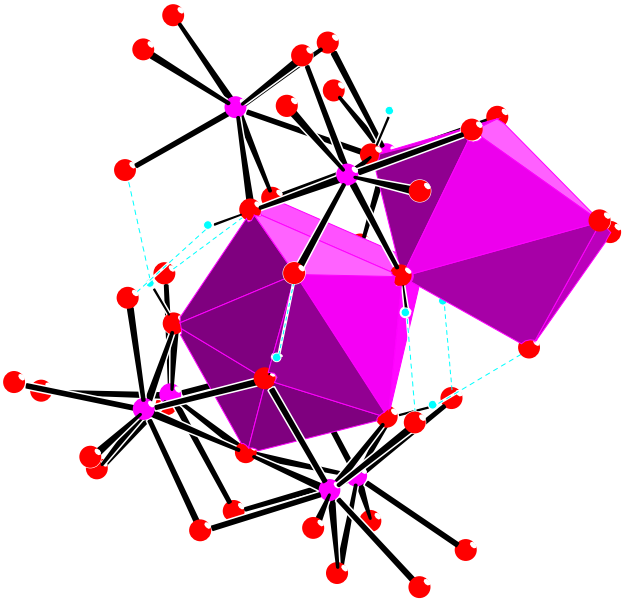

Figure 3-54 Coordination polyhedral of the yttrium atoms in **11c**.

11c is disordered, with respect to the μ_5-O and μ_4-OH groups, with 50 % occupancy for both groups, leading to a higher symmetry for the average structure and indistinguishable Y_5 square pyramids. The average Y(1)--O(2) (μ_5-O/μ_4-OH) distance is 2.86(1) pm and hence shorter than for $[Na(EtOH)_6][Y_9O_2(OH)_8(etac)_{16}]$ (2.89(2) and 2.94(2) pm), but quite similar to the average distance in **9c** (2.841(9) pm)[xxiii]. The Y--Y distances (3.6786(9) pm for Y(1)--Y(2) and 3.585(1) pm for Y(2)--Y(2)) are longer than for **9c** (3.624(4) pm and 3.401(1) pm)[xxiii], most probably caused by the higher steric demand of the μ-^{i}prac ligands compared to the μ-O^{i}Pr ligands in **9c** and the increase of the coordination number at the yttrium atoms from seven to eight. This is in accordance to the similarity to the Y--Y distances of $[Na(EtOH)_6][Y_9O_2(OH)_8(etac)_{16}]$. The Y–($\mu_3$-OH) bond distances of 2.423(6) (Y(1)–O(1)) and 2.277(6) pm (Y(2)–O(1)) are in the range of those of **9c** and **10c**. The Y–O bond distances of the ^{i}prac ligands increase in the order Y–O^{keto,t} (2.274(6) pm) < Y–O^{ester,t} (2.332(6) pm) < Y–O^{ester,b} (2.366(6) pm) < Y–(μ-O^{keto}) (2.392(6) and 2.405(6) pm). This order is the same as for **10c** but with slightly longer average distances for each type. The Y–(μ-O^{keto}) bonds are also significantly longer than the Y–(μ-O^{i}Pr) bonds in **9c** (2.266(3)–2.295(3) pm). The bite angles of the μ-^{i}prac ligands are smaller than for the terminal ones (70.9(2)° compared to 73.6(2)°). Selected bond distances and angles are given in Table 3-15.

[xxiii] Average values because of lower symmetry of **9c** with distinguishable Y_5 pyramides.

Table 3-15 Selected bond distances [pm] and angles [°] of **11c**.

Y(1)–O(1)	236.5(2)	Y(2)–O(1)[a]	227.5(2)
Y(1)–O(2)	232.5(2)	Y(2)–O(8)[a]	238.4(2)
Y(1)–O(3)	233.2(2)	Y(2)–O(9)[a]	232.7(2)
Y(1)–O(5)	227.5(2)	Y(2)–O(14)	237.2(2)
Y(1)–O(11)	245.2(2)	Y(2)–O(15)	234.3(2)
Y(1)–O(14)	242.8(2)	O(1)–H(1)	85(2)
Y(2)–O(1)	230.0(2)	O(3)[d] ···H(1)	198(3)
O(1)–Y(1)–O(1)[a]	73.88(11)	O(2)–Y(2)–O(4)	137.17(15)
O(1)–Y(1)–O(1)[b]	141.9(2)	O(2)–Y(2)–O(6)	64.89(17)
O(1)–Y(1)–O(1)[c]	116.4(2)	O(2)–Y(2)–O(6)[f]	65.03(17)
O(1)–Y(1)–O(1)[d]	142.2(2)	O(2)–Y(2)–O(7)	135.55(18)
O(1)–Y(1)–O(1)[e]	76.4(2)	O(3)–Y(2)–O(4)	73.74(17)
O(1)–Y(1)–O(1)[g]	76.6(2)	O(3)–Y(2)–O(6)	135.05(17)
O(1)–Y(1)–O(2)	58.21(11)	O(3)–Y(2)–O(6)[f]	137.88(16)
O(1)–Y(1)–O(2)[e]	121.79(11)	O(3)–Y(2)–O(7)	80.84(17)
O(1)–Y(2)–O(1)[f]	79.3(2)	O(4)–Y(2)–O(6)	126.18(16)
O(1)–Y(2)–O(2)	65.09(18)	O(4)–Y(2)–O(6)[f]	74.12(17)
O(1)–Y(2)–O(3)	77.45(17)	O(4)–Y(2)–O(7)	72.97(18)
O(1)–Y(2)–O(4)	151.17(17)	O(6)–Y(2)–O(6)[f]	86.4(2)
O(1)–Y(2)–O(6)	76.46(16)	O(6)–Y(2)–O(7)	70.68(17)
O(1)–Y(2)–O(6)[f]	129.94(17)	O(6)[f]–Y(2)–O(7)	114.39(17)
O(1)–Y(2)–O(7)	103.63(17)	Y(1)–O(1)–Y(2)	102.77(17)
O(1)[f]–Y(2)–O(2)	65.05(18)	Y(1)–O(1)–Y(2)[a]	102.70(17)
O(1)[f]–Y(2)–O(3)	79.32(16)	Y(1)–O(2)–Y(2)	85.4(2)
O(1)[f]–Y(2)–O(4)	94.17(16)	Y(2)–O(1)–Y(2)[a]	103.46(19)
O(1)[f]–Y(2)–O(6)	129.76(16)	Y(2)–O(2)–Y(2)[a]	89.63(3)
O(1)[f]–Y(2)–O(6)[f]	76.62(17)	Y(2)–O(2)–Y(2)[c]	170.8(4)
O(1)[f]–Y(2)–O(7)	158.76(17)	Y(2)–O(6)–Y(2)[a]	96.91(17)
O(2)–Y(2)–O(3)	131.6(2)	O(1)–H(1)···O(3)[d]	166(7)

Symmetry transformations used to generate equivalent atoms:
[a] x,z,-y+1/2; [b] -x+3/2,z,y; [c] x,-y+1/2,-z+1/2; [d] -x+3/2,y,-z+1/2; [e] -x+3/2,-y+1/2,z;
[f] x,-z+1/2,y; [g] -x+3/2,-z+1/2,-y+1/2

The μ-^{i}prac ligands are strongly twisted with respect to the basal plane, as observed for one type of μ-^{i}prac ligands in **10c** (compare chapter 3.4.2) and the μ-^{i}prac in $[Na(EtOH)_6][Y_9O_2(OH)_8(etac)_{16}]$, and show a envelop-like conformation with respect to the chelated yttrium center, as it is also observed for the terminal ^{i}prac ligands.

Again, the structure is stabilized by eight hydrogen bonds between the μ_3-OH groups and the keto carbonyl oxygens of the terminal ^{i}prac ligands.

9c crystallized in the cubic space group *P*n−3n. Each unit cell contains six Y_9 clusters, leading to large voids, forming channels along the [111] direction (Figure 3-55). These channels are filled with four chloroform molecules per Y_9 cluster. An identical arrangement was observed for analogous nonanuclear lanthanide clusters [107].

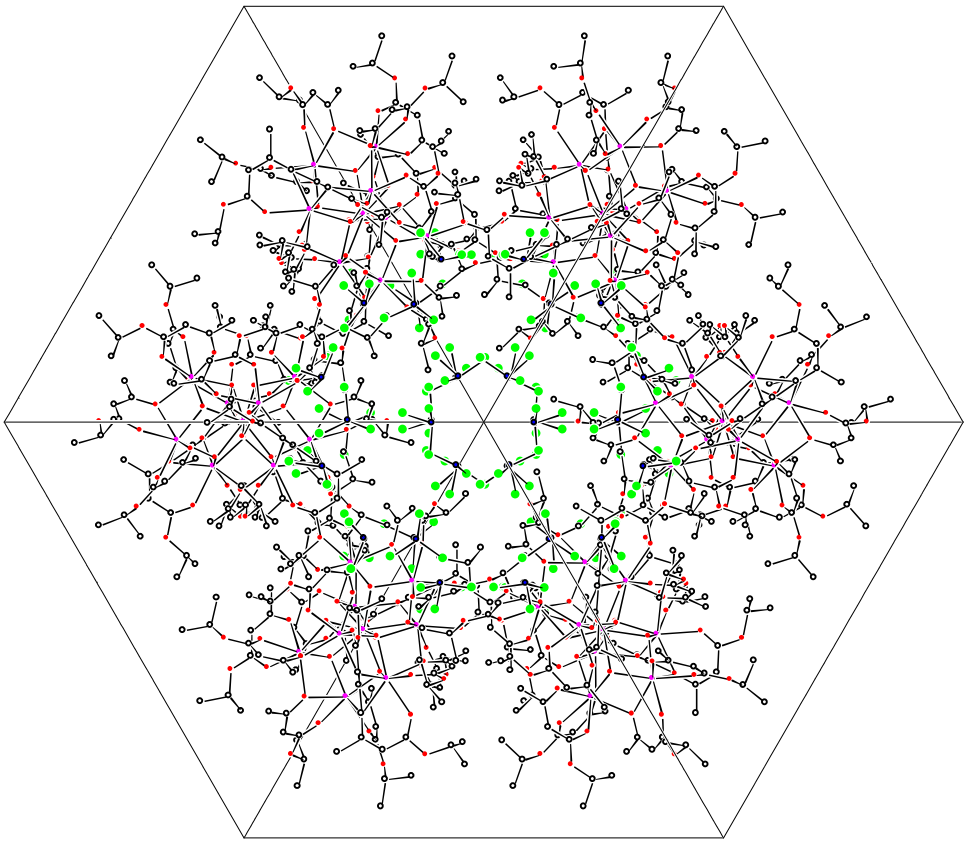

Figure 3-55 Representation of the unit cell of **11c**, along the [111] direction (hydrogen atoms omitted for clarity, carbon atoms of solvent molecules colored blue).

3.4.4 Conclusions

The three compounds $Y_9O(OH)_9(O^iPr)_8(^i prac)_8$ (**9c**), $[Y_2(OH)(^i prac)_5]_2$ (**10c**), and $Y_9O(OH)_9(^i prac)_{16}$ (**11c**) reported here are new products of the modification of yttrium isopropoxide with β-ketoesters.

9c is one of rare examples of modified yttrium alkoxides. It should be applicable as precursor to sol-gel derived yttria materials. Because of the well defined structure it might be capable to preserve these structural features in the final materials.

From **10c** to **11c**, the ^{i}prac/Y ratio decreases from 2.5 to 1.78, indicating a "higher degree of hydrolysis" for the latter. The fact, that **10c** posses only μ_3-OH groups besides the ^{i}prac ligands, whereas **10c** also features μ_5-O and μ_4-OH groups can also be regarded as an increase of the "degree of condensation". The transformation of **10c** to **11c** can be interpreted as a condensation step with elimination of a ^{i}prac ligand. Therefore, these two structures can be seen as "snapshots" of intermediates formed during hydrolysis/condensation of organically modified yttrium alkoxides. This formation of **11c** from **10c** also shows for the first time the close relationship between these structural motives, both known from the literature for yttrium.

4 Summary

Modification of metal alkoxides by coordination of organic ligands is a prerequisite to adjust the reactivity towards hydrolysis and condensation reactions. Thus they become useful and versatile precursors for sol-gel materials. Concomitant to the influence on the reactivity of the precursors also the structure of the final material is influenced upon modification of the metal alkoxide. Furthermore, the (partial) preservation of the organic ligand in the final material opens a route to inorganic-organic hybrid materials. In the case of organic ligands bearing additional functionalities these functional groups remain available in the material and can act as reactive sites for further reactions, *e.g.* cross-linking or post-synthesis modification.

β-Diketonic ligands are widely used for this purpose, but there is a lack of systematic studies on the relation between the ligand properties and the structure and reactivity of the resulting modified metal alkoxide. The aim of this work was to investigate these relations.

Compounds Al(*β*-ketoesterate)$_3$ (*β*-ketoesterate = meac, etac, ^{i}prac, ^{t}buac, aaa, meaa, me(ome)ac, et(tfl)ac, et(^{i}pr)ac) (Figure 4-1) were obtained upon reaction of [Al(OR)$_3$]$_n$ (OR = O^{t}Bu, O^{i}Pr) with three equivalents of *β*-ketoesters at room temperature, except for et(^{i}pr)ac-H, where elevated temperatures had to be applied. All complexes show a mononuclear structure with an octahedrally coordinated aluminum center, giving rise to C_1 and C_3 symmetric isomers, coexisting in solution without a preference for either isomer. No influence of the ligand on the structure or stability of the product was observed, with one exception: Al(^{t}buac)$_3$ underwent transesterification with liberated ^{i}PrOH, giving Al(^{i}prac)$_x$(^{t}buac)$_{3-x}$. This behavior is attributed to the steric bulk of the *tert.*-butoxo groups, since it is not observed for a lower substitution degree.

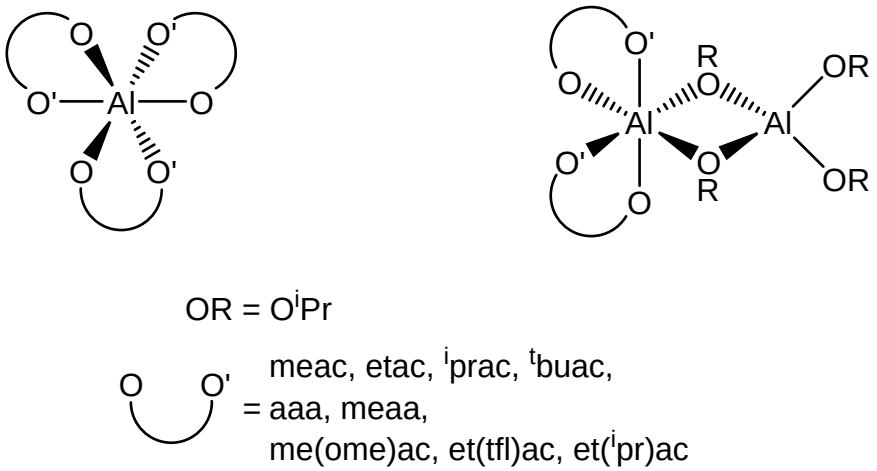

Figure 4-1 Schematic representation of the products obtained for the modification of aluminum alkoxides with *β*-ketoesters (O,O' indicates the asymmetric nature of the ligand, only one possible isomer shown in each case).

Al(β-ketoesterate)$_3$ was also the product for the reaction of [Al(O^{i}Pr)$_3$]$_4$ with one equivalent of β-ketoester at room temperature instead of an anticipated monosubstituted species. Raising the reaction temperature eventually yielded dinuclear monosubstituted products Al$_2$(μ-O^{i}Pr)$_2$(O^{i}Pr)$_2$(β-ketoesterate)$_2$ (β-ketoesterate = meac, etac, ^{i}prac, ^{t}buac, aaa, meaa, me(ome)ac, et(tfl)ac, et(^{i}pr)ac) (Figure 4-1), with one exception: modification with meaa failed due to the thermal instability of the ligand under the reaction conditions. Synthesis of Al$_2$(μ-O^{i}Pr)$_2$(O^{i}Pr)$_2$(meaa)$_2$ was achieved by an alternative procedure, *viz.* previous thermal de-oligomerization of [Al(O^{i}Pr)$_3$]$_4$, enabling the formation of the desired monosubstituted product at room temperature. Al$_2$(μ-O^{i}Pr)$_2$(O^{i}Pr)$_2$(β-ketoesterate)$_2$ (β-ketoesterate = me(ome)ac, et(tfl)ac) were directly formed at room temperature, not showing preferred formation of Al(β-ketoesterate)$_3$.

Complexes Al$_2$(μ-O^{i}Pr)$_2$(O^{i}Pr)$_2$(β-ketoesterate)$_2$ were asymmetrically substituted dimers, giving rise to one C_1 and two C_2 symmetric isomers. The structure was confirmed for Al$_2$(μ-O^{i}Pr)$_2$(O^{i}Pr)$_2$(^{t}buac)$_2$ in the solid state by single crystal XRD and is retained in solution. This was confirmed by NMR spectroscopic methods, which also indicated dynamic behavior and exchange between the bridging and terminal O^{i}Pr groups.

For the reactions with et(^{i}pr)ac-H, coordination of the ligand and formation of Al(et(^{i}pr)ac)$_3$ and Al$_2$(μ-O^{i}Pr)$_2$(O^{i}Pr)$_2$(et(^{i}pr)ac)$_2$ was accompanied by hydrodeacylation reactions, leading to cleavage of the ligand.

Compounds of the general formula [Al(OR)(β-ketoesterate)$_2$]$_n$ were not obtained in any case. Corresponding reactions yielded only mixtures of Al(β-ketoesterate)$_3$ and Al$_2$(μ-OR)$_2$(OR)$_2$(β-ketoesterate)$_2$ (OR = O^{i}Pr) or [Al(OR)$_3$]$_2$ (OR = O^{t}Bu)$_3$. Reaction of [Al(O^{t}Bu)$_3$]$_2$ with less than three equivalents of β-ketoester yielded mixtures of Al(β-ketoesterate)$_3$ and [Al(O^{t}Bu)$_3$]$_2$ in all cases, indicating the incapability of O^{t}Bu to occupy a bridging position.

These results for the modification of aluminum alkoxides with β-ketoesters lead to following conclusions:

- Al$_2$(μ-O^{i}Pr)$_2$(O^{i}Pr)$_2$(β-ketoesterate)$_2$ is the most stable species for an Al/β-ketoester ratio of 1:1.
- Formation of Al(β-ketoesterate)$_3$ at room temperature for a Al/β-ketoesterate ratio of 1:1 is due to a kinetic effect.
- De-oligomerized [Al(O^{i}Pr)$_3$]$_4$, *i.e.* dimeric and trimeric species, reacts faster with the β-ketoesters than the tetramer.
- Dimeric and trimeric Al(O^{i}Pr)$_3$ species also react faster than intermediate [Al(O^{i}Pr)$_x$(β-ketoesterate)$_{3-x}$]$_n$ species, giving Al$_2$(μ-O^{i}Pr)$_2$(O^{i}Pr)$_2$(β-ketoesterate)$_2$ compounds already at room temperature.
- Substitution in the 4 position of the β-ketoester (me(ome)ac-H, et(tfl)ac-H) influences the reaction kinetics, yielding Al$_2$(μ-O^{i}Pr)$_2$(O^{i}Pr)$_2$(β-ketoesterate)$_2$ at room temperature.
- Substitution at the 2 position of the β-ketoester (et(^{i}pr)ac-H) favors hydrodeacylation as competing side reaction to coordination.

- Products $Al_2(\mu\text{-}O^iPr)_2(O^iPr)_2(\beta\text{-ketoesterate})_2$ (β-ketoesterate = aaa, meaa) are potential precursors for covalently linked dual inorganic-organic hybrid polymers due to the preservation of the polymerizable C=C double bond.
- The alkoxo group of the esters had no influence on the structure of the products.
- Transesterification was observed only in the case of $Al(^tbuac)_3$ with ^iPrOH, favored due to steric constraint around the aluminum center.

Compounds Al(malonate)$_3$ (malonate = dmem, detm, d^{i}prm, d^{t}bum) (Figure 4-2) were obtained upon reaction of $[Al(O^tBu)_3]_n$ with three equivalents of malonate at room temperature. The reaction proceeded in a similar manner as for the analogous β-ketoesterate derivatives, but longer reaction times were required.

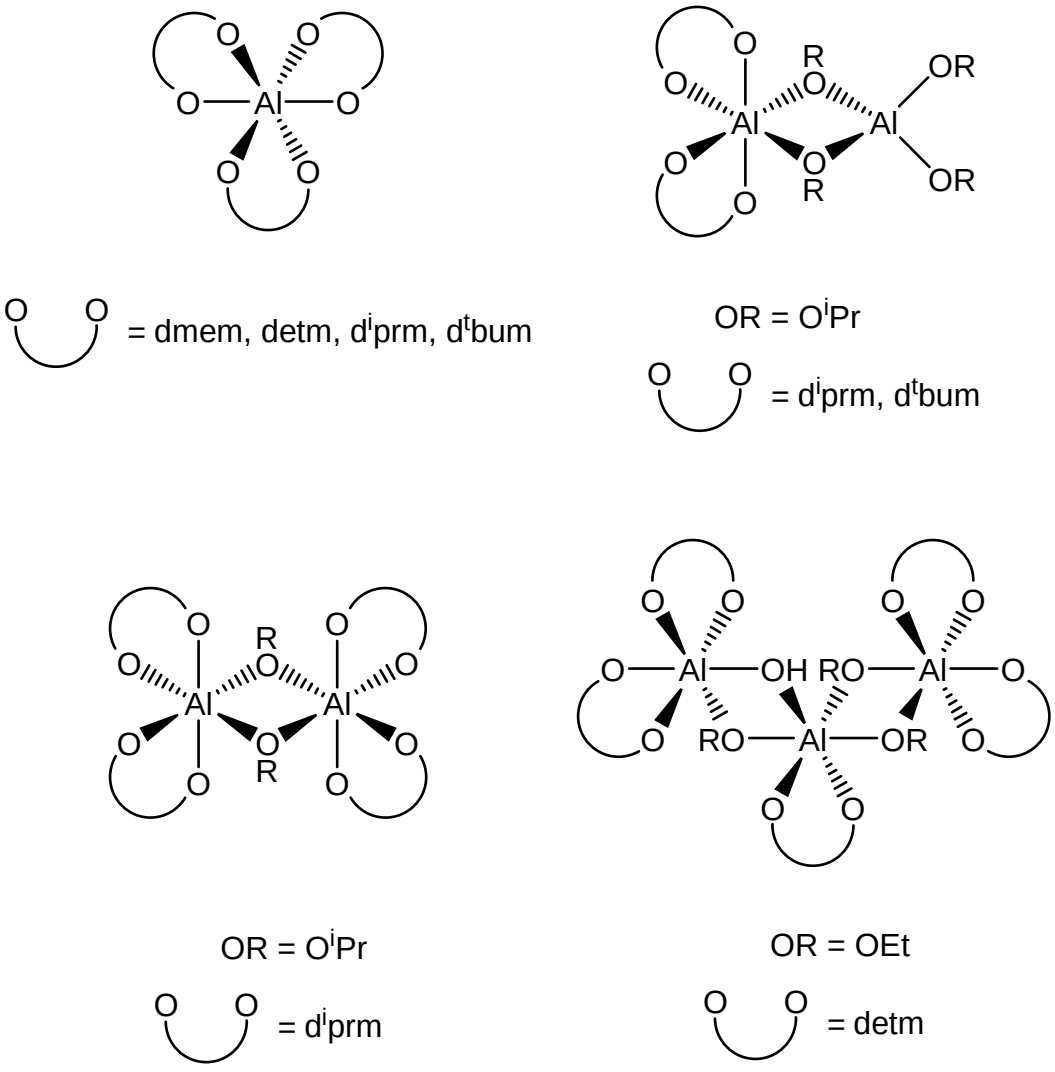

Figure 4-2 Schematic representation of the products obtained for the modification of aluminum alkoxides with dialkylmalonates (only one possible isomer shown in each case).

Reaction of $Al(O^iPr)_3$ with d^{i}prm-H and d^{t}bum-H yielded analogous products, but required elevated reaction temperatures. Alternatively, the reaction could be accelerated by

de-oligomerization of $[Al(O^iPr)_3]_4$ prior to the substitution reaction. For the modification of $Al(O^iPr)_3$ with dmem-H and detm-H transesterification occurred. The complexes were mononuclear, with an octahedrally coordinated aluminum center, as confirmed in the solid state by single crystal XRD. The structure is retained in solution.

Modification of $Al(O^iPr)_3$ with one equivalent of d^iprm-H or d^tbum-H gave $Al_2(\mu\text{-}O^iPr)_2(O^iPr)_2(malonate)_2$ (malonate = d^iprm, d^tbum) (Figure 4-2), exhibiting an asymmetrically substituted dinuclear structure, confirmed for $Al_2(\mu\text{-}O^iPr)_2(O^iPr)_2(d^tbum)_2$ by single crystal XRD.

Reaction of $Al(O^tBu)_3$ with less then three equivalents of malonate only gave mixtures of $Al(malonate)_3$ and $[Al(O^tBu)_3]_2$, again showing the incapability of O^tBu to occupy bridging positions. Transesterification was not observed in any case for the reactions of $Al(O^tBu)_3$. Reactions of $Al(O^iPr)_3$ with two equivalents of d^iprm-H or d^tbum-H only yielded mixtures of $Al(malonate)_3$ and $Al_2(\mu\text{-}O^iPr)_2(O^iPr)_2(malonate)_2$, as observed for reactions with β-ketoesters. Interestingly, $[Al(\mu\text{-}O^iPr)(d^iprm)_2]_2$ – a symmetric dimer with a Al/malonate ratio of 1:2 (Figure 4-2) – was obtained by crystallization upon storage of $Al_2(\mu\text{-}O^iPr)_2(O^iPr)_2(d^iprm)_2$ (or mixtures with $Al(d^iprm)_3$) and identified by single crystal XRD. This conversion was only observed upon storage of the isolated products but did not take place in solution, indicating the importance of crystallization as driving force in this transformation.

For the modification of $Al(OEt)_3$ with three equivalents of detm-H, unexpected $Al_3(\mu\text{-}OH)(\mu\text{-}OEt)_3(detm)_5$ was obtained as the product (Figure 4-2). Single crystal XRD revealed a trinuclear structure with a Al/malonate ratio of 3:5 for this complex, bearing an Al–OH group, most likely formed by scission of an OEt group. This is supported by the fact that this compound was also obtained by an alternative experiment starting from $Al(O^tBu)_3$ and detm-H.

These results for the modification of aluminum alkoxides with malonates lead to the following conclusions:

- Dialkylmalonates can be used for the modification of aluminum alkoxides in a similar manner as β-ketoesters, although longer reaction times/elevated reaction temperatures are required.
- The reaction rate of the substitution is inversely correlated to the degree of oligomerization of the aluminum alkoxide.
- The lower degree of oligomerization of $[Al(O^tBu)_3]_2$ compared to $[Al(O^iPr)_3]_4$ leads to higher reaction rates for the former, despite the higher steric demand of the O^tBu groups compared to the O^iPr groups, which lowers the reactivity towards substitution reactions.
- Diisopropyl malonate is capable to stabilize $[Al(\mu\text{-}O^iPr)(d^iprm)_2]_2$, a rare example for an aluminum alkoxide modified with a β-diketonic ligand with a Al/ligand ratio of 1:2. Nevertheless, crystallization appears to be evident as driving force for the formation of $[Al(\mu\text{-}O^iPr)(d^iprm)_2]_2$.

- Transesterification was only observed for reactions of $Al(O^iPr)_3$ with dmem-H and detm-H, showing the influence of both, the ester and metal alkoxo group on the reactivity.

Modification of $Al(O^iPr)_3$ with a β-ketoamide (detaca-H) yielded $Al(detaca)_3$ and $Al_2(\mu\text{-}O^iPr)_2(O^iPr)_2(malonate)_2$ as products (Figure 4-3), proving that the substitution reaction between aluminum alkoxides and acetoacetamides is an easy applicable alternative for the modification of aluminum alkoxides with other β-diketonic compounds. Both products show structures analogous to the related β-ketoesterate and malonate complexes, confirmed for $Al(detaca)_3$ by single crystal XRD.

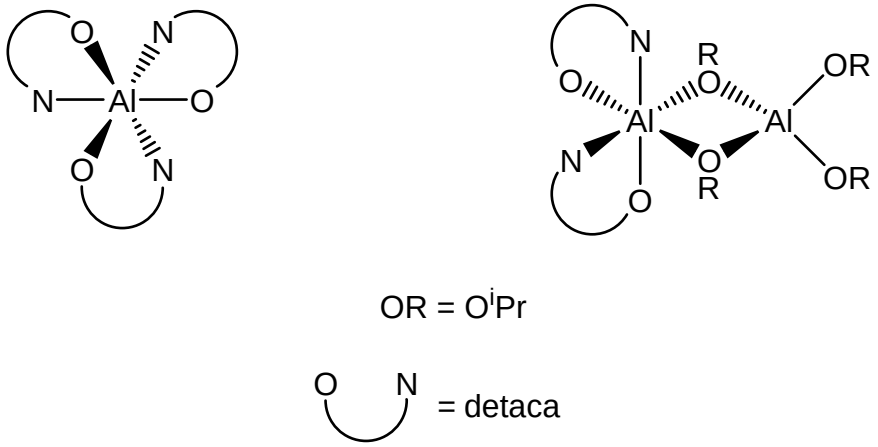

Figure 4-3 Schematic representation of the products obtained for the modification of aluminum alkoxides with dialkylmalonates (only one possible isomer shown in each case).

Modification of $Y_5O(O^iPr)_{13}$ with isopropyl acetoacetate yielded three new yttrium complexes, all characterized by single crystal XRD. Reaction with one equivalent of ^{i}prac-H per yttrium atom yielded $Y_9O(OH)_9(O^iPr)_8(^i prac)_8$ (Figure 4-4). This complex is a rare example of a modified yttrium alkoxide bearing alkoxo groups and β-diketonic ligands. The compound is a nonanuclear cluster built from two Y_5 square pyramids connected through their vertices.

Reaction with three equivalent of ^{i}prac-H per yttrium atom yielded $[Y_2(OH)(^i prac)_5]_2$ (Figure 4-4), a tetranuclear cluster with ^{i}prac and OH groups coordinated to the yttrium centers. In this cluster, two types of ^{i}prac ligands are present, one coordinating in a terminal chelating binding mode and the other in a bridging chelating binding mode.

Crystallization of $[Y_2(OH)(^i prac)_5]_2$ from chloroform gave $Y_9O(OH)_9(^i prac)_{16}$ (Figure 4-4) as product, exhibiting an Y_9 core analogous to $Y_9O(OH)_9(O^iPr)_8(^i prac)_8$, but with bridging chelating ^{i}prac ligands replacing the O^iPr groups. This transformation shows the close relationship of the known Y_4 and Y_9 cluster motives as well as the importance of the Y_9 structure for yttrium clusters. During this transformation, the ^{i}prac/Y ratio decreases from 2.5

to 1.78, indicating a "higher degree of hydrolysis" for the latter complex. The fact, that $[Y_2(OH)(^{i}prac)_5]_2$ posses only μ_3-OH groups besides the ^{i}prac ligands, whereas $Y_9O(OH)_9(^{i}prac)_{16}$ also features μ_5-O and μ_4-OH groups can also be regarded as an increase of the "degree of condensation". Therefore, this transformation can be interpreted as a condensation step with elimination of an ^{i}prac ligand and these two structures can be seen as "snapshots" of intermediates formed during hydrolysis/condensation of organically modified yttrium alkoxides.

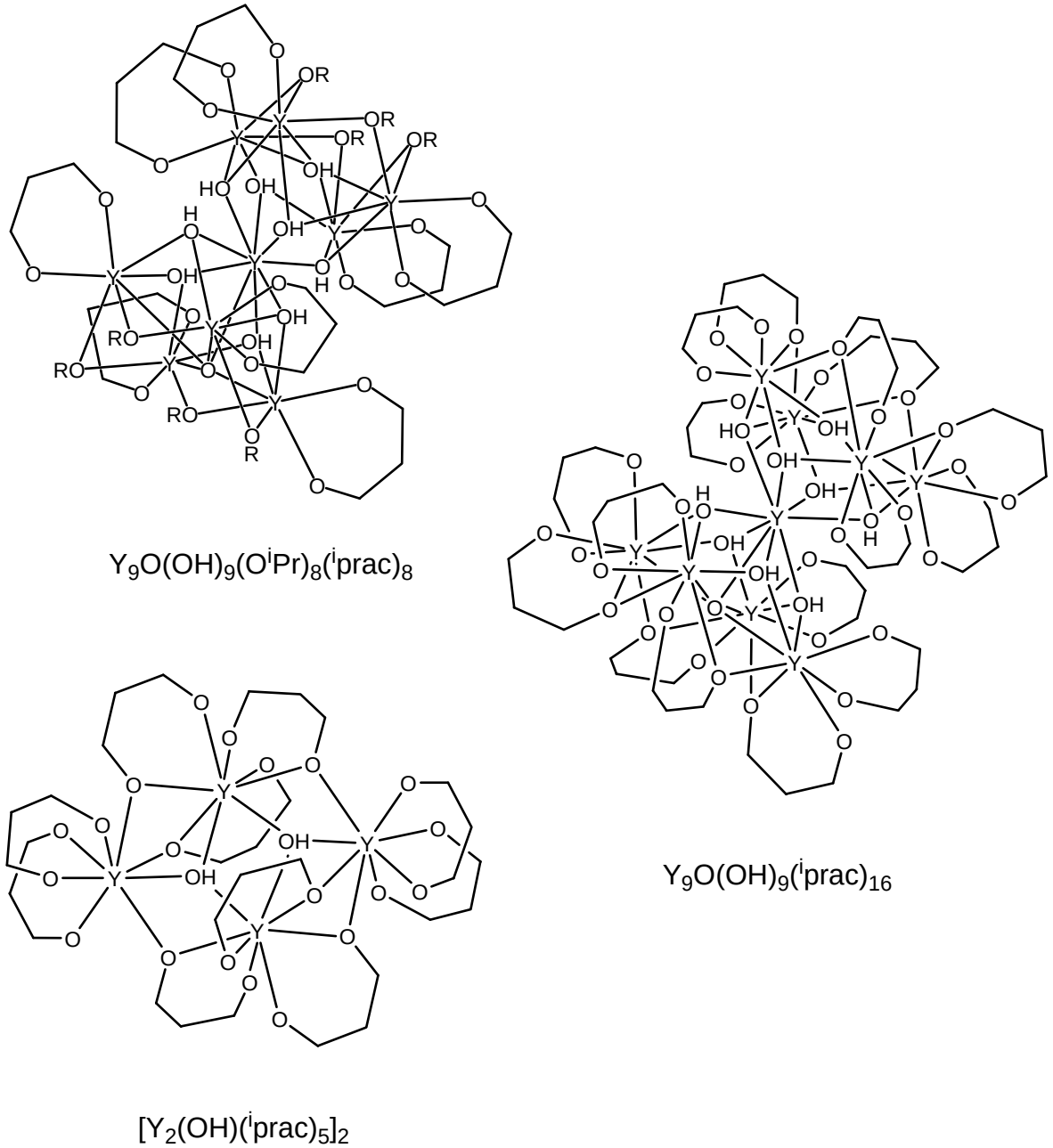

Figure 4-4 Schematic representation of the products obtained for the modification of yttrium alkoxides with isopropyl acetoacetate (OR = O^{i}Pr; methyl and ester groups omitted for clarity).

These results show the versatility and complexity of the – at first glance – simple and well known modification of metal alkoxides with *β*-diketonic ligands. Minor variations of the ligand class as well as of the alkoxide can result in very different structures and stabilities of the products, also with respect to undesired side reactions like transesterification or hydrodeacylation. Modification of aluminum and yttrium alkoxides with *β*-diketonic ligands opens a way to a variety to modified metal alkoxide precursors for sol-gel processing as well as for inorganic-organic hybrid materials, including precursors with anchoring points for covalent linkage between inorganic and organic polymers.

5 Experimental Section

5.1 General Methods and Materials

All manipulations were carried out in a moisture- and oxygen-free atmosphere of dry argon using standard Schlenk or glove box techniques. Solvents were purified and desiccated by standard methods [108] and stored under an argon atmosphere over molecular sieve (3 or 4 Å, respectively). All chemicals were purchased, used as received (Table 5-1) and stored under argon after opening them the first time.

Table 5-1 Chemicals used.

Name	Abbreviation	Supplier	purity
aluminum triethoxide	$Al(OEt)_3$	Aldrich	97 %
aluminum triisopropoxide	$Al(O^iPr)_3$	Aldrich	98+ %
aluminum tri-*sec.*-butoxide	$Al(O^sBu)_3$	Fluka	pract.
aluminum tri-*tert.*-butoxide	$Al(O^tBu)_3$	Aldrich	techn.
yttrium triisopropoxide	$Y(O^iPr)_3$	Aldrich	25 % in toluene
2-(methacryloyloxy)ethyl acetoacetate	meaa-H	Aldrich	95 %
allyl acetoacetate	aaa-H	Fluka	98 %
ethyl 2-isopropylacetoacetate	et(^{i}pr)ac-H	Fluka	prakt.
ethyl 2-methylacetoacetate	et(me)ac-H	Aldrich	90 %
ethyl 4,4,4-trifluoroacetoacetate	et(tfl)ac-H	Fluka	≥98.0 %
ethyl acetoacetate	etac-H	Fluka	p.a., ≥99.0 %
isopropyl acetoacetate	^{i}prac-H	Alfa Aesar	98 %
methyl 4-methoxyacetoacetate	me(ome)ac-H	Fluka	pract.
methyl acetoacetate	meac-H	Aldrich	99 %
tert.-butyl acetoacetate	^{t}buac-H	Aldrich	98 %
N,N-diethyl acetoacetamide	detaca-H	ABCR	97 %
diethyl malonate	detm-H	Fluka	≥99 % (GC)
diisopropyl malonate	d^{i}prm-H	Aldrich	99 %
dimethyl malonate	dmem-H	Aldrich	98 %
di-*tert.*-butyl malonate	d^{t}bum-H	Aldrich	98 %
acetylacetone	acac-H	Aldrich	99+ %

Solvents used for NMR experiments (Table 5-2) were dried and stored over molecular sieve (3 Å) and degassed by "pump-and-freeze" technique prior to first use.

Table 5-2 Deuterated solvents used.

Name	Abbreviation	Supplier	quality
[D_6]benzene	C_6D_6	euriso-top	99.5 % D
[D_8]toluene		euriso-top	99.5 % D
[D]chloroform	$CDCl_3$	euriso-top	99.8 % D

5.2 Analytical Techniques

5.2.1 NMR spectroscopy

1D ^{1}H NMR and $^{13}C\{^{1}H\}$ spectra were recorded on a Bruker AVANCE 250 (250.13 MHz $\{^{1}H\}$, 62.86 MHz $\{^{13}C\}$) and a Bruker AVANCE 300 (300.13 MHz $\{^{1}H\}$, 75.47 MHz $\{^{13}C\}$) spectrometer, respectively, both equipped with a 5 mm broadband probe head and a *z*-gradient unit. ^{27}Al and 2D NMR experiments were recorded on the Bruker AVANCE 300 spectrometer (78.21 MHZ $\{^{27}Al\}$). COSY (Correlated Spectroscopy), HSQC (Heteronuclear Single Quantum Correlation), HMBC (Heteronuclear Multiple-Bond Correlation, evolution delay for long range coupling 100 ms), and EXSY (Exchange Spectroscopy, t_{mix} = 1.2 s) were measured with Bruker standard pulse sequences. The ^{27}Al NMR signals were referenced externally against a 2M solution of $AlCl_3$ in water (0 ppm).

5.2.2 Single Crystal XRD

Crystals suitable for single crystal XRD were mounted on a Siemens SMART diffractometer with a CCD area detector or a Bruker AXS KAPPA diffractometer with an APEX II CCD area detector using graphite-monochromated Mo-K_α radiation (λ = 71.073 pm). Data collection at 100 K in a nitrogen stream covered a hemisphere of the reciprocal space by recording three sets of exposures, each of them exhibiting a different Φ angle. Each exposure covered 0.3° in ω. The data was corrected for polarization and Lorentz effects, and an empirical absorption correction (SADABS) was applied. The cell dimensions were refined with all unique reflections. The structures were solved with direct methods (SHELXS97) and refinement to convergence was carried out with the full-matrix least squares method based on F^2 (SHELXL97) with anisotropic structure parameters for all non-hydrogen atoms. The hydrogen atoms were placed on calculated positions and refined riding on their parent atoms.

5.3 Modification of Aluminum Alkoxides

5.3.1 Modification with *β*-Ketoesters

5.3.1.1 Synthesis of Al(meac)$_3$ (1a)

1.004 g (4.92 mmol) of Al(O^{i}Pr)$_3$ was dissolved in toluene (10 mL) at room temperature and 1.59 mL (1.710 g, 14.71 mmol) of methyl acetoacetate was slowly added under stirring. The clear reaction solution was stirred at room temperature for 18 h. The volatiles were removed *in vacuo*, the crude product washed with n-pentane, and a colorless solid was obtained.

Yield: 1.746 g (95 %).

^{1}H NMR (δ [ppm], C_6D_6, 20 °C): 5.17 (s, 3H, COC***H***CO), 3.43/3.38/3.34/3.33 (s, 9H, OC***H***$_3$), 1.83/1.82/1.80/1.79/1.77 (s, 9H, C***H***$_3$CO).

^{13}C {^{1}H} NMR (δ [ppm], [D_8]toluene, 20 °C): 188.3/188.2/187.9/187.8 (***C***O), 174.8/174.6 (***C***OO), 85.0/84.7/84.5 (CO***C***HCO), 51.0/50.9/50.8/50.7 (O***C***H$_3$), 25.8 (***C***H$_3$CO).

5.3.1.2 Synthesis of Al(etac)$_3$ (1b)

1.001 g (4.90 mmol) of Al(O^{i}Pr)$_3$ was dissolved in toluene (20 mL) at room temperature and 1.86 mL (1.914 g, 14.71 mmol) of ethyl acetoacetate was slowly added under stirring. The clear reaction solution was stirred at room temperature for 18 h. The volatiles were removed *in vacuo*, and a white solid was obtained.

Yield: 1.890 g (93 %).

^{1}H NMR (δ [ppm], C_6D_6, 20 °C): 5.18/5.17 (s, 3H, COC***H***CO), 4.15–3.85 (m, 6H, OC***H***$_2$Me), 1.85/1.84/1.81/1.80 (s, 9H, C***H***$_3$CO), 1.00/0.99/0.91/0.90 (t, J = 7.1 Hz, 9H, OCH$_2$C***H***$_3$).

^{13}C {^{1}H} NMR (δ [ppm], [D_8]toluene, 20 °C): 188.1/188.0/187.7/187.6 (***C***O), 174.5/174.3/174.2 (***C***OO), 85.2/85.0/84.8 (CO***C***HCO), 60.4/60.3/60.2/60.1 (O***C***H$_2$Me), 25.9 (***C***H$_3$CO), 14.1/13.9 (OCH$_2$***C***H$_3$).

^{27}Al NMR (δ [ppm], [D_8]toluene, 20 °C): 4.8 ppm (octahedral).

5.3.1.3 Synthesis of Al(^{i}prac)$_3$ (1c)

1.005 g (4.92 mmol) of Al(O^{i}Pr)$_3$ was dissolved in toluene (10 mL) at room temperature and 2.16 mL (2.125 g, 14.74 mmol) of isopropyl acetoacetate was slowly added under stirring. The clear reaction solution was stirred at room temperature for 18 h. The volatiles were removed *in vacuo*, and a white, partially crystalline solid was obtained.

Yield: 2.130 g (95 %).

^{1}H NMR (δ [ppm], C_6D_6, 20 °C): 5.16 (s, 3H, COC***H***CO), 5.12–4.94 (m, 3H, OC***H***Me_2), 1.86/1.84/1.81/1.79 (s, 9H, C***H***$_3$CO), 1.20–0.95 (m, 18H, OCH(C***H***$_3)_2$).

^{13}C {^{1}H} NMR (δ [ppm], [D_8]toluene, 20 °C): 187.9/187.6/187.4/187.3 (***C***O), 174.1/175.0/173.9/173.8 (***C***OO), 85.6/85.4/85.1 (CO***C***HCO), 67.9/67.8/67.7/67.6 (O***C***HMe_2), 25.8/25.7 (***C***H_3CO), 21.7/21.6/21.5/21.4 (OCH(***C***$H_3)_2$).

5.3.1.4 Synthesis of Al(^{t}buac)$_3$ (1d)

0.999 g (4.89 mmol) of Al($O^iPr)_3$ was dissolved in toluene (10 mL) at room temperature and 2.43 mL (2.318 g, 14.65 mmol) of *tert.*-butyl acetoacetate slowly added under stirring. The clear reaction solution was stirred at room temperature for 18 h. The volatiles were removed *in vacuo*, the crude product washed with dichloromethane, and a white, partially crystalline solid was obtained.

Yield: 2.278 g (93 %).

^{1}H NMR (δ [ppm], C_6D_6, 20 °C): 5.13/5.10/5.08 (s, 3H, COC***H***CO), 1.83/1.82/1.79 (s, 9H, C***H***$_3$CO), 1.46/1.45 (s, 27H, OC(C***H***$_3)_3$).

^{13}C {^{1}H} NMR (δ [ppm], [D_8]toluene, 20 °C): 187.2/187.0/186.9/186.6 (***C***O), 174.5/174.4/174.3/174.1 (***C***OO), 86.4/86.2/86.1/86.8 (CO***C***HCO), 80.6/80.3/80.2/80.0 (O***C***Me_3), 28.8/28.3 (OC(***C***$H_3)_3$), 26.0/25.9/25.7 (***C***H_3CO).

5.3.1.5 Synthesis of Al(aaa)$_3$ (1e)

0.999 g (4.89 mmol) of Al($O^iPr)_3$ was dissolved in toluene (10 mL) at room temperature and 2.01 mL (2.084 g, 14.66 mmol) of allyl acetoacetate was slowly added under stirring. The slightly turbid reaction solution was stirred at room temperature for 18 h. The volatiles were removed *in vacuo*. The crude product was washed with dichloromethane, and an orange oil was obtained.

Yield: 2.167 g (98 %).

^{1}H NMR (δ [ppm], C_6D_6, 20 °C): 5.95–5.55 (m, 3H, OCH_2C***H***=CH_2), 5.15 (s, 3H, COC***H***CO), 5.10–4.85 (m, 6H, OCH_2CH=C***H***$_2$), 4.60–4.30 (m, 6H, OC***H***$_2CH$=CH_2), 1.81/1.79/1.78/1.76 (s, 9H, C***H***$_3$CO).

^{13}C {^{1}H} NMR (δ [ppm], [D_8]toluene, 20 °C): 188.6/188.4/188.2/188.0 (***C***O), 174.1/174.0/173.9/173.8 (***C***OO), 132.7/132.6/132.5/132.4 (OCH_2***C***H=CH_2), 117.8/117.6/117.4/117.3 (OCH_2CH=***C***H_2), 85.1/84.9/84.8/84.7 (CO***C***HCO), 65.2/65.0/64.8 (O***C***H_2CH=CH_2), 25.9/25.8 (***C***H_3CO).

5.3.1.6 Synthesis of Al(meaa)$_3$ (1f)

1.001 g (4.90 mmol) of Al($O^iPr)_3$ was dissolved in toluene (10 mL) at room temperature and 2.81 mL (3.153 g, 14.72 mmol) of 2-(methacryloyloxy)ethyl acetoacetate was slowly added under stirring. The clear reaction solution was stirred at room temperature for 18 h. The

volatiles were removed *in vacuo*, the crude product was washed with dichloromethane, and a colorless rubber-like mass was obtained.

Yield: 3.114 g (95 %).

^{1}H NMR (δ [ppm], C_6D_6, 20 °C): 6.12/6.08 (s, 3H, OC(O)C(Me)=C***H***$_2$), 5.25–5.15 (m, 3H, OC(O)C(Me)=C***H***$_2$), 5.14 (s, 3H, COC***H***CO), 4.40–3.90 (m, 12H, OC***H***$_2$C***H***$_2$O), 1.85–1.75 (m, 18H, OC(O)C(C***H***$_3$)=CH$_2$), 1.85 (s, 9H, C***H***$_3$CO).

^{13}C {^{1}H} NMR (δ [ppm], [D_8]toluene, 20 °C): 189.2/189.0/188.6/188.5 (***C***O), 174.2/174 (***C***OO), 166.3/166.2/166.1 (O***C***(O)C(Me)=CH$_2$), 136.1 (OC(O)***C***(Me)=CH$_2$), 125.3/125.0/124.8 (OC(O)C(Me)=***C***H$_2$), 85.1/84.9/84.8 (CO***C***HCO), 62.5/62.4/62.3/62.2 (O***C***H$_2$***C***H$_2$O), 25.9/15.1 (***C***H$_3$CO), 17.9 (OC(O)C(***C***H$_3$)=CH$_2$).

5.3.1.7 Synthesis of Al(me(ome)ac)$_3$(1g)

0.532 g (2.61 mmol) of Al(O^{i}Pr)$_3$ was dissolved in toluene (7 mL) at room temperature and 1.10 mL (1.14 g, 7.81 mmol) of methyl 4-methoxyacetoacetate was slowly added under stirring. The reaction solution was stirred at room temperature for 3 d. The volatiles were removed *in vacuo*, and a yellow solid was obtained.

Yield: 1.034 g (82 %).

^{1}H NMR (δ [ppm], C_6D_6, 20 °C): 5.89/5.87/5.86 (s, 3H, COC***H***CO), 3.94/3.91/3.88/3 (s, 6H, C***H***$_2$OMe), 3.40/3.35/3.32/3.30 (s, 9H, COOC***H***$_3$), 3.00/2.96/2.96 (s, 9H, CH$_2$OC***H***$_3$).

^{13}C {^{1}H} NMR (δ [ppm], [D_8]toluene, 20 °C): 187.7/187.3 (***C***O), 175.8/175.8/175.6 (***C***OO), 82.7/82.5/82.3 (CO***C***HCO), 74.7 (***C***H$_2$OMe), 58.5/58.3 (CH$_2$O***C***H$_3$), 51.1/51.6/51.4/51.3 (COO***C***H$_3$).

5.3.1.8 Synthesis of Al(et(tfl)ac)$_3$ (1h)

0.505 g (2.47 mmol) of Al(O^{i}Pr)$_3$ was dissolved in toluene (7 mL) at room temperature and 1.09 mL (1.372 g, 7.45 mmol) of ethyl 4,4,4-trifluoraocetoacetate was slowly added under stirring. The reaction solution was stirred at room temperature for 18 h. The volatiles were removed *in vacuo*, and a white solid was obtained.

Yield: 1.257 g (88 %).

^{1}H NMR (δ [ppm], C_6D_6, 20 °C): 5.60/5.55 (s, 3H, COC***H***CO), 4.00–3.65 (m, 6H, OC***H***$_2$Me), 0.85 (t, J = 6.7 Hz, 3H, OCH$_2$C***H***$_3$), 0.80–0.70 (m, 6H, OCH$_2$C***H***$_3$).

^{13}C {^{1}H} NMR (δ [ppm], C_6D_6, 20 °C): 176.1/176.0 (***C***OO), 170.0/169.3/169.2 (quart, J^2_{CF} = 35 Hz, ***C***O), 119.3/119.2 (quart, J^1_{CF} = 280 Hz, ***C***F$_3$), 86.1/85.8/85.3 (CO***C***HCO), 63.3/63.0/62.7 (O***C***H$_2$Me), 13.4/13.2 (OCH$_2$***C***H$_3$).

5.3.1.9 Synthesis of Al(et(^{i}pr)ac)$_3$ (1i)

Method A: 0.528 g (2.14 mmol) of Al(O^{t}Bu)$_3$ was dissolved in toluene (7 mL) at room temperature and 1.15 mL (1.11 g, 6.52 mmol) of ethyl 2-isopropylacetoacetate was slowly added under stirring. The reaction solution was stirred at 100 °C for 18 h. The volatiles were removed *in vacuo*, the crude product washed twice with n-pentane, and a white solid was obtained.

Yield: 0.965 g (83 %).

Method B: 0.518 g (2.54 mmol) of Al(O^{i}Pr)$_3$ was dissolved in toluene (10 mL) at room temperature and 1.36 mL (1.31 g, 7.60 mmol) of ethyl 2-isopropylacetoacetate was slowly added under stirring. The reaction solution was stirred at 80 °C for 4 d. The volatiles were removed *in vacuo*, the crude product washed with n-pentane, and a white solid was obtained.

Yield: 0.786 g (57 %).

^{1}H NMR (δ [ppm], C_6D_6, 20 °C): 4.20–3.95 (m, 6H, OC***H***$_2$Me), 2.85–2.70 (m, 3H, CC***H***Me$_2$), 1.85 (s, 6H, C***H***$_3$CO), 1.28–1.19 (m, 18H, CCH(C***H***$_3$)$_2$).

^{13}C {^{1}H} NMR (δ [ppm], [D_8]toluene, 20 °C): 185.5/185.2/185.0/184.7 (***C***O), 173.4/173.3/173.2 (***C***OO), 101.8/101.6/101.5/101.3 (CO***C***(i Pr)CO), 60.6/60.5/60.3/60.2/60.0 (O***C***H$_2$Me), 27.5/27.4 (C***C***HMe$_2$), 25.1/25.0/24.9 (***C***H$_3$CO), 21.8 (CCH(***C***H$_3$)$_2$), 14.2/14.0/14.0/13.8 (OCH$_2$***C***H$_3$).

5.3.1.10 Synthesis of Al$_2$(*μ*-O^{i}Pr)$_2$(O^{i}Pr)$_2$(meac)$_2$(2a)

1.003 g (4.91 mmol) of Al(O^{i}Pr)$_3$ was dissolved in toluene (10 mL) at room temperature and 0.53 mL (0.570 g, 4.91 mmol) of methyl acetoacetate was slowly added under stirring. The clear reaction solution was stirred at 120 °C for 18 h. The volatiles were removed *in vacuo*, the crude product was washed with n-pentane, and a colorless oil was obtained.

Yield: 1.217 g (95 %).

^{1}H NMR (δ [ppm], C_6D_6, 20 °C): 5.07 (s, 2H, COC***H***CO), 4.45 (sept, *J* = 5.9 Hz, 2H, OC***H***Me$_2^{b}$)[xxiv], 4.16 (sept, *J* = 6.2 Hz, 2H, OC***H***Me$_2^{t}$), 3.59 (s, 6H, COOC***H***$_3$), 1.66 (s, 6H, C***H***$_3$CO) 1.49–1.30 (m, 24H, OCH(C***H***$_3$)$_2$).

^{13}C {^{1}H} NMR (δ [ppm], [D_8]toluene, 20 °C): 186.8 (***C***O), 175.2 (***C***OO), 85.5 (CO***C***HCO), 66.0 (O***C***HMe$_2^{b}$), 63.1 (O***C***HMe$_2^{t}$), 51.8 (COO***C***H$_3$), 28.0 (OCH(***C***H$_3$)$_2^{b}$), 25.5 (***C***H$_3$CO), 25.3 (OCH(***C***H$_3$)$_2^{t}$).

5.3.1.11 Synthesis of Al$_2$(*μ*-O^{i}Pr)$_2$(O^{i}Pr)$_2$(etac)$_2$ (2b)

0.999 g (4.89 mmol) of Al(O^{i}Pr)$_3$ was dissolved in toluene (20 mL) at room temperature and 0.62 mL (0.638 g, 4.90 mmol) of ethyl acetoacetate slowly added under stirring. The clear

[xxiv] ^{t} and ^{b} indicate terminal or bridging binding of OR groups.

reaction solution was stirred at room temperature for 12 h and then at 120 °C for additional 18 h. The volatiles were removed *in vacuo*, and a colorless oil was obtained.

Yield: 1.297 g (97 %).

^{1}H NMR (δ [ppm], C_6D_6, 20 °C): 5.10 (s, 2H, COC***H***CO), 4.60–4.00 (m, 8H, OC***H***Me_2^b + OC***H***$_2Me^t$), 1.68 (s, 6H, C***H***$_3$CO), 1.48 (d, *J* = 6.2 Hz, 12H, OCH(C***H***$_3)_2^b$), 1.39 (d, *J* = 5.9 Hz, 12H, OCH(C***H***$_3)_2^t$), 1.10 (t, *J* = 7.1 Hz, 6H, OCH_2C***H***$_3$).

^{13}C {^{1}H} NMR (δ [ppm], [D_8]toluene, 20 °C): 186.5 (***C***O), 174.6 (***C***OO), 86.0 (CO***C***HCO), 65.9 (O***C***HMe_2^b), 63.1 (O***C***HMe_2^t), 61.1 (O***C***H_2Me), 28.0 (OCH(***C***$H_3)_2^b$), 25.5 (***C***H_3CO), 25.2 (OCH(***C***$H_3)_2^t$), 14.1 (OCH_2***C***H_3).

5.3.1.12 Synthesis of $Al_2(\mu\text{-}O^iPr)_2(O^iPr)_2(^i\text{prac})_2$ (2c)

1.006 g (4.93 mmol) of $Al(O^iPr)_3$ was dissolved in toluene (10 mL) at room temperature and 0.72 mL (0.708 g, 4.91 mmol) of isopropyl acetoacetate was slowly added under stirring. The clear reaction solution was stirred at 120 °C for 18 h. The volatiles were removed *in vacuo*, and a colorless oil was obtained.

Yield: 1.388 g (98 %).

^{1}H NMR (δ [ppm], C_6D_6, 20 °C): 5.39 (quin, *J* = 6.2 Hz, 2H, COOC***H***Me_2), 5.06 (s, 2H, COC***H***CO), 4.50 (quint, *J* = 5.8 Hz, 2H, OC***H***Me_2^b), 4.21 (quint, *J* = 6.2 Hz, 2H, OC***H***Me_2^t), 1.66 (s, 6H, C***H***$_3$CO), 1.48 (d, *J* = 6.2 Hz, 12H, OCH(C***H***$_3)_2^b$), 1.39 (d, *J* = 5.8 Hz, 12H, OCH(C***H***$_3)_2^t$), 1.30 (d, *J* = 6.2 Hz, 6H, COOCH(C***H***$_3)_2$), 1.12 (d, *J* = 6.2 Hz, 6H, COOCH(C***H***$_3)_2$).

^{13}C {^{1}H} NMR (δ [ppm], [D_8]toluene, 20 °C): 186.2 (***C***O), 174.6 (***C***OO), 86.5 (CO***C***HCO), 68.6 (COO***C***HMe_2), 65.8 (O***C***HMe_2^b), 63.2 (O***C***HMe_2^t), 28.0 (OCH(***C***$H_3)_2^b$), 25.5 (***C***H_3CO), 25.2 (OCH(***C***$H_3)_2^t$), 21.8 (COOCH(***C***$H_3)_2$).

5.3.1.13 Synthesis of $Al_2(\mu\text{-}O^iPr)_2(O^iPr)_2(^t\text{buac})_2$ (2d)

1.006 g (4.93 mmol) of $Al(O^iPr)_3$ was dissolved in toluene (10 mL) at room temperature and 0.82 mL (0.709 g, 4.92 mmol) of *tert.*-butyl acetoacetate was slowly added under stirring. The clear reaction solution was stirred at 120 °C for 18 h. The volatiles were removed *in vacuo*, and a white microcrystalline precipitate was obtained. Crystals suitable for single crystal XRD analysis were obtained upon recrystallization from toluene at 4 °C.

Yield: 1.331 g (89 %).

^{1}H NMR ((δ [ppm], C_6D_6, 20 °C): 5.06/5.05/4.98 (s, 2H, COC***H***CO), 4.65–4.45 (m, 2H, OC***H***Me_2^b), 4.35–4.15 (m, 2H, OC***H***Me_2^t), 1.67 (s, 6H, C***H***$_3$CO), 1.62–1.25 (m, 42H, OCH(C***H***$_3)_2^b$ + OCH(C***H***$_3)_2^t$ + OC(C***H***$_3)_3$).

^{13}C {^{1}H} NMR (δ [ppm], [D_8]toluene, 20 °C): 189.9/185.3 (***C***O), 175.0 (***C***O), 86.2/87.4 (CO***C***HCO), 81.05/80.5/80.0 (O***C***Me_3), 65.8 (O***C***HMe_2^b), 63.1 (O***C***HMe_2^t), 28.5 (OC(***C***$H_3)_3$), 28.0 (OCH(***C***$H_3)_2^b$), 25.3 (***C***H_3CO), 25.2 (OCH(***C***$H_3)_2^t$).

^{27}Al NMR (δ [ppm], [D_8]toluene, 20 °C): 100–40 (tetrahedral), 2.4 (octahedral).

5.3.1.14 Synthesis of $Al_2(\mu\text{-}O^iPr)_2(O^iPr)_2(aaa)_2$ (2e)

0.998 g (4.89 mmol) of $Al(O^iPr)_3$ was dissolved in toluene (10 mL) at room temperature and 0.67 mL (0.695 g, 4.89 mmol) of allyl acetoacetate was slowly added under stirring. The slightly turbid reaction solution was stirred at 120 °C for 18 h. The volatiles were removed *in vacuo*, the crude product washed with dichloromethane, and a pale yellow, slightly turbid oil was obtained.

Yield: 1.300 g (93 %).

^{1}H NMR (δ [ppm], C_6D_6, 20 °C): 6.05–5.85 (m, 2H, $OCH_2C\boldsymbol{H}{=}CH_2$), 5.10 (s, 2H, $COC\boldsymbol{H}CO$), 5.30–5.00 (m, 4H, $OCH_2CH{=}C\boldsymbol{H}_2$), 4.95–4.55 (m, 4H, $OC\boldsymbol{H}_2CH{=}CH_2$), 4.48 (quint, J = 5.9 Hz, 2H, $OC\boldsymbol{H}Me_2^b$), 4.18 (quint, J = 6.2 Hz, 2H, $OC\boldsymbol{H}Me_2^t$), 1.66 (s, 6H, $C\boldsymbol{H}_3CO$), 1.50–1.25 (m, 24H, $OCH(C\boldsymbol{H}_3)_2^b$ + $OCH(C\boldsymbol{H}_3)_2^t$).

^{13}C {^{1}H} NMR (δ [ppm], [D_8]toluene, 20 °C): 188.0 (***C***O), 174.0 (***C***OO), 132.8 ($OCH_2\boldsymbol{C}H{=}CH_2$), 117.5 ($OCH_2CH{=}\boldsymbol{C}H_2$), 86.0 ($CO\boldsymbol{C}HCO$), 66.1 ($O\boldsymbol{C}HMe_2^b$), 66.0 ($O\boldsymbol{C}H_2CH{=}CH_2$), 63.1 ($O\boldsymbol{C}HMe_2^t$), 28.0 ($OCH(\boldsymbol{C}H_3)_2^b$), 25.5 ($\boldsymbol{C}H_3CO$), 25.0 ($OCH(\boldsymbol{C}H_3)_2^t$).

5.3.1.15 Synthesis of $Al_2(\mu\text{-}O^iPr)_2(O^iPr)_2(meaa)_2$ (2f)

1.009 g (4.94 mmol) of $Al(O^iPr)_3$ was dissolved in toluene (10 mL) at room temperature and then stirred at 120 °C for 18 h. After cooling to room temperature 0.93 mL (1.055 g, 4.92 mmol) of 2-(methacryloyloxy)ethyl acetoacetate was slowly added under stirring. The clear reaction solution was stirred at room temperature for additional 18 h. The volatiles were removed *in vacuo*, and a colorless oil was obtained.

Yield: 1.696 g (97 %).

^{1}H NMR (δ [ppm], C_6D_6, 20 °C): 6.12 (s, 2H, $OC(O)C(Me){=}C\boldsymbol{H}_2$), 5.18 (s, 2H, $OC(O)C(Me){=}C\boldsymbol{H}_2$), 5.05 (s, 2H, $COC\boldsymbol{H}CO$), 4.80–3.90 (m, 12H, $OC\boldsymbol{H}Me_2^b$ + $OC\boldsymbol{H}Me_2^t$ + $OC\boldsymbol{H}_2C\boldsymbol{H}_2O$), 1.79 (s, 6H, $OC(O)C(C\boldsymbol{H}_3){=}CH_2$), 1.63 (s, 6H, $C\boldsymbol{H}_3CO$), 1.55–1.25 (m, 24H, $OCH(C\boldsymbol{H}_3)_2^b$ + $OCH(C\boldsymbol{H}_3)_2^t$).

^{13}C {^{1}H} NMR (δ [ppm], [D_8]toluene, 20 °C): 187.5 (***C***O), 174.4 (***C***OO), 166.3 ($O\boldsymbol{C}(O)C(Me){=}CH_2$), 136.2 ($OC(O)\boldsymbol{C}(Me){=}CH_2$), 125.0 ($OC(O)C(Me){=}\boldsymbol{C}H_2$), 85.8 ($CO\boldsymbol{C}HCO$), 66.0 ($O\boldsymbol{C}HMe_2^b$), 63.1 ($O\boldsymbol{C}HMe_2^t$), 62.3 ($O\boldsymbol{C}H_2\boldsymbol{C}H_2O$), 27.9 ($OCH(\boldsymbol{C}H_3)_2^b$), 25.4 ($\boldsymbol{C}H_3CO$), 25.0 ($OCH(\boldsymbol{C}H_3)_2^t$) 17.8 ($OC(O)C(\boldsymbol{C}H_3){=}CH_2$).

5.3.1.16 Synthesis of $Al_2(\mu\text{-}O^iPr)_2(O^iPr)_2(me(ome)ac)_2$ (2g)

1.075 g (5.26 mmol) of $Al(O^iPr)_3$ was dissolved in toluene (10 mL) at room temperature and 0.68 mL (0.769 g, 5.13 mmol) of methyl 4-methoxyacetoacetate was slowly added under stirring. The reaction solution was stirred at room temperature for 3 d. The volatiles were removed *in vacuo*, the crude product washed with n-pentane, and an orange oil was obtained.

Yield: 1.244 g (83 %).

^{1}H NMR (δ [ppm], C_6D_6, 20 °C): 5.78 (s, 2H, COC***H***CO), 4.48 (quint, *J* = 5.9 Hz, 2 H, OC***H***Me_2^b), 4.20 (quint, *J* = 6.1 Hz, 2 H, OC***H***Me_2^t), 3.72 (s, 4 H, C***H***$_2$OMe), 3.59 (s, 6 H, COOC***H***$_3$), 2.96 (s, 6 H, CH_2OC***H***$_3$), 1.60–1.40 (m, 24 H, OCH(C***H***$_3)_2^b$ + OCH(C***H***$_3)_2^t$).

^{13}C {^{1}H} NMR (δ [ppm], [D_8]toluene, 20 °C): 186.4 (***C***O), 176.1 (***C***OO), 83.7 (CO***C***HCO), 74.0 (***C***H_2OMe), 66.5 (O***C***HMe_2^b), 63.5 (O***C***HMe_2^t), 58.6 (CH_2O***C***H_3), 52.5 (COOC***H***$_3$), 28.4 (OCH(***C***$H_3)_2^b$), 25.5 (OCH(***C***$H_3)_2^t$).

5.3.1.17 Synthesis of $Al_2(\mu\text{-}O^iPr)_2(O^iPr)_2(et(tfl)ac)_2$ (2h)

0.539 g (2.64 mmol) Al(O^iPr)$_3$ was dissolved in toluene (7 mL) at room temperature and 0.39 mL (0.486 g, 2.67 mmol) of ethyl 4,4,4-trifluorocetoacetate was slowly added under stirring. The reaction solution was stirred at room temperature for 18 h. The volatiles were removed *in vacuo*, the crude product washed with n-pentane, and a white solid was obtained.

Yield: 0.733 g (85 %).

^{1}H NMR (δ [ppm], C_6D_6, 20 °C): 5.57 (s, 2H, COC***H***CO), 4.60–3.60 (m, 8H, OC***H***Me_2^t + OC***H***Me_2^b + OC***H***$_2$Me), 1.70–0.70 (m, 30H, OCH(C***H***$_3)_2^t$ + OCH(C***H***$_3)_2^b$ + OCH_2C***H***$_3$).

^{13}C {^{1}H} NMR (δ [ppm], C_6D_6, 20 °C): 175.9/175.6/175.5 (***C***OO), 169.0/168.0 (quart, J^2_{CF} = 35 Hz, ***C***O), 121.3/119.2 (quart, J^1_{CF} = 280 Hz, ***C***F_3), 86.6/86.3 (CO***C***HCO), 66.7 (O***C***HMe_2^b), 63.7 (O***C***H_2Me), 63.3 (O***C***HMe_2^t), 28.0 (OCH(***C***$H_3)_2^b$), 25.1 (OCH(***C***$H_3)_2^t$), 13.6 (OCH_2C***H***$_3$).

5.3.1.18 Synthesis of $Al_2(\mu\text{-}O^iPr)_2(O^iPr)_2(et(^ipr)ac)_2$ (2i)

0.514 g (2.52 mmol) of Al(O^iPr)$_3$ was dissolved in toluene (7 mL) at room temperature and 0.45 mL (0.43 g, 2.51 mmol) of ethyl 2-isopropylacetoacetate was slowly added under stirring. The reaction solution was stirred at room temperature, 80 °C, and 100 °C for 24 h each. The volatiles were removed *in vacuo*. The crude product was washed with n-pentane, and a yellow oil was obtained.

Yield: 0.444 g (56 %).

^{1}H NMR (δ [ppm], C_6D_6, 20 °C): 4.49 (quint, *J* = 5.9 Hz, 2H, AlOC***H***Me_2^b), 4.20 (quint, *J* = 6.0 Hz, 2H, AlOC***H***Me_2^t), 4.05–3.75 (m, 4H, OC***H***$_2$Me), 2.71 (quint, *J* = 6.7 Hz, 2H, CC***H***Me_2), 1.85 (s, 6H, C***H***$_3$CO), 1.55–1.05 (m, 42H, AlOCH(C***H***$_3)_2^b$ + AlOCH(C***H***$_3)_2^t$ + CCH(C***H***$_3)_2$ + OCH_2C***H***$_3$).

^{13}C {^{1}H} NMR (δ [ppm], [D_8]toluene, 20 °C): 183.4 (***C***O), 173.8 (***C***OO), 102.2 (CO***C***(^{i}Pr)CO), 65.9 (AlO***C***HMe_2^b), 62.8 (AlO***C***HMe_2^t), 60.8 (O***C***H_2Me), 27.9 (AlOCH(***C***$H_3)_2^b$), 27.5/27.2 (CCH(***C***$H_3)_2$), 25.1 (***C***H_3CO), 25.0 (AlOCH(***C***$H_3)_2^b$), 14.0 (OCH_2***C***H_3).

5.3.2 Modification with Dialkylmalonates

5.3.2.1 Synthesis of Al(dmem)$_3$ (3a)

0.498 g (2.02 mmol) of Al(O^{t}Bu)$_3$ was dissolved in toluene (7 mL) at room temperature and 0.69 mL (0.798 g, 6.04 mmol) of dimethyl malonate was added under stirring. The reaction mixture was stirred at room temperature for 6 d and at 50 °C for 2 d. The volatiles were removed *in vacuo*, and a colorless microcrystalline precipitate was obtained, including crystals suitable for single crystal XRD.

Yield: 0.801 g (94 %).

^{1}H NMR (δ [ppm], [D$_8$]toluene, 20 °C): 4.91 (s, 3H, COC***H***CO), 3.48 (s, 18H, OC***H***$_3$).

^{13}C {^{1}H} NMR (δ [ppm], [D$_8$]toluene, 20 °C): 175.8 (***C***O), 66.2 (CO***C***HCO), 51.1 (O***C***H$_3$).

5.3.2.2 Synthesis of Al(detm)$_3$ (3b)

0.498 g (2.02 mmol) of Al(O^{t}Bu)$_3$ was dissolved in toluene (5 mL) at room temperature and 0.92 mL (0.971 g, 6.06 mmol) of diethyl malonate was added under stirring. The reaction mixture was stirred at room temperature for 11 d and at 50 °C for 3 d. The volatiles were removed *in vacuo*, and a colorless solid was obtained.

Yield: 0.967 g (95 %).

^{1}H NMR (δ [ppm], C$_6$D$_6$, 20 °C): 4.99 (s, 3H, COC***H***CO), 4.18−3.96 (m, 12H, OC***H***$_2$Me), 1.00 (t, *J* = 7.0 Hz, 18 H, OCH$_2$C***H***$_3$).

^{13}C {^{1}H} NMR (δ [ppm], C$_6$D$_6$, 20 °C): 175.9 (***C***O), 67.1 (CO***C***HCO), 60.8 (O***C***H$_2$Me), 14.6 (OCH$_2$***C***H$_3$).

5.3.2.3 Synthesis of Al(d^{i}prm)$_3$ (3c)

Method A: 0.502 g (2.04 mmol) of Al(O^{t}Bu)$_3$ was dissolved in toluene (7 mL) at room temperature and 1.16 mL (1.150 g, 6.11 mmol) of diisopropyl malonate was added under stirring. The reaction mixture was stirred at room temperature for 3 d and at 50 °C for 7 d. The solvent volume was reduced *in vacuo*. Colorless crystals were obtained after recrystallization and storage for few days at room temperature.

Yield: 0.804 g (67 %).

Method B: 0.994 g (4.86 mmol) of Al(O^{i}Pr)$_3$ was dissolved in toluene (10 mL) at room temperature and 2.77 mL (2.745 g, 14.58 mmol) of diisopropyl malonate was added under stirring. The reaction mixture was stirred at 120 °C for 3 d. The volatiles were removed *in vacuo*, and a colorless solid was obtained.

Yield: 2.651 g (93 %).

Method C: 9.18 mL (9.097 g, 48.33 mmol) of diisopropyl malonate was added to 0.992 g (4.86 mmol) of $Al(O^iPr)_3$ and the mixture was stirred at 120 °C for 3 d. Toluene (2 mL) was added, resulting in dissolution of the colorless solid. Colorless crystals were obtained upon storage for few days at room temperature.

Yield: 2.102 g (74 %).

^{1}H NMR (δ [ppm], C_6D_6, 20 °C): 5.09 (sept, J = 6.1 Hz, 6H, OC***H***Me_2), 4.96 (s, 3H, COC***H***CO), 1.18 (d, J = 6.1 Hz, 18H, OCH(C***H***$_3)_2$), 1.07 (d, J = 6.1 Hz, 18H, OCH(C***H***$_3)_2$).

^{13}C {^{1}H} NMR (δ [ppm], C_6D_6, 20 °C): 175.5 (***C***O), 68.0 (CO***C***HCO), 67.9 (O***C***HMe_2), 22.2 (OCH(***C***$H_3)_2$), 22.0 (OCH(***C***$H_3)_2$).

^{27}Al NMR (δ [ppm], d_8-toluene, 20 °C): 5.3 (octahedral).

5.3.2.4 Synthesis of Al(d^{t}bum)$_3$(3d)

Method A: 0.506 g (2.05 mmol) of $Al(O^tBu)_3$ was dissolved in toluene (7 mL) at room temperature and 1.36 mL (1.314 g, 6.08 mmol) di-*tert.*-butyl malonate was added under stirring. The reaction mixture was stirred at 80 °C for 4 d. The solvent volume was reduced *in vacuo* to approximately 3 mL, and colorless crystals were obtained after recrystallization and storage for a few days at room temperature.

Yield: 0.822 g (59 %).

Method B: 0.995 g (4.87 mmol) of $Al(O^iPr)_3$ was dissolved in toluene (10 mL) at room temperature and 3.27 mL (3.159 g, 14.61 mmol) of di-*tert.*-butyl malonate was added under stirring. The reaction mixture was stirred at 80 °C for 5 d. The volatiles were removed *in vacuo*, and a colorless solid was obtained. Colorless crystals suitable for single crystal XRD were obtained upon recrystallization from toluene at room temperature.

Yield: 3.144 g (96 %).

^{1}H NMR (δ [ppm], C_6D_6, 20 °C): 4.81 (s, 3H, COC***H***CO), 1.50 (s, 54H, OC(C***H***$_3)_3$).

^{13}C {^{1}H} NMR (δ [ppm], C_6D_6, 20 °C): 175.6 (***C***O), 79.9 (O***C***Me_3), 69.0 (CO***C***HCO), 29.0 (OC(***C***$H_3)_3$).

5.3.2.5 Synthesis of Al$_2$(*μ*-O^{i}Pr)$_2$(O^{i}Pr)$_2$(d^{i}prm)$_2$(4c)

1.020 g (4.99 mmol) of $Al(O^iPr)_3$ was dissolved in toluene (10 mL) at room temperature and 0.95 mL (0.941 g, 5.00 mmol) of diisopropyl malonate was added under stirring. The reaction mixture was stirred at 100 °C for 3 d. The volatiles were removed *in vacuo*, and a colorless oil was obtained.

Yield: 1.577 g (95 %).

^{1}H NMR (δ [ppm], C_6D_6, 20 °C): 5.41 (quint, *J* = 6.2 Hz, 2H, COOC***H***Me_2), 4.96 (quint, *J* = 6.2 Hz, 2H, COOC***H***Me_2), 4.83 (s, 2H, COC***H***CO), 4.52 (quint, *J* = 6.2 Hz, 2H, AlOC***H***Me_2^b), 4.26 (quint, *J* = 6.2 Hz, 2H, AlOC***H***Me_2^t), 1.49 (d, *J* = 6.2 Hz, 6H, AlOCH(C***H***$_3)_2^b$), 1.45–1.35 (m, 18H, AlOCH(C***H***$_3)_2^b$ + AlOCH(C***H***$_3)_2^t$), 1.28 (d, *J* = 6.2 Hz, 6H, COOCH(C***H***$_3)_2$), 1.23 (d, *J* = 6.2 Hz, 6H, COOCH(C***H***$_3)_2$), 1.10 (d, *J* = 6.2 Hz, 6H, COOCH(C***H***$_3)_2$), 1.05 (d, *J* = 6.2 Hz, 6H, COOCH(C***H***$_3)_2$).

^{13}C {^{1}H} NMR (δ [ppm], C_6D_6, 20 °C): 175.3 (***C***O), 175.0 (*C*O), 68.1 (COO***C***HMe_2), 68.0 (CO***C***HCO), 66.3 (AlO***C***HMe_2^b), 63.5 (AlO***C***HMe_2^t), 28.4 (AlOCH(***C***H$_3)_2^t$), 25.5 (AlOCH(***C***H$_3)_2^b$), 25.4 (AlOCH(***C***H$_3)_2^b$), 22.4 (COOCH(***C***H$_3)_2$), 22.3 (COOCH(***C***H$_3)_2$), 22.3 (COOCH(***C***H$_3)_2$), 22.2 (COOCH(***C***H$_3)_2$).

^{27}Al NMR (δ [ppm], [D_8]toluene, 20 °C): 130–20 (tetrahedral), 5.1 (octahedral).

5.3.2.6 Synthesis of $Al_2(\mu\text{-}O^iPr)_2(O^iPr)_2(d^tbum)_2$ (4d)

1.008 g (4.94 mmol) of $Al(O^iPr)_3$ was dissolved in toluene (10 mL) at room temperature and 1.11 mL (1.072 g, 4.96 mmol) of di-*tert.*-butyl malonate was added under stirring. The reaction mixture was stirred at 80 °C for 3 d. The volatiles were removed *in vacuo*, and a colorless crystalline solid was obtained, including crystals suitable for single crystal XRD.

Yield: 1.741 g (98 %).

^{1}H NMR (δ [ppm], [D_8]toluene, 20 °C): 4.68 (s, 2H, COC***H***CO), 4.52 (quint, *J* = 5.9 Hz, 2H, AlOC***H***Me_2^b), 4.34 (quint, *J* = 6.3 Hz, 2H, AlOC***H***Me_2^t), 1.62 (s, 18 H, COOC(C***H***$_3)_3$), 1.55 (d, *J* = 6.3 Hz, 6H, AlOCH(C***H***$_3)_2^b$), 1.51 (s, 6H, OC(C***H***$_3)_3$), 1.40 (s, 12H, COOC(C***H***$_3)_3$, 1.32–1.40 (m, 18H, AlOCH(C***H***$_3)_2^b$ + AlOCH(C***H***$_3)_2^t$).

^{13}C {^{1}H} NMR (δ [ppm], [D_8]toluene, −60 °C)[xxv]: 175.5 (***C***O), 175.4 (***C***O), 80.5 (O***C***Me_3), 79.9 (O***C***Me_3), 69.8 (CO*C*HCO), 65.8 (AlO***C***HMe_2^b), 63.5 (AlO***C***HMe_2^t), 29.1 (OC(***C***H$_3)_3$), 28.7 (OC(***C***H$_3)_3$), 28.3 (OC(***C***H$_3)_3$), 27.4 (AlOCH(***C***H$_3)_2^t$), 25.9 (AlOC(***C***H$_3)_2^b$), 24.5 (AlOCH(***C***H$_3)_2^b$).

^{27}Al NMR (δ [ppm], [D_8]toluene, 20 °C): 120–40 (tetrahedral), 4.8 (octahedral).

5.3.2.7 Synthesis of $Al_2(\mu\text{-}O^iPr)_2(d^iprm)_4$ (5c)

Storage of 1.557 g (2.342 mmol) of $Al_2(\mu\text{-}O^iPr)_2(O^iPr)_2(d^iprm)_2$, a colorless oil, for few days at room temperature gave colorless crystals, including crystals suitable for single crystal XRD.

Yield: 0.468 g (43 %).

[xxv] Measurement at −60 °C because *C*O resonances were not detectable at 20 °C.

^{1}H NMR (δ [ppm], C_6D_6, 20 °C): 5.28 (t, *J* = 5.9 Hz, 4H, COOC***H***Me_2), 5.17 (t, *J* = 6.1 Hz, 4H, COOC***H***Me_2), 4.91 (s, 4H, COC***H***CO), 4.76 (quint, *J* = 6.1 Hz, 2H, AlOC***H***Me_2), 1.55 (d, *J* = 6.1 Hz, 6H, AlOCH(C***H***$_3)_2$), 1.43 (d, *J* = 6.1 Hz, 6H, AlOCH(C***H***$_3)_2$), 1.32 (d, *J* = 5.9 Hz, 12H, COOCH(C***H***$_3)_2$), 1.20–1.25 (m, 24H, COOCH(C***H***$_3)_2$), 1.13 (d, *J* = 6.1 Hz, 12H, COOCH(C***H***$_3)_2$).

^{13}C {^{1}H} NMR (δ [ppm], C_6D_6, 20 °C): 175.1 (***C***O), 174.5 (***C***O), 68.4 (CO***C***HCO), 67.2 (COO***C***HMe_2), 67.1 (COO***C***HMe_2), 64.4 (AlO***C***HMe_2), 25.4 (AlOCH(***C***$H_3)_2$), 24.0 (AlOCH(***C***$H_3)_2$), 23.2 (COOCH(***C***$H_3)_2$), 22.6 (COOCH(***C***$H_3)_2$), 22.5 (COOCH(***C***$H_3)_2$).

^{27}Al NMR (δ [ppm], [D_8]toluene, 20 °C): 3.5 (octahedral).

5.3.2.8 Synthesis of $Al_3(\mu\text{-OH})(\mu\text{-OEt})_3(detm)_5$ (6b)

Toluene (10 mL) and subsequently 2.80 mL of diethyl malonate (2.954 g, 18.44 mmol) were added to $Al(OEt)_3$ (1.007 g, 6.21 mmol) at room temperature. The mixture was stirred at 90 °C for 4 d, whereupon it cleared. Removal of the volatiles *in vacuo* gave a slightly greenish oil which crystallized upon storage at room temperature for several days to give colorless crystals suitable for single crystal XRD.

Yield: 1.874 g (88 %).

^{1}H NMR (δ [ppm], C_6D_6, 20 °C): 4.91 (s, 5H, COC***H***CO), 4.43–4.60 (m, 6H, AlOC***H***$_2$Me), 3.92–4.12 (m, 22H, COOC***H***$_2$Me + AlOC***H***$_2$Me), 3.72–3.84 (m, 4H, AlOC***H***$_2$Me), 1.33 (t, *J* = 6.6 Hz, 9H, $AlOCH_2C$***H***$_3$), 1.14 (t, *J* = 6.9 Hz, 15H, $COOCH_2C$***H***$_3$), 0.99 (t, *J* = 6.9 Hz, 15H, $COOCH_2C$***H***$_3$).

^{13}C {^{1}H} NMR (δ [ppm], C_6D_6, 20 °C): 175.4 (***C***O), 66.4 (CO***C***HCO), 60.1 (COO***C***H_2Me), 60.0 (COO***C***H_2Me), 56.6 (AlO***C***H_2Me), 18.4 ($AlOCH_2$***C***H_3), 14.6 ($COOCH_2$***C***H_3), 14.4 ($COOCH_2$***C***H_3).

^{27}Al NMR (δ [ppm], [D_8]toluene, 20 °C): 5.9 (octahedral).

5.3.3 Modification with N,N-Diethyl Acetoacetamide

5.3.3.1 Synthesis of $Al(detaca)_3$ (7b)

0.513 g (2.51 mmol) of $Al(O^iPr)_3$ was dissolved in toluene (7 mL) at room temperature and 1.19 mL (1.18 g, 7.53 mmol) of N,N-diethyl acetoacetamide was added under stirring. The reaction mixture was stirred at room temperature for 3 d. The volatiles were removed *in vacuo* and colorless crystals obtained upon recrystallization from toluene and storage at room temperature for few days, including crystals suitable for single crystal XRD.

Yield: 1.124 g (91 %).

^{1}H NMR (δ [ppm], C_6D_6, 20 °C): 4.87/4.86 (s, 3H, COC***H***CO), 3.45–2.60 (m, br, 12H, NC***H***$_2$Me), 1.97/1.96/1.93 (s, 9H, C***H***$_3$CO), 1.25–0.55 (m, br, 18H, NCH_2C***H***$_3$).

^{13}C {^{1}H} NMR (δ [ppm], C_6D_6, 20 °C): 182.6/182.3/182.1/182.0 (***C***O), 169.6/169.5/169.4 (***C***ON), 83.3/83.1/82.9/82.6 (CO***C***HCO), 41.9/40.9 (br, N***C***H_2Me), 27.0/26.9 (C***H***$_3$CO), 13.7/13.4 (NCH$_2$***C***H_3).

5.3.3.2 Synthesis of $Al_2(\mu\text{-}O^iPr)_2(O^iPr)_2$ (detaca)$_3$ (8b)

0.526 g (2.51 mmol) of Al(O^iPr)$_3$ was dissolved in toluene (7 mL) at room temperature and 0.41 mL (0.405 g, 2.58 mmol) of N,N-diethyl acetoacetamide was added under stirring. The reaction mixture was stirred at room temperature for 18 h. The volatiles were removed *in vacuo*, and a yellow oil was obtained.

Yield: 0.703 g (91 %).

^{1}H NMR (δ [ppm], C_6D_6, 20 °C): 4.83/4.81/4.79 (2H, s, COC***H***CO), 4.59 (quint, J = 6.0 Hz, 2H, AlOC***H***Me$_2^b$), 4.50–4.35 (m, 2H, AlOC***H***Me$_2^t$), 3.40–2.50 (m, br, 8H, NC***H***$_2$Me), 1.83/1.82 (s, 6H, C***H***$_3$CO), 1.65–1.35 (m, 24H, AlOCH(C***H***$_3$)$_2^b$ + AlOCH(C***H***$_3$)$_2^t$), 1.25–0.65 (m, br, 12H, NCH$_2$C***H***$_3$).

^{13}C {^{1}H} NMR (δ [ppm], C_6D_6, 20 °C): 183.4/181.3/180.8 (***C***O), 169.2/169.1 (***C***ON), 84.2/83.8/82.7 (CO***C***HCO), 66.3/65.6/65.0 (AlO***C***HMe$_2^b$), 63.2/63.0/62.9 (AlO***C***HMe$_2^t$), 42.0/41.9/41.2/41.0 (br, N***C***H_2Me), 28.1/27.0 (AlOCH(***C***H$_3$)$_2^b$), 25.7/25.6 (AlOCH(***C***H$_3$)$_2^t$), 25.3 (***C***H$_3$CO) 13.8/13.5 (br, NCH$_2$***C***H_3).

5.4 Modification of Yttrium Alkoxides

5.4.1 Modification with *β*-Ketoesters

5.4.1.1 Synthesis of $Y_9(\mu_5\text{-}O)(\mu_4\text{-}OH)(\mu_3\text{-}OH)_8(\mu\text{-}O^iPr)_8(^i$prac)$_8$ (9c)

0.922 g of a 25 % solution of Y(O^iPr)$_3$ in toluene – corresponding to 0.231 g (0.188 mmol) of $Y_5(\mu_5\text{-}O)(\mu_3\text{-}O^iPr)_4(\mu\text{-}O^iPr)_4(O^iPr)_5$ – was diluted with toluene (2 mL). 0.127 mL (0.125 g, 0.867 mmol) of isopropyl acetoacetate was slowly added at room temperature under stirring. The reaction solution was stirred at room temperature for 2 d and at 90 °C for 18 h. The volatiles were removed *in vacuo*, and a white solid was obtained. Colorless crystals suitable for single crystal XRD were obtained upon recrystallization from toluene at room temperature.

Yield: 0.095 g (35 %)[xxvi]

[xxvi] Only the first crop of crystals was isolated and used for the determination of the yield. Due to their high solubility in toluene the yield is relatively low.

5.4.1.2 Synthesis of $[Y_2(\mu_3\text{-}OH)(\mu\text{-}^i prac)_3(^i prac)_2]_2$ (10c)

0.926 g of a 25 % solution of $Y(O^iPr)_3$ in toluene – corresponding to 0.232 g (0.188 mmol) of $Y_5(\mu_5\text{-}O)(\mu_3\text{-}O^iPr)_4(\mu\text{-}O^iPr)_4(O^iPr)_5$ – was diluted with toluene (2 mL). 0.38 mL (0.374 g, 2.594 mmol) of isopropyl acetoacetate was slowly added at room temperature under stirring. After addition of additional toluene (2 mL), the reaction solution was stirred at room temperature for 6 d and at 80 °C for 18 h. Storage of the reaction solution at room temperature yielded colorless crystals suitable for single crystal XRD.

Yield: 0.102 g (24 %)[xxvi]

5.4.1.3 Synthesis of $Y_9(\mu_5\text{-}O)(\mu_4\text{-}OH)(\mu_3\text{-}OH)_8(\mu\text{-}^i prac)_8(^i prac)_8$ (11c)

A solution of 0.051 g (0.028 mmol) of $[Y_2(\mu_3\text{-}OH)(\mu\text{-}^i prac)_3(^i prac)_2]_2$ (**10c**) in $CDCl_3$ in an NMR tube seald with a cap and Parafilm® yielded colorless crystals suitable for single crystal XRD upon slow evaporation of the solvent at room temperature over a periode of one week.

Yield: 0.032 g (80 %)

5.5 Crystallographic Data

Table 5-3 Crystallographic and structural parameters of **2d**, **3a**, and **3c**.

	2d	**3a**	**3c**
Empirical formula	$C_{28}H_{54}Al_2O_{10}$	$C_{15}H_{21}AlO_{12}$	$C_{27}H_{45}AlO_{12}$
Formula weight	604.70	420.30	588.61
crystal system	monoclinic	monoclinic	monoclinic
space group	$P2_1/n$	$C2/c$	$P2_1/c$
Unit cell dimensions			
a [pm]	955.3(4)	1557.41(18)	1617.19(9)
b [pm]	1802.9(7)	1634.10(19)	1164.64(6)
c [pm]	2047.5(9)	766.74(9)	1721.08(9)
α [°]	90	90	90
β [°]	91.825(8)	103.132(2)	97.672(1)
γ [°]	90	90	90
Volume [pm^3] $\cdot 10^6$	3525(3)	1900.3(4)	3212.5(3)
Z	4	4	4
Calcd. density [$g \cdot cm^{-3}$]	1.139	1.469	1.217
Absorption coefficient μ [mm^{-1}]	0.129	0.169	0.119
Crystal size [mm]	1.60×1.40×0.10	0.56×0.23×0.17	0.32×0.21×0.20
crystal-to-detector distance [mm]	50	50	50
Θ range (°)	2.41–28.45	3.02−27.49	1.27−30.52
Reflections coll./unique	12759/6606	6283/2170	27148/9793
Data/parameters	6606/377	2170/131	979373/380
GOF on F^2	0.991	1.138	1.042
R [I>2σ(I)]	0.1165	0.0382	0.0628
w*R*2	0.3253	0.0951	0.1687
Largest diff. peak/hole [$e \cdot Å^{-3}$]	0.581/−0.375	0.292/−0.296	1.063/−0.444

Table 5-4 Crystallographic and structural parameters of **3d**, **4d**, and **5c**.

	3d·0.5toluene	**4d**	**5c**
Empirical formula	$C_{73}H_{122}A_{l2}O_{24}$	$C_{34}H_{66}Al_2O_{12}$	$C_{42}H_{74}Al_2O_{18}$
Formula weight	1437.67	720.83	920.97
crystal system	Triclinic	Triclinic	Orthorhombic
space group	*P*−1	*P*−1	$P2_12_12_1$
Unit cell dimensions			
a [pm]	1011.89(5)	1270.21(9)	1233.3(2)
b [pm]	1118.28(5)	1949.16(14)	2118.3(4)
c [pm]	1901.72(8)	1980.94(14)	3965.2(8)
α [°]	74.787(1)	64.924(1)	90
β [°]	85.206(1)	74.446(1)	90
γ [°]	81.489(1)	84.206(1)	90
Volume [pm^3] ·10^6	2051.41(16)	4279.1(5)	10359(3)
Z	1	4	8
Calcd. density [$g·cm^{-3}$]	1.164	1.119	1.181
Absorption coefficient μ [mm^{-1}]	0.105	0.120	0.121
Crystal size [mm]	0.57×0.48×0.37	0.53×0.37×0.16	0.60×0.30×0.10
crystal-to-detector distance [mm]	55	55	60
Θ range (°)	2.60−25.00	1.78−25.00	1.73−25.00
Reflections coll./unique	11229/7168	38427/15018	54453/9938
Data/parameters	7168/497	15018/965	9938/1175
GOF on F^2	1.023	0.957	1.094
R [I>2σ(I)]	0.0365	0.0536	0.0749
w*R*2	0.0954	0.1362	0.1825
Largest diff. peak/hole [$e·Å^{-3}$]	0.265/−0.268	0.582/−0.485	0.744/−0.403

Table 5-5 Crystallographic and structural parameters of **6b**, $[Al(\mu\text{-}O^sBu)(acac)_2]_2$, and **7b**.

	6b	$[Al(\mu\text{-}O^sBu)(acac)_2]_2$	**7b**
Empirical formula	$C_{41}H_{71}Al_3O_{24}$	$C_{28}H_{46}Al_2O_{10}$	$C_{24}H_{42}AlN_3O_6$
Formula weight	1028.92	596.61	495.59
crystal system	Triclinic	Tetragonal	Triclinic
space group	*P*−1	$I4_1/acd$	*P*−1
Unit cell dimensions			
a [pm]	1237.19(14)	1481.20(8)	965.89(17)
b [pm]	1479.98(17)	1481.20(8)	981.57(17)
c [pm]	1500.80(17)	2945.7(3)	1659.0(4)
α [°]	74.305(2)	90	94.334(4)
β [°]	81.936(2)	90	103.178(4)
γ [°]	77.301(2)	90	112.795(3)
Volume $[pm^3] \cdot 10^6$	2571.2(5)	6462.7(8)	1388.2(5)
Z	2	8	2
Calcd. density $[g \cdot cm^{-3}]$	1.329	1.226	1.186
Absorption coefficient μ $[mm^{-1}]$	0.154	0.140	0.113
Crystal size [mm]	0.57×0.47×0.26	0.35×0.15×0.10	0.31×0.18×0.09
crystal-to-detector distance [mm]	55	50	55
Θ range (°)	2.44−25.00	2.39–28.28	2.94–24.99
Reflections coll./unique	26695/9065	20486/2010	8035/4861
Data/parameters	9065/709	2010/146	4861/316
GOF on F^2	1.073	1.06	1.029
R [I>2σ(I)]	0.0342	0.0456	0.0356
w*R*2	0.0903	0.1193	0.0912
Largest diff. peak/hole $[e \cdot Å^{-3}]$	0.590/−0.544	0.268/−0.157	0.277/–0.225

Table 5-6 Crystallographic and structural parameters of **9c**, **10c**, and **11c**.

	9c·4.0toluene	**10c**	**11c**·4.0choroform
Empirical formula	$C_{108}H_{185}O_{42}Y_9$	$C_{70}H_{112}O_{32}Y_4$	$C_{116}H_{185}Cl_{12}O_{58}Y_9$
Formula weight	2955.75	1821.24	3733.23
crystal system	Tetragonal	Monoclinic,	Cubic
space group	*P*4/n	$P2_1/n$	*P*n−3n
Unit cell dimensions			
a [pm]	2076.9(4)	1417.2(5)	3109.91(12)
b [pm]	2076.9(4)	2004.8(7)	3109.91(12)
c [pm]	1497.9(6)	1656.9(6)	3109.91(12)
α [°]	90	90	90
β [°]	90	114.755(5)	90
γ [°]	90	90	90
Volume [pm^3] ·10^6	6461(3)	4275(3)	30078(2)
Z	2	2	6
Calcd. density [$g \cdot cm^{-3}$]	1.519	1.415	1.237
Absorption coefficient μ [mm^{-1}]	4.068	2.766	2.796
Crystal size [mm]	0.27×0.05×0.04	0.15×0.14×0.11	0.47×0.44×0.29
crystal-to-detector distance [mm]	55	55	55
Θ range (°)	2.39–28.28	1.59–28.31	2.62–23.99
Reflections coll./unique	44166/7977	56717/10612	139939/3955
Data/parameters	7977/414	10612/526	3955/300
GOF on F^2	1.002	1.109	1.118
R [I>2σ(I)]	0.0358	0.0361	0.0609
w*R*2	0.0782	0.0827	0.1819
Largest diff. peak/hole [$e \cdot Å^{-3}$]	0.896/−0.660	0.851/−1.218	1.846/−0.578

6 References

[1] Gomez-Romero, P.; Sanchez, C. *New J. Chem.* **2005**, *29*, 57-58.

[2] Brinker, C. J.; Scherer, G. W., *Sol-Gel Science*. Academic Press: Boston, Massachus, **1990**.

[3] Livage, J.; Henry, M.; Sanchez, C. *Prog. Solid State Chem.* **1988**, *18*, 259-341.

[4] Schubert, U.; Huesing, N., *Synthesis of Inorganic Materials*. 2 ed.; Wiley-VCH Verlag GmbH & Co. KGaA: Weinheim, Germany, **2005**.

[5] Schubert, U., Sol-gel processing of metal compounds. In *Compr. Coord. Chem. II*, McCleverty, J. A.; Meyer, T. J., Eds. Elsevier: Amsterdam, 2004; Vol. 7, pp 629-656.

[6] Schubert, U. *J. Sol-Gel Sci. Technol.* **2003**, *26*, 47-55.

[7] Turova, N. Y.; Kozuniv, V. A.; Yanovskii, A. I.; Bokii, N. G.; Struchkov, Y. T.; Tarnopol'skii, B. L. *J. Inorg. Nuc. Chem.* **1979**, *41*, 5-11.

[8] Shiner, V. J., Jr.; Whittaker, D.; Vernandez, V. P. *J. Am. Chem. Soc.* **1963**, *85*, 2318-2322.

[9] Vaartstra, B. A.; Huffman, J. C.; Gradeff, P. S.; Hubert-Pfalzgraf, L. G.; Daran, J. C.; Parraud, S.; Yunlu, K.; Caulton, K. G. *Inorg. Chem.* **1990**, *29*, 3126-3131.

[10] Kundu, D.; Ganguli, D. *J. Mater. Sci. Lett.* **1986**, *5*, 293-295.

[11] Gladstone, J. H.; Tribe, A. *J. Chem. Soc., Trans.* **1881**, *39*, 1-12.

[12] Mehrotra, R. C. *J. Indian Chem. Soc.* **1953**, *30*, 585-591.

[13] Mehrotra, R. C. *J. Indian Chem. Soc.* **1954**, *31*, 85-90.

[14] Bradley, D. C. *Nature (London, U. K.)* **1958**, *182*, 1211-1214.

[15] Cayton, R. H.; Chisholm, M. H.; Davidson, E. R.; DiStasi, V. F.; Du, P.; Huffman, J. C. *Inorg. Chem.* **1991**, *30*, 1020-1024.

[16] Bains, M. S. *Can. J. Chem.* **1962**, *40*, 381-383.

[17] Kriz, O.; Casensky, B.; Lycka, A.; Fusek, J.; Hermanek, S. *J. Magn. Reson.* **1984**, *60*, 375-81.

[18] Bradley, D. C.; Mehrotra, R. C.; Rothwell, I.; Singh, A., *Alkoxo and Aryloxo Derivatives of Metals*. 1st ed.; Academic Press: London, **2001**.

[19] Oliver, J. G.; Phillips, P. K.; Worrall, I. J. *J. Inorg. Nuc. Chem.* **1969**, *31*, 1609-1613.

[20] Ulich, I. H.; Nespital, W. *Z. physik. Chem.* **1933**, *A165*, 294-310.

[21] Bradley, D. C.; Mehrotra, R. C.; Gaur, D. P., *Metal Alkoxides*. Academic Press: London, **1978**.

[22] Lichtenberger, R.; Puchberger, M.; Schubert, U. *unpublished results*.

[23] Robinson, R. A.; Peak, D. A. *J. Phys. Chem.* **1935**, *39*, 1125-1133.

[24] Kleinschmidt, D. C.; Shiner, V. J., Jr.; Whittaker, D. *J. Org. Chem.* **1973**, *38*, 3334-3337.

[25] Oliver, J. G.; Worrall, I. J. *J. Chem. Soc. A* **1970**, 1389-1391.

[26] Oliver, J. G.; Worrall, I. J. *J. Chem. Soc. A* **1970**, 2347-2348.

[27] Abraham, A.; Prins, R.; van Bokhoven, J. A.; Van Eck, E. R. H.; Kentgens, A. P. M. *J. Phys. Chem. B* **2006**, *110*, 6553-6560.

[28] Saegusa, T.; Ueshima, T. *Inorg. Chem.* **1967**, *6*, 1679-1681.

[29] Parente, V.; Bredas, J.-L.; Dubois, P.; Ropson, N.; Jerome, R. *Macromol. Theory Simul.* **1996**, *5*, 525-546.

[30] Duda, A.; Penczek, S. *Macromol. Rapid. Commun.* **1995**, *16*, 67-76.

[31] Duda, A. *Macromolecules* **1996**, *29*, 1399-406.

[32] Kowalski, A.; Duda, A.; Penczek, S. *Macromolecules* **1998**, *31*, 2114-2122.

[33] Shiner, V. J., Jr.; Whittaker, D. *J. Am. Chem. Soc.* **1963**, *85*, 2337-2338.

[34] Shiner, V. J., Jr.; Whittaker, D. *J. Am. Chem. Soc.* **1969**, *91*, 394-398.

[35] Starikova, Z. A.; Kessler, V. G.; Turova, N. Y.; Tcheboukov, D. E.; Suslova, E. V.; Seisenbaeva, G. A.; Yanovsky, A. I. *Polyhedron* **2004**, *23*, 109-114.

[36] Abrahams, I.; Bradley, D. C.; Chudzynska, H.; Motevalli, M.; Sinclair, R. A. *J. Chem. Soc., Dalton Trans.* **2002**, 259-266.

[37] Sangokoya, S. A.; Pennington, W. T.; Byers-Hill, J.; Robinson, G. H.; Rogers, R. D. *Organometallics* **1993**, *12*, 2429-2431.

[38] Poncelet, O.; Sartain, W. J.; Hubert-Pfalzgraf, L. G.; Folting, K.; Caulton, K. G. *Inorg. Chem.* **1989**, *28*, 263-267.

[39] Poncelet, O.; Hubert-Pfalzgraf, L. G.; Daran, J. C.; Astier, R. *J. Chem. Soc., Chem. Commun.* **1989**, 1846-1848.

[40] Pfalzgraf, L. G. H.; Morlens, S.; Daniele, S.; Thozet, A. *Inorg. Chem. Commun.* **2004**, *7*, 751-755.

[41] Bradley, D. C.; Chudzynska, H.; Hursthouse, M. B.; Motevalli, M. *Polyhedron* **1991**, *10*, 1049-1059.

[42] Daniele, S.; Hubert-Pfalzgraf, L. G.; Hitchcock, P. B.; Lappert, M. F. *Inorg. Chem. Commun.* **2000**, *3*, 218-220.

[43] Herrmann, W. A.; Anwander, R.; Denk, M. *Chem. Ber.* **1992**, *125*, 2399-2405.

[44] Hubert-Pfalzgraf, L. G.; Daniele, S. *C. R. Chim.* **2004**, *7*, 521-527.

[45] Hubert-Pfalzgraf, L. G. *New J. Chem.* **1995**, *19*, 727-750.

[46] Arnold, P. L.; Buffet, J.-C.; Blaudeck, R. P.; Sujecki, S.; Blake, A. J.; Wilson, C. *Angew. Chem., Int. Ed.* **2008**, *47*, 6033-6036.

[47] Spassky, N.; Simic, V.; Montaudo, M. S.; Hubert-Pfalzgraf, L. G. *Macromol. Chem. Phys.* **2000**, *201*, 2432-2440.

[48] McLain, S. J.; Drysdale, N. E. *Polym. Prepr. (Am. Chem. Soc., Div. Polym. Chem.)* **1992**, *33*, 174-175.

[49] Oliver, J. G.; Worrall, I. J. *J. Inorg. Nuc. Chem.* **1971**, *33*, 1281-1285.

[50] Wengrovius, J. H.; Garbauskas, M. F.; Williams, E. A.; Goint, R. C.; Donahue, P. E.; Smith, J. F. *J. Am. Chem. Soc.* **1986**, *108*, 982-989.

[51] Garbauskas, M. F.; Wengrovius, J. H.; Going, R. C.; Kasper, J. S. *Acta Crystallogr., Sect. C: Cryst. Struct. Commun.* **1984**, *C40*, 1536-40.

[52] Sharma, N.; Sharma, R. K.; Bohra, R.; Drake, J. E.; Hursthouse, M. B.; Light, M. E. *J. Chem. Soc., Dalton Trans.* **2002**, 1631-1634.

[53] Sharma, N.; Jain, A. K.; Sharma, R. K.; Bohra, R.; Drake, J. E.; Hursthouse, M. B.; Light, M. E. *Polyhedron* **2003**, *22*, 2943-2952.

[54] Garbauskas, M. F.; Wengrovius, J. H. *Acta Crystallogr., Sect. C: Cryst. Struct. Commun.* **1987**, *C43*, 2441-2442.

[55] Lichtenberger, R.; Benodvá, M.; Schubert, U. *unpublished results*.

[56] Hoebbel, D.; Reinert, T.; Schmidt, H.; Arpac, E. *J. Sol-Gel Sci. Technol.* **1997**, *10*, 115-126.

[57] Bhardwaj, N. C.; Singh, R. V. *J. Indian Chem. Soc.* **1992**, *69*, 850-852.

[58] Bhardwaj, N. C.; Jadon, S. C. S.; Singh, R. V. *Synth. React. Inorg. Met.-Org. Chem.* **1994**, *24*, 1267-1279.

[59] Saxena, C.; Bhardwaj, N. C.; Singh, D.; Singh, R. V. *Synth. React. Inorg. Met.-Org. Chem.* **1993**, *23*, 1391-1405.

[60] Malhotra, K. C.; Sharma, N.; Chaudhry, S. C. *J. Indian Chem. Soc.* **1992**, *69*, 381-382.

[61] Dhammani, A.; Bohra, R.; Mehrotra, R. C. *Polyhedron* **1995**, *14*, 733-739.

[62] Dhammani, A.; Bohra, R.; Mehrotra, R. C. *Polyhedron* **1996**, *15*, 733-737.

[63] Dhammani, A.; Bohra, R.; Mehrotra, R. C. *Polyhedron* **1998**, *17*, 163-171.

[64] Nagar, S.; Bohra, R.; Mehrotra, R. C. *Synth. React. Inorg. Met.-Org. Chem.* **2002**, *32*, 1825-1838.

[65] Ko, B.-T.; Wu, C.-C.; Lin, C.-C. *Organometallics* **2000**, *19*, 1864-1869.

[66] Liu, Y.-C.; Ko, B.-T.; Huang, B.-H.; Lin, C.-C. *Organometallics* **2002**, *21*, 2066-2069.

[67] Lugmair, C. G.; Fujdala, K. L.; Tilley, T. D. *Chem. Mater.* **2002**, *14*, 888-898.

[68] Akitt, J. W.; Duncan, R. H. *J. Chem. Soc., Dalton Trans. (1972-1999)* **1976**, 1119-1120.

[69] Bains, M. S.; Bradley, D. C. *Can. J. Chem.* **1962**, *40*, 2218-2228.

[70] Shiner, V. J., Jr.; Whittaker, D. *J. Am. Chem. Soc.* **1965**, *87*, 843-846.

[71] Bains, M. S.; Bradley, D. C. *Can. J. Chem.* **1962**, *40*, 1350-1354.

[72] Stepovik, L. P.; Dodonov, V. A.; Vaulina, E. N.; Sofronova, S. M. *Zh. Obshch. Khim.* **1992**, *62*, 861-866.

[73] Velez, K.; Quinson, J. F.; Fenet, B. *J. Sol-Gel Sci. Technol.* **1999**, *16*, 201-208.

[74] Tadanaga, K.; Minami, T.; Tohge, N. *Chem. Lett.* **1994**, 1507-1510.

[75] Amini, M. M.; Sharbatdaran, M.; Mirzaee, M.; Mirzaei, P. *Polyhedron* **2006**, *25*, 3231-3237.

[76] Francis, J. A.; Bott, S. G.; Barron, A. R. *J. Organomet. Chem.* **2000**, *597*, 29-37.

[77] Lin, C.-Y.; Lee, H. M.; Huang, J.-H. *J. Organomet. Chem.* **2007**, *692*, 3718-3722.

[78] Munoz-Hernandez, M.-A.; Keizer, T. S.; Parkin, S.; Zhang, Y.; Atwood, D. A. *J. Chem. Crystallogr.* **2000**, *30*, 219-222.

[79] Amgoune, A.; Lavanant, L.; Thomas, C. M.; Chi, Y.; Welter, R.; Dagorne, S.; Carpentier, J.-F. *Organometallics* **2005**, *24*, 6279-6282.

[80] Taden, I.; Kang, H.-C.; Massa, W.; Spaniol, T. P.; Okuda, J. *Eur. J. Inorg. Chem.* **2000**, 441-445.

[81] Chmura, A. J.; Chuck, C. J.; Davidson, M. G.; Jones, M. D.; Lunn, M. D.; Bull, S. D.; Mahon, M. F. *Angew. Chem., Int. Ed.* **2007**, *46*, 2280-2283.

[82] Liu, Y.-C.; Ko, B.-T.; Lin, C.-C. *Macromolecules* **2001**, *34*, 6196-6201.

[83] Hubert-Pfalzgraf, L. G.; Cauro-Gamet, L.; Brethon, A.; Daniele, S.; Richard, P. *Inorg. Chem. Commun.* **2007**, *10*, 143-147.

[84] Gleizes, A.; Sans-Lenain, S.; Medus, D.; Hovnanian, N.; Miele, P.; Foulon, J. D. *Inorg. Chim. Acta* **1993**, *209*, 47-53.

[85] Poncelet, O.; Hubert-Pfalzgraf, L. G.; Daran, J. C. *Polyhedron* **1990**, *9*, 1305-1310.

[86] Kickelbick, G., Introduction to hybrid materials. In *Hybrid Materials*, Kickelbick, G., Ed. Wiley-VCH Verlag GmbH & Co. KGaA: Weinheim, Germany, 2007; pp 1-48.

[87] Sanchez, C.; Ribot, F. *New J. Chem.* **1994**, *18*, 1007-47.

[88] Cauro-Gamet, L. C.; Hubert-Pfalzgraf, L. G.; Lecocq, S. *Z. Anorg. Allg. Chem.* **2004**, *630*, 2071-2077.

[89] Ivanovici, S.; Puchberger, M.; Fric, H.; Kickelbick, G. *Monatsh. Chem.* **2007**, *138*, 529-539.

[90] Dharmaprakash, M. S.; Thamotharan, S.; Neelgund, G. M.; Shivashankar, S. A. *Acta Crystallogr., Sect. E: Struct. Rep. Online* **2006**, *E62*, m434-m436.

[91] Diaz-Acosta, I.; Baker, J.; Cordes, W.; Pulay, P. *J. Phys. Chem. A* **2001**, *105*, 238-244.

[92] Baker, R. H. *J. Am. Chem. Soc.* **1938**, *60*, 2673-2675.

[93] Pajot, N.; Papiernik, R.; Hubert-Pfalzgraf, L. G.; Vaissermann, J.; Parraud, S. *J. Chem. Soc., Chem. Commun.* **1995**, 1817-19.

[94] Bader, A. R.; Cummings, L. O.; Vogel, H. A. *J. Am. Chem. Soc.* **1951**, *73*, 4195-4197.

[95] Reeder, J. A.; Schlabitz, J. *J. Org. Chem.* **1966**, *31*, 3415-3416.

[96] Puchberger, M.; Rupp, W.; Bauer, U.; Schubert, U. *New J. Chem.* **2004**, *28*, 1289-1294.

[97] Metelkina, O.; Schubert, U. *Monatsh. Chem.* **2003**, *134*, 1065-1069.

[98] Shulman, G. P.; Trusty, M.; Vickers, J. H. *J. Org. Chem.* **1963**, *28*, 907-910.

[99] Bader, A. R.; Vogel, H. A. *J. Am. Chem. Soc.* **1952**, *74*, 3992-3994.

[100] Patil, U.; Winter, M.; Becker, H.-W.; Devi, A. *J. Mater. Chem.* **2003**, *13*, 2177-2184.

[101] Honda, A.; Waltz, K. M.; Carroll, P. J.; Walsh, P. J. *Chirality* **2003**, *15*, 615-621.

[102] Gornshtein, F.; Kapon, M.; Botoshansky, M.; Eisen, M. S. *Organometallics* **2007**, *26*, 497-507.

[103] Hitchcock, P. B.; Huang, Q.-G.; Lappert, M. F.; Wei, X.-H. *J. Mater. Chem.* **2004**, *14*, 3266-3273.

[104] Poncelet, O.; Hubert-Pfalzgraf, L. G.; Daran, J. C. *Inorg. Chem.* **1990**, *29*, 2883-2885.

[105] Hubert-Pfalzgraf, L. G.; Miele-Pajot, N.; Papiernik, R.; Vaissermann, J. *J. Chem. Soc., Dalton Trans.* **1999**, 4127-4130.

[106] Barash, E. H.; Coan, P. S.; Lobkovsky, E. B.; Streib, W. E.; Caulton, K. G. *Inorg. Chem.* **1993**, *32*, 497-501.

[107] Xu, G.; Wang, Z.-M.; He, Z.; Lue, Z.; Liao, C.-S.; Yan, C.-H. *Inorg. Chem.* **2002**, *41*, 6802-6807.

[108] Armarego, W. L. F.; Perrin, D. D., *Purification of Laboratory Chemicals, Fourth Edition*. **1997**.

Curriculum Vitae

Name	Robert Lichtenberger
Date and Place of Birth	28.08.1981, Linz
Citizenship	Austrian
Address	Schallergasse 9/18, 1120 Wien
Marital Status / Children	married, two children (1 ¾ years, ½ year)

Education

03/2007– present	PhD Thesis Institut of Materials Chemistry, Vienna University of Technology, Vienna
10/2001–11/2003	University Education in Chemistry Graduation with distinction as "Diplom Ingineur" (comparable to a M.Sc.) Vienna University of Technology, Vienna
09/1992–06/2000	Secondary School Gratuation with "Matura" (comparable to High School Graduation) Europagymnasium Auhof, Linz

Work Experinece

01/2007–present	Research and Teaching Assistant Institute of Materials Chemistry, Vienna Univesity of Technology, Vienna
08/2005	Internship (Polymerdesign and -modification) Borealis Polyolefine GmbH, Linz
09/2004	Internship (Technical translation) Borealis Polyolefine GmbH, Schwechat
07/2004	Internship (Oil and fuel analytics) Shell Austria GmbH, Vienna
07–08/2003	Internship (Qualitiy assurance, method validiation) Aventis Behring GmbH, Vienna